Energy Metabolism of Platelets

Miriayi Aibibula, BSc, MSc

Doctorate of Philosophy (PhD) in Medical Sciences

The University of Hull and the University of York

Hull York Medical School

March 2017

Abstract

Undesired platelet activation is associated with a number of diseases characterised by metabolic imbalance, such as hyperlipidaemia. Changes in platelet energy metabolism associated with disease states are unclear. This thesis presents a detailed investigation of platelet energy metabolism under normal physiological conditions as well as platelet mitochondrial dysfunction in hyperlipidaemia.

Platelets rapidly take up exogenous glucose at rest. Following platelet-thrombin activation, the secretion of ADP and TxA_2 are the most glucose dependent processes. Platelets have a wide 'scope' for glycolysis, which reaches full capacity when activated with thrombin, mainly mediated by the PAR1 receptor. Despite being a major fuel for platelets, the absence of exogenous glucose is not able to prevent platelet adhesion, secretion and aggregation, suggesting metabolic redundancy and an important role for endogenous metabolic fuels. Furthermore, glycogen or endogenous fatty acids alone are sufficient to facilitate platelet activation. Moreover, activated platelets adopt a glycolytic phenotype regardless of extracellular fuel availability and irrespective of the thrombin dose.

Analysis of the mitochondrial function revealed remarkable fuel flexibility for platelets under normal physiological conditions. After identifying that amino acids have a minimal role as an oxidative fuel, it is further revealed that platelets can switch freely between glucose and fatty acid oxidation. Under conditions where these substrates are limited for mitochondrial oxidation, platelets can up-regulate glycolysis to meet the energy demand of activation. The transition of platelets from resting to an activated state is associated with an increase in mitochondrial oxygen consumption, despite the shift to a glycolytic state. Thrombin-stimulated platelets have higher ATP-coupled respiration and higher spare respiratory capacity. Interestingly, platelets from hyperlipidaemic mice show an increased mitochondrial proton leak and a complete loss of mitochondrial spare respiratory capacity.

This thesis presents for the first time the impact of high fat diet on the function of platelet mitochondria. The data are important in investigating the potential impact of altered platelet metabolism on disease outcome.

Table of Content

List of Figures

List of Tables

Acknowledgement

I would like to express my deepest appreciation to my principle supervisor, Dr Roger Sturmey and co-supervisor Professor Khalid Naseem, for their constant guidance, encouragement, and patience throughout my PhD, without which this work would not have been possible. I am tremendously fortunate to have Professor Henry Leese as my TAP chair, whom I would like to express my gratitude for providing me with thoughtful feedbacks and guiding me on scientific writing.

I would like to thank University of Hull, for covering my tuition fees with the International Student Scholarship, without which I would not be writing this acknowledgement. On that note, words cannot describe how thankful I am to my family. My parents, Habibulla Omer and Faride Kahar, my brothers Nesrulla and Asrulla, my sister Munevver and their families have been assisting me financially, helping me with my living expenses throughout my PhD. Expressing my gratitude with a few lines can not in million years counterbalance all the sacrifices you have all made in this unique and remarkable journey of my life. I would like to say a special thank you to my biggest sponsor, my elder brother Nesrulla, for paying my tuition fee and living expenses during my master degree (You could have bought a nice 4 bedroom house back home instead). Your generosity has paved the way for everything I have dreamed for. Above all, I would like to thank my family for their unconditional love and support, which have been the reason for the resilience and determination in me all the way through.

I would also like to thank all members of CCMR, my colleagues from Thrombosis Lab, especially Dr Casey Woodward (thank you for showing me all the platelet assays) and all the old and new members of Sturmey Group. I would like to extend my appreciation to all, whom I have met along the way, for being a part of this journey; especially Sophie, a friend and sister for life. A heartfelt appreciation goes to Riza for his selfless support, love and tolerance of me throughout the last stage of the PhD.

Finally, this work is dedicated to my community.

Declaration

I confirm that this work is original and that if any passage(s) or diagram(s) have been copied from academic papers, books, the Internet or any other sources these are clearly identified by the use of quotation marks and the reference(s) is fully cited. I certify that, other than where indicated, this is my own work and does not breach the regulations of HYMS, the University of Hull or the University of York regarding plagiarism or academic conduct in examinations. I have read the HYMS Code of Practice on Academic Misconduct, and state that this piece of work is my own and does not contain any unacknowledged work from any other sources.

Miriayi Aibibula
March 2017

Abbreviations

ATP	Adenosine triphosphate
ADP	Adenosine diphosphate
AMP	Adenosine monophosphate
ANT	Adenine nucleotide translocase
ACD	Acid citrate dextrose
A/R	Antimycin A and rotenone
AMPK	AMP- activated protein kinase
β-ME	β-mercaptoethanol
BAPTA-AM	1,2-Bis(2-aminophenoxy)ethane-N,N,N,N-tetraacetic acid tetrakis
BPTES	Bis-2-(5-phenylacetamido-1,3,4-thiadiazol-2-yl)ethyl sulfide
CS	Canalicular system
cAMP	cyclic AMP
cGMP	cyclic GMP
CD	Cluster of differentiation
CD40L	CD40 ligand
CVD	Cardiovascular diseases
COX-1	Cyclooxygenase-1
CoA	Co-enzyme A
CPTI	Carnitine O-palmitoyltransferase
CPT1A	Carnitine palmitoyltransferase 1A
CPTII	Carnitine O-palmitoyltransferase II
CACT	Carnitine acylcarnitine translocase
DAG	1,2- diacylglycerol
DABA	Dl-2-4-diaminobutyric acid
ESAM	Endothelial cell-selective adhesion molecule
ETC	Electron transport chain
EDTA	Ethylenediaminetetraacetic acid
ECAR	Extracellular acidification rate

eNOS	Endothelial nitric oxide synthase
$FADH_2$	Flavin adenine dinucleotide
FCCP	Carbonyl cyanide-4 phenylhydrazone
GLUT3	Glucose transporter 3
GPVI	Glycoprotein VI
GP	Glycoprotein
GLUTs	Glucose transporter proteins
G6P	Glucose 6-phosphate
GLS	Glutaminase
GTP	Guanosine-5'-triphosphate
G6PD	Glucose-6-phosphate dehydrogenase
HK	Hexokinase
HPLC	High performance liquid chromatography
HIF	Hypoxia inducible factor
HFD	High fat diet
ITAM	Immunoreceptor tyrosine-based activation motifs
IP_3	Inositol 1, 4, 5 triphosphate
ITIM	Immunoreceptor tyrosine-based inhibition motif
IL-1β	Interleukin 1β
ICAM-1	Intracellular adhesion molecule1
ITP	Idiopathic thrombocytopenic purpura
iNOS	Inducible nitric oxide synthase
JAMA	Junctional adhesion molecule A
LED	Light-emitting diode
MK	Megakaryocytes
MIM	Mitochondrial inner membrane
MCP	Monocyte chemoattractin
MMP	Matrix metalloproteinase
MPC	Mitochondrial pyruvate carrier
NO	Nitric oxide
NOS	Nitric oxide synthase
nNOS	Neuronal nitric oxide synthase
NADPH	Nicotinamide adenine dinucleotide phosphate

NADH	Nicotinamide adenine dinucleotide
OXPHOS	Oxidative phosphorylation
OMM	Outermitochondrial membrane
OCR	Oxygen consumption rate
OD	Optical density
OPA	Ortho-phthalaldehyde
PI3K	Phosphoinositol 3-kinase
PGI_2	Prostacyclin
PKG	Protein kinase G
PKA	Protein kinase A
PLC γ2	Phospholipase Cγ2
PKC	Protein kinase C
PARs	Protease-activated receptors
PLA_2	Phospholipase A_2
PF4	Platelet factor 4
PFK	Phosphofructokinase
PK	Pyruvate kinase
PDH	Pyruvate dehydrogenase
Pi	Inorganic phosphate
PRP	Platelet-rich-plasma
PGE_1	Prostaglandin
PPP	Pentose phosphate pathway
RNA	Ribonucleic acid
RANTES	Regulated on activation, normal T cell expressed and secreted
ROS	Reactive oxygen species
2-DG	2-Deoxy glucose
TEM	Transmission electron microscopy
TCA	Tricarboxylic acid
TxA_2	Thromboxane A_2
UCPs	Uncoupling proteins
vWF	Von-Willebrand factor

"Knowledge is a type of wealth that cannot turn to poverty

and cannot fall pray to theft or fraud"

(Yusuf Khass Hajib (1018-1069) line 313 from *kutadgu Bilig*)

بىلىم بايلىق ئول گادايلاشمايدىغان

قاراقچى ۋە ئوغرى ئالالمايدىغان

يۈسۈف خاس هاجىپ(1018-106) قۇتادغۇبىلىك ،313- بىيت

1. General Introduction

1.1 Overview

Haemostasis is a dynamic and indispensable system for maintaining the integrity of the circulatory system, by preventing excessive bleeding at the sites of vascular injury. There are three central elements that contribute to this process. First, the injured vascular wall exposes pro-thrombotic proteins in the extracellular matrix when damaged, such as collagen, to capture and activate blood platelets. Secondly, blood platelets adhere, spread and aggregate on the damaged endothelium to form a platelet plug. Finally, the coagulation cascade is activated, with the formation of a fibrin mesh to stabilise the thrombi (Gale et al., 2011). However, the inappropriate activation of platelets can lead to inflammatory responses that drive atherogenesis and thrombosis (Patzelt et al., 2015; Nording et al., 2015). While there have been great strives in understanding the primary signalling mechanisms that drive platelet activation in health and disease, the metabolic components of platelet biology have been overlooked. Understanding the regulation of platelet energy metabolism at rest and following activation is paramount in the endeavour of designing effective interventions to target diseases of platelet dysfunction in both hyper- and hypo-thrombotic events.

1.2 Platelets

Platelets are one of the smallest anuclear cells. They originate from megakaryocytes (MK) in the bone marrow as a product of thromopoiesis in haematopoiesis. Platelet formation from MK can be divided into two phases. The first phase involves the maturation and development, during which MK accumulate cytoskeletal proteins, platelet specific granules and sufficient membrane to complete platelet assembly. In the second phase, MK go through cytoplasmic remodelling to generate pro and pre platelets, from which discoid platelets are generated by subsequent fission events (Machlus and Italiano, 2013). In their quiescent state, platelets are discoid with a diameter of approximately 2 to 3μm and a thickness of 0.5μm, giving a mean cell volume of 6 to 10 femtoliters. Around 1×10^{11} platelets are formed daily and once released, platelets persist in the blood stream of human for 7-10 days (Machlus and Italiano, 2013). Old platelets are destroyed in the spleen and liver by phagocytosis, maintaining the normal range of $150\text{-}350\times10^{9}$ platelets/L in a healthy individual (Broos et al., 2012).

1.2.1 Platelet morphology

Although anucleate, platelets have a complex structure (Figure 1-1). Morphologically, platelets are divided into three distinct zones, peripheral, cytoskeleton and organelle zones (Smyth et al., 2010). The '*Peripheral zone'* consists of the plasma membrane that is invaginated with an open canalicular system (Figure 1-1B, CS), which links platelet organelles to the external factors. The plasma membrane is embedded in a bilayer of phospholipids that are rich in cholesterol, glycolipids and glycoproteins. The lipid-rich plasma membrane contains a multitude of protein receptors, transporters and channels required for platelets to tailor their physiological responses to external environment. These include proteins that are important for haemostatic, immune and metabolic functions, such as cluster of differentiation (CD) 36, CD9, CD63, $\alpha_{IIb}\beta_3$, and glucose transporter (GLUT) 3. The plasma membrane is responsible for maintaining ionic balance in platelets. In particular, the concentration of the calcium store in platelets is facilitated by the activity of sodium and calcium adenosine triphosphate pumps on the plasma

membrane. Finally, membrane phospholipids provide arachidonic acid as substrate for the formation of thromboxane A_2 (TxA_2), an important secondary mediator of platelet activation (Ghoshal and Bhattacharyya, 2014).

The *'Cytoskeletal zone'* is composed of basic elements for platelet cytoskeletal support for contraction, including microtubule coil and actin cytoskeleton, which are continuous with the sub-membrane area of the peripheral zone. Functionally, the cytoskeleton maintains the integrity and discoid shape of platelets even in the presence of high shear stress in circulation under quiescent state. However, dynamic cytoskeletal rearrangement facilitates platelet shape change, spreading and adhesion when activated. This is achieved by a close interaction of actin-microtubule filament network with platelet transmembrane proteins such as glycol protein (GP) GPIb-IX, $\alpha_{IIb}\beta_3$, and $\alpha_2\beta_1$ (Symth et al., 2010).

The '*Organelle zone'* contains α granules, dense granules, peroxisomes (lipid metabolism), lysosomes (acid hydrolase), mitochondria and glycosomes (glycogen) that are distributed throughout the cytoplasm. As such, functionally, this zone serves as a storage site for enzymes, adenine nucleotides, serotonin, calcium, coagulation factors, chemokines as well as a wide variety of proteins. Secondly, it is involved in metabolic processes of platelet activation (White, 1979).

A

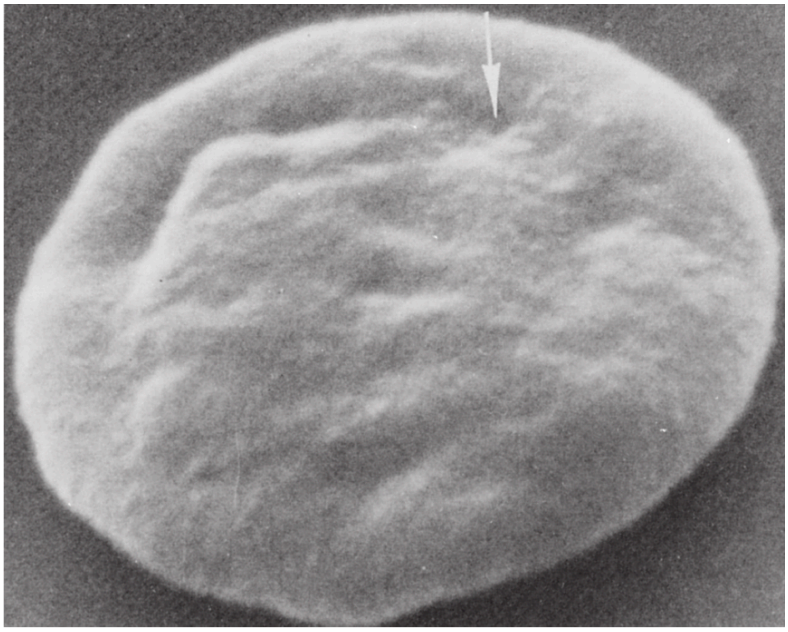

B

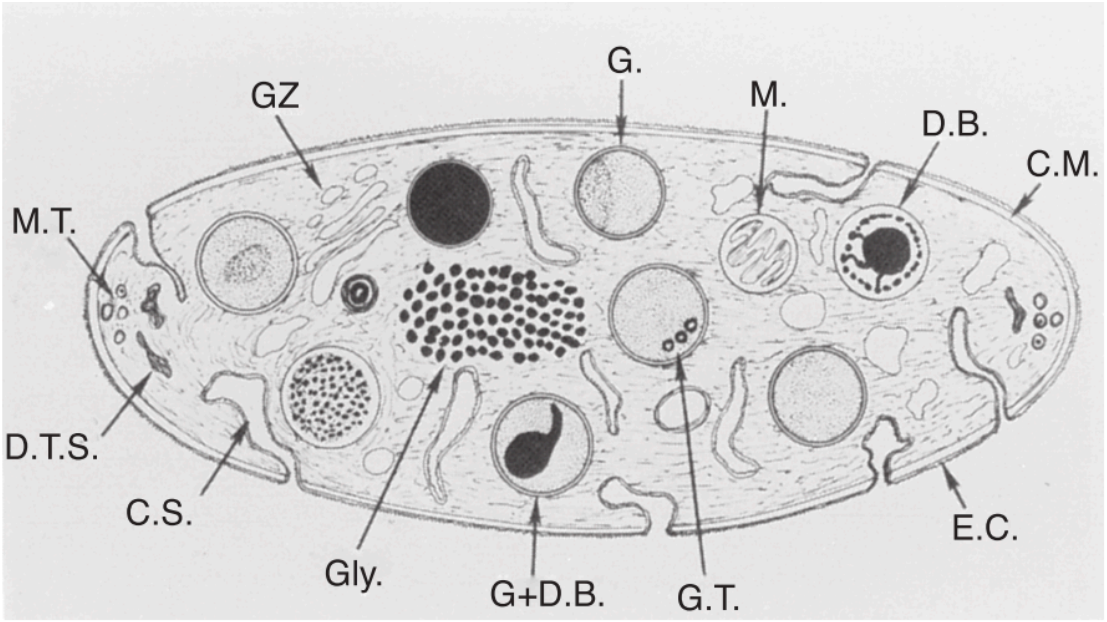

Figure 1-1: Platelet Structure. (A) Electron microscopy image of discoid platelets, magnification *13,200. White arrow shows the open canalicular system. (B) Ultrastructure of cross-sectioned discoid platelets. EC: exterior coat; C.M. tri-laminar membrane (lipid-bilayers); D.B. dense granules; M. mitochondria; G: a granules; GZ: Golgi zone; M.T. circumferential band of microtubules; D.T.S: dense tubular system; C.S. surface connected open canalicular system; Gly: glycogen granules; (Image taken from Symth et al., (2010), platelet morphology, biochemistry and function).

1.2.2 Platelets in primary haemostasis

The endothelium serves as a protective surface under normal physiological conditions. Platelets circulate in the vascular system and monitor for areas of damage on the endothelium. The presence of larger cells in the blood flow and rheological forces push platelets near to the vessel wall due to their small size. Consequently, platelets are positioned in close proximity of the vessel wall, where they carry out their function (Bye et al., 2016). Under normal conditions, the healthy, undamaged endothelium generates platelet inhibitory molecules (Figure 1-2), such as nitric oxide (NO) and prostacyclin (PGI_2). These molecules increase the intracellular cyclic GMP (cGMP) and cyclic AMP (cAMP) in platelets. cAMP and cGMP activate a series of signalling events through protein kinase G (PKG) and protein kinase A (PKA), which inhibit platelet activation and maintain platelets in a quiescent state in the circulation. Other inhibitory mechanisms co-exist, including CD39 and junctional adhesion molecule A (JAMA). CD39 hydrolyses adenosine triphosphate (ATP) and adenosine diphosphate (ADP), important secondary mediators of platelet activation, released by red blood cells. JAMA inactivates $\alpha_{IIb}\beta_3$ integrin complex on platelet surface (Rivera et al., 2009; Bye et al., 2016). However, the healthy endothelium is damaged during a vascular injury and the endogenous inhibitory mechanisms are overcome (Figure 1-2), to initiate platelet activation to minimise blood loss. This process involves a series of coordinated events including platelet adhesion, activation, amplification as well as a self-regulatory mechanism. The initial stages, platelet adhesion and activation are also termed as primary aggregation while the amplification stages are referred as secondary aggregation (Born and Cross, 1963)

Platelet adhesion begins with the exposure of platelets to the extracellular matrix proteins, such as collagen, von-Willebrand factor (vWF), laminin, fibronectin and thrombospondin (Rivera et al., 2009; Broos et al., 2011& 2012; Clemetson, 2012). The interaction of platelets with these extracellular matrix proteins is influenced largely by the rheological conditions. Platelets primarily interact with collagen, fibronectin and laminin under low shear stress, such as in veins and large arteries. However, in the presence of high shear stress, such as in microvasculature, platelets adhere to collagen on the damaged surface of endothelium via glycoprotein (GP) IB-

V-XI, facilitated by vWF (Bye et al., 2016). Collagen binds to platelet surface receptors, GPVI and $\alpha_2\beta_1$, which enable stable platelet adhesion, activation and signalling. GPVI is functionally linked to the FcRγ-chain containing immunoreceptor tyrosine-based activation motifs (ITAM), which transduces activatory signalling response to the interior of the cell.

Platelet activation (Figure 1-2). GPVI dimerization induces the Src tyrosine phosphorylation of ITAM, leading to the recruitment of tyrosine kinase Syk, which in turn activates phospholipase Cγ2 (PLCγ2). PLCγ2 facilitates the production of inositol 1, 4, 5 triphosphate (IP_3) and 1,2- diacylglycerol (DAG), which induce an efflux of calcium from dense tubular system increasing cytoplasmic calcium concentration (Broos et al., 2012). Calcium, together with the hydrophobic DAG, activates the serine/threonine protein kinase C (PKC), which plays an important role in the secretion of secondary mediators and activation of integrin $\alpha_{IIb}\beta_3$ (Bye et al., 2016). Calcium signalling plus the activation of integrins result in the acceleration of platelet activation. Highly activated platelets enable the assembly of the prothrombinase complex, leading to the production and release of thrombin. Thrombin converts the soluble fibrinogen into insoluble fibrin, consolidating the haemostatic plug. Moreover, thrombin can also act as a potent platelet activator, by cleaving and activating protease-activated receptors (PARs) PAR1 and PAR4 on human platelets. Activation of PARs triggers a variety of cell signalling processes through Gα proteins, Gq, G_{12}/G_{13} and perhaps Gi, of which downstream signalling result in shape change, secretion and integrin activation responses. These are mediated by Rho-dependent cytoskeletal response, as well as calcium mobilisation and PKC activation mediated through the activation of phospholipase Cβ.

Amplification In order to ensure the formation of a thrombus, platelets generate secondary mediator thromboxane A_2 (TxA_2) and release platelet granule contents, such as ADP (Figure 1-2). These platelet-derived soluble mediators act to amplify initial platelet activation. TxA_2 is generated in response to rising calcium levels and the PLA_2. PLA_2 cleaves fatty acids from phospholipids to generate arachidonic acid, which serves as a substrate for cyclooxygenase to generate TxA_2. TxA_2 acts on its G-protein coupled receptor on platelet surface, activating additional platelets via the phosphorylation of Rho/Rho-kinase and myosin-light chain. ADP instead is released

from dense granules, which also acts on its G-protein coupled receptors on platelet surface. The downstream signalling of ADP inhibits cAMP generation and stimulates PI3K, thus enhancing platelet activation. After the adhesion and activation, the binding of integrin $\alpha_{IIb}\beta_3$ to fibrinogen crosslink different platelets and result in platelet aggregation, thrombus growth and stabilisation (Rivera et al., 2009).

Self-regulation is essential to avoid excessive thrombus formation leading to blood vessel occlusion. This is achieved by several negative feedback signalling mechanisms, including immunoreceptor tyrosine-based inhibition motif (ITIM) containing receptors and endothelial cell-selective adhesion molecule (ESAM). They are responsible for negatively regulating integrin activities, receptor desensitisation for secondary mediators, and activating phosphatases that counteract phosphorylation-dependent positive signalling (Bye et al., 2016).

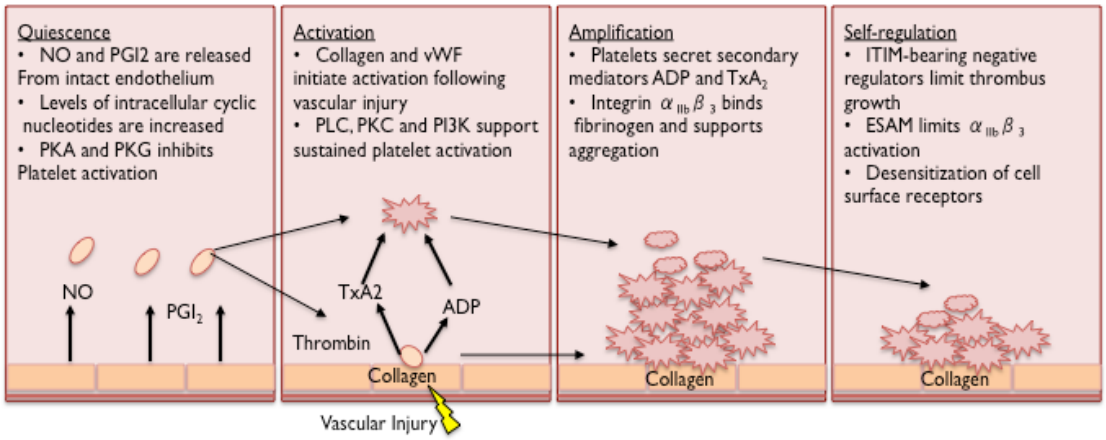

Figure 1-2: Simplified schematic of platelets in primary haemostasis. The healthy endothelium generates NO and PGI_2, which increase intracellular cyclic nucleotides that initiate inhibitory signals in platelets via PKA and PKG. When the vascular endothelium is damaged, the pro-thrombotic sub-endothelium exposes matrix proteins, such as collagen and vWF, which attract platelets via platelet surface specific ligands and initiate platelet adhesion and activation. The ligand occupancy by collagen and vWF on platelet surface initiate a series of signalling events, leading to the generation of TxA_2 and release reaction of ADP, which in turn amplificate platelet activation process and recruits more platelets. The binding of integrin $\alpha_{IIb}\beta_3$ to fibrinogen supports further platelet-platelet aggregation. There are several self-regulating mechanisms to prevent undesired thrombus growth. (Modified from Bye et al., 2016).

1.3 Cardiovascular disease and atherothrombosis

Cardiovascular diseases (CVD) are a group of disorders that affect the heart and blood vessels, and share similar pathology and risk factors. CVD accounted for 17.5 million deaths worldwide in 2012 (World Health Organization, 2016) making it the largest non-communicable cause of mortality. Among these, death due to atherothrombotic vascular diseases, such as myocardial infarction and stroke, account for nearly 80%.

1.3.1 Platelets in the development of atherothrombosis

Haemostasis is the first line of defence against uncontrolled bleeding in the human body and the beneficial role of platelets in forming primary haemostatic plug is clear. However, a growing body of evidence supports the notion that platelets have a pathophysiological role in the development of various diseases, such as atherothrombosis (Jennings, 2009), arthritis, diabetes (Haouari and Rosado, 2008), tumour biology (tumour killing), inflammation, multiple sclerosis (Mathur et al., 2014; Wachowicz et al., 2016), endometriosis (Du et al., 2017), liver and renal diseases (Ghoshal and Bhattacharyya, 2014). This pathological role of platelets is in part credited to its ability to interact with different cell types in circulation, including endothelial cells, neutrophils, monocytes, dendritic cell, leukocytes and various tumour cells (Kaplan and Jackson, 2011). Among these cells, the interaction of platelets with endothelial cells and leukocytes were shown to be critical during both atherogenesis and acute thrombosis coupled to plaque rupture of atherosclerotic lesion (Figure 1-3) via promoting the deposition of pro-inflammatory mediators at the vascular wall (Patzelt et al., 2015; Nording et al., 2015).

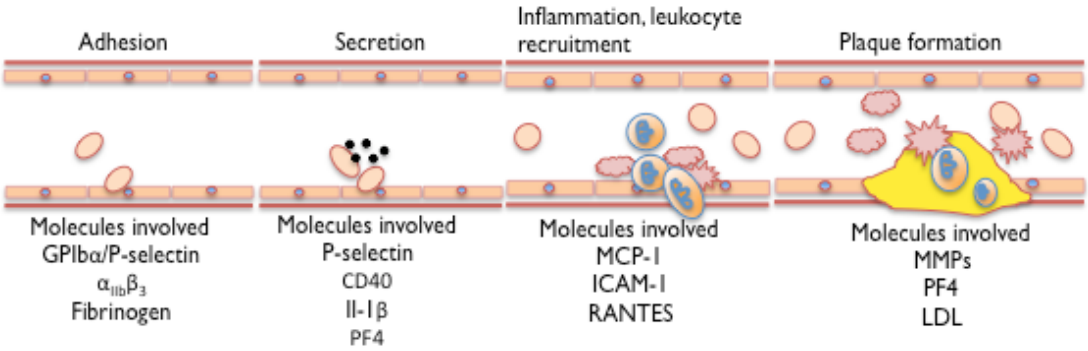

Figure 1-3: Simplified schematic of platelet-triggered atherogenesis. The endothelial adhesion molecules induced by inflammatory responses, such as P-selectin, support platelet endothelial interaction. This induces the counter receptors for P-selectin on platelet surface including glycoprotein Ibα, initiating platelet adhesion. This is further stabilised by the interaction of fibrinogen and integrin $\alpha_{IIb}\beta_3$ or the ICAM-1 on endothelial cells. Adherent platelets secret numerous inflammatory compounds, such as CD40L, IL-1β, PF4, which alter the adhesive properties of endothelial cells and lead to the surface expression of monocyte chemoattractin 1 (MCP-1), regulated on activation, normal T cell expressed and secreted (RANTES). This further supports the recruitment of leukocytes and monocytes, which migrates into intima along with accumulated modified lipoproteins, leading to the development of atherogenic plaque. MMP: matrix metalloproteinase. (Image modified from Langer et al., 2013).

Briefly, increased systemic inflammation in the circulation, such as the accumulation of modified oxidised lipoproteins and increased reactive oxygen species, results in the activation of endothelial cell monolayer. Activated endothelial cells attract platelets even in the absence of thrombogenic sub-endothelial matrix through the interaction with platelet surface glycoproteins and integrin, such as P-selectin (Anfossi and Trovati, 2009), initiating platelet adhesion (Figure 1-3). Adhered platelets then release pro-inflammatory compounds, such as CD40 ligand (CD40L), interleukin 1β (IL-1β), and platelet factor 4 (PF4), as well as promoting the expression of inflammatory adhesive receptors like intracellular adhesion molecule1 (ICAM-1) on endothelial cells. This enables platelets to recruit circulating leukocytes, monocytes and inflame them by receptor interaction, leading to the migration into the intima and formation of foam cells. This plaque is then enriched with various immune cells as well as oxidised lipids, exposure of which to the lumen activates more platelets, initiating the coagulation cascade with fibrin generation, eventually leading to the undesired atherosclerotic thrombus formation (Kaplan and Jackson, 2011).

1.3.2 Risk factors of atherothrombosis and alteration of platelet biochemistry

The pathology that underlies the development of atherothrombosis is multifactorial. Its origins may be traced to early childhood and can progress asymptomatically through adult life. Manifestation as a pathological event depends largely on the life style choices of an individual. An unhealthy diet, physical inactivity and smoking are the most important behavioural risk factors of CVD, which manifest as impaired glucose tolerance or diabetes, atherogenic dyslipidaemia, hypertension, endothelial dysfunction (Tziomalos et al., 2010) and visceral obesity (Durina and Remkova, 2007). These risk factors are often described as metabolic syndrome (MS), a disorder of energy utilization and storage by human body (Ren et al., 2010; Santilli et al., 2012; Rooy and Pretorius, 2015) (Figure 1-4).

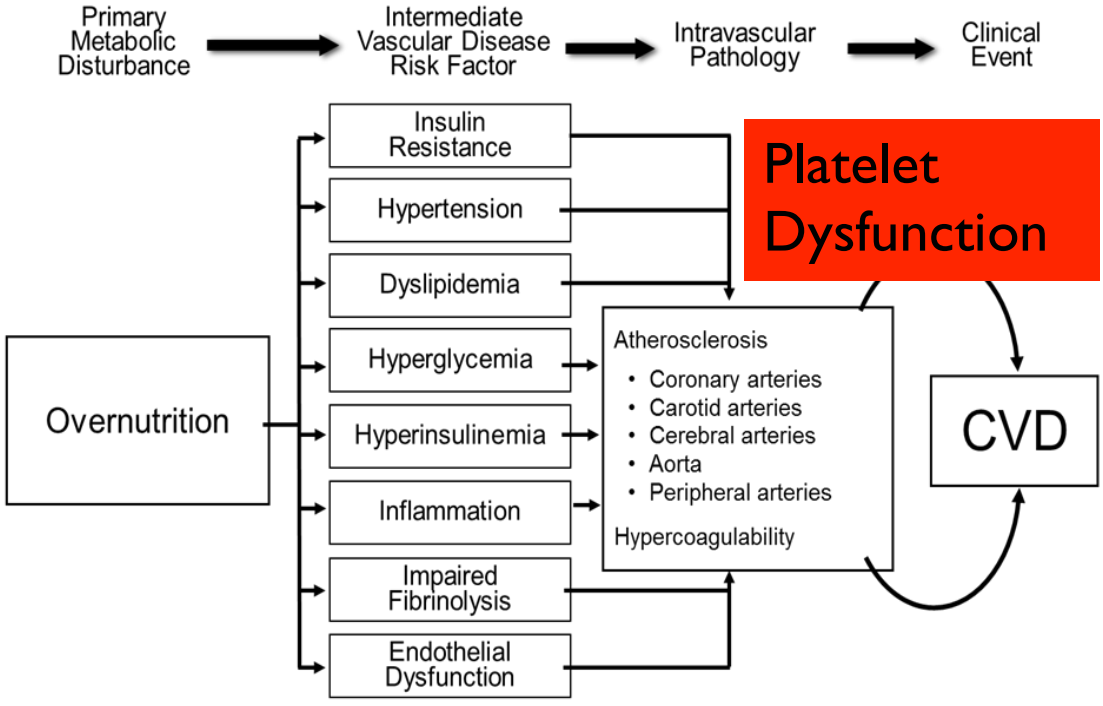

Figure 1-4: Proposed role of platelets in CVD. The role of platelets in the potential road map from primary metabolic disturbance to the development of a clinical CVD event. As circulatory cells, platelets are exposed to all risk factors of CVD, which have been shown to alter platelet morphology, biochemistry and function, exacerbating the development of clinical manifestation of atherosclerotic cardiovascular diseases.

MS is often associated with chronic systemic inflammation and oxidative stress, which creates a pro-thrombotic environment (Davi and Santilli, 2007; Durina and Remkova, 2007; Kapoor, 2008; Palomo et al., 2010; Russo, 2012) (Figure 1-3) for the development of atherosclerotic disease (Anfossi et al., 2009; Santilli et al., 2012; Suslova et al., 2015). However, morphophysiological and chemical changes (Table 1-1) in platelets have been reported in obesity/hyperlipidaemia (Anfossi et al., 2009; Santilli et al., 2012), insulin resistance and type 2 diabetes (Keaney et al., 1999; Sobol and Watala, 2000; Watala, 2005; Michno et al., 2007; Haouari and Rosado, 2008; Natarajan et al., 2008; Kakouros et al., 2011; Avila et al., 2012; Santilli et al., 2015).

Table 1-1: Platelet morphophysiological and chemical changes with MS

Morphophysiological Changes	Chemical Changes
Membrane fluidity Increased Mean Volume Increased platelet count Increased P-selectin expression Increased *in vivo* spontaneous aggregation Enhanced platelet turn over Enhanced expression of adhesive receptors	Increased intracellular calcium Increased TxA_2 production Decreased mitochondrial membrane potential Modified mitochondrial stress proteins Increased ROS generation Increased CD40L release Elevated ATP/ADP ratio Insensitivity to NO & PGI_2

Abnormalities in TxA_2 generation are among the earliest characterised effects of diabetes and obesity on platelets (Natarajan et al., 2008). TxA_2 is a potent secondary mediator of platelet activation, which is generated from the platelet membrane phospholipid derived arachidonic acids via cyclooxygenase-1 (COX-1). Aspirin is a common first-line anticoagulant prescribed to people with MS since it inhibits COX-1, thus minimises TxA_2 generation. Although the health benefits and pharmacological mechanism of aspirin are widely accepted, nearly 20% of the aspirin treated patients may experience diminished or nil response to treatment. There is no direct evidence showing the mechanism of increased TxA_2 generation in these conditions and how aspirin is failing to reduce it. It is mostly accredited to the elevated concentration of blood glucose or lipids (Santilli et al., 2015), rather than increased interaction between platelets and endothelial cell, thus intrinsic to platelets. Thomas et al., (2014) used a systems biology approach to create a functionally tested and biochemically validated reaction network of platelet metabolism. In this approach, redirection of glycolytic, fatty acid and nucleotide metabolism reaction fluxes to accommodate increased TxA_2 and reactive oxygen

species (ROS) generation were shown, suggesting a potential metabolic fingerprint of aspirin resistance in platelets. Unfortunately, there is virtually no experimental data on platelet metabolism in disease states and how the metabolic alterations in platelets itself play a role in the progression of atherosclerotic cardiovascular diseases.

1.4 Energy metabolism in eukaryotic cell

Although anucleate, platelets share many of the characteristic of eukaryotic cells as described in 1.2.1. Quiescent platelets utilise energy for maintaining ionic and osmotic homeostasis, as well as to support the polymerization and depolymerization of actin, and turnover of inositol phosphate and proteins. Platelet activation involves integrated biochemical signalling events to drive morphological changes, such as shape change and spreading, as well as the expression of large numbers of proteins and the release of various mediators of coagulation or inflammation. There is increasing evidence showing that transition between quiescent and activated state of platelets requires the apportioning of numerous nutrients into different metabolic pathways for energy generation, and thus there is a growing interest in understanding how metabolic fuels and pathways are regulated to support or direct functional changes (Chacko et al., 2013; Pearce and Pearce, 2013; Ravi et al., 2015).

Metabolic processes in eukaryotic cells provide energy required for cell work in the form of ATP formed principally through glycolysis and oxidative phosphorylation (OXPHOS), both of which are active in platelets (Ravi et al., 2015). In the cytoplasm of eukaryotic cells, glucose and glycogen can be metabolised through glycolysis, producing pyruvate, which can be reduced to lactate by lactate dehydrogenase. Alternatively, pyruvate can be converted to acetyl co-enzyme A (CoA) by pyruvate dehydrogenase (PDH) in the mitochondria and enter tricarboxylic acid (TCA) cycle, converging glycolysis with oxidative phosphorylation (Dashty, 2013).

1.4.1 Glycolysis

Degradation of glucose in cells is termed glycolysis, or glycogenolysis if the source of the glucose is endogenous glycogen (Maughan, 2013), both of which take place in the cytosol. The two major purposes for glycolysis are the generation of ATP and providing carbon skeleton for biosynthesis. Glucose is transported into cells via specialised GLUTs and immediately phosphorylated by an isoform of hexokinase (HK), to form glucose 6-phosphate (G6P) in a reaction requiring ATP. HK is the first rate limiting enzyme as it catalyses an irreversible reaction and can be inhibited by its own product G6P. Glycogen phosphorylase catalyses the breakdown of glycogen polymer into glucose 1-phosphate if glycogen is the starting point, with no requirement for ATP. Glucose 1-phosphate is then rapidly converted to G6P by phosphoglucomutase, which continues along the glycolytic pathway. G6P can be converted back to glycogen if ATP is abundant, or commit to the pentose-phosphate pathway (PPP) for the generation of nicotinamide adenine dinucleotide phosphate (NADPH). NADPH takes part in the regeneration of reduced glutathione against the toxicity of reactive oxygen species and generation of ribose sugar for nucleotide biosynthesis.

The next step in glycolysis is the isomerisation of G6P into fructose 6-phosphate, which is then phosphorylated by phosphofructokinase 1 (PFK) into fructose 1,6-bisphosphate in a reaction requiring ATP. PFK is the second important rate-limiting enzyme that dictates the pace of glycolysis. PFK is allosterically activated by fructose 2,6-bisphosphate, formed by hormone sensitive phosphofructokinase 2 in the abundance of fructose 6-phosphate. PFK is activated by high levels of ADP, AMP and inhibited by ATP as well as citrate (Berg et al., 2002; Dashty, 2013). This first stage of glycolysis requires 2 ATP for glucose or 1 ATP for glycogen degradation instead of producing ATP, and is thus referred to as the preparatory or investment phase.

The second stage of glycolysis, the energy yielding or 'pay off' phase, starts with splitting fructose 1,6-bisphosphate by aldolase into glyceraldehyde 3- phosphate and dihydroxyacetone phosphate. These two three carbon units are interconvertible, thus each of the succeeding steps in glycolysis occur in duplicate, however, further

metabolism only proceeds with glyceraldehyde 3-phosphate. Two glyceraldehyde 3-phosphates are then oxidised by NAD^+ into two 1,3-bisphosphoglycerates. In the next step, two molecules of 1,3-bisphosphoglycerate and ADP are catalysed by phosphoglycerate kinase to form two ATPs and two molecules of 3-phosphoglycerate. Each 3-phosphoglycerate is then converted to the second high-energy intermediate, phosphoenolypyruvate, of which the conversion to pyruvate yields one molecule of ATP, in a reaction catalysed by the third rate limiting enzyme pyruvate kinase (PK). Four ATPs are formed from each molecule of glucose, two compensate for the preparatory phase of glycolysis, leaving the net generation of two molecules of ATP, pyruvate and nicotinamide adenine dinucleotide (NADH). The regeneration of NAD^+ from NADH is a prerequisite for continuing glycolysis in the process of reducing pyruvate to lactate. Alternatively, both pyruvate and NADH that are generated in the process of glycolysis can be transported into mitochondria for further metabolism in TCA cycle, connecting glycolysis and OXPHOS.

1.4.2 TCA cycle

Glycolysis only releases part of the ATP available from glucose. Higher yield of ATP may be generated in the mitochondria from the complete oxidation of glucose-derived pyruvate and fatty acids in the form of acetyl CoA. The series of reactions that oxidise and reduce acetyl CoA, generated from pyruvate and fatty acids, as well as the intermediary substrates from amino acids, are termed the TCA cycle (known also as the citric acid cycle or Krebs cycle). TCA cycle generates high-energy electron carriers for electron transport chain (ETC) to be reduced in OXPHOS.

Acetyl CoA is the common intermediate from the metabolism of glucose and fatty acids that enters the TCA cycle (Berg et al., 2002; Figure 1-5). Glucose-derived pyruvate is transported to the mitochondria via mitochondrial pyruvate carrier (MPC) and decarboxylated by pyruvate dehydrogenase in the presence of CoA. This releases one molecule of carbon dioxide and the two remaining carbons combine with CoA to form acetyl CoA, a general carrier of acyl groups.

Acetyl CoA can also be produced by the β-oxidation of fatty acids. Fatty acids are imported into cells by either passive diffusion, in the case of short and medium

chain fatty acids, or by fatty acid transport proteins for long chain fatty acids. They are then converted to fatty acyl-CoA ester by acyl-CoA synthetase. The fatty acyl-CoA combines with carnitine in a reaction catalysed by carnitine O-palmitoyltransferase I (CPTI) forming fatty acylcarnitine, which is transported across the mitochondrial inner membrane via carnitine acylcarnitine translocase (CACT). Carnitine O-palmitoyltransferase II (CPTII) converts fatty acylcarnitine back to fatty acyl-CoA ester, which goes through a series of dehydrogenation, hydration to yield acetyl-CoA as well as NADH and flavin adenine dinucleotide ($FADH_2$).

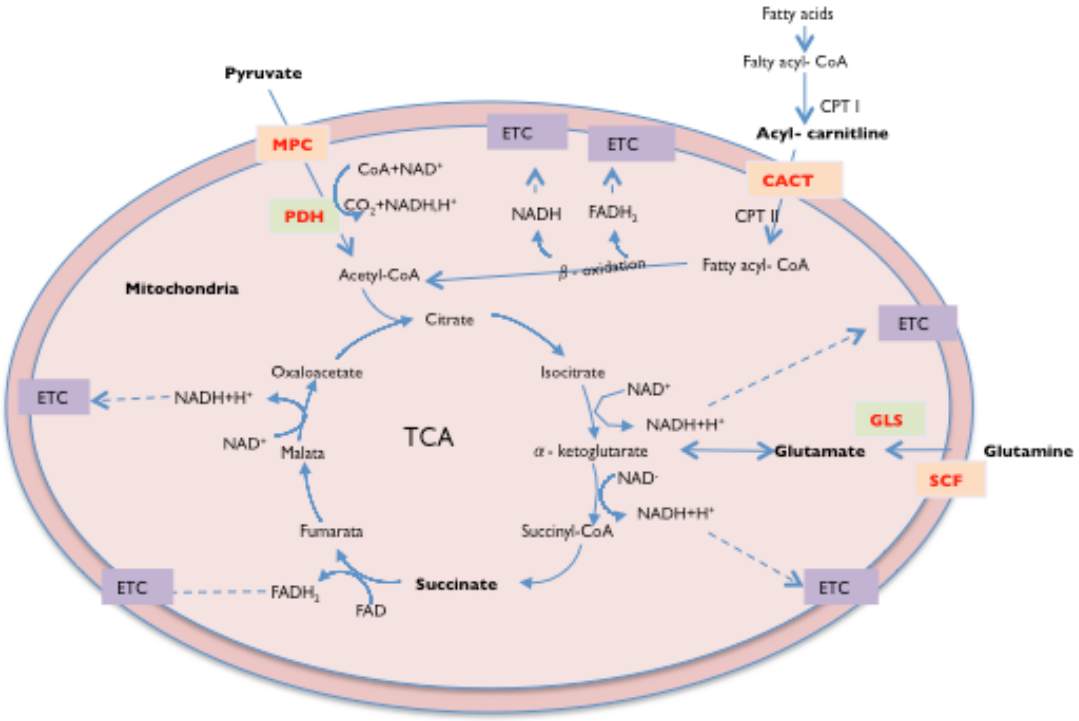

Figure 1-5: Simplified schematic of TCA cycle. Illustration of pyruvate, fatty acids and glutamine entry to TCA cycle. Two-carbon Acetyl-CoA generated from the decarboxylation of pyruvate and β-oxidation of fatty acids condensate with four-carbon oxaloacetate to form six- carbon citrate. After two steps of oxidative decarboxylation of citrate, a four-carbon succinate is produced, from which the oxaloacetate is reproduced. Glutamine is transported into mitochondria and generates glutamate via glutaminase, which provides carbon skeletons to TCA producing a-ketoglutarate. The reduced NADH and $FADH_2$ are utilised by ETC in the process of OXPHOS to generate ATP. MPC: mitochondrial pyruvate carrier; PDH: pyruvate dehydrogenase; CACT: carnitine acylcarnitine translocase; SCF: solute carrier family; GLS: glutaminase

Acetyl-CoA that is generated from pyruvate or fatty acids condenses with the four-carbon molecule oxaloacetate, forming six-carbon citrate. This citrate can be

exported to the cytosol, where it serves as a substrate for fatty acid and cholesterol synthesis in highly proliferating cells. However, citrate proceeds in the TCA cycle in highly oxidative tissues or cells as shown in Figure 1-5 in detail, where it regenerates oxaloacetate with series of decarboxylation, phosphorylation and oxidation processes. Similar to citrate, oxaloacetate can provide the carbon skeleton for the formation of aspartate and other amino acids, contributing to protein synthesis in cell proliferation. In some cells, glutamine may be converted to glutamate and then α-ketoglutarate, which replenishes the TCA cycle intermediates, thus maintaining TCA cycle flux. During the cycle of regenerating oxaloacetate, one guanosine-5'-triphosphate (GTP) is formed from the substrate level phosphorylation of succinyl CoA into succinate. GTP is then catalysed by nucleoside diphosphokinase to synthesise ATP. Overall, two carbon atoms enter TCA cycle in the form of the acetyl unit and two carbon atoms leave as carbon dioxide, as well as generating three NADH and one $FADH_2$ per cycle. Thus, similar to glycolysis, the TCA cycle itself does not generate large amounts of ATP nor does it require oxygen as reactant. It does transfer the electrons from acetyl CoA to NADH and $FADH_2$. NADH and $FADH_2$ need to be re-oxidised to harvest the energy, which occurs principally in oxidative phosphorylation.

1.4.3 Oxidative phosphorylation (OXPHOS)

NADH and $FADH_2$ are high-energy molecules, in which the free energy is not directly available for the cells unless re-oxidised in ETC (Figure 1-6). The majority of the oxygen taken up by mammalian cells is used in mitochondrial respiration, as the final acceptor of electrons released from the re-oxidation of NADH and $FADH_2$ in ETC forming water (Figure 1-6). The ETC is composed of four oxidative phosphorylation complexes (Figure 1-6, I-IV) and ATP synthase, which is also referred as complex V. Apart from complex II, the complexes couple electron transport with pumping protons across the mitochondrial inner membrane. It is generally assumed that complex I and III pump four protons each, while complex IV pumps two with the transport of two electrons (Stock et al., 1999). NADH dehydrogenase (complex I) and succinate dehydrogenase (complex II) transfer electrons to coenzyme Q from NADH and $FADH_2$ respectively, linking the TCA

cycle to the respiratory chain. Coenzyme Q transfers electrons to cytochrome c reductase (complex III), which carries the electrons to cytochrome c oxidase (complex IV) mediated by cytochrome c. Finally, the electrons are accepted by oxygen to form water. As protons are pumped out of the matrix without any associated anions, a charge separation is formed, with the matrix side of the mitochondrial inner membrane being negatively charged. This proton electrochemical gradient, the proton motive force, across the mitochondrial inner membrane is then used to synthesis ATP via complex V with the energetically favourable flow of protons back to the matrix (Cooper, 2000; Lodish et al., 2000; Dudkina et al., 2010).

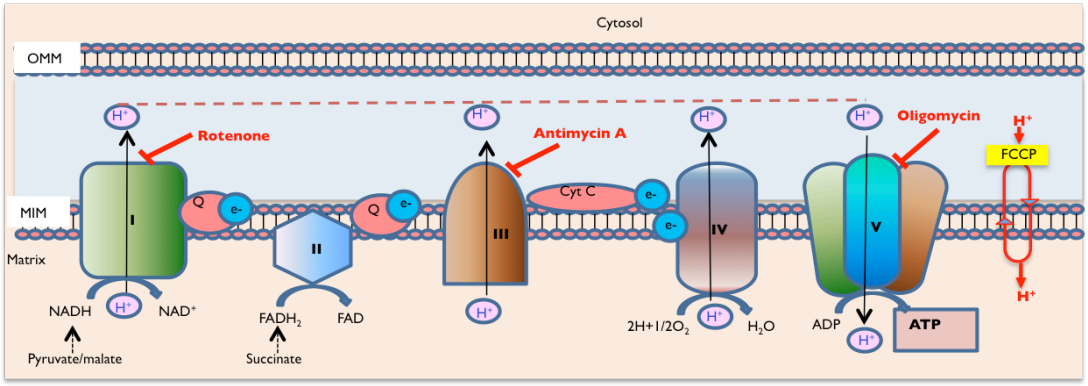

Figure 1-6: Simplified representative schematic of ETC. Electron transport chain consists of 5 enzyme complexes. Complex I: NADH-CoQ reductase or NADH dehydrogenase; Complex II: Succinate-CoQ reductase or succinate dehydrogenase; Complex III: cytochrome bc1 complex; Complex IV: cytochrome C oxidase. Complex V: ATP synthase. Pharmacological inhibitors of complex I, III and V are rotenone, antimycin A and oligomycin, respectively. FCCP is an ionophore, used to uncouple oxidative phosphorylation. MIM: mitochondrial inner membrane; OMM: outermitochondrial membrane

The amount of ATP generated by the re-oxidation of NADH and $FADH_2$ is dictated by the amount of inorganic phosphate (Pi) incorporated into ATP per oxygen atom reduced by ETC, which is also termed as P/O ratio (Kadenbach, 2003; Hinkle, 2005). There are parameters that can disrupt the proton gradient across the membrane, thus decreasing the P/O ratio (Kadenbach et al., 2010). These factors include unspecific proton leak across the mitochondrial inner membrane, uncoupling proteins, proton phosphate carrier, classical uncouplers such as fatty acids and transportation of protons through aspartate/glutamate carrier (Hinkle, 2005). Taking these factors into consideration and the structural analysis of ATP synthase (Stock et al., 1999), it is now proposed that $H^+/O=10$ for NADH and 6 for

$FADH_2$. From these protons, H^+/ATP=3 is used by ATP synthase and H^+/ATP=1 for ATP transport to cytoplasm, thus total four H^+ per ATP synthesized. Thus, the ATP generated by per molecule NADH and $FADH_2$ re-oxidation is 2.5 and 1.5 respectively, using the ration of H^+/ATP=4.

Using above ratio, it is possible to estimate indirectly the amount of ATP formed by the oxidation of glucose. As discussed in section 1.4.1, 2 molecules of ATP, 2 molecules of pyruvate and 2 molecules of NADH are the products of one molecule of glucose metabolised by glycolysis. The transportation of the pyruvate to the mitochondria results in additional 2 molecules of NADH (Figure 1-5) by the PDH reaction. Pyruvate metabolism in the TCA cycle yields an additional 6 NADH and 2 $FADH_2$. During this process, 2 molecules of GTP are also formed. GTP requires a phosphate carrier to be transported from the mitochondrial matrix to the cytosol, which requires the import of one proton per GTP exported, diverting 2 protons from ATP synthesis. Thus the conversion of 2GTP to ATP actually gives 1.5 molecules of ATP. Similarly, the 2 molecules of NADH produced during the process of glycolysis must be transported into the mitochondria by malate/aspartate shuttle, which diverts two protons from ATP synthesis, thus resulting in the net loss of 0.5 ATP. As a result, these 2 molecules of NADH only produce 4.5 molecules of ATP instead of 5 ATP. The remaining 8 molecules of NADH and 2 molecules $FADH_2$ result in 23 molecules of ATP. Thus, oxidation of one molecule glucose produces 31 ATP if the malate/aspartate shuttle is used. However, the NADH from glycolysis can also be transported into mitochondria by glycerol phosphate shuttle, which transforms NADH to $FADH_2$, thus only generating 3 ATP instead of 4.5. In this way, the net production of ATP is only 29.5 per molecule of glucose (Cooper, 2000).

Using similar approaches, it is also possible to calculate the amount of ATP generated by β-oxidation of fatty acids. The β-oxidation of a 16-carbon fatty acid, such as palmitate, generates 7 of each of NADH and $FADH_2$ as well as 8 acetyl CoA molecules. The TCA cycle, generates a further 8 GTP, 8 $FADH_2$ and 24 NADH. Thus 31 NADH equals 77.5 ATP and 15 $FADH_2$ equals 22.5 ATP. 8 GTP require 8 protons for the phosphate carrier, which looses the equivalent of 2 molecules of ATP, generating 6 ATP in total. Activation of acetyl CoA synthetase requires 2 ATP,

thus giving a net production of 104 ATPs per molecule of palmitate. This means that the amount of ATP generated by one molecule of palmitate is almost three times more than one molecule of glucose, reflecting the advantage of lipid as energy storage molecules.

1.4.4 Mitochondrial components of respiration

ATP production in the mitochondria is not completely coupled to substrate oxidation. Protons can leak back to the mitochondrial matrix prior to being used by the ATP synthase. Apart from proton leak, non-mitochondrial enzymes such as NADPH-oxidase comprise the majority of cellular oxygen consumption in cells like macrophages (Brand and Nicholls, 2011). As cellular oxygen consumption is central to mitochondrial function, it is important to understand its individual components.

Using pharmacological inhibitors of different complexes in the ETC (Figure 1-6), it is possible to measure basal, ATP-linked, maximum respiration and proton leak in a single experiment at the whole cell level. From such data, spare respiratory capacity and coupling efficiency can also be derived. However, compared to isolated mitochondria, whole cells are obviously more complicated and the permeability of the cell membrane (Brand and Nicholls, 2011) as well as the respiratory complex threshold for inhibition (Murphy, 2001) may limit the effectiveness of mitochondrial inhibitors. Thus, such experiments require careful titration of the target inhibitors for the cell type under investigation.

Basal respiration is a reflection of a cell's ATP demand, proton leak, and substrate availability. As such, basal respiration can alter to a large extent with the presence or absence of certain substrates. Increase in the ATP demand for various cell work can also increase basal respiration. Although basal proton leak contributes to the basal respiration, any increase in basal respiration does not directly reflect an increase in the proton leak until further measurements are made. Therefore, the remaining components of mitochondrial respiration must be measured to elucidate the changes in basal respiration rate for a given cell.

ATP-linked oxygen consumption can be determined with the addition of oligomycin (Figure 1-6). Oligomycin binds to the ATP synthase and blocks the F_0 subunit, the proton channel, which is necessary for the oxidative phosphorylation of ADP to ATP (Jastroch et al., 2010). In most cells, the inhibition of the ATP synthase causes the production of ATP from glycolysis, thus requiring the cells to have sufficient glycolytic 'capacity' to satisfy the demand for ATP. Caution should be taken as oligomycin itself is a mitochondrial toxin, which can slightly increase proton leak by increasing proton motive force leading to less coupling efficiency. However, the increase in proton leak caused by oligomycin has been shown to be less than 10% (Divakaruni and Brand, 2010) if the concentration of oligomycin is optimised to the minimal concentration that generates the maximal ratio between uncoupled and oligomycin inhibited respiration rate. In other words, reversing its effect in the presence of an uncoupler can validate the effect of the oligomycin (Brand and Nicholls, 2011).

Maximal respiration caused by the addition on an uncoupler means a loss of coupling between the ATP generation (phosphorylation) and the rate of electron transport in ETC (respiration). Weak lipid-soluble acid ionophores, such as FCCP (Figure 1-6), dissolve in MIM and diffuse into matrix compartment, where they dissociate into acid anions and protons (Figure 1-7). The weakly charged acid anions can diffuse through the MIM into intermitochondrial (IM) space where they bind to protons, increasing the permeability of the lipid bilayer by facilitating proton transport across the hydrophobic barrier. This results in high rate of proton transport through membrane, thus uncontrolled maximum respiration (Benz and McLaughlin, 1983; Terada, 1990). Proton ionophores must be titrated carefully (Section 2.6.3) for each cell type and experimental conditions, as too high a concentration can inhibit respiration (Benz and McLaughlin, 1983; Terada, 1990). Carefully titrated FCCP can report the maximum activity of electron transport and substrate oxidation. As such, a drop in the maximal respiration is an indicator of mitochondrial dysfunction.

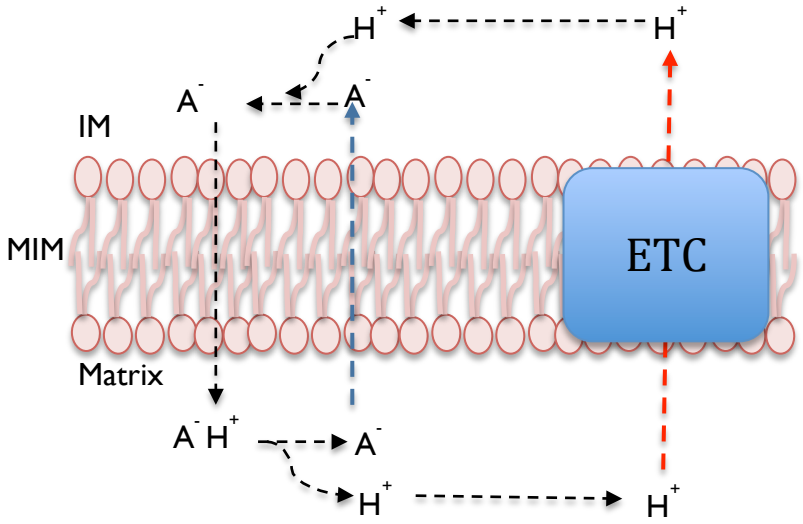

Figure 1-7: Mechanism of uncoupling by FCCP (Image modified from: Benz and McLaughlin, 1983). A^- stands for the weakly charged acid anions of lipid-soluble ionophores, such as FCCP

Non-mitochondrial respiration Rotenone and antimycin A (Figure 1-6) are inhibitors of complex I and III, respectively. A flavin mononucleotide cofactor and several iron-sulfur clusters facilitate electron transport from Complex I to CoQ. Rotenone inhibits the iron-sulfur cluster of Complex I, resulting in the inhibition of electrons from NADH oxidation (Lümmen, 1998). Antimycin A binds to the Qi site of Complex III, which inhibits the electron transport between cytochrome b and c (Ma et al., 2011). To account for the non-mitochondrial respiration, it is necessary to inhibit the ETC completely; this is often achieved by the simultaneous addition of rotenone and antimycin A until a constant rate is achieved for the experimented cell line, which should be subtracted from all other rates (Brand and Nicholls, 2011) to get mitochondrial respiration.

The basal *Proton leak* is defined as the proportion of respiration rate that is insensitive to oligomycin. The total proton leak in cells comprises two processes: 1) basal leak, of which the mechanism of regulation is not fully understood and contributes to 20-30% of the resting metabolic rate depending on cell types and; 2) inducible leak, which can be caused by, for example fatty acids, via the activation of uncoupling proteins (UCPs) and adenine nucleotide translocase (ANT) (Jastroch et al., 2010; Divakaruni and Brand, 2011). Proton leak is not affected by changes in substrate oxidation or ATP demand. A mild increase in proton leak may suggest a change in proton leakiness of the mitochondrial membrane or a change in

mitochondrial membrane potential caused by substrate oxidation. Large increase in proton leak can be used as an indicator of severe mitochondrial damage (Brand and Nicholls, 2011).

Coupling efficiency and spare respiratory capacity are calculated based on the other components of mitochondrial respiration described above. Coupling efficiency is defined as the ratio between the proportions of oxygen used for ATP generation and the basal oxygen consumption after correcting for the non-mitochondrial respiration. Coupling efficiency indicates the productivity of mitochondria in producing ATP or in other words, how well the mitochondrion is coupled to ATP generation. Spare respiratory capacity is the difference between the maximal and basal respiration. It is the ability of the cell to increase the respiration rate above basal in response to a sudden increase in energy demand, thus indicating the bioenergetic limit of a cell can operate. A decreased spare respiratory capacity undermines the cell's ability to respond under conditions where ATP demands are high, which may not be apparent under basal conditions where respiration rate is highly controlled by ATP turn over (Brand and Nicholls, 2011).

1.5 Platelet energy metabolism

Platelet energy metabolism has been the subject of research from early 1960s. However, the current understanding of platelet metabolism, in terms of fuel choice, fuel dependency, regulation and how this is coupled to platelet function is largely unknown compared to other blood cells, such as macrophages (Kelly and O'Neil, 2015) and lymphocytes (Pearce et al., 2013).

1.5.1 Glucose metabolism in platelets

Glucose is the most abundant readily available nutrient for platelets in blood. Glucose uptake in platelets is facilitated by GLUT3, which is the dominant GLUT subtype in human platelets (Craik et al., 1995); platelets express minimal amount of GLUT1. In quiescent platelets, approximately 15% of the GLUT3 is present in the plasma membrane with the remainder located in intracellular α-granule membranes,

which is shown to translocate to plasma membrane upon platelet activation (Sorbara et al., 1997; Heijnen et al., 1997). Little is known about the regulation of GLUT3 in platelets, however, of all the GLUT transporters, GLUT3 has the highest affinity for binding glucose with K_m of 1-2 mM and the highest V_{max} for glucose transport. Thus under normal conditions (5mM glucose), this transporter works near saturation (Heijnen et al., 1997; Sorbara et al., 1997; Ferreira et al., 2005), indirectly implicating the importance of glucose as a substrate for platelet functions.

The reported rates of glucose uptake (10^{11} to 110^{5}µmols/hr/10^{11}platelets) and lactate generation (15^{11} to 320^{12} µmols/hr/10^{11}platelets) under basal conditions (Doery and Cooper, 1970) vary significantly across studies (Table 1-2). Likely explanations for this include technical variations in platelet preparations, such as the use of different anticoagulants, temperature, washing buffers, and suspension mediums, thus making it difficult to make direct comparisons between studies. Table 1-2 summarises studies that have used similar methods for the measurement of glucose and lactate. Despite the variations, these data potentially indicates that platelets can take up glucose under basal conditions and have active glycolysis.

Table 1-2: Comparison of platelet glycolysis from different methods

Publication	Platelet isolation method	Suspension Buffer	Glycolysis
Karpatkin., (1967)	ACD (5°C); differential centrifugation method (Mustard et al., 1989); washed twice with Ringer Solution[1]	Ringer Solution (pH 7.1)	Glucose uptake =21µmols/hr/10^{11}platelets; Lactate production =34.8 µmols/hr/10^{11}platelets in 5mM glucose containing Ringer solution
Doery et al., (1970)	2% EDTA saline (0.42% saline, 6°C); Differential centrifugation; Washed once with ice cold EDTA-Tyrode solution; washed once more in Krebs-Ringer bicarbonate solution, pH 7.4	Krebs-Ringer solution[2] (pH 7.4)	Glucose uptake =39.4 µmols/hr/10^{11}platelets; Lactate production = 92 µmols/hr/10^{11}platelets in 5mM glucose containing Krebs-Ringer solution
Akkerman et al., (1977)	Citrate; Tangen et al., (1972) gel filtration method	Calcium free Tyrode's (pH 7.2) solution[3]	Lactate production = 180 µmols/hr/10^{11}platelets

1.Ringer solution: 4mM KCl, 107mM NaCl, 20mM $NaHCO_3$, and 2mM Na_2SO_4 gassed with 5%CO_2-95%O_2 to pH 7.1

2. Modified Krebs-Ringer solution: 0.9% NaCl solution gassed with 5%CO_2-95%O_2 to pH 7.4

3. Calcium free Tyrode's solution: 137mM NaCl, 2.68 mM KCl, 0.42mM NaH_2PO_4, 12mM $NaHCO_3$, 17mM $MgCl_2$, 2g/L bovine albumin and 1mM KCN.

Early studies used 6-^{14}C-glucose to confirm the metabolic fate of glucose both at rest and activated conditions. Both aerobic glycolysis and OXPHOS were functional for glucose metabolism (Doery and Cooper, 1970). Two studies have shown that thrombin stimulation increases glucose uptake, lactate production as well as oxygen consumption in the presence of physiological (5mM) concentration of glucose (Karpatkin, 1967; Ravi et al., 2015). Thus, while it is generally accepted that platelets have active glycolysis and OXPHOS pathways for glucose metabolism (Karpatkin, 1967; Cohen and Wittels, 1970; Niu et al., 1996; Ravi et al., 2015), the relative importance of each in terms of platelet function remains unknown. Quantitative measurement of platelet function and specific glucose partitioning in glycolysis and OXPHOS under a defined experimental condition has the potential to provide a tool for assessing platelet malfunction in the development of different pathologies.

1.5.2 Glycogen metabolism in platelets

Enzymes for glycogenolysis, glycogenesis and gluconeogenesis were shown to be active in platelets (Scott, 1967; Karpatkin, 1967; Karpatkin et al., 1970), suggesting functionally active glycogen store in platelets. Washed human platelets were shown to have active glycogen phosphorylase and synthetases, of which the latter was inhibited upon platelet activation. Furthermore, human platelets incorporated pyruvate-^{14}C and citrate-^{14}C into platelet glycogen as well as showing fructose-1, 6-bisphosphate as the regulatory substrate for this process, which was activated by AMP, ADP and inhibited by ATP.

Glycogenolysis was shown to be a potential pathway for lactate production in resting platelets (Karpatkin et al., 1970). Platelets incubated in glucose-free medium with CN^- produced lactate at a rate of 0.79±0.23 pmol glycosyl residues/min/10^{11} platelet, which was linear for 40 minutes, indicating that platelets have active glycogenolysis in the absence of glucose and OXPHOS (Akkerman et al., 1978). Prior to this, Karpatkin (1967) had reported that in the absence of glucose, the lactate production lasted 60-90 minutes at a rate of 15.6 μmols/ml/hr. The relationship between endogenous glycogen and exogenous glucose in platelets is unclear. It was suggested that lactate production originated mainly from glycogen

when extracellular glucose was less then 50μM (Akkerman et al., 1978). However, earlier studies have shown that approximately 50% of glycolytic flux originated from glycogen in the presence of physiological concentrations of glucose (Karpatkin, 1967). These data suggests a role for platelet glycogen as a potential energy source, however, its physiological role is largely undiscovered. Also, it is not clear how platelet glycogen metabolism is regulated and whether it has similar metabolic fate with glucose in glycolysis and OXPHOS.

1.5.3 Fatty acid metabolism in platelets

Fatty acid metabolism in platelets was studied mainly by investigating the metabolic fate of ^{14}C-labeled fatty acids in platelet suspensions (Cohen et al., 1970). Most of these studies showed that platelets could synthesise neutral lipids and phospholipids via *de novo* fatty acid biosynthesis (Cohen et al., 1970). The first line of evidence was the measurement of enzyme activity resulting in the incorporation of acetate-1-[14C] into platelet lipids, and the enzyme activity was similar to that of human liver per milligram of soluble protein (Majerus et al., 1969). Apart from the lipid synthesis, exchanges between platelet membrane lipids and plasma lipids were observed. Palmitic acid-1-[14C] added to the plasma was incorporated into platelets, of which nearly 40% was recovered in plasma as free fatty acids, and ceramide (Deykin and Deseer, 1968; Joist et al., 1976). The incorporation pattern at rest and thrombin stimulation was also reported. Washed human platelets incorporated radioactive glycerol mainly into phosphoglycerides, including phosphatidic acid, phosphatidylinositol, phosphatidyl ethanolamine and phosphatidyl serine. Thrombin (1U/ml) activation decreased the incorporation of glycerol into all phopholipids but increased phosphatidyl serine (Lewis and Majerus, 1969). The exact mechanism by which thrombin exerts its effect on lipid synthesis remains unexplained. A separate study has shown that platelets exhibit high affinity esterification of eicosanoid precursor fatty acids, such as arachidonate and 5,8,11,14,17-eicosapentaenoste compared to stearate, oleate and linoleate (Neufeld et al., 1983).

Fatty acid oxidation was also measured using radiolabelled fatty acids. Platelets oxidised U-[14C] palmitate at a rate of 0.19 μmole/hr/10^{11} platelets, which increased in the absence of glucose (Doery and Cooper, 1970). The oxidation rates of different fatty acids can be summarized as linoleic > oleic = stearic > palmitic (Spector et al., 1970) when supplied at a concentration of 70 pM. However, fatty acid utilization is very sensitive to the fatty acid/albumin ratio, and the free concentrations of different fatty acids will differ at the same fatty acid/albumin ratio. Thus the experimental conditions need to be considered when interpreting these data; however, it indicates the metabolic potential of platelets to utilise fatty acids and potential pathways involved.

1.5.4 Amino acid metabolism in platelets

The metabolism of amino acids by platelets has been little investigated, with very few studies available. *De novo* protein synthesis in platelets was reported, indicating that platelets inherit metabolically stable messenger ribonucleic acid (RNA) from MK (Kieffer et al., 1987). Apart from this, protein biosynthesis was measured in normal and splenectomised patients with idiopathic thrombocytopenic purpura (ITP) using radiolabelled amino acids or carbohydrates. Radioactivity in ITP patients was 10 fold higher than control and involved the incorporation of ^{35}S-methionine and ^{3}H-leucine into major membrane glycoproteins. Similarly, the incorporation of D- (U-^{14}C) glucose into four major amino acids was measured in platelets from healthy patients and those with myologenous leukemia. Healthy platelets incorporated most of the labelled glucose into glutamine and asparagine, while patient platelets were not able to synthesize these amino acids, which was interpreted as a defect in platelet TCA cycle in myologenous leukemia (Patel et al., 1976). The activity of phosphate-activated GLS was reported in platelets (Sahai, 1983). However, the fate of glutamine as a potential energy substrate is controversial (Murphy et al., 1992; Vasta et al., 1995).

1.5.5 Oxygen consumption

Mitochondrial oxygen consumption is often used as an indicator of its function in cell bioenergetics, since it can be measured in isolated mitochondria, in intact cells or *in vivo*. Studies using isolated mitochondria from platelets require large amount of blood, which is often not practical during *in vitro* experiments, making the measurement of mitochondrial function in whole platelets an attractive option.

Various methods have been used for oxygen profiling in platelets over time, including the Clark electrode, and Clark electrode based instruments such as the vibrating O_2 cathode, and the oxygraph. While the instruments based on the Clark electrode can measure oxygen consumption in isolated mitochondria, permeablised cells and intact cells, Clark electrode based methods often require large amount of samples, substrates, and inhibitors. The major limitations of Clark electrode based methods are low –time resolution and limited possibility of making additions during the experimental procedure. These limitations are mainly due to measuring cellular respiration in a sealed chamber throughout the experimentation. Clark electrode based systems may also experience oxygen leaking into the instrument due to the system assembly process (Simonnet et al., 2014).

The reported oxygen consumption by platelets varies significantly across studies, again due possibly to differences in the platelet preparation, suspension medium, use of various units and normalisations (Table 1-3) as well as the time resolution and sensitivity of the instruments. In some cases, despite the application of similar methods, different units were used. Using an oxygen cathode, the oxygen consumption rate (OCR) at rest was measured as 14.5 mμmols/10^9 and 18 natoms oxygen/min/10^9, respectively by Hussain and Newcomb (1964) and Muenzer et al., (1975). Without knowing how these units were defined and the experimental context, it is difficult to compare the data. Other differences exist between the studies, such as varying substrates. Thus these data only suggest that platelets have functional mitochondria and that platelet activation is accompanied by increased oxygen consumption (Table 1-3).

Table 1-3: Platelet oxygen consumption with various instruments

Instrument	Basal OCR	Thrombin OCR	Reference
Clark-type Electrode	3nmol/min/10^{16} platelets	Not reported	Protti et al., 2012
Clark Electrode	18±1.6 natoms oxygen/min/10^9 platelets	(1.9U/ml thrombin) 138±14 natoms oxygen/min/10^9 platelets	Muenzer et al., 1975
Vibrating O_2 cathode	14.5±4.8 mμmols/min/10^9 platelets	11 fold increase with thrombin	Hussain and Newcomb, 1963
Oxygraph-2K	11±0.6 pmolO_2/s/10^8 platelets	Not- reported	Sjovall et al., 2013
Seahorse bio-analyser	2-6 pmol/min/μg protein	(0.5U/ml thrombin) 4-9 pmol/min/μg protein	Ravi et al., 2015 Chacko et al., 2013
Seahorse bio-analyser	79±7 pmol/min/μg DNA	Not reported	Fink et al., 2012

1.5.6 Energy requirements of platelet functions

Measuring the relationship between various platelet functions and metabolic responses has always been difficult. This requires a clear discrimination between different processes involved in the initial platelet activation leading to full platelet aggregation (Akkerman and Holmsen, 1981). Platelets tend to stay quiescent in the blood circulation under normal physiological conditions. The anucleate nature of platelets does not require complicated energy demanding anabolic processes. As such platelets have only a relatively low energy demand for homeostatic functions, which are maintaining ionic and osmotic homeostasis, circulating and screening for injury.

However, like many other activatory cells, it has been shown that the activation of platelets is accompanied by an increase for ATP demand (Akkerman and Holmsen, 1981; Holmsen et al., 1982; Verhoeven et al., 1984; Ravi et al., 2015). Platelets can be activated by many different agonists (Huang and Detwiler, 1981), and there have been numerous attempts to measure the energy requirements of platelet activation

processes (Chapter 1.2.2). The poor time resolution of the methodologies used mainly consisted of single point determination of secreted compounds or metabolic end products, and therefore insufficiently characterised the platelet function specific energy requirements. In addition, various units were used in the quantification process. The complete secretion of dense, α and acid hydrolase granules required was reported as 2.5-4.0, 4.2-6.5, and 6.7 μmol of ATP equivalents *(10^{11} platelets) (Akkerman et al., 1983; Holmsen et al., 1982; Vorhoeven et al., 1984 & 1985). The results are expressed as ATP equivalents, defined as the number of moles of ATP produced per mole of substrate converted in the reaction. This is based on the assumption that all the sequences are stoichiometrically coupled to ATP generation and all the metabolic processes are 100% energy efficient (Atkinson, 1977), which are not the case in real biological systems. Although suggesting the variation in the potential energy requirements of these processes, it is difficult to interpret these data without understanding the experimental context. Understanding the energy requirements that various agonists impose on platelets to meet a functional end point might offer potential biomarkers for diagnosing platelet dysfunction. However, there is a clear need for new approaches to simplify measuring platelet function dependent energy demand for the use in both experimental research and clinical environments.

1.6 Aims

This literature review has revealed that the understanding of platelet substrate metabolism and its partitioning in various metabolic pathways under basal and activated conditions have been relatively little studied. Although the roles of glucose, glycogen, amino acids and fatty acids as potential substrates for platelet metabolism are agreed, the metabolic fate of these substrates and their relation to platelet function has yet to be described. The role of platelet mitochondria has received little attention, in terms of their function, fuel choice, dependency and flexibility on different substrates. Apart from this, the effect of metabolic disturbance, such as dyslipidaemia on platelet function has not been investigated.

The aim of this study was therefore to perform a detailed analysis of the fuel choices of human platelets at rest and following activation, to increase our knowledge of the metabolic capacity of platelets. This was achieved through the following objectives:

- Quantifying platelet function-specific glucose metabolism at rest and activation as well as the partitioning between glycolysis and OXPHOS
- Quantifying platelet glycogen and its metabolic fate at rest and following activation of platelets
- Measuring mitochondrial components of respiration, fuel choice and flexibility as well as the impact of a high-fat diet on platelet mitochondria

2. General Materials and Methods

2.1 Source of Reagents and Equipment

A detailed list of all the reagents used throughout this study and their suppliers are given in Appendix 1. Buffer compositions and equipment used are provided in Appendix 2.

2.2 Isolation of Human Blood Platelets

Platelets were isolated from healthy human donors to investigate the intrinsic metabolic pathways in platelets independent of factors present in vivo.

2.2.1 Volunteers and Blood Withdrawal

The Ethics Committee at Hull York Medical School (University of Hull) granted approval for this study. Blood was obtained from healthy human volunteers ranging from 21-60 years old, who had given their informed consent. It had been confirmed that the volunteers were not taking medication that might interfere with platelet function in the 14 days prior to each donation. The volunteers were asked to sit in an armchair while a rubber band was applied to the upper arm, above the elbow, tight enough to occlude superficial venous blood flow but not to prevent arterial blood flow (Figure 2-1). Blood was drawn from cubital vein into 20 ml syringes containing ACD, 1:5 ratio (Appendix 2) as anticoagulant (Cazenave et al., 2004), and mixed gently before being moved to a 50 ml Falcon tube for centrifugation.

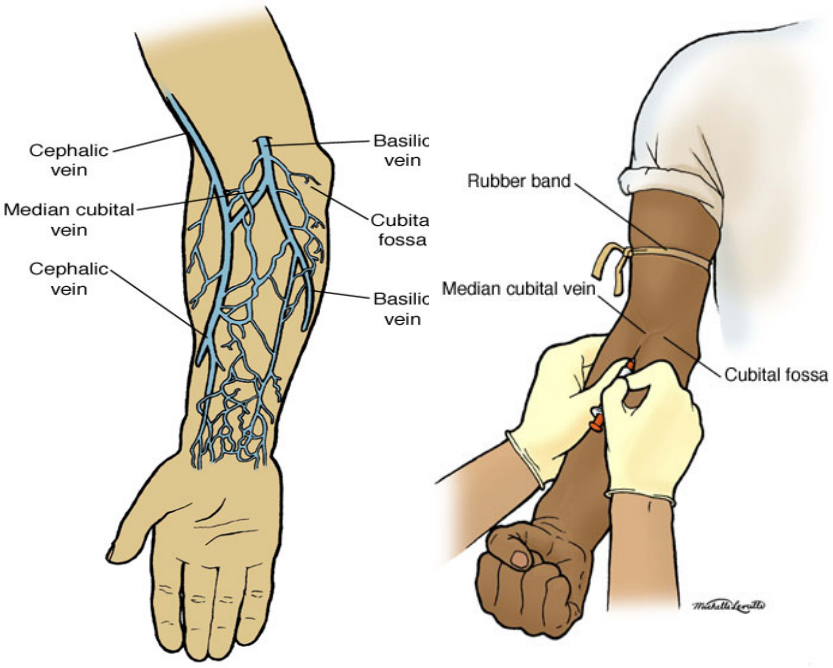

Figure 2-1: A simplified schematic of the blood withdrawal process. The median cubital vein as first choice, cephalic vein second, and basilica vein was the third choice palpated and located at the cubital fossa before being sanitised with alcohol wipes and dried. Blood was drawn using a 21g needle. The first 2 ml of blood was discarded to minimise the presence of artificially activated platelets during the sampling process. Blood was collected into 20 ml syringes containing acid citrate dextrose (ACD), 1:5 ratio as anticoagulant (Image From: Anatomy Atlases™ (Michael P. D'Alessandro, M.D. and Ronald A. Bergman, Ph.D; URL: http://www.anatomyatlases.org/)

2.2.2 Isolation of platelets from whole blood

The well-established differential centrifugation method (Magwenzi et al., 2015) adapted from Mustard et al., (1989) was used for platelet isolation. PRP was obtained by centrifugation of whole blood at 200 × *g* at room temperature for 15 minutes. The centrifugation separated the blood into three layers (Figure 2-2), comprising of red blood cells in the bottom layer, buffy coat (leukocytes) in the thin middle layer and PRP in the top layer. The top layer of PRP was aspirated carefully using a Pasteur pipette into a clean 15 ml Falcon tube without disturbing the bottom two layers. Isolation of platelets from PRP requires high-speed centrifugation, which can lead to undesired platelet activation. However, inhibitors can be added to minimise platelet activation. Those commonly used include prostaglandin (PGE_1) and citric acid. PGE_1 elevates intracellular cAMP levels and in this manner inhibits

platelet aggregation. Numerous studies have shown that the addition of PGE_1 to PRP, before the centrifugation step, improves the separation, re-suspension of the platelet pellet and minimizes the activation as well as minimizing spontaneous aggregation (Menitove et al., 1986 &1988; Bode and Norris, 1992; Hawker et al., 1996). Citric acid, an alternative to PGE_1, lowers the pH of PRP to 6.5, at which platelets are shown to be non-aggregative (Flatow and Freireich, 1966).

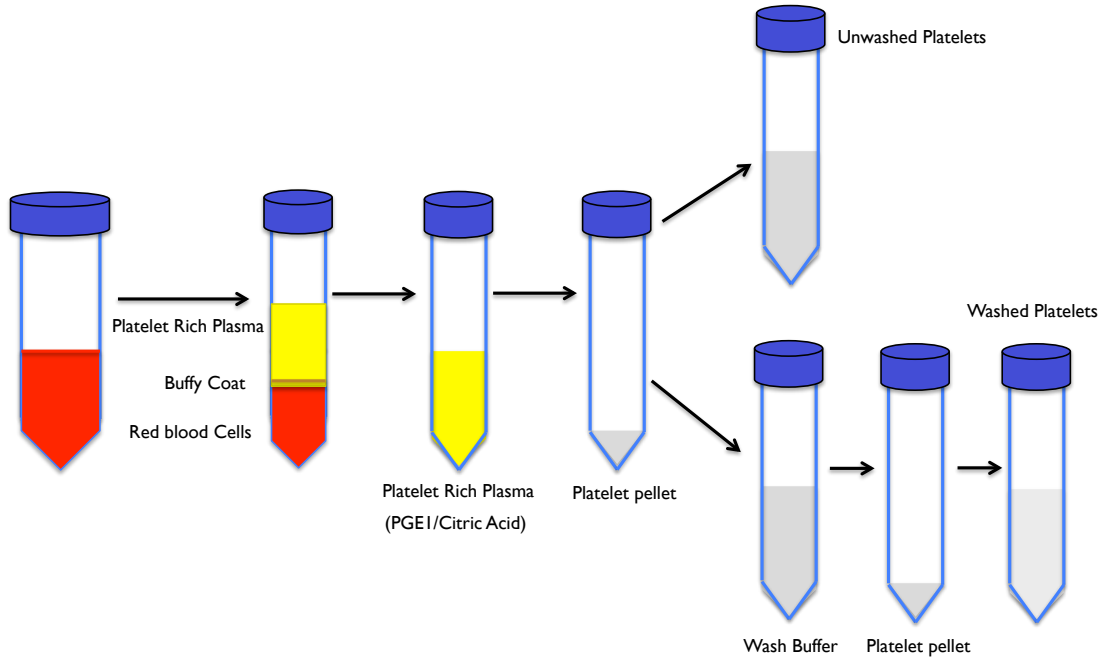

Figure 2-2: Schematic diagram of the platelet isolation process. Platelets that were washed with wash buffer (Appendix 2) were defined as 'washed platelets'.

PRP was treated with either PGE_1 (50ng/ml) or citric acid (300mM, at a ratio of 1:50, v/v) to prevent activation in subsequent aggregation step, and then centrifuged at 800× *g* for 12 minutes. This resulted in the separation of platelet poor plasma (PPP) and a platelet pellet at the bottom of the Falcon tube, which was re-suspended in modified Tyrode's buffer (Appendix 2) to yield un-washed platelets. Modified Tyrode's buffer was chosen as being close to physiological. In some experiments, the platelet pellet was re-suspended in wash-buffer (Appendix 2) and centrifuged once more at 800 × *g* for 12 minutes to provide washed platelets, which were re-suspended in modified Tyrode's buffer to ensure that the final platelet suspension was free of plasma protein. Washed platelets prepared in wash buffer

were shown to be relatively pure and plasma protein-free as well as being functionally responsive to weak agonists, such as low concentrations of ADP (Patscheke et al., 1981). Platelets prepared by the PGE_1 method needed to be kept in suspension medium at 37 °C for at least 40-50 minutes before experimentation to allow the cAMP levels to return to normal. However, the platelets prepared by the pH method could be used immediately after re-suspension.

2.2.3 Platelet counting

Platelets were counted using a Beckman Coulter Z1 Particle Counter (Figure 2- 3). It counts the cells by inserting an aperture tube with electrodes into particle containing low –concentration electrolyte. There are two electrodes, of which one is inside and one is outside the aperture, with a current path provided by electrolyte when the electric field is applied. The aperture creates a 'sensing zone', through which the particles pass creating a voltage pulse. This voltage pulse is used to derive the cell number in the suspension. 5μl platelets were suspended in 10mls of Beckman Coulter Isotone II diluent in a Beckman Coulter Accuvette, which was placed within the Beckman Coulter Z1 particle Counter. The platelets are counted and the value is displayed as platelet number per millilitre.

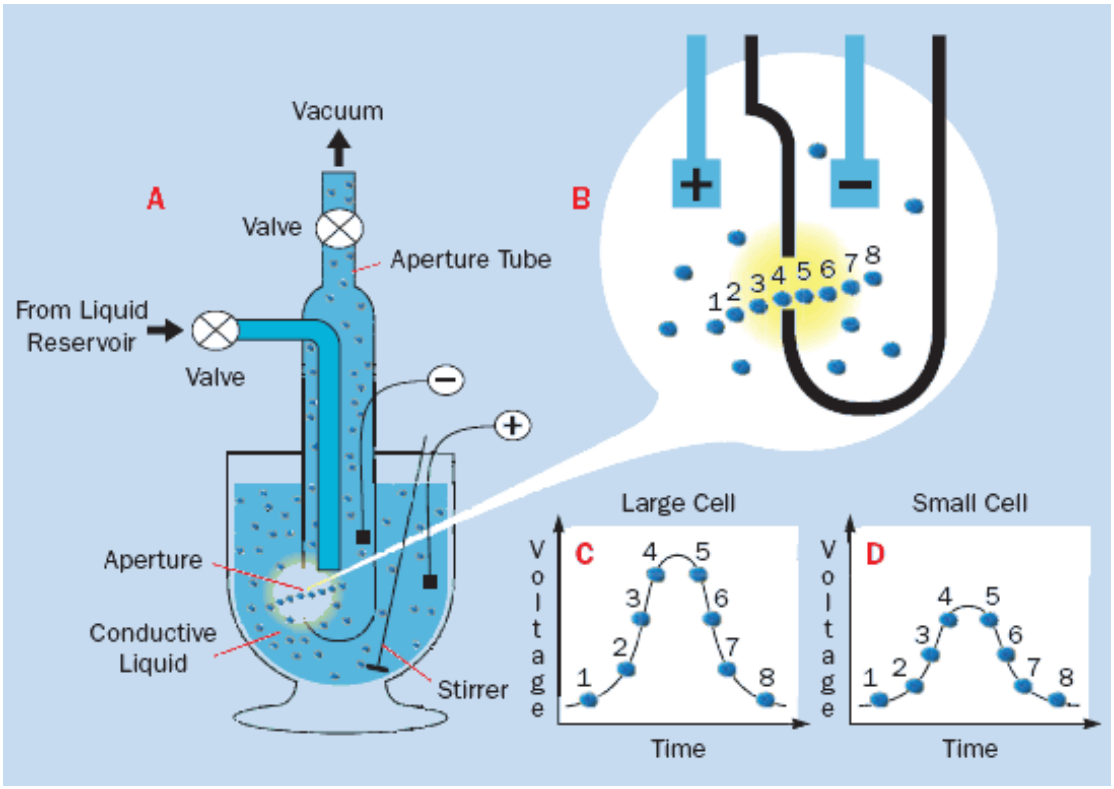

Figure 2-3: Simplified schematic of a Coulter Counter. The vacuum pulls the particle- containing suspension through aperture A, and an electric current flows between the two electrodes creating the sensing zone in B. As individual particles pass through the sensitive zone, voltage pulses are generated as shown in C and D. The larger cells create larger amplitude pulses since they cause a larger resistance (Image from: Beckman Coulter Life Science, URL: http://uk.beckman.com/particle/instruments/cell-sizing-and-processing/z-series-coulter-counter)

2.3 Measurement of Platelet function

The different phases of platelet activation including adhesion, granule release and aggregation were measured *in vitro* to characterise the fuel requirements of platelets during these processes. A 96-well plate Collagen platelet adhesion assay was used to determine platelet adhesion. Light transmission aggregometry and lumi-aggregometry were used to assess platelet aggregation and ATP secretion, respectively.

2.3.1 Platelet Collagen 96-well Adhesion assay

One early feature of platelet function is adhesion to injured blood vessel walls during the haemostatic process. Adhesion is a complex process in which a variety of plasma and sub-endothelial tissue components bind to different membrane proteins. As such, studying the adhesion process of platelets on different surfaces enable the characterisation of fuel requirements during platelet-matrix protein interactions. In this study, a multi-well microplate assay was used to determine the activity of acid phosphatase, a platelet enzyme whose activity is stable independent of platelet stimulation, and proportional to the number of adhered platelets (Bellavite et al., 1994).

A 96-well plate was coated with 50μg/ml collagen overnight at 4 °C. Platelets were suspended in Tyrode's buffer with +/- glucose. The platelet suspension was incubated with Tirofiban (1:50) for 20 minutes before use, gently mixed by rolling and maintained at 37 °C prior to the experiment. The wells were washed twice with phosphate buffered saline (PBS, Appendix 2) before the addition of 50μl, $1*10^8$ platelets/ml +/- glucose in triplicates with controls. The plate was incubated at 37 °C for 60 minutes before being subjected to two washes with PBS. 150μl of the p-nitro-phenyl phosphate citrate solution was added to all wells and incubation carried out at room temperature for 1 hour. The reaction was stopped by adding 100μl of 2M NaOH and the absorbance of p-nitrophenol produced was measured at 405nm using a plate reader.

p-nitrophenyl phosphate + $H_2O \xrightarrow{\text{Acid Phosphatase}}$ p-nitrophenol + P_i

2.3.2 Light transmission aggregometry

Measuring platelet aggregation with light transmission aggregometry was first described by Born (1962). Briefly, light is passed through a uniform suspension of platelets with constant stirring (Figure 2-4) in a cuvette. The presence of platelets in the suspension obstructs the passage of light through the suspension, thereby resulting in a high optical density (OD). The aggregometer is then calibrated in a way that the optical density of the un-stimulated platelets represents 0% aggregation. When platelets are activated with an agonist, they first undergo a shape change, which briefly reduces the optical density further as the surface area of the platelets increase, followed by aggregation. Aggregation results in a space clearing between aggregates in the suspension, leading to reduced OD. The OD without free platelets present in the suspension represents 100% aggregation (Figure 2-4).

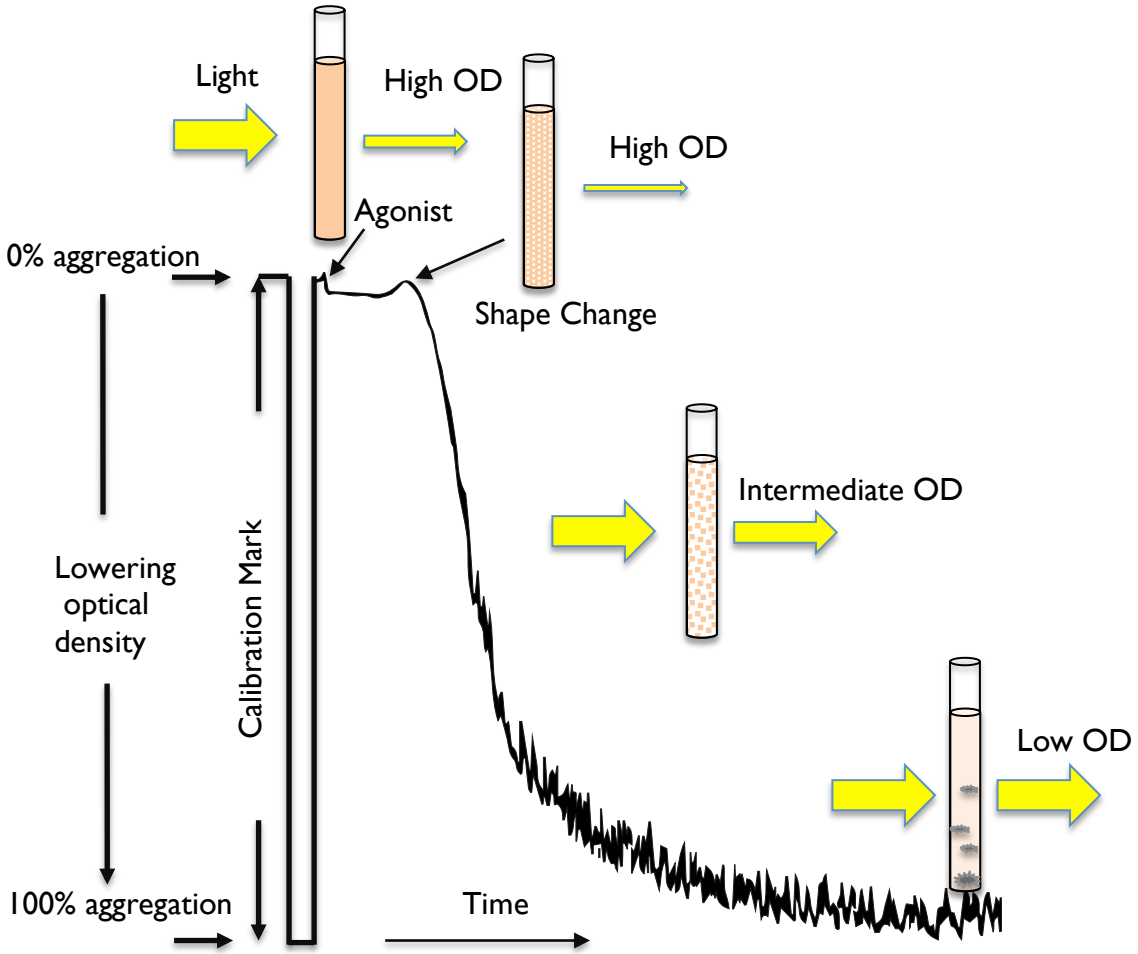

Figure 2-4: Diagram of a typical light transmission aggregometry trace. The un-stimulated washed platelet suspension has a relatively high optical density (OD), allowing less light transmission and represents 0% aggregation. Following addition of the agonist, platelets undergo a shape change, which leads to an increase in the surface area of platelets resulting in less light transmission for a short period. With constant stirring, aggregation proceeds, allowing more light transmission, which leads to reduced OD. Autologous platelet-poor suspension gives an optical density equivalent to 100% aggregation as indicated by the calibration mark.

In the present study, washed platelets (250µl, $2.5*10^8$ platelets/ml) were re-suspended in Tyrode's buffer plus or minus (+/-) glucose and equilibrated at 37°C before aggregation was recorded under constant stirring conditions (1000 rpm). Aggregation was carried out for three and half minutes, unless stated otherwise, using a Chrono-log aggregation module-dual channel light aggregometer. For each sample, the aggregometer was calibrated using a resting platelet suspension for 0% aggregation and modified Tyrode's buffer for 100% aggregation.

2.3.3 Measurement of platelet ATP secretion

Platelet aggregation occurs in two phases (Born and Cross., 1963) as reviewed in Chapter 1.2.2. Primary aggregation occurs following activation with various physiological stimuli, when platelets undergo shape change and initiate the primary reversible phase of aggregation. Secondary aggregation, which is irreversible, results in the release of granules to assist and amplify the recruitment of additional platelets. ATP release is an indicator of dense granule secretion during the secondary aggregation process given 60% of the nucleotide pool is stored in dense granules (Ghoshal and Bhattacharyya, 2014). This can be measured by 'lumiaggregometry', which is a modified version of light transmission aggregometry. It is based on the bioluminescent determination of ATP, in which ATP reacts with luciferin and luciferase, resulting in light emission. It uses a light-emitting diode (LED), which emits light in the infrared range detectable by a phototransistor. A photomultiplier tube located on the light path of LED then detects the luminescence produced by the reduction of ATP.

Luciferin + ATP ⟶ Luciferyl Adenylate + Inorganic phosphate (ppi)

Luciferyl Adenylate + O_2 ⟶ oxyluciferin + AMP + LIGHT

In this study, a Chrono-log 400vs Lumi-aggregometer was used to detect ATP secretion. The assay was performed using 225µl of washed platelets $2.5*10^8$ platelets/ml suspended in Tyrode's buffer +/- glucose. Each sample was pre-incubated with 25µl of luciferin-luciferase reagent for 1 minute prior to further incubation for 1 minute in the channel under stirring conditions. The samples were then stimulated with different agonists for 90 seconds before 2.5µl of ATP standard (2nM final concentration) was added (Figure 2-5). The ATP secretion was calculated using the equation provided below. The luminescence of the sample and ATP standard were measured on the Chart recorder in mm using a ruler.

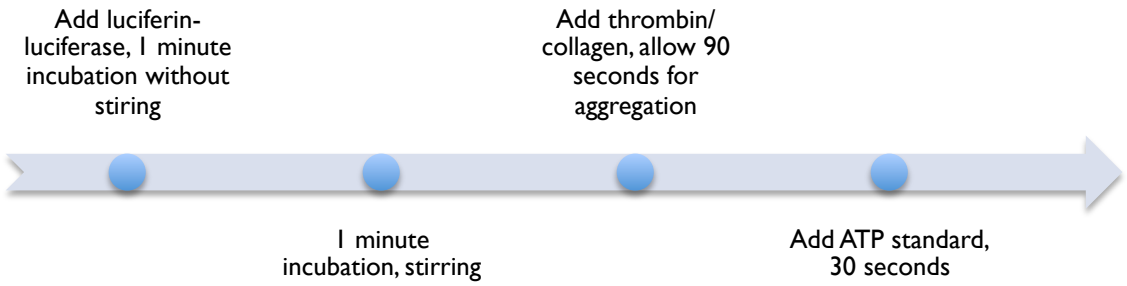

Figure 2-5: Flow chart of the experimental procedure for lumiaggregation
The ATP released from the sample was calculated using the following formula:

$$\frac{Luminescense\ of\ the\ sample}{luminescense\ of\ the\ standard} \times [ATP\ standard]$$

2.4 Enzymatic Determination of Glucose

Glucose is one of the major fuels in the blood available to platelets. Quantifying platelet function-specific glucose consumption will provide insights in the partitioning of different fuels to support normal platelet activation. Platelet glucose uptake was measured by a rapid and specific fluorimetric assay, which in its modern form was first described by Bergmeyer et al., (1974). In the first step of the pentose phosphate pathway, glucose-6-phosphate dehydrogenase (G6PD) catalyses the conversion of GP6 produced from glucose, to phosphoglucono- δ lactone. This results in the production of highly fluorescent NADPH (Figure 2-6). The change in the fluorescence, which is proportional to the amount of glucose, can be detected with a fluorescence microplate reader with excitation/emission of 340/460nm.

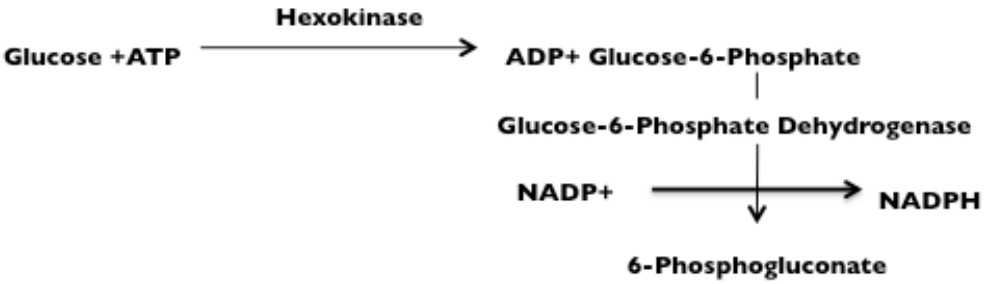

Figure 2-6: Enzymatic reaction for glucose quantification

In this study, a glucose reaction cocktail (Guerif et al., 2013; Appendix 2) was prepared prior to the experiments and aliquoted to be stored at -20 °C. It was kept for a maximum of 3 months. Before each experiment, a new aliquot was thawed, mixed well and placed on ice. Glucose standard was prepared using a 5mM glucose solution to create a six point glucose standard ranging from 0-1mM (Figure 2-7). 45µl/well of the cocktail mixture was added to a Costar black clear bottom microplate, before being centrifuged for 30 seconds in a microplate spinner. The fluorescence was measured to obtain a value for pre-assay background fluorescence of the cocktail (defined as the 'pre-blank reading'). 5µl of the glucose standard, at six increasing concentrations were added, and centrifuged again for 30 seconds to achieve uniform distribution and mixture before being incubated for 10 minutes at 25 °C. The plate was centrifuged once more after the incubation before measuring the end point fluorescence. A linear standard curve was created using the glucose standard concentrations against the fluorescence. Curves with a correlation coefficient (R^2)<0.99 were rejected. The final glucose concentration in the samples was determined against the standard curve.

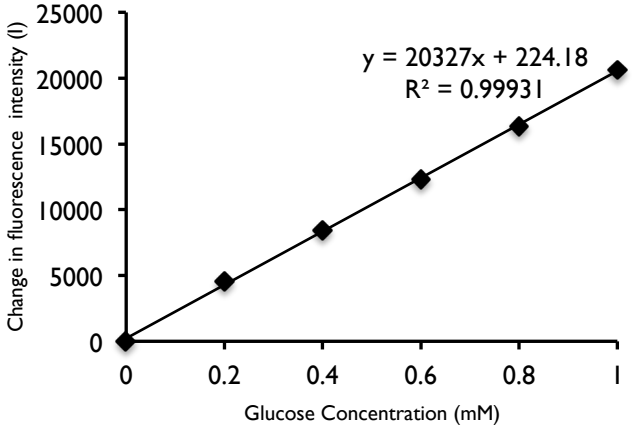

Figure 2-7: An example standard curve for glucose assay

2.4.1 Glycogen determination

Glycogen granules are abundant in platelet cytoplasm, with levels approaching that of skeletal muscle on a gram-to-gram basis (1.6g/cm^3) (Karpatkin et al., 1970). The presence of a large amount of glycogen in platelets and enzymes related to its metabolism suggest a putative biological role for this polymeric form of glucose (Rocha et al., 2014).

In this study, glycogen was acid-hydrolysed with 4M HCl plus boiling, and the liberated glucose was quantified as in section 2.4 (Rocha et al., 2014). In each experiment, a glycogen standard was prepared from 1mg/ml of glycogen solution to create a five point standard curve ranging from 0-200μg/ml glycogen (Figure 2-8). The standards and samples were boiled on a block heater (100 °C) for 10 minutes to denature all enzymes before adding 300μl of 4M HCl and boiling for a further 60 minutes. 300μl of 2M Na_2CO_3 was added to neutralize the reaction. Supernatants from standards and samples were subjected to enzyme coupled fluorometric assay for glucose quantification as in section 2.4. Glucose standard curve was generated, which was used to determine the concentrations of glucose liberated from glycogen standards. Glycogen standard curve was then created from the free glucose concentrations obtained from the hydrolysis of glycogen standards ranging from 0-200μg/ml glycogen.

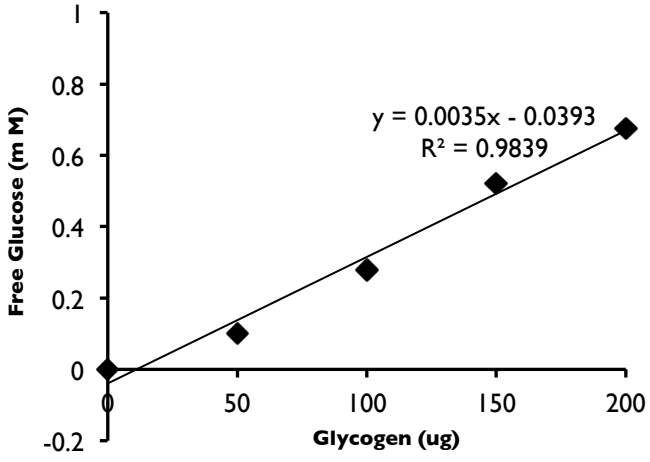

Figure 2-8: An example standard curve for glycogen assay

The amount of glycogen in the samples then was calculated from the glycogen standard curve (Figure 2-8) and expressed as μg glycogen/10^8 platelets.

2.5 Seahorse XFp Extracellular Flux Analyser

The real time oxygen consumption rate (OCR) and extracellular acidification rate (ECAR) of platelets were measured simultaneously using a Seahorse XFp extracellular flux analyser (Agilent). OCR is an indicator of mitochondrial respiration and ECAR is predominantly the result of glycolysis. It measures the dissolved oxygen (pmol/min) and pH (mpH/min) in the media as a rate of change at intervals of approximately 2-5 minutes, using optical fluorescent biosensors embedded in a disposable cartridge. This is achieved by isolating as little as 2µl of the medium above the cell monolayer to create a transient micro chamber, in which the cellular oxygen consumption and proton excretion (glycolysis) cause rapid and easily measurable changes in the dissolved oxygen and free protons. This change is then measured every few seconds until the rate of change is linear to calculate the slopes to determine the OCR and ECAR. It also allows the injection of up to four compounds of interest (Figure 2-9) from which the rates of cellular oxygen consumption and glycolytic rate are then determined in a precise, non-invasive, and label–free manner.

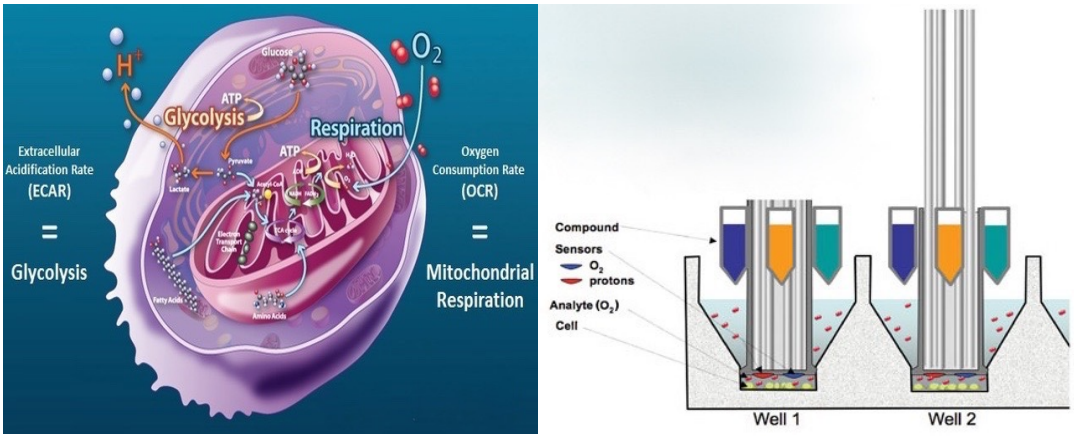

Figure 2-9: Simplified mechanism of XFp extracellular flux analyser. (Image modified from: Agilent Seahorse Bioscience). In each well of the XFp mircoplate, the sensor cartridge forms a transient microchamber above the cell monolayer. It detects the change in oxygen consumption rate and proton excretion rate by the cell in real time (Left). It also allows the injection of up to four compounds of interest (Right).

2.5.1 XFp assay workflow

Table 2-1: Simplified XFp assay workflow used in this study

Day Before Assay	Day of the assay
1.Hydrate sensor cartridge overnight at 37 °C in non-CO_2 incubator 2. Design the assay protocol using the XFp software if required and load it on to the XFp machine 3.Design the experimental procedure	1. Prepare the cell suspension 2. Coat the cell culture mini plate if required 30 mins prior to the experiment and warm up the medium (Appendix 2) to 37 °C in non-CO_2 incubator 3. Seed the cells using optimised cell concentration and spin if required to achieve maximum coverage 4. Load the cartridge with the compound of interest 5. Equilibrate the loaded cartridge and start the assay by changing the cell plate with utility plate

2.5.2 Hydration of a sensor cartridge

Each seahorse experiment used an 8 well cell culture mini plate and a cartridge pack, which included a utility plate and sensor cartridge (Figure 2-10).

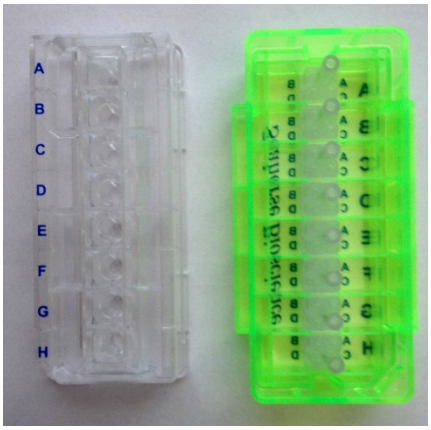

Figure 2-10: The cartridge pack. Utility plate on the left next to upside down sensor cartridge on the right

Each probe tip is equipped with a solid-state sensor material, which must be hydrated (XFp Basic Procedures, Agilent). To do this, the utility plate and sensor cartridge are separated, and the sensor cartridge is placed upside down on the lab bench (Figure 2-10). Each well is filled with approximately 200µl XFp calibrant solution. The moats around the utility plate outside the wells are filled with 400µl/chamber to achieve maximum sealing between the utility plate and sensor

cartridge. The sensor cartridge is placed on top of the utility plate before overnight incubation at 37°C. The incubator is humidified to minimise evaporation of the calibrant solution.

2.5.3 Preparation of platelets for XFp assay

This method was adapted from Kramer et al., (2014). Platelets were isolated using the prostaglandin method described in section 2.2.2. The final pellet after the wash step was re-suspended in 200μl-1ml PBS-PGI_2 (1μg/ml) depending on pellet size, before being counted and diluted to the desired concentration. Adding prostacyclin (PGI_2) effectively prevented platelet activation during the cell seeding procedure (2.5.5) when observed under microscopy after the centrifugation step. Platelets were counted and diluted in XFp assay medium +/- 5.6mM of glucose (Appendix 2) to $1*10^8$/ml platelets.

2.5.4 Coating of cell culture miniplate

Since measurement of OCR and ECAR by the seahorse takes place in the microchamber that is created between the cartridge sensor and platelet monolayer, it is a prerequisite for the platelets in the suspension to adhere at the bottom of the plate. Cell lines, such as platelets, that could become activated by the plate material require a plate coating with Cell-Tak, poly-D/L-lysine or gelatin depending on the specific cell type (XFp Basic Procedure, Agilent).

To avoid unnecessary platelet activation during the seahorse experiments, the plates were coated with Cell-Tak as recommended by Agilent seahorse bioscience for suspension cells. The optimum Cell-Tak concentration for an XFp miniplate is 22.4 μg/ml (Agilent, UK). Cell-Tak is a non-immunogenic extracellular matrix protein isolated from marine mussels, which is re-suspended in 5% acetic acid. The optimum pH for Cell-Tak absorption is between 6.5-8.0 and it starts being absorbed by the plate immediately after re-suspension within the correct pH window. 500μl (22.4 μg/ml) of Cell-Tak solution was prepared from a stock of 2.03mg/ml in 0.1M sodium bicarbonate solution (pH-8.0). The pH was adjusted before coating each

well with 50μl of Cell-Tak solution. The plate was incubated at 37°C for 30 minutes before being washed twice with PBS.

2.5.5 Cell seeding

Each XFp cell culture miniplate has eight wells, A-H. A and H were kept as blank wells if there were two experimental conditions. These two experimental conditions were: platelets with (B, C, D) or without (E, F, G) stressors of interest, or platelets from different donors and under the same experimental conditions (Figure 2-11). In either case, 50μl of platelet suspension ($1*10^8$/ml) was loaded in to each well of miniplate before being put into the XFp plate carrier tray. The plate was centrifuged at 200×*g* for 1second without break and rotated 180 degrees before being spun again at 300×*g* for 1 second. The cell-loaded plate was balanced with a separate plate, which was loaded with 50μl PBS/well, using a different XFp plate carrier tray. After the centrifugation step, the assay volume was brought up to 180μl by adding 130μl of the XFp assay medium (Appendix 2).

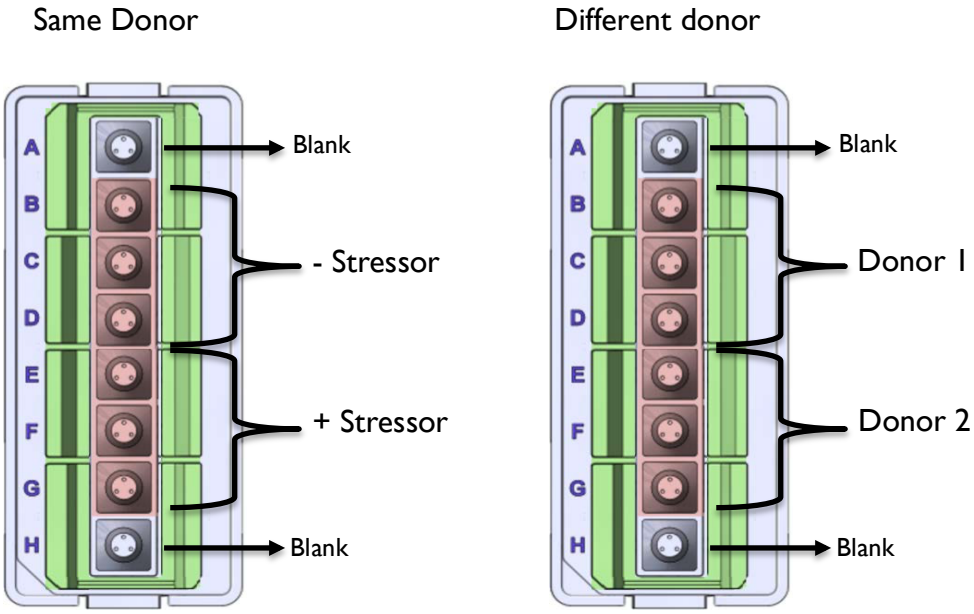

Figure 2-11: Typical cell seeding designs in this study. Platelets from the same donor (on the left) were treated with a stressor of interest to measure the effect on OCR & ECAR simultaneously. B, C, D wells were kept as controls, which were not treated with the stressor. Well A was not seeded with cells and kept as a background well for wells B, C, D. Wells E, F, G were treated with the stressor and well H was not seeded but injected with the stressor. Platelets from different donors were compared in parallel (on the right) with the same experimental conditions. Wells A and H were kept as blanks for each. The results of the OCR, ECAR and protein quantification were corrected for the blank background wells (modified from XFp Basic Procedure).

2.5.6 Cartridge port loading procedure

The recommended initial assay volume range for the XFp assay is 150-275µl. The recommended injection volume range is 20-30µl per port (XFp Basic Procedure, Agilent). In this study, the starting assay volume was 180µl, of which 50µl was the cell-seeding volume and 130µl was the added volume before any injections. The stressor compounds of interest or the inhibitors were freshly prepared in the XFp medium (Appendix 2) prior to each assay and warmed to 37°C. The desired volume of stressors was injected into the ports of the cartridge (Figure 2-12) using a p100 pipette carefully with a 60 ° angle in between the cartridge surface and pipette tip, leaving the port sleeve dry. The stressors or inhibitors for the cartridge loading were prepared as a 10x stock, meaning that the final well concentrations decided the loading volume (Table 2-2). This meant that with different injection numbers, the final assay volume varied slightly. As the cell seeding density was $1*10^8$

platelet/ml, the different final volume resulted in different cell numbers in the final assay. This was corrected for the total proteins in each well to avoid differences between assays.

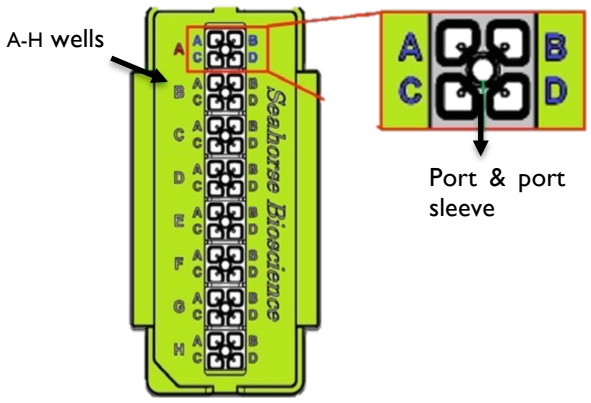

Figure 2-12: Diagram of the XFp sensor cartridge. The XFp sensor cartridge has eight wells, A-H, labelled on the left hand side. Each well has four injection ports A, B, C, D. (modified from XFp Basic Procedure, Agilent)

Table 2-2: XFp port injection volumes and well volumes

No. Of Injections	1	2	3	4
Assay medium at Start	180µl	180µl	180µl	180µl
Port A	20µl	20µl	20µl	20µl
Port B	0	22µl	22µl	22µl
Port C	0	0	28µl	28µl
Port D	0	0	0	30µl
Total volume/well	200µl	222µl	250µl	280µl

2.6 XFp protocols

For many Seahorse experiments there are ready-programmed protocols available (Figure 2-13). In a standard protocol, each measurement takes 3-5 minutes with triplicate measurements. Injections depend on the number of inhibitors or stressor of interest as shown in Table 2-2. However, this may be modified if required depending on the cell line of interest.

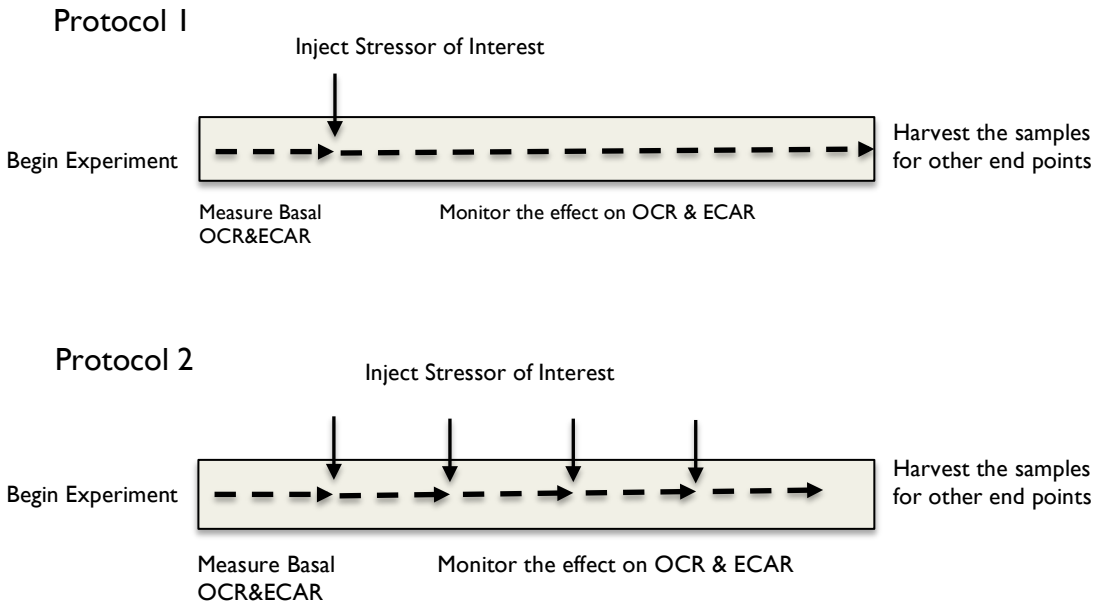

Figure 2-13: Example standard XFp protocols. Protocol 1 is used to investigate a single stressor of interest. After a baseline measurement of OCR & ECAR, a stressor is added and the effect on the cell line monitored over a certain length of time. Protocol 2 is used to investigate the effect of multiple stressors or inhibitors of interest on the cell line. After a baseline measurement of OCR & ECAR, a sequential injection of up to four stressors can be achieved. This can be flexible depending on how many inhibitors are used or the focus of the experiment. Dotted lines represent periods of measurement.

2.6.1 XFp glycolysis stress test

In this study, the glycolytic capacity of platelets was measured using the glycolysis stress test (XFp Glycolysis Stress Test User Guide, Agilent). Platelets were re-suspended in a glucose-free XFp assay medium (Appendix 2) and the ECAR, which was indicative of glycolysis (Figure 2-14, right), was measured in response to the addition of glycolysis stressors (Table 2-3) using XFp.

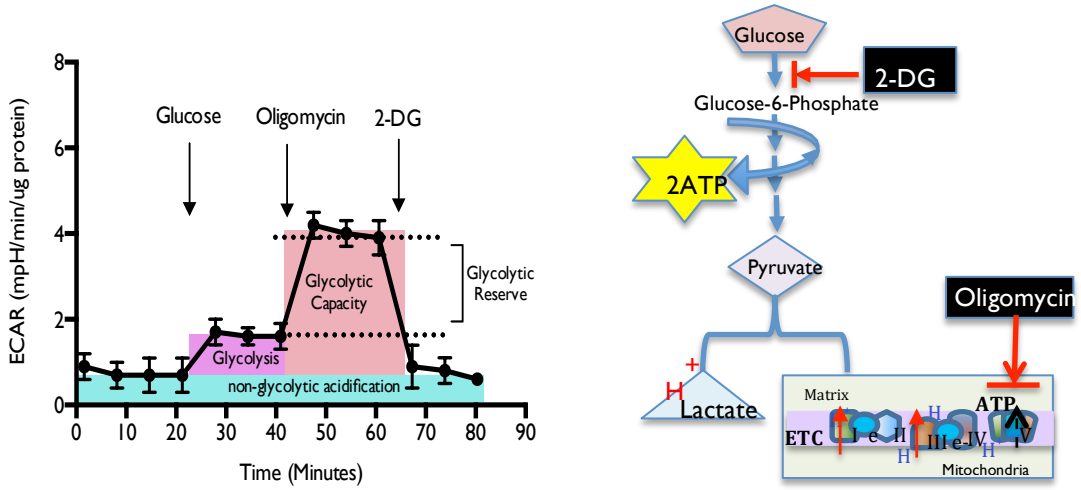

Figure 2-14: Example glycolytic stress profile. Glycolytic stress profiles of platelets (Left) and key inhibitors used to modulate glycolysis (Right). After measuring the basal ECAR in glucose-free medium, the injection of 5.6mM of glucose increases ECAR, illustrating the ability of platelets to utilise glucose through glycolysis. The subsequent injection of oligomycin to inhibit mitochondrial ATP synthesis, results in a further increase in ECAR, providing the ability of platelets to switch to glycolysis alone when mitochondrial ATP production is inhibited. The injection of the glucose analog, 2-deoxy-glucose (2-DG), inhibits glycolysis through competitive binding to hexokinase, reducing ECAR. This confirms that the ECAR produced in the experiment is due to glycolysis and the remaining ECAR after 2-DG gives the non-glycolytic acidification.

The basal rate of extracellular acidification was established in glucose-free medium before injecting 5.6mM of glucose, which increased ECAR. This was reported as the ability of platelets to utilise exogenous glucose via glycolysis. The injection of oligomycin (1μM) inhibited mitochondrial ATP synthesis meaning that glycolysis became the sole pathway for the production of ATP. The typical response in this situation is a further increase in ECAR, reported as the maximum glycolytic rate of platelets. The difference between the maximum ECAR and basal glycolysis after glucose injection was reported as the glycolytic reserve, the extent to which glycolysis may be increased if needed. The injection of 2-deoxy glucose (2-DG,

50mM) inhibited glycolysis through competitive binding to the hexokinase resulting in the decrease in ECAR. This confirmed that this ECAR was due to glycolysis. The remaining ECAR was reported as the non-glycolytic acidification. Every stage was measured three times and the final result was taken as the average of the three measurements.

Table 2-3: Inhibitors and working concentration for glycolysis stress test

Ports	Compounds	Stock	Cartridge	Well
A	Glucose	1M	56mM	5.6mM
B	Oligomycin	10mM	10μM	1μM
C	2-DG	500mM	500mM	50mM

The standard glycolysis stress test described above was modified to study the glycolytic capacity of platelets when stimulated with an agonist, such as thrombin. To achieve this, the port injections were modified as shown in Table 2-4.

Table 2-4: Modified injection of stressors for glycolysis stress test

Conditions	Ports			
	A	B	C	D
Control	Media	Glucose	Oligomycin	2-DG
Thrombin (0.1U/ml)	Thrombin	Media	Oligomycin	2-DG
Thrombin+Glucose	Thrombin+Glucose	Media	Oligomycin	2-DG
Thrombin/Glucose	Thrombin	Glucose	Oligomycin	2-DG

2.6.2 XFp mitochondrial stress test

By measuring oxygen consumption in the presence of multiple mitochondrial electron transport chain inhibitors (Table 2-5), the key parameters of mitochondrial function were assessed (Figure 2-15) (XFp Mito Stress Test User Guide, Agilent).

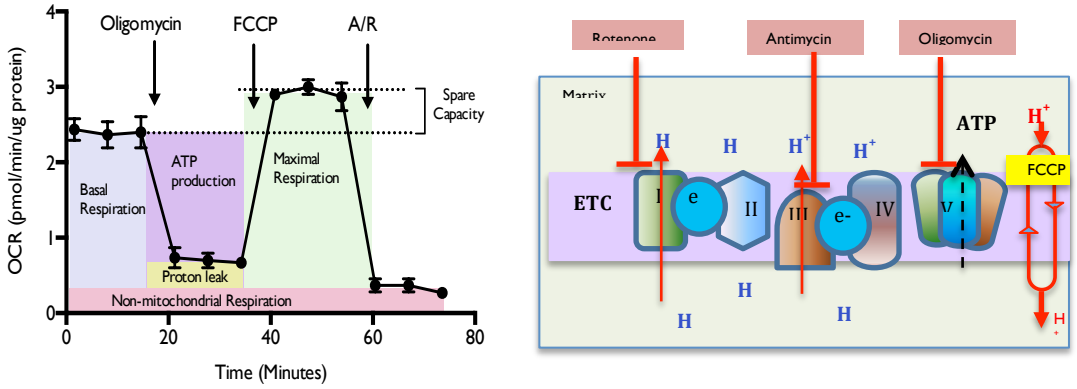

Figure 2-15: Example mitochondrial stress profile. Mitochondrial stress profile of platelets (Left) and the inhibitors used to assess the key mitochondrial parameters (Right). Sequential injection of oligomycin, FCCP and the combination of antimycin A/Rotenone yielded the following parameters: basal mitochondrial respiration, ATP coupled respiration, proton leak, maximal respiration, spare respiratory capacity and non-mitochondrial respiration.

Platelets were re-suspended in the presence or absence of glucose (5.6mM) in XFp medium (Appendix 2). A cell culture mini plate and cartridge were prepared as described in section 2.5.4. The basal oxygen consumption rate (OCR) was established with three measurements prior to the injection of oligomycin (1μM), which inhibits mitochondrial ATP synthase (Complex V) (Figure 2-15, Right). This was accompanied by a reduction in OCR, which was correlated to mitochondrial ATP synthesis, and reported as ATP-coupled OCR. Carbonyl cyanide-4 phenylhydrazone (FCCP) is an ionophore that increases proton transport across mitochondrial membrane. This results in unhindered electron flow and maximal oxygen consumption by the mitochondria. Thus, the injection of FCCP (2μM) increased the OCR to the maximum, which was reported as the maximal OCR. The combined injection of antimycin A and rotenone (A/R, 2.5uM) inhibited complexes I and III on the electron transport chain, which resulted in the complete inhibition of electron flow. As a result, the mitochondrial OCR was abolished. The remaining OCR was reported as the non-mitochondrial component. The difference

between the maximal and basal OCR was reported as the spare respiratory capacity and the difference between ATP-coupled OCR and non-mitochondrial OCR was reported as the proton leak. The compounds in Table 2-5 are dissolved in ethanol and please refer to Figure 5-19B in Chapter 5 for vehicle control.

Table 2-5: Inhibitors and working concentrations for mitochondrial stress

Ports	Compounds	Stock	Cartridge	Well
A	Oligomycin	10mM	10μM	1μM
B	FCCP	50mM	20μM	2μM
C	A/R	5mM	25μM	2.5μM

The standard XFp mitochondrial stress test was modified to study the key components of platelet mitochondrial function in the presence of a stimulator, such as thrombin or a stressor (X). To achieve this, the injection protocol of the test was modified as shown in Table 2-6.

Table 2-6: Modified injection of stressors for mitochondrial stress test

Ports	Compounds	Stock	Cartridge	Well
A	Thrombin/X	10U/ml	1U/ml	0.1U/ml
B	Oligomycin	10mM	10μM	1μM
C	FCCP	50mM	20μM	2μM
D	A/R	5mM	25μM	2.5μM

2.6.3 FCCP Titration

FCCP must be carefully titrated for every new experimental condition and cell line to achieve fully uncontrolled respiration, as too high concentrations of FCCP can inhibit respiration (Brand and Nicholls, 2011). A five-point titration curve was used in this study to optimize the concentration of FCCP (XFp Basic Procedure, Agilent). To achieve this, different concentrations of FCCP were first prepared (Figure 2-16)

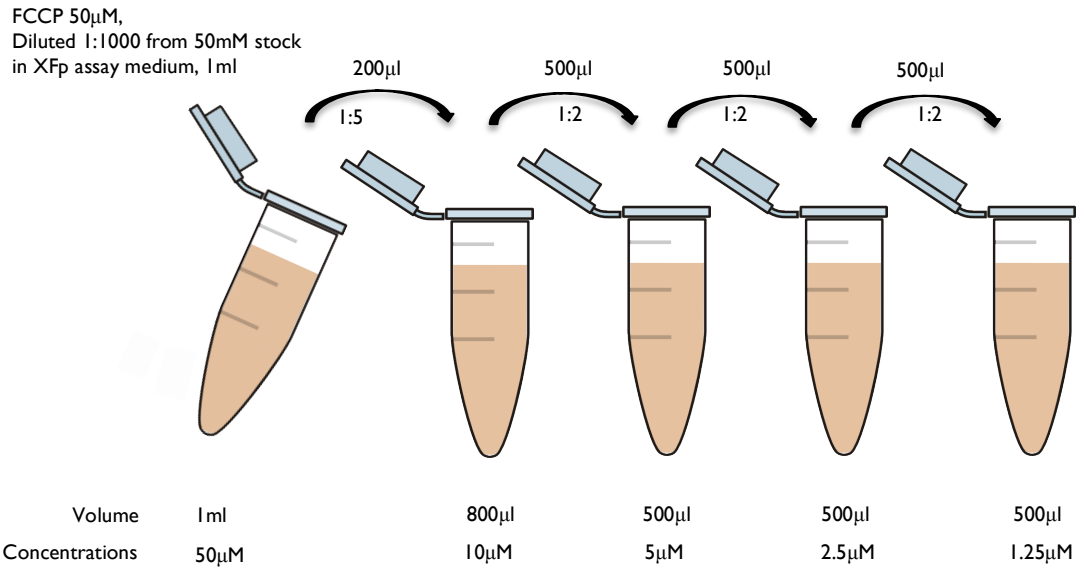

Figure 2-16: FCCP dilution procedures

The XFp assay plate was then divided into a low FCCP concentration range (0.125, 0.25, 0.5µM) and a high FCCP concentration range (0.5, 1.0, 2.0µM) as shown in Figure 2-17.

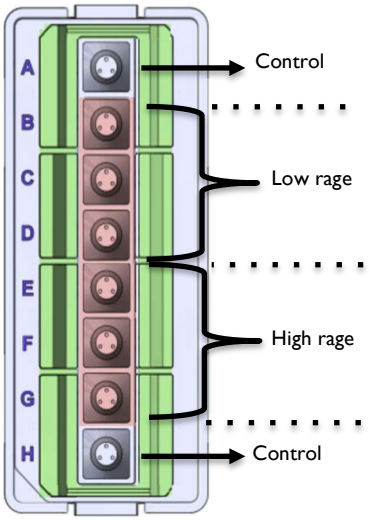

Cartridge Loading Concentration/well		Well Concentration	
A 10μM oligomycin	B 1.25μM FCCP	A 1μM oligomycin	B 0.125μM FCCP
C 1.25μM FCCP	D 2.5μM FCCP	C 0.125μM FCCP	D 0.25μM FCCP
A 10μM oligomycin	B 5μM FCCP	A 1μM oligomycin	B 0.5μM FCCP
C 5μM FCCP	D 10μM FCCP	C 0.5μM FCCP	D 1μM FCCP

Figure 2-17: Cartridge loading procedure for FCCP titration. FCCP titration was carried out in the presence of 1μM oligomycin.

FCCP titrations were carried out in the presence of 1μM oligomycin by measuring the OCR in the XFp (Figure 2-18). In low range FCCP wells, the final well concentrations were: 0.125μM, 0.125+0.125=0.25μM, and 0.25+0.25=0.5μM. In high range FCCP wells, the final well concentrations were: 0.5μM, 0.5+0.5=1μM, and1+1=2μM.

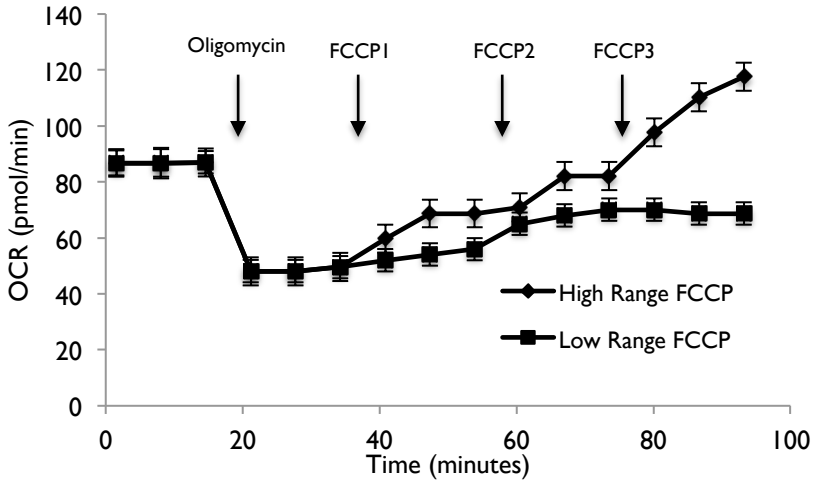

Figure 2-18: Example FCCP titration curve

The concentration of FCCP that induced the highest OCR was chosen for the mitochondrial stress test.

2.6.4 XFp cell phenotype test

The metabolic phenotype, glycolysis versus OXPHOS, of platelets was determined by measuring the ECAR and OCR at baseline (XFp Cell Phenotype Test User Guide, Agilent). The stressed phenotype, defined as the glycolysis vs. OXPHOS under an induced energy demand with stressor compounds, was measured using the combined injection of oligomycin and FCCP (Figure 2-19, Table 2-7). Inhibition of mitochondrial ATP synthesis by oligomycin causes a compensatory increase in ECAR as the cells attempt to meet energy demand through glycolysis, if the cells have the ability to do so. FCCP depolarizes the mitochondrial inner membrane and drives the oxygen consumption rates to their highest level as the mitochondria tries to restore the mitochondrial membrane potential. Thus, the combination of oligomycin and FCCP results in the maximum ECAR and OCR under stress, giving the stressed energy phenotype. The metabolic potential was calculated as the percentage increase of stressed ECAR and OCR above baseline.

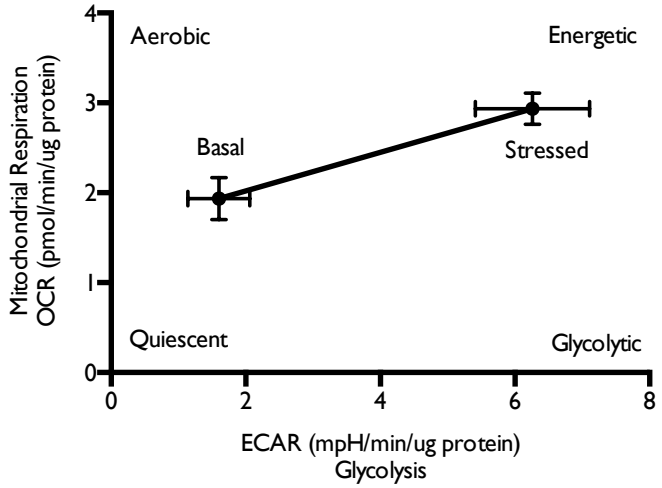

Figure 2-19: Example cell phenotype map

Table 2-7: Inhibitors and working concentrations for cell phenotype test

Ports	Compounds	Stock	Cartridge	Well
A	Oligomycin+FCCP	10mM, 50mM	10μM, 20μM	1μM, 2μM

The standard XFp cell phenotype assay was modified to investigate the platelet energy phenotype when platelets were activated with thrombin. To achieve this, the injection protocol of the standard test was modified as shown in Table 2-8.

Table 2-8: Modified injection of stressors for cell phenotype test

Ports	Compounds	Stock	Cartridge	Well
A	Thrombin	10U/ml	1U/ml	0.1U/ml
B	Oligomycin+FCCP	10mM, 50mM	10μM, 20μM	1μM, 2μM

After the injection of thrombin, only one measurement was taken instead of the standard three measurements before the second injection of oligomycin and FCCP.

2.6.5 XFp cell mitochondrial fuel flexibility test

Platelets can oxidise glucose, fatty acids and amino acids, such as glutamine as substrates for ATP production. This substrate flexibility of platelets to utilise these molecules was investigated using specific inhibitors of relevant metabolic pathways (Figure 2-20). UK5099, a MPC inhibitor, was used to inhibit glucose derived pyruvate oxidation in the platelet mitochondria. Etomoxir, which inhibits carnitine palmitoyltransferase 1A (CPT1A), was used to inhibit long chain fatty acid oxidation. For glutamine, BPTES was used to inhibit glutaminase (GLS1). Basal OCR was established before injecting a given inhibitor of the selected pathway (e.g. glucose oxidation), which reduced the OCR (XFp Mitochondrial Fuel Flexibility Test User Guide, Agilent). This OCR was reported as the target pathway's dependency of platelet for energy generation from that substrate by oxidation. Since one of the pathways has already been inhibited (e.g. glucose oxidation), the sequential injection of the combined inhibitors of other two pathways (e.g. fatty acid & glutamine) should reduce the OCR further. This OCR was then reported as the total OCR contributed from all three pathways (Figure 2-21)

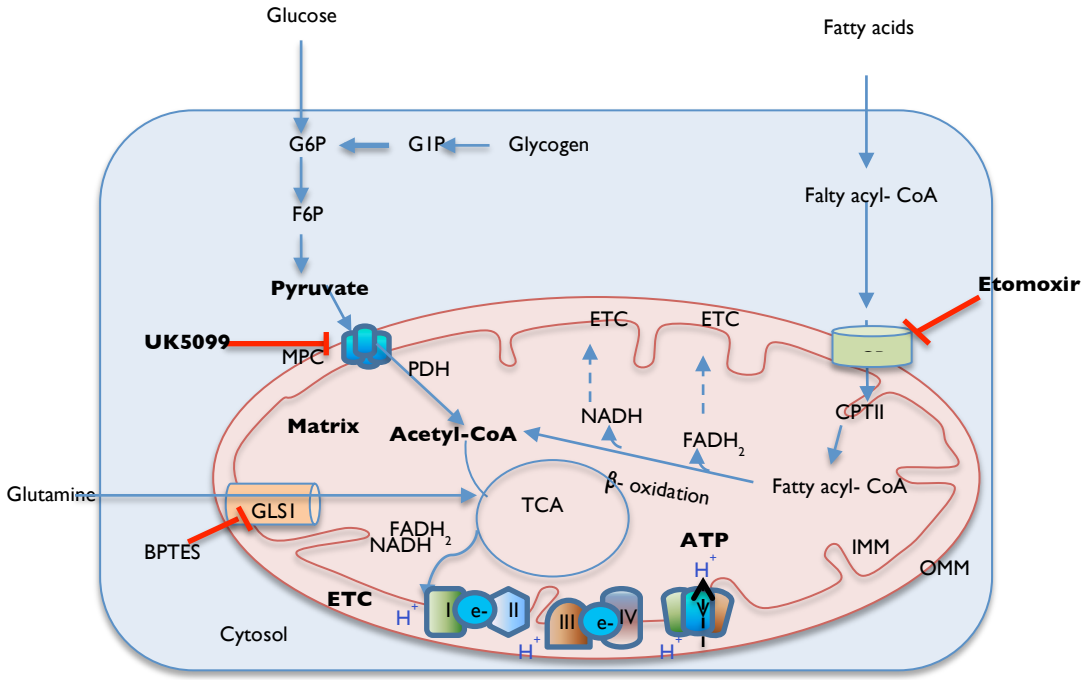

Figure 2-20: Simplified schematics of mitochondrial fuel pathway inhibitors

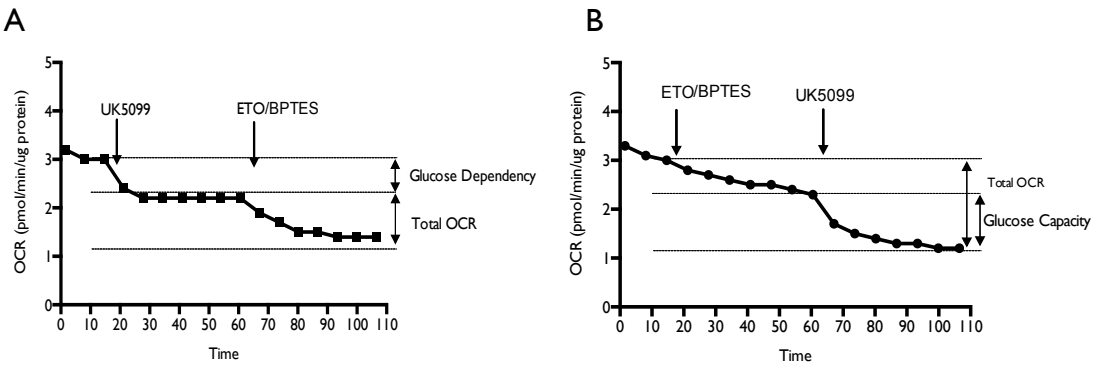

Figure 2-21: Example XFp glucose flexibility test. Glucose dependency assay (A) and glucose capacity assay (B). After establishing a baseline OCR (A), inhibiting glucose derived pyruvate oxidation by UK5099 reduced OCR, which represented the platelet dependency on glucose oxidation. As platelet glucose oxidation was already inhibited, the only possible fuels were endogenous fatty acids and glutamine. The combined inhibition of fatty acid oxidation with glutamine using etomoxir and BPTES, resulted in further reduction giving the platelet dependency on glucose + endogenous fatty acids + glutamine. Using these OCR data, % platelet dependency on glucose oxidation can be expressed as the % of total (glucose + endogenous fatty acids + glutamine). By changing the sequence (Right), platelet capacity to oxidise glucose can be measured. Inhibiting glutamine and endogenous fatty acid oxidation first leaves glucose as the only fuel, thus maximising glucose oxidation. Similarly, % capacity can be expressed as the % of total (glucose + endogenous fatty acids + glutamine).

For investigating the full capacity of a chosen metabolic pathway (e.g. glucose oxidation) when other metabolic pathways were inhibited, the above sequence was

reversed around (Figure 2-21). The other two metabolic pathways (e.g. fatty acid & glutamine) were inhibited after establishing basal OCR, and the target pathway was then inhibited (e.g. glucose oxidation). As the other pathways were inhibited first, the target pathway increased the OCR to compensate for the loss of the other two. This OCR was then reported as the full capacity of platelet mitochondria to utilise this target pathway (Figure 2-21, B). The results were expresses as the percentage of the total OCR used by all three substrates. The following calculations (Table 2-9) were used to calculate the %dependency, %capacity and %flexibility.

Table 2-9: Calculation used for mitochondrial fuel flexibility

Parameters	Equations
Dependency (%)	$(\frac{Baseline\ OCR - Target\ inhibitor\ OCR}{Baseline\ OCR - All\ inhibitors\ OCR})$*100%
Capacity (%)	$(1-\frac{Baseline\ OCR - Other\ 2\ inhibitors\ OCR}{Baseline\ OCR - All\ inhibitors\ OCR})$*100%
Flexibility (%)	Capacity % -Dependency %

The cartridge loading protocols for glucose, fatty acids and glutamine were carried out as shown in table 2-10.

Table 2-10: Cartridge loading protocol for mitochondrial fuel flexibility assay

Assay Group	Ports	Compounds	Stock	Port Concentrations	Well Concentration
Glucose Dependency	A	UK5099	20mM	20μM	2μM
	B	BPTES/Etomoxir		30μM/400μM	3μM/40μM
Glucose Capacity	A	BPTES/Etomoxir		30μM/400μM	3μM/40μM
	B	UK5099		20μM	2μM
Fatty acid Dependency	A	Etomoxir	4mM	400μM	40μM
	B	BPTES/UK5099		30μM/20μM	3μM/2μM
Fatty acid Capacity	A	BPTES/UK5099		30μM/20μM	3μM/2μM
	B	Etomoxir		400μM	40μM
Glutamine Dependency	A	BPTES	15mM	30μM	3μM
	B	UK5099/Etomoxir		20μM/400μM	2μM/40μM
Glutamine Capacity	A	UK5099/Etomoxir		20μM/400μM	2μM/40μM
	B	BPTES		30μM	3μM

The assay was modified to investigate the fuel flexibility of activated platelets in the presence of thrombin. 0.1U/ml thrombin was injected in to the port A and the rest of the assays were carried out as shown in Table 2-10.

2.7 Measurement of amino acids

High performance liquid chromatography (HPLC) was used to detect the amino acid utilisation by platelets. An automated pre-column derivatization method of amino acids with ortho-phthalaldehyde (OPA) in the presence of β-mercaptoethanol (β-ME) was used to form their isoindole-derivative conjugate (Figure 2-22), making them suitable for fluorescence detection at excitation/emission of 330/450nm (Bartolomeo and Maisano, 2006).

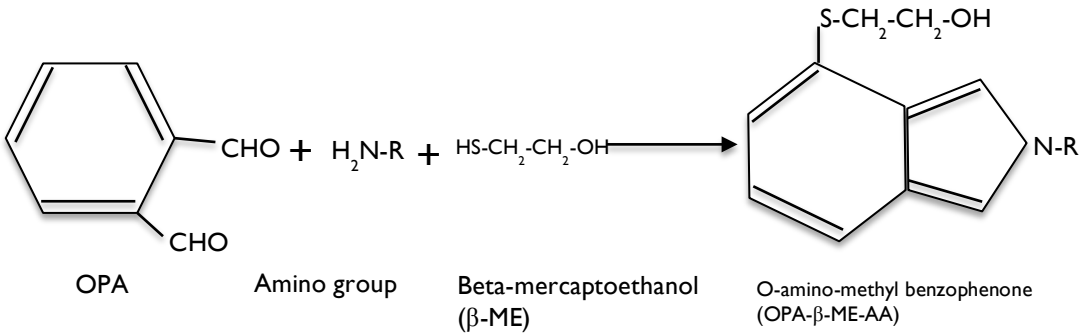

Figure 2-22: Simplified reaction mechanism for OPA, AA, β-ME conjugation. OPA reacts with the free amino group of the amino acids in the presence of the reducing reagent, β-ME, and produces the fluorogenic OPA- β-ME-AA, which can be detected with a fluorescence detector using HPLC at excitation/emission of 330/450nm

An internal standard dl-2-4-diaminobutyricc acid (DABA) and 18 amino acid standards: aspartic acid, asparagine, serine, histidine, glutamine, glycine, threonine, arginine, alanine, trypotophan, methionine, valine, phenylalanine, isoleucine, leucine, lysine, glutamic acid and tyrosine (12.5μM) were derivatized with OPA in the presence of 1mg/ml β-ME, using the automated pre-column derivatisation. After the derivatisation, reverse phase chromatography was performed using an Agilent 1100 HPLC coupled with Phenomenex Hyperclone™ 5μm ODC (C18) column (250*4.6nm). The gradient elution by buffers A and B (Appendix 2) was carried out for 60 minutes with a flow rate of 1.3ml/min at 30 °C. The amino acid composition of the samples were confirmed against the retention times and peak area of standards (Figure 2-23).

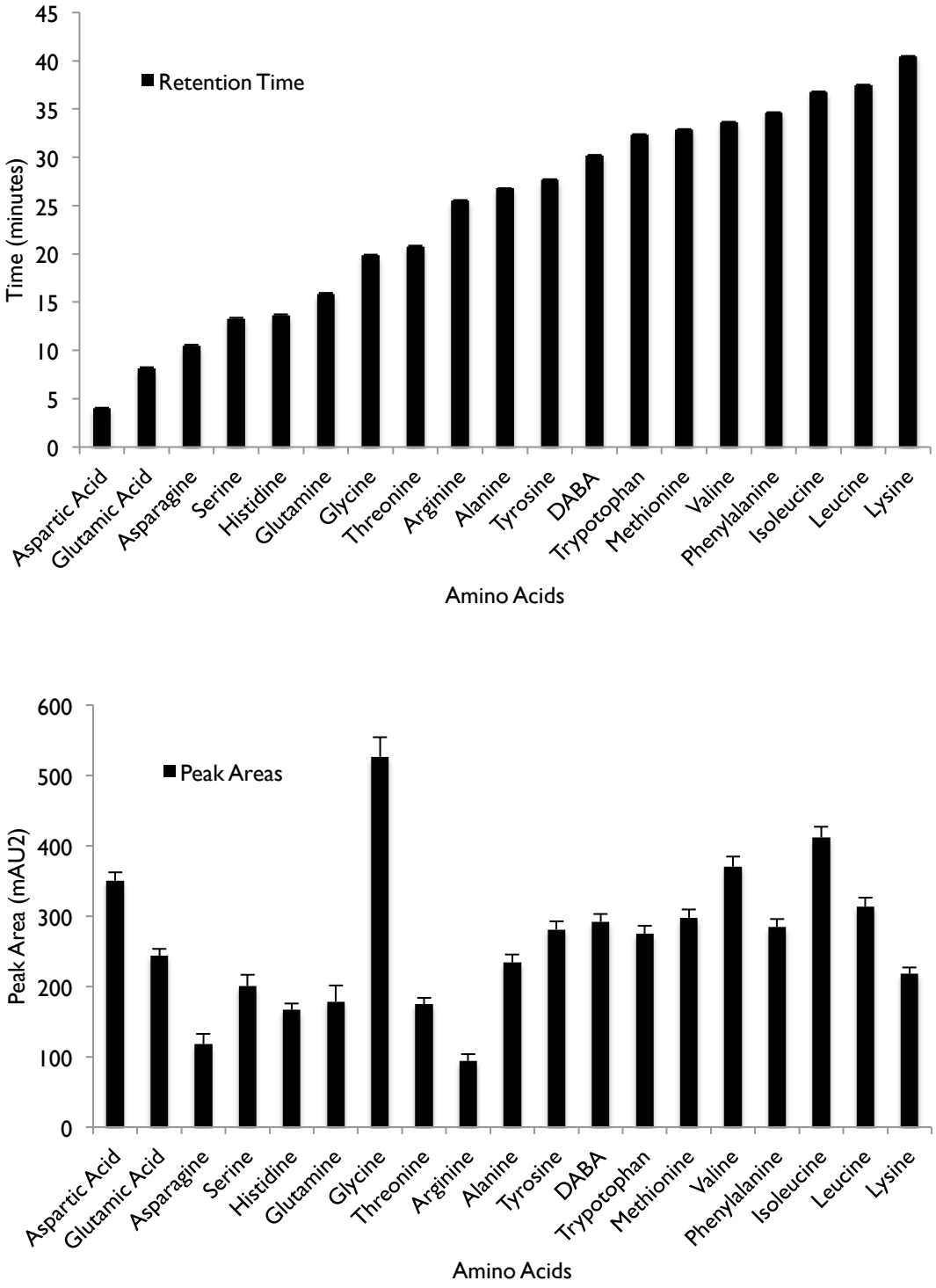

Figure 2-23: Example amino acid standard retention time and peak area. 18 standard amino acids (12.5μM)

2.8 Protein quantification

The Bio-Rad protein DC microplate assay was used to quantify proteins in this study. The microplate assay requires as little as a 5µl sample volume and the detection sensitivity is between 5-250µg/ml. A six-point protein standard was prepared ranging from 0-1.5mg/ml from 10mg/ml bovine serum albumin. 5µl of each standard was pipetted into a 90-well round bottom clear plate. For each ml of reagent A (Alkaline copper tartrate solution), 20µl of reagent S (surfactant solution) was added. 25µl of reagent A+S was pipetted into each well using a multichannel pipette. Immediately after, 200µl of reagent B (dilute folin reagent solution) was added into each well. The plate was then placed on a plate rotater for 15 minutes gently mixing the reagents before reading the absorbance at 750nm with the plate reader. A standard curve was created (Figure 2-24) and the amount of proteins in the sample was determined against the standards.

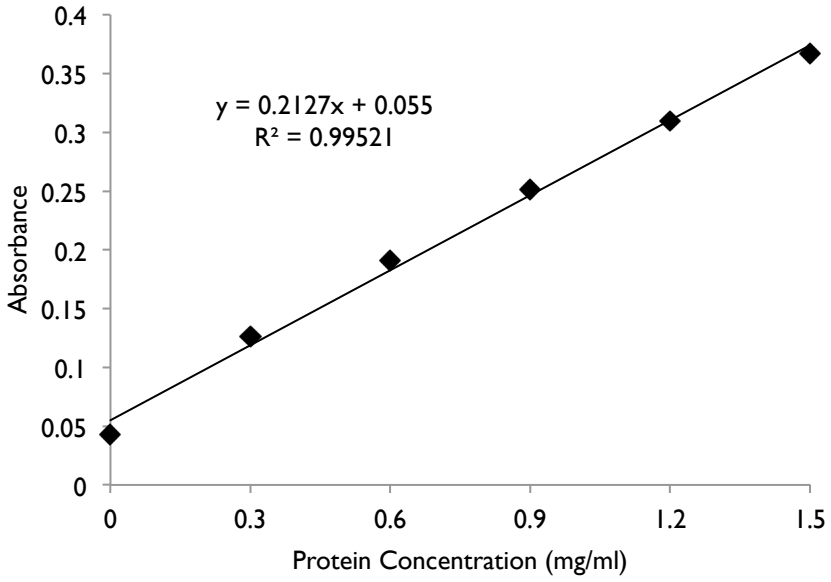

Figure 2-24: Example protein standard curve

2.9 Statistics

T-test (nonparametric tests) was used to compare two groups. Values obtained from more than three groups were compared using analysis of variance (Anova) followed by either Dunn's multiple comparisons for one-way Anova or Holm-Sidak multiple comparison test for two-way Anova. Non-linear regression (dose-response curve) was used to compare the concentration of agonist (EC_{50}) that gives half of the maximal response. Data presented as mean ± SEM for assays with three technical replicates per biological replicate or mean ± SD for three biological replicate. * represents $p<0.05$, ** $p<0.01$, *** $p<0.001$, and ****<0.0001

3. Glucose Metabolism in Platelets

3.1 Introduction

Glucose is an abundant, readily available nutrient for platelets *in situ*, yet our current understanding of platelet glucose metabolism is limited. The abundance of GLUT3 suggests that a sustained glucose transport into platelets is guaranteed even in a low glucose environment, and is indirectly indicative of the importance of glucose to platelet function, both at rest and following activation. It is well established that glucose can be catabolised by two integrated pathways to produce ATP; glycolysis and OXPHOS (Karpatkin, 1967; Cohen and Wittels, 1970; Ravi et al., 2015). However, if we are to exploit platelet metabolism as a potential biomarker or therapeutic target in various disease conditions, a better understanding of glucose metabolism beyond its mere metabolic fate is required. This includes the platelet function-specific glucose dependency, partitioning between glycolysis and OXPHOS and maximal capacity for glucose utilization.

In this chapter, a combination of enzyme-coupled fluorometric assays and XFp Seahorse bio-analyser measurements are used to profile platelet glucose uptake and metabolic fate following activation by thrombin. It is well established that most of the platelet agonists induce characteristic pattern of responses, which may be divided into weak and strong, depending on the threshold concentration required to induce full aggregation. A lower dose of a strong agonist, such as thrombin, can also act as a weak agonist (Huang and Detwiler, 1981). Consequently, the key platelet activation processes, such as shape change and secretion of granules can be distinguished using relatively low dose of a strong agonist in dose response experiments during *in vitro* platelet aggregation as described in 2.3.2. The fluorometric method chosen to examine platelet glucose metabolism is based largely on those used to study the metabolism of single early mammalian embryos (Guerif et al., 2013); thus the assay has been optimised for sensitivity in low volumes of sample. Consequently, it is possible to sample as little as 1μl at different time points of the aggregation assay for quantitative analysis of platelet function-specific glucose uptake. Alternatively, the XFp Seahorse bio-analyser allows the continuous monitoring of the interaction between different functional and metabolic responses in the same platelet suspension, with better time resolution. As mentioned previously, ADP (Weber et al., 1999) and TxA_2 (Kocsis et al., 1973) are

important mediators of platelet secondary aggregation, which have been used as drug targets for decades. The commercially available apyrase can be used to hydrolyse the ADP released, thereby preventing its action on platelets. Similarly, indomethacin can be used to inhibit the generation of TxA_2 by inhibiting the cyclooxygenase in platelets. By treating platelets with these inhibitors, it is possible to measure the energy demand placed on platelets to generate these two major mediators. Similarly, the partitioning of glucose between glycolysis and OXPHOS can be measured in real time with various agonists.

The concept of the 'metabolic capacity' of activated cells is emerging. Activatory cells have a metabolic 'scope', which enables them to respond quantitatively and sensitively to changing energy demands, despite the fact that under normal conditions, they operate at a lower metabolic rate. In this context, metabolic capacity reflects the maximum rate of the cell, an upper limit on the cellular metabolism, to respond an acute increase in energy demand (Mookerjee et al., 2016). For cells that depend on glucose as a major source of energy, glycolytic capacity is then the maximum rate of conversion of glucose to lactate that can be achieved acutely by the cell. Since the generation of lactate necessarily generates two H^+ that are exported to maintain cytosolic pH, the rate of glycolysis can be assessed by measuring the ECAR of the medium using XFp seahorse bioanalyser. OXPHOS is the major and alternative pathway in most cell types for generating ATP, and blocking this pathway with oligomycin (Figure 2-14) will force the cells to supply ATP entirely by glycolysis, thereby achieving the glycolytic capacity of the cell. In cells with limited glycolytic machinery, this is detrimental and leads to cell death. By contrast, if the cell already has a high glycolytic capacity, it is totally capable of providing ATP entirely from this pathway in the absence of OXPHOS without even reaching the maximum glycolytic capacity. Thus measuring the glycolytic capacity of platelets can provide crucial information on their energy phenotype during normal physiological conditions as well as with the development of pathology.

3.2 Aim

The **aims** of this chapter are to:

- Define the system for measuring platelet metabolism
- Quantify glucose uptake by platelets at rest and activation
- Determine the impact of secondary mediators on platelet glycolysis
- Measure the maximal glycolytic capacity of platelets at rest and following activation
- Examine the partitioning of glucose metabolism between glycolysis and oxidative phosphorylation at rest and activation

3.3 Materials & Methods

Washed platelets were prepared as described in Chapter 2 using PGE_1 method unless stated otherwise. All the chemicals and buffer compositions are provided in Appendix 1&2. Unless stated otherwise, platelets were prepared as described in 2.5.3 for the XFp assays, seeded as described in 2.5.5 and the cartridge loaded as described in 2.5.6. All the XFp experiments were corrected for protein concentrations as described in 2.8, thus, the OCR results are reported as pmol/min/μg protein, and ECAR is reported mpH/min/μg protein. Unless stated otherwise, all data are analysed from three independent experiments using platelets from three different individuals. For aggregation experiments, the data were presented as log (Thrombin dose) Vs. response (%Aggregation), from which the concentration of thrombin that gave half of the full platelet aggregation response (EC_{50}) was compared for two time points, to better represent the aggregation pattern. For representative aggregation traces, refer to Chapter 4 (Figure 4-9).

3.3.1 Choosing a system for measuring platelet metabolism

Various systems have been used for measuring platelet metabolism (Table 1-2), which may partly explain the discrepancies in current understanding of platelet metabolism. Thus, it is important to define the system in which platelet metabolism is investigated, to facilitate a better understanding of the impact of technical differences on the experimental outcome. Unwashed and washed platelets (Chapter 2.2.2) were compared functionally in the presence of glucose, to investigate the potential effect of the purity of the platelet suspension on metabolism. Also, the basal metabolic profile was compared for platelets isolated by the pH and PGE_1 methods, in terms of the basal OCR and ECAR using the XFp, to select the most appropriate platelet anti-aggregating reagent.

3.3.1.1 Aggregation of washed vs. unwashed platelets with thrombin

Washed and unwashed human platelets were prepared as described in 2.2.2. PRP was split into two equal volumes in a 15ml falcon tube after treating with PGE_1 to

generate two separate pellets. One of the pellets was re-suspended in Tyrode's buffer containing 5.6mM glucose (Appendix 2) without a further wash step and the other, after a wash step (Appendix 2). Platelets were counted as described in 2.2.3, and the final platelet count adjusted to 2.5 $*10^8$ platelets/ml. Platelet aggregation was carried out for 3.5 minutes/dose on both suspensions with thrombin. Thrombin was added at 0.01, 0.0125, 0.025, 0.05 and 0.1U/ml. Aggregation experiments were carried out starting from the highest dose of thrombin and alternating between washed and unwashed platelet suspensions, for each dose.

3.3.1.2 Aggregation of washed vs. unwashed platelets with collagen

Platelet aggregation with collagen was carried out as for thrombin in 3.3.1.1. Collagen was added at 0.5, 1, 2.5, 5 and 10μg/ml. The aggregation experiment was carried out starting from the highest dose of collagen and alternated in between washed and unwashed groups for each dose.

3.3.1.3 XFp Cell seeding density

To examine the bioenergetics function of a specific cell type effectively, it was essential to characterise metabolic activity under basal and test conditions. To generate metabolic rate within the dynamic rage of the XFp, it is recommended that the cells should cover 50-90% of the XFp cell culture miniplate, with visual assessment suitable for approximation (XFp basic procedure, Agilent). The XFp mitochondrial stress test described in 2.6.2 was used to optimise cell-seeding density. Three different cell concentrations, $5*10^7$, $8*10^7$ and $1*10^8$ platelets/ml were prepared. Each cell concentration was seeded in duplicate (Figure 3-1). The cartridge was loaded with the drug concentrations recommended by the XFp mitochondrial stress test kit (Agilent) shown in table 3-1. Mitochondrial indices were measured.

Table 3-1: Inhibitors and working concentrations for cell seeding density

Ports	Compounds	Stock	Cartridge	Well
A	Oligomycin	10mM	10μM	1μM
B	FCCP	50mM	10μM	1μM
C	A/R	5mM	5μM	0.5μM

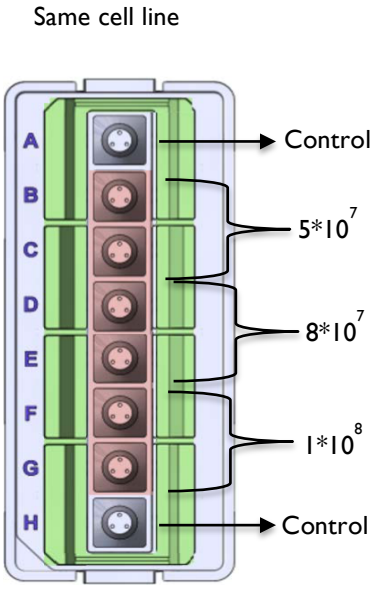

Figure 3-1: XFp cell seeding density optimization. A&H wells were not seeded with cells; H well was treated with inhibitors.

3.3.1.4 Comparison of basal ECAR and OCR of platelets isolated with the pH or PGE_1 method

The basal ECAR and OCR rate of platelets isolated with pH and PGE_1 methods were compared using XFp assay. Washed platelets were isolated as described in 2.2.2. PRP was split into two equal volumes in a 15ml falcon tube. One was treated with citric acid (pH method) while the other was treated with PGE_1. For platelets that were treated with the pH method, the final pellet was directly re-suspended in 200µl of PBS, counted and diluted to $1*10^8$/ml platelets in XFp assay medium (Appendix 2) containing 5.6mM of glucose. With the PGE_1 method, platelets were prepared as described in 2.5.3 (Kramer et al., 2014; Ravi et al., 2015). The cells were seeded as shown in Figure 2-11, Left. Six measurements were taken for OCR and ECAR, and the means calculated.

3.3.2 Glucose uptake by resting and activated platelets

Experiments were conducted to determine the rate of glucose depletion by platelets in response to various doses of thrombin quantitatively. The details of each experiment are given below.

3.3.2.1 Glucose uptake by resting platelets

Washed platelets from three different donors were re-suspended in Tyrode's buffer (Appendix 2) containing 5.6mM glucose at two different cell counts; $3*10^8$ platelets/ml and $5*10^8$ platelets/ml. Platelet suspensions were kept in an incubator at 37 °C during the entire experiment. 10μl of sample was taken every 30 minutes for 120 minutes in total and the glucose was determined using the enzyme-coupled fluorometric assay as described in Chapter 2.4.

3.3.2.2 Glucose uptake by platelets with high dose thrombin

Platelet aggregation was carried out as described in 2.3.2. Washed platelets ($2.5*10^8$ platelets/ml) were stimulated with 0.1U/ml of thrombin. 10μl of sample was taken out at 0, 1, 3, 5, 7 and 9^{th} minute for the analysis of glucose concentration using enzyme-coupled fluorometric assay as described in 2.4. Time 0 was defined as the injection of thrombin. The time between platelet re-suspension in modified Tyrode's buffer (5.6mM glucose) and aggregation was recorded and kept the same for every experiment. The resting rate of glucose consumption was calculated for the time, from starting the stirring for aggregation experiment for calibration, until time 0.

3.3.2.3 Glucose uptake by platelets with low dose thrombin

Platelet aggregation was carried out as described in 2.3.2. Washed platelets ($2.5*10^8$ platelets/ml) were stimulated with 0.01U/ml of thrombin. The experimental procedure was as in 3.3.2.2.

3.3.2.4 The effect of secondary mediators on platelet glycolysis

Washed platelets were re-suspended in XFp assay medium containing 5.6mM glucose. Cells were split into three equal portions; one was kept as control, one was treated with 2U/ml apyrase, and one treated with 10μM indomethacin. All the samples were incubated for 20 minutes in a non-CO_2 incubator at 37 °C before being seeded into XFp plates as shown in Figure 3-2. Cells were stimulated with 0.1U/ml thrombin. ECAR was measured as a qualitative analysis for glycolysis.

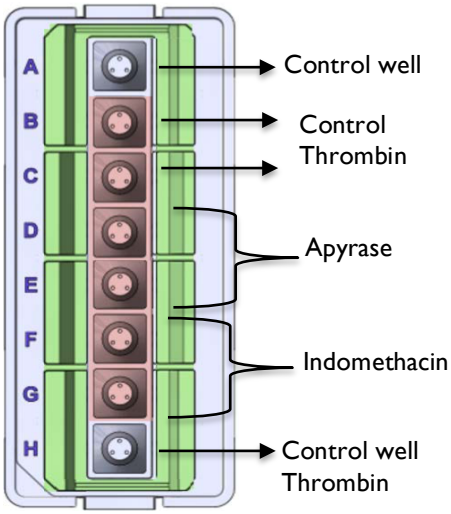

Figure 3-2: Cell seeding plan for measuring the effect of secondary mediators on platelet glycolysis. A & H wells were kept as absolute controls with no cells; H well was injected with the same amount of thrombin as the other wells to correct for protein content. B & C wells were kept as cell and cell thrombin controls. D & E wells were seeded with platelets treated with apyrase. F & G wells were seeded with platelets treated with indomethacin.

3.3.3 Glycolytic Capacity of resting and activated platelets

The 'scope' of platelet glycolysis under resting and activated conditions was investigated using thrombin. The receptor mediation of thrombin induced glycolytic response was also investigated using the commercially available peptide fragments of thrombin-dependent PARs, PAR1 (SFLLRN) and PAR4 (AYPGKF) receptor agonists, from Cambridge Bioscience, UK.

3.3.3.1 Glycolytic capacity of platelets at rest and following activation with thrombin

Washed platelets were re-suspended in glucose-free XFp assay medium (Appendix 2). Platelets were seeded into XFp plates from B to G wells. A and H wells were left as absolute controls without cells. Well A was injected with same compounds with B to D wells. Well H was injected with same compounds with E to G wells (Figure 3-3). Cells were stimulated with 0.1U/ml thrombin and ECAR was measured. The concentration of oligomycin required to induce maximum glycolytic rate was determined using the cell mitochondrial test similar to that shown in Table 3-1 and OCR was measured.

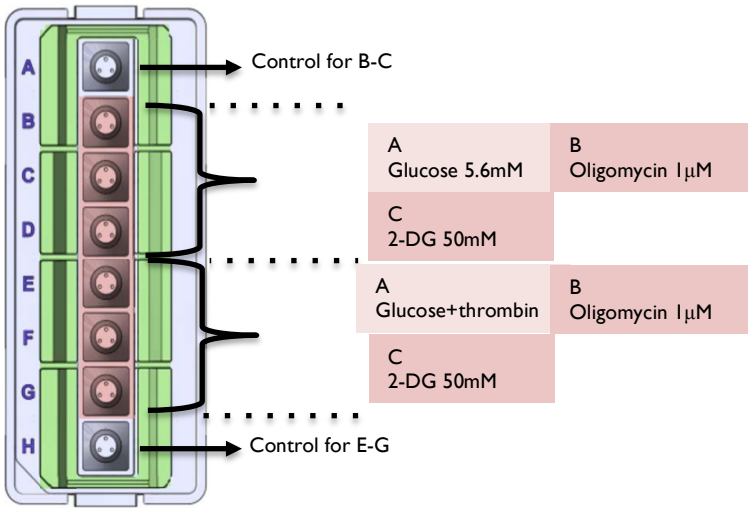

Figure 3-3: Cartridge compound loading map for measuring platelet glycolytic capacity. Platelets are stimulated with 0.1U/ml thrombin. The final well concentrations of the compounds added are shown.

3.3.3.2 Glycolytic capacity of platelets with PAR1

Washed platelets were re-suspended in XFp assay medium (Appendix 2) containing 5.6mM glucose. The experimental procedures were the same as in 3.3.3.1. Three different dose of PAR1 were used instead of thrombin, as shown in Figure 3-4.

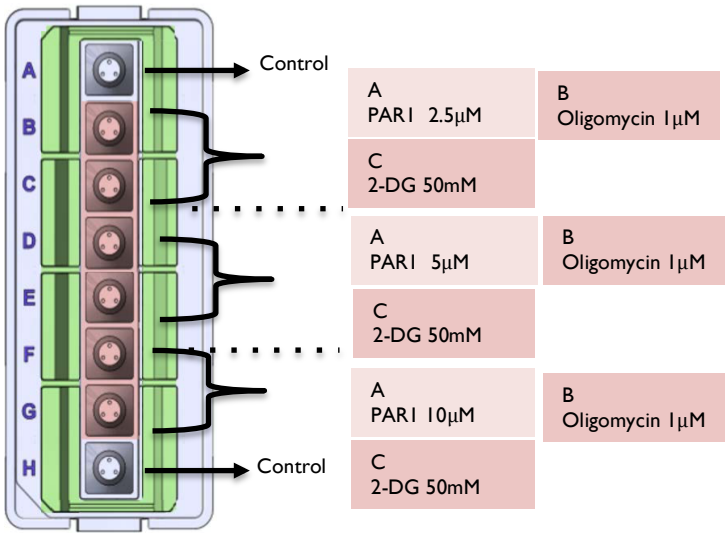

Figure 3-4: Cartridge compound loading map for measuring platelet glycolytic function with PAR1. The final well concentrations of the compounds added are shown.

3.3.3.3 Glycolytic capacity of platelets with PAR4

Glycolytic capacity of platelets with various concentrations of PAR4 was carried out as described for PAR1 in 3.3.3.2. The cartridge compound-loading map is shown in Figure 3-5.

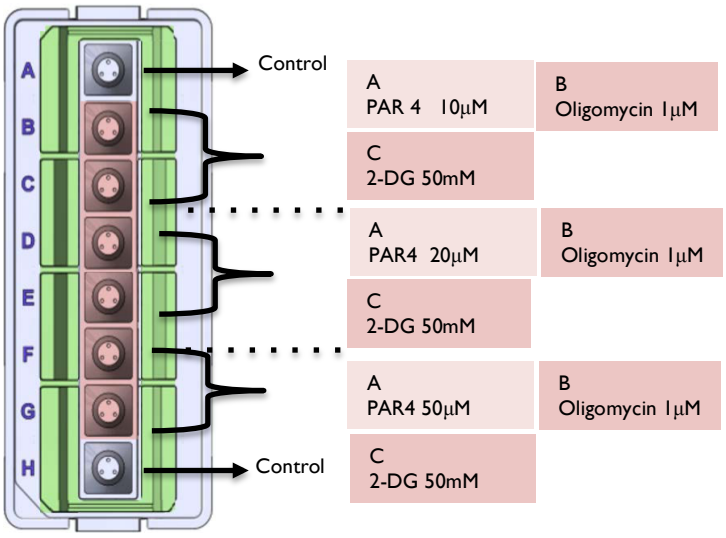

Figure 3-5: Cartridge compound loading map for measuring platelet glycolytic function with PAR4. The final well concentrations of the compounds added are shown.

3.3.4 Glycolytic and oxidative metabolism of glucose

In this series of experiments, thrombin dose-dependent glycolysis and OXPHOS were measured using the XFp assay. In addition, thrombin dependent partitioning of glucose between glycolysis and OXPHOS was measured. Platelets were re-suspended in XFp assay medium containing 5.6mM glucose. Further experimental details are described below.

3.3.4.1 OCR & ECAR of platelets stimulated with thrombin

Platelets were seeded onto a XFp plate from B to G wells and treated with 0.01 and 0.1U/m thrombin as shown in Figure 3-6. OCR and ECAR were measure simultaneously.

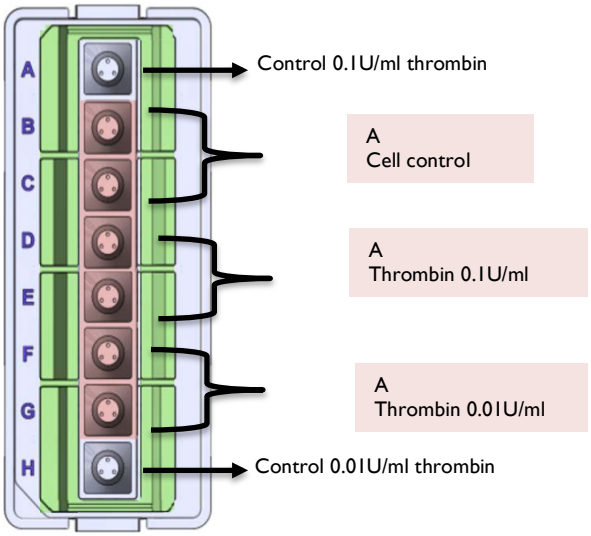

Figure 3-6: Cartridge compound loading map for measuring OCR & ECAR. Platelets are stimulated with either 0.01 or 0.1U/ml thrombin. The final well concentrations of the compounds added are shown.

3.3.4.2 Partitioning of glucose metabolism between OXPHOS and glycolysis with high dose thrombin

Platelets were seeded onto a XFp plate from B to G wells and treated with sequential injections of etomoxir, media/thrombin, a combination of antimycin and rotenone (A/R), and finally with 2-DG as shown in Figure 3-7. OCR and ECAR were measured simultaneously.

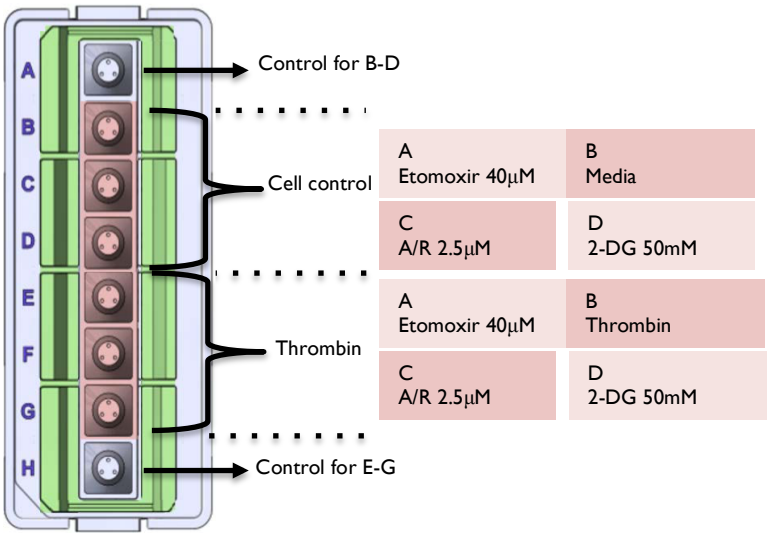

Figure 3-7: Cartridge compound loading map for measuring the partitioning of glucose between OXPHOS and glycolysis. The final well concentrations of the compounds added are shown.

3.3.4.3 Partitioning of glucose metabolism between OXPHOS and glycolysis with low dose thrombin

Partitioning of glucose between OXPHOS and glycolysis was measured in response to 0.01U/ml thrombin, as described in 3.3.4.2.

3.3.4.4 Energy phenotype of platelets in the basal state and after activation with thrombin

Platelets were seeded onto the XFp plate from B to G wells. The experiment was carried out as described in 2.6.4. The cartridge compound-loading map was shown in Table 2-8.

3.4 Results

3.4.1 Choosing a system for measuring platelet metabolism

3.4.1.1 Aggregation of washed vs. unwashed platelets with thrombin

Aggregation responses of washed and unwashed platelets were compared in Tyrode's buffer containing glucose (Appendix 2) and with various doses of thrombin. The aggregation was carried out for three and half minutes, however, the data were analysed at 1.5 and 3 minutes of aggregation to better understand the aggregation pattern. The EC_{50} values for washed and unwashed platelets at 1.5 minute were 0.08 and 0.03, respectively ($p<0.0001$). Similarly, the EC_{50} values for 3 minutes were 0.04 for washed platelets but only 0.003 for unwashed platelets ($p<0.0001$) (Figure 3-8A, B).

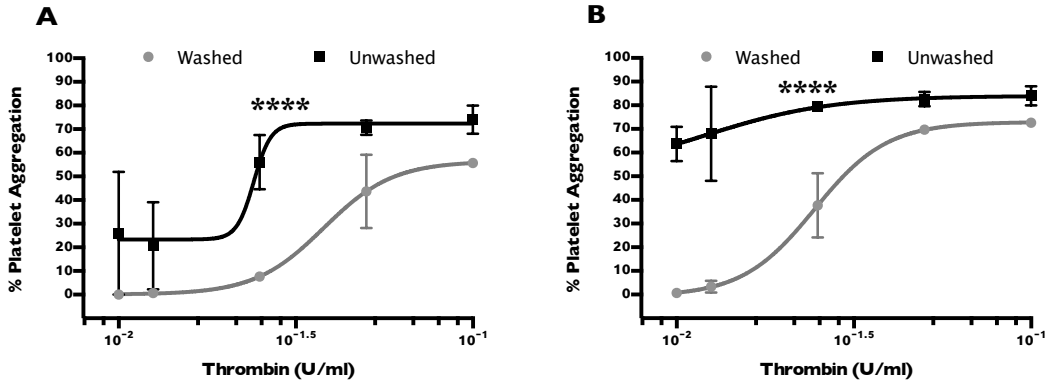

Figure 3-8: Aggregation of washed & un-washed platelet with thrombin. Data presented as log (Thrombin dose) Vs. response (%Aggregation), n=3. (A) Dose response curve for platelets stimulated with 0.01, 0.0125, 0.025, 0.05 and 0.1U/ml thrombin in Tyrode's buffer at 1.5 minutes. (B) Dose response curve for platelets stimulated with 0.01, 0.0125, 0.025, 0.05 and 0.1U/ml thrombin in Tyrode's buffer at 3 min. EC_{50} was compared for each data set, ****<0.0001.

3.4.1.2 Aggregation of washed vs. unwashed platelets with collagen

Aggregation responses of washed and unwashed platelets in response to various doses of collagen were compared in Tyrode's buffer containing glucose at 1.5 and 3 minutes of aggregation as for thrombin in Figure 3-8. The EC_{50} at 1.5 for washed and unwashed platelets were 14.75 and 0.33, respectively ($p<0.0001$). Similarly, the EC50 at 3 minutes was different for washed (5.7) and unwashed (0.3) platelets ($p<0.0001$) (Figure 3-9A, B).

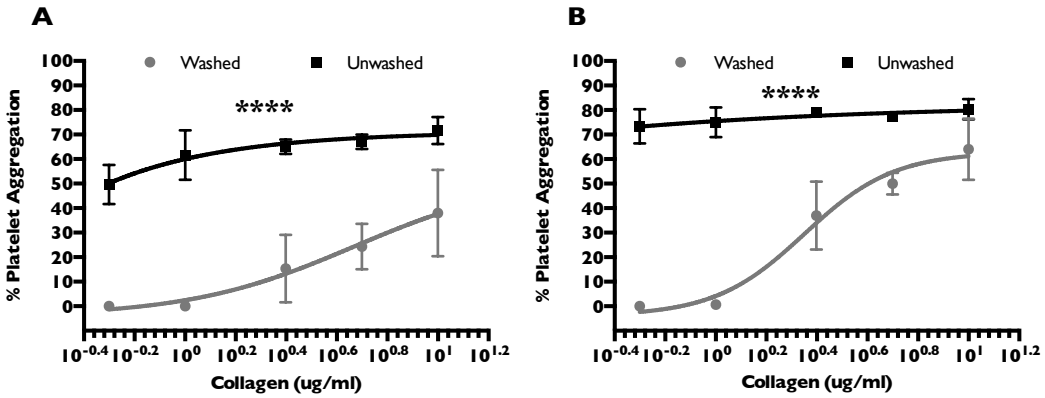

Figure 3-9: Aggregation of washed & un-washed platelets with collagen. Data presented as log (collagen dose) Vs. response (%Aggregation), n=3. (A) Dose response curve for platelets stimulated with 0.5, 1, 2.5, 5 and 10μg/ml collagen in Tyrode's buffer at 1:30 minutes. (B) Dose response curve for platelets stimulated with 0.5, 1, 2.5, 5 and 10μg/ml collagen in Tyrode's buffer at 3 minutes. EC_{50} was compared for each data set, ****<0.0001.

3.4.1.3 XFp cell seeding density

OCR was measured using the cell mitochondrial stress test for three different cell concentrations, $5*10^7$, $8*10^7$ and $1*10^8$ platelets/ml (Figure 3-10). $5*10^7$platelets/ml of cell concentration was too low for detecting OCR in this experimental condition. Although $8*10^7$ platelets/ml gave reasonable basal OCR, platelets did not survive the subsequent oligomycin injection. $1*10^8$ platelets/ml gave readings that were significantly and proportionally higher than the lower concentrations. Platelets remained viable throughout the experiment and the OCR was comparable with that published by Ravi et al., (2015). On the basis of these data and visual observation of the plate coverage, $1*10^8$ platelets/ml was used for XFp experiments throughout this study.

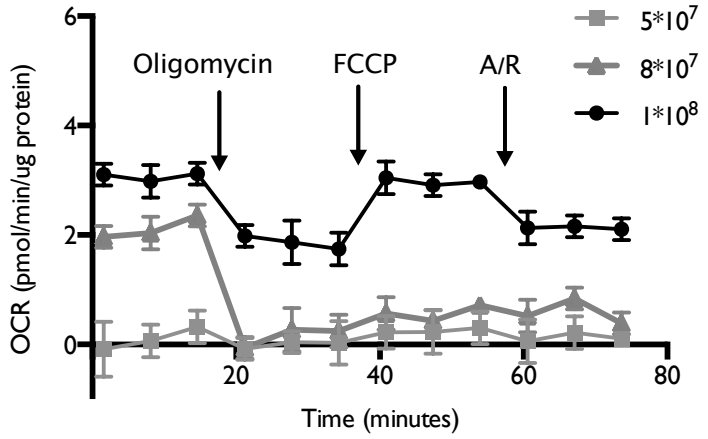

Figure 3-10: XFp mitochondrial stress test for cell seeding density optimization. OCR was measured with the sequential injection of oligomycin (1μM), FCCP (1μM) and the combination of antimycin and rotenone (A/R; 0.5μM) for three different cell concentrations $5*10^7$, $8*10^7$ and $1*10^8$ platelets/ml. Mean ± SEM, n=3.

3.4.1.4 Basal ECAR and OCR of platelets isolated with pH Vs. PGE_1 method

The basal metabolic profile, as indicated by platelet oxygen consumption and extracellular acidification, was compared between platelets isolated by the pH and PGE_1 methods. Mean OCRs of platelets isolated with the pH and PGE_1 methods were 2.96±1.6 pmol/min/μg protein and 2.6±0.3 pmol/min/μg protein (Figure 3-11A). The values were not significantly different ($p>0.05$). Mean ECARs of platelets isolated with pH and PGE_1 methods were 1.87±1.8 mpH/min/μg protein and 1.65±0.6 mpH/min/μg protein (Figure 3-11B). The values were not significantly different ($p>0.05$).

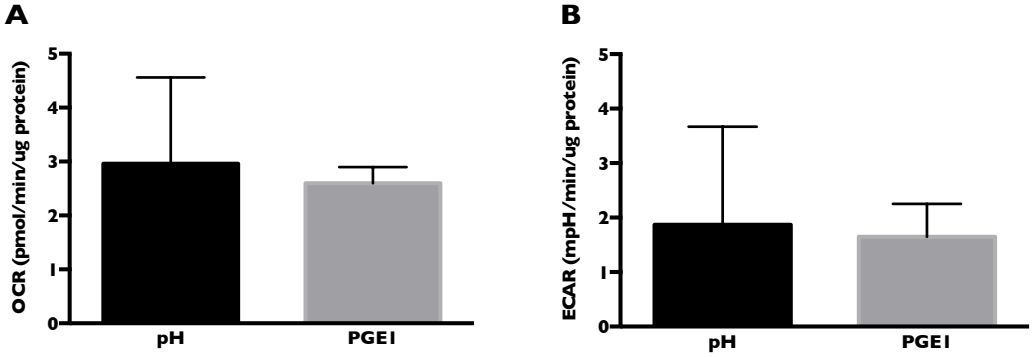

Figure 3-11: Comparison of basal OCR & ECAR. (A) Average OCR of platelets isolated with pH (2.96±1.6 pmol/min/ug protein) and PGE_1 (2.6±0.3 pmol/min/ug protein) methods over six measurements (40 mins). Data shown as mean OCR±SEM, n=3. (B) Average ECAR of platelets isolated with pH (1.87±1.8 mpH/min/ug protein) and PGE_1 (1.65±0.6 mpH/min/ug protein) methods over six measurements. Data shown as mean ECAR±SEM, n=3.

3.4.2 Glucose uptake by resting and activated platelets

3.4.2.1 Glucose uptake by resting platelets

There was a linear decrease in the concentration of glucose in the medium over time for both cell concentration, $3*10^8$ platelets/ml and $5*10^8$ platelets/ml (Figure 3-12, A, B). It is noteworthy that there was apparently considerable variation in glucose depletion rate of platelets from different donors but the differences were not significant ($p>0.05$). The mean rate of glucose depletion from the medium was calculated for both cell numbers and different donors, and did not differ significantly ($p>0.05$).

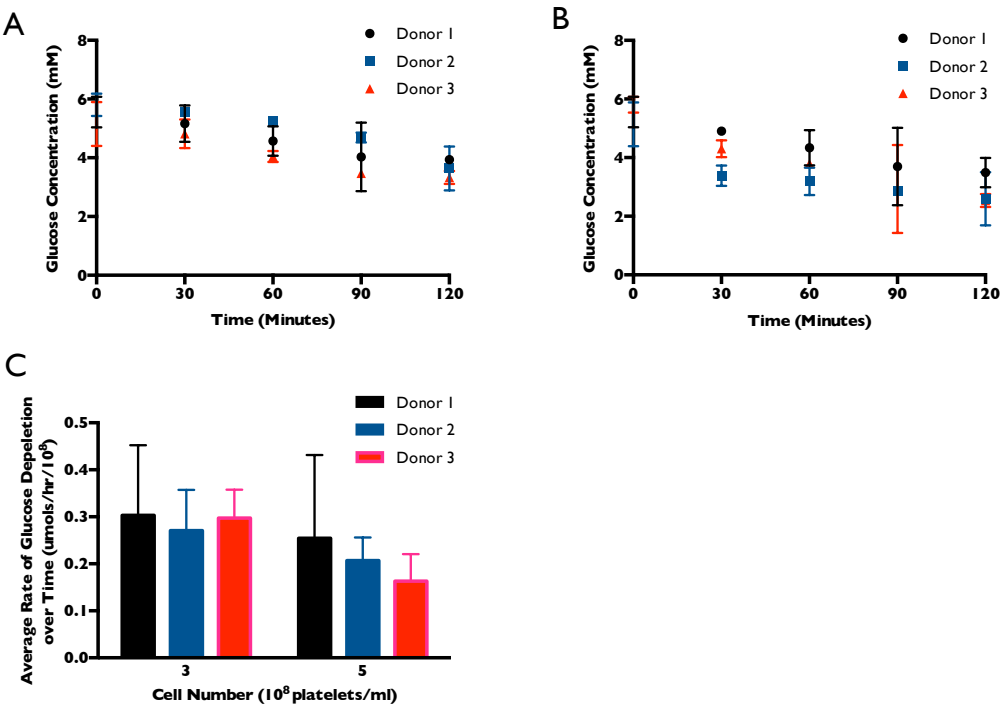

Figure 3-12: Glucose consumption of platelets at rest from different donors. (A) Glucose concentration in the media containing $3*10^8$ platelets/ml over 120 minutes from three different donors with samples taken every 30 minutes (B) Glucose concentration in the media containing $5*10^8$ platelets/ml over 120 minutes from three different donors, with samples taken every 30 minutes (C) Mean rate of glucose depletion by platelets over 120 minutes for two cell concentrations from three different donors, calculated from A&B. The data were shown as mean± SD, n=3. The rate of glucose consumption was calculated as μmol/hr/10^8 for two different cell concentrations for three different donors.

3.4.2.2 Glucose uptake by platelets with high dose thrombin

Under basal conditions, platelets depleted glucose from the medium at a steady rate (0.03±0.03µmol/min/10^8 cells). Stimulation with the potent agonist thrombin (0.1U/ml) induced aggregation (Figure 3-13A) and increased glucose depletion from the medium 15-fold (0.50±0.19 µmol/min/10^8 cells; $p<0.05$) over the first minute (Figure 3-13B). This initial burst of glucose uptake declined over time, falling to 0.24±0.09 µmols/min/10^8 ($p<0.05$) cells over the next two minutes and had returned to basal levels by three minutes post thrombin stimulation (Figure 3-13A and B).

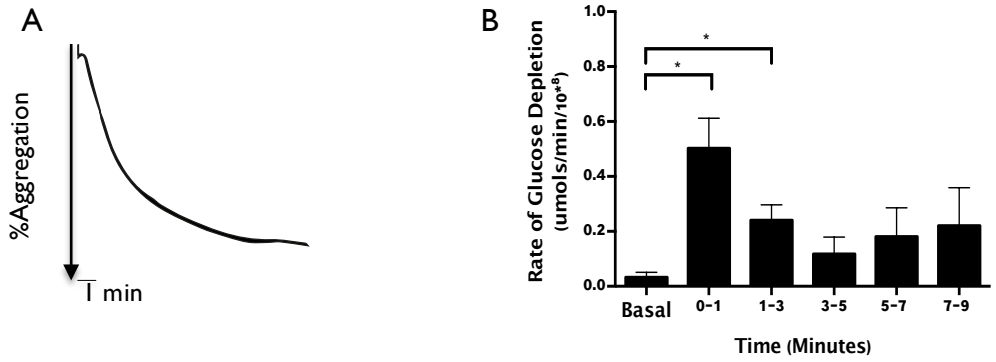

Figure 3-13: High dose thrombin-induced glucose depletion from the medium by platelets (A) Representative aggregation trace of platelets stimulated with 0.1U/ml thrombin (n=3). (B) Upon stimulation with 0.1U/ml thrombin, there was a significant increase in the rate of glucose depletion from the media within first minute ($p<0.05$), which was sustained until the third minute ($p<0.05$). Data shown as mean ± SEM, n=3, *<0.05.

3.4.2.3 Glucose uptake by platelets with low dose thrombin

To differentiate the primary and secondary aggregation responses, the dose of thrombin was reduced. Stimulation with thrombin (0.01U/ml) led to a delayed primary aggregation response followed by a secondary response beginning around 5 minutes post treatment (Figure 3-14A). Under these conditions, a biphasic depletion of glucose was observed that was linked to the aggregation response. The rate of glucose depletion increased 8-fold (0.03±0.004 µmol/min/10^8 to 0.28±0.03 µmols/min/10^8; $p<0.001$) within the first minute and was maintained for up to 5 minutes as aggregation plateaued. Interestingly, glucose uptake then increased again to 0.54±0.1 µmols/min/10^8 ($p<0.001$ compared to basal) as the secondary aggregation response was initiated (Figure 3-14A, B). The rate of glucose depletion for the secondary aggregation response (5-7min) was significantly higher ($p<0.05$) than the initial aggregation response (1-3 min).

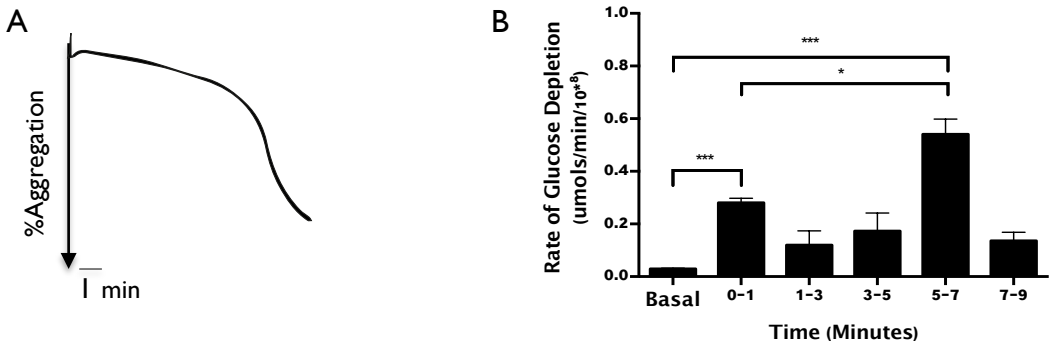

Figure 3-14: Low dose thrombin-induced glucose depletion from the medium by platelets (A) Representative aggregation trace of platelets stimulated with 0.01U/ml thrombin (n=3). (B) Upon stimulation with 0.01U/ml thrombin, there was a significant increase in glucose depletion rate from the media within first minute and a second rise at 5-7 minutes ($p<0.001$, $p<0.001$). The rate of glucose depletion for the secondary aggregation response (5-7min) was significantly higher ($p<0.05$) than the initial aggregation response (1-3 min). Data shown as mean ± SEM, n=3. *<0.05, ***<0.001.

3.4.2.4 The effect of secondary mediators on platelet glycolysis

Platelet derived mediators are required to amplify the wider functions of platelets. It was reasoned that given that two such mediators, ADP and TxA_2, were required to potentiate platelet activation they might also influence platelet glycolysis (Figure 3-15). Stimulation with thrombin increased ECAR significantly in both apyrase and indomethacin treated platelets ($p<0.0001$). Inhibition of platelet derived ADP with apyrase decreased ECAR in response to thrombin; however, the effect was not as significant as indomethacin. In contrast, inhibition of TxA_2 generation by indomethacin significantly reduced thrombin induced ECAR from 4.2 ± 0.7 mpH/min/μg protein to 3.4 ± 0.6 mpH/min/μg protein ($P<0.05$).

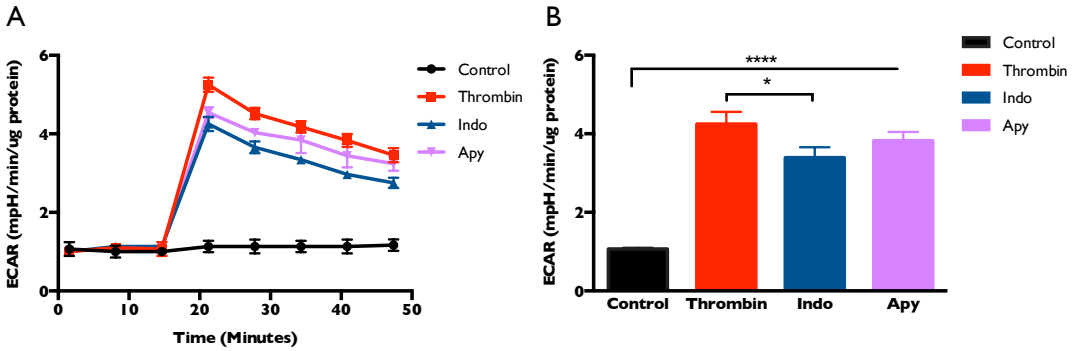

Figure 3-15: The effect of secondary mediators on platelet glycolysis. (A) ECAR of platelets in the presence of thrombin (0.1U/ml), thrombin with apyrase (2U/ml) and thrombin with indomethacin (10μM). (B) Average ECAR quantified from (A). Data shown as mean ± SEM, n=3. *<0.05, ****<0.0001

3.4.3 Glycolytic Capacity of resting and activated platelets

3.4.3.1 Glycolytic capacity of platelets at rest and following activation with thrombin

The glycolytic capacity of platelets at rest and after activation was assessed using the XFp glycolytic stress test (2.6.1). After establishing a basal ECAR in glucose-free XFp medium, 5.6mM of glucose was injected (Figure 3-16A). ECAR increased from 0.7 to 1.63 ± 0.6 mpH/min/μg protein ($p<0.01$), giving the basal glycolytic function of platelets when extracellular glucose was provided. The injection of mitochondrial complex V inhibitor oligomycin further elevated the ECAR to a maximum of 4.03 ± 0.2 mpH/min/μg protein ($p<0.001$), resulting in a shift towards glycolysis for ATP generation in the absence of mitochondrial ATP. The addition of 2-DG ablated the ECAR, indicating that the ECAR was from glycolysis and there was minimum non-glycolytic ECAR. Platelets were activated by injecting glucose and thrombin (0.1U/ml) together, which prompted a notable rise in ECAR from 0.63 ± 0.06 to a maximum of 5.9 ± 0.4 mpH/min/μg protein ($p< 0.01$). As observed previously (Figure 3-13 & Figure 3-15), the glycolytic rate fell over time prior to the injection of oligomycin, which increased the ECAR to 5.43 ± 0.4 mpH/min/μg protein. The thrombin and thrombin + oligomycin-induced ECAR were both higher than oligomycin alone, indicating that the glycolytic capacity of stimulated platelets is higher than that of un-stimulated. The addition of 2-DG caused ECAR to fall, again indicative that this ECAR was from glycolysis and that platelets express minimal non-glycolytic ECAR (Figure 3-16B). For the cell concentration of $1*10^8$ platelets/ml, 1μM oligomycin was optimal as platelets did not respond to FCCP with 2μM oligomycin (Figure 3-16C).

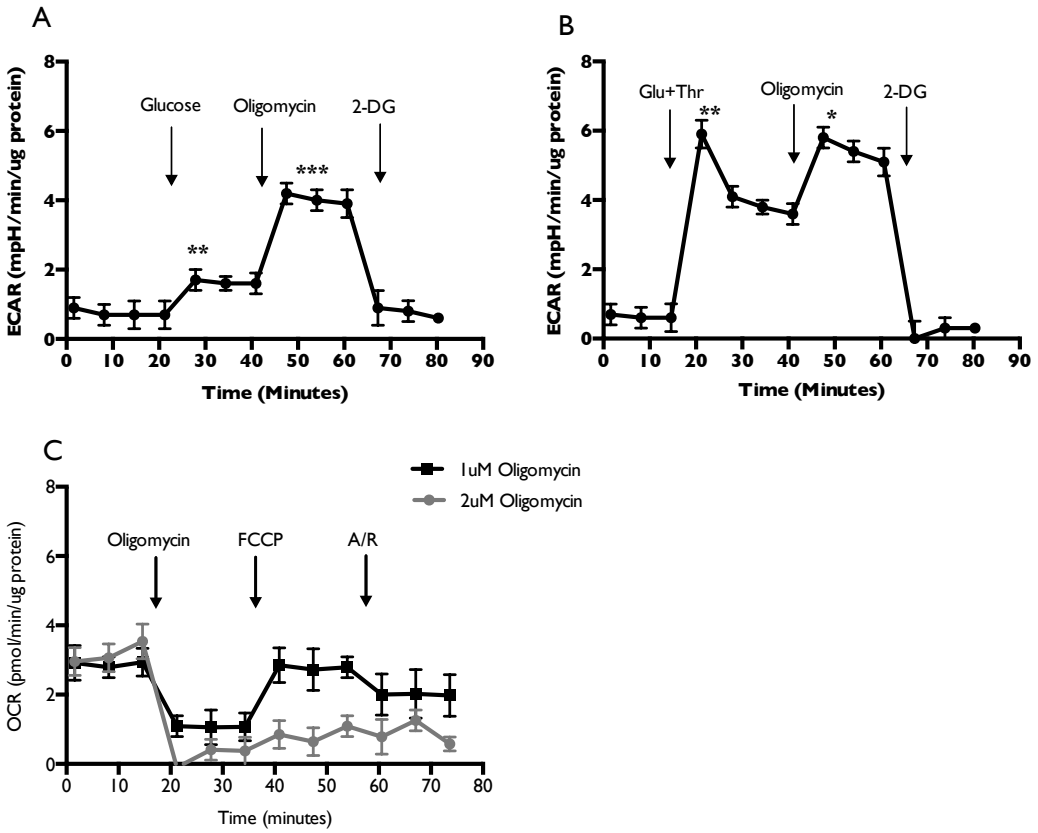

Figure 3-16: Glycolytic capacity of platelets at rest and following activation. (A) ECAR of platelets with sequential injection of glucose (5.6mM), oligomycin (1μM) and 2-deoxy glucose (2-DG, 50mM). The injection of glucose increased ECAR significantly ($p<0.01$). Oligomycin further increased ECAR ($p<0.001$). 2-DG was added to correct for non-glycolytic extracellular acidification. (B) ECAR of platelets with sequential injection with glucose and thrombin (0.1U/ml) combined, oligomycin and 2-DG. Thrombin stimulation increased ECAR markedly ($p<0.01$) above basal ECAR. Oligomycin further increased ECAR ($p<0.05$). (C) Oligomycin concentrations were optimised in order to achieve complete inhibition of OXPHOS and thereby maximise glycolysis. 1μM and 2μM of oligomycin were tested using the cell mitochondrial stress test for $1*10^8$ platelets/ml. FCCP (1μM) and A/R (0.5μM). Data shown as mean ± SEM, n=3. *<0.05, **<0.01,***<0.001.

3.4.3.2 Glycolytic capacity of platelets with PAR1

The interaction of thrombin with platelets is achieved by a small family of G-protein coupled PARs. Human platelets express PAR1 and PAR4; activation of either is sufficient to trigger platelet activation (Coughlin, 2000). The synthetic peptides of PAR1 (SFLLRN) and PAR4 (AYPGKF) receptor agonists were used to discover whether there were differences in the glycolytic function of platelets induced by these two different signalling peptides. Basal glycolytic rate (0.9 ± 0.6 mpH/min/μg protein) of platelets at rest was established in glucose-containing XFp medium (5.6mM) (Figure 3-17A, B). The injection of 5μM and 10μM PAR1 induced comparable rises in ECAR, to 3.5 ± 0.6 and 3.56 ± 0.5mpH/min/μg protein respectively (Figure 3-17B). This was not surprising given that the aggregation response induced by 5μM and 10μM PAR1 was almost similar (Figure 3-17C). However, 2.5μM PAR1 induced a smaller rise in ECAR (2.3 ± 0.5 mpH/min/μg protein; $p<0.001$). As a result, 2.5μM PAR1 induced the smallest oligomycin-induced ECAR (4.4 ± 0.05 mpH/min/μg protein) compared to 5 and 10μM PAR1 (5.8 ±0.1 and 5.5 ± 0.1 mpH/min/μg protein), indicating that the glycolytic response to PAR agonists was dose dependent.

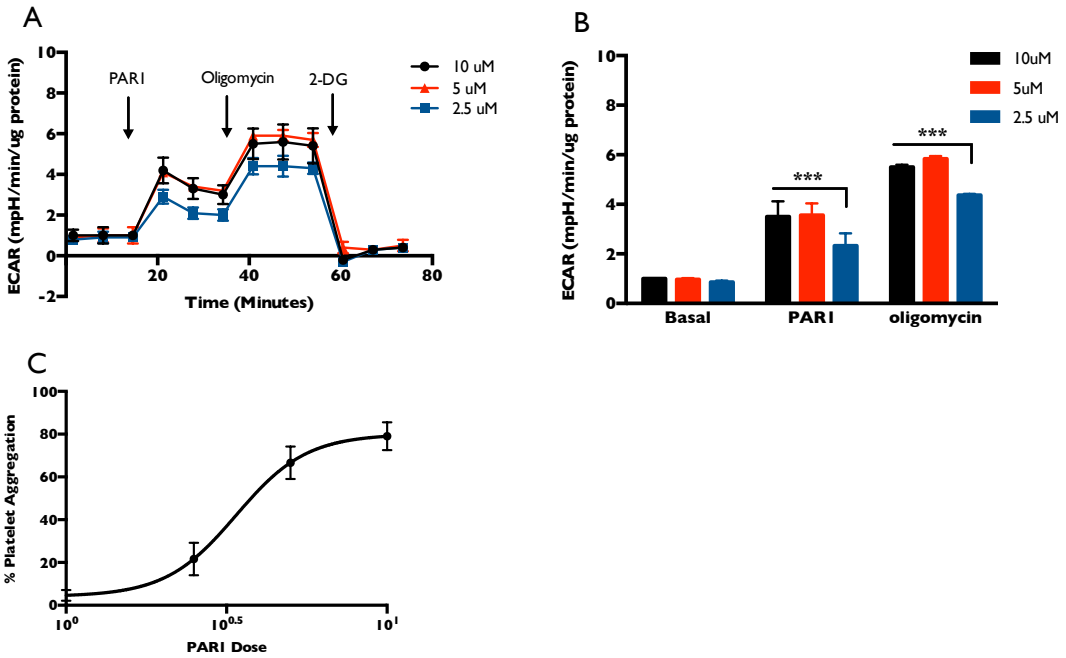

Figure 3-17: Glycolytic capacity of platelets with various doses of PAR1 (A) ECAR of platelets stimulated with 2.5, 5, and 10μM of PAR1. Oligomycin and 2-DG were injected subsequently to obtain the maximum glycolytic capacity and non-glycolytic ECAR of platelets. (B) ECAR was quantified from A after correction for non-glycolytic ECAR. ECAR increased in a dose dependent manner compared to basal when stimulated with increasing doses of PAR1. 2.5μM of PAR1 induced less ECAR compared to both 5 & 10μM PAR1 ($p<0.001$). Similarly, the glycolytic shift with 2.5μM PAR1 upon oligomycin injection was the lowest compared to 5 & 10μM PAR1 ($p<0.001$) Data shown as mean ± SEM, n=3. (C) Dose response curve of platelet aggregation when stimulated with 1, 2.5, 5 and 10μM PAR1 for three minutes; Data shown as mean ± SD, n=3. ***<0.001.

3.4.3.3 Glycolytic capacity of platelets with PAR4

Like PAR1 (SFLLRN), the glycolytic capacity of platelets stimulated with various doses of PAR4 (AYPGKF) was assessed (Figure 3-18). The basal glycolytic rate of resting platelets was 0.93 ± 0.6 mpH/min/μg protein (Figure 3-18A, B). The addition of 20μM and 50μM of PAR4 induced a comparable rise in ECAR, to 2.4 ± 0.5 and 2.6 ± 0.5 mpH/min/μg protein respectively (Figure 3-18B). This was not surprising given that the aggregation response induced by 20μM and 50μM PAR4 was similar (Figure 3-18C). However, 10μM PAR4 induced less significant rise in ECAR: 1.6 ± 0.2 mpH/min/μg protein ($p<0.001$). As a result, 10μM PAR4 induced the lowest oligomycin-induced ECAR (3.1 ± 0.06 mpH/min/μg protein) compared to 20 and 50μM PAR4 (4.1 ±0.1 and 4.03 ± 0.05 mpH/min/μg protein), indicating that the glycolytic response induced by PAR4 was dose dependent.

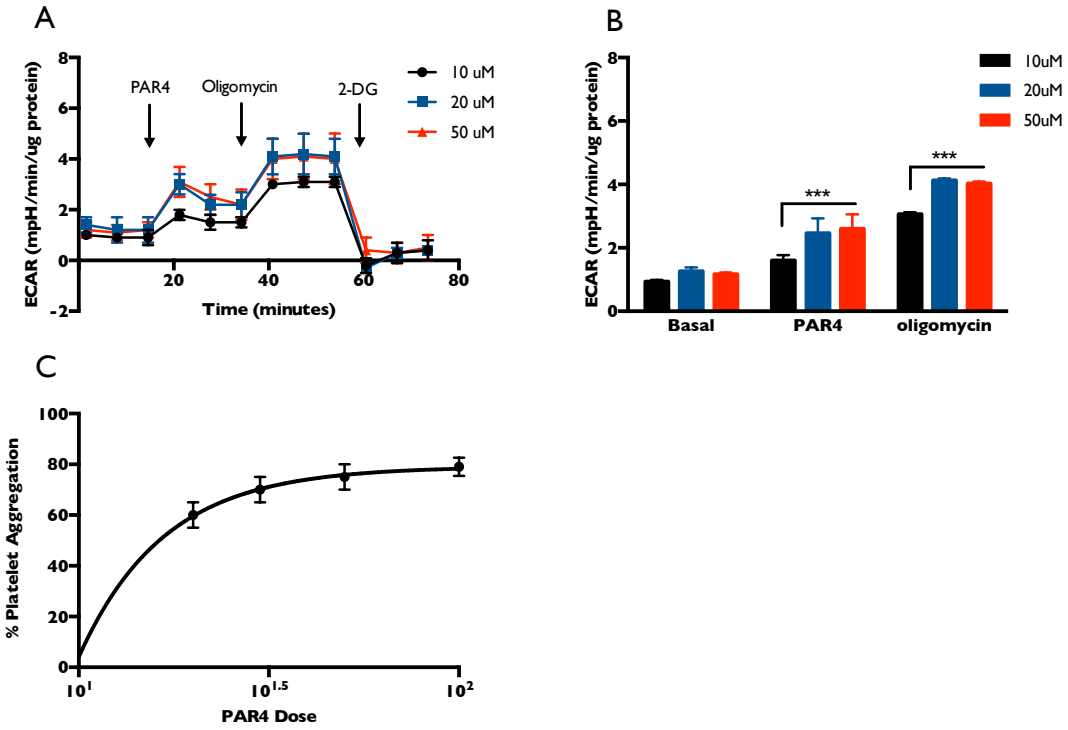

Figure 3-18: Glycolytic capacity of platelets with various doses of PAR4 (A) ECAR of platelets stimulated with 10, 20, and 50μM of PAR4. Oligomycin and 2-DG were injected subsequently to obtain the glycolytic capacity of platelets and non-glycolytic ECAR. (B) ECAR quantified from (A). ECAR increased in a dose dependent manner compared to basal when stimulated with various dose of PAR4. 10μM PAR4 induced a lower rise in ECAR compared to both 20 & 50μM PAR4 ($p<0.001$). Similarly, the glycolytic shift with 10μM PAR4 upon oligomycin injection was below that of 20 & 50μM PAR1 ($p<0.001$) Data shown as mean ± SEM, n=3. (C) Dose response curve of platelet aggregation when stimulated with 10, 20, 30, 50 and 100μM PAR4 for three minutes. Data shown as mean ± SD, n=3, ***<0.001.

3.4.4 Glycolytic and oxidative metabolism of glucose

3.4.4.1 OCR & ECAR of platelets stimulated with thrombin

To discover whether OXPHOS is involved in the process of platelet activation, the OCR and ECAR of platelets were measured both at basal and when activated with thrombin. When platelets were stimulated with 0.1U/ml thrombin, the OCR increased from 2.84 ± 0.02 pmol/min/μg protein to 4.2 ± 0.11 pmol/min/μg protein ($p<0.05$; Figure 3-19A, C). 0.01U/ml thrombin prompted a smaller increase in OCR (3.55 ± 0.07 pmol/min/μg protein). ECAR was measured simultaneously and showed a similar pattern to OCR (Figure 3-19C, D); 0.1U/ml thrombin increased ECAR drastically from 1.85 ± 0.08 mpH/min/μg protein to an average 6.35 ± 1.76 mpH/min/μg protein ($p<0.05$) whereas 0.01U/ml increased ECAR to a mean 3.63 ± 1.2 mpH/min/μg protein.

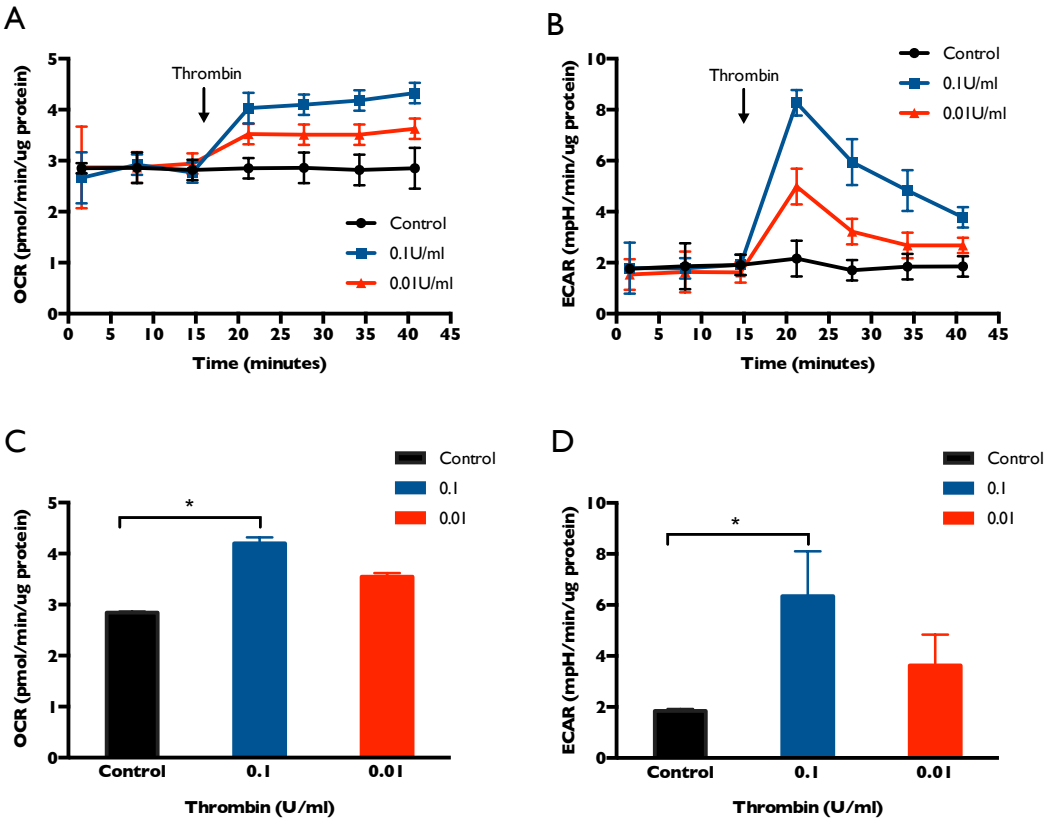

Figure 3-19: OCR & ECAR of platelets stimulated with high and low dose thrombin (A) OCR of platelets stimulated with 0.1 and 0.01U/ml thrombin over time. (B) ECAR of platelets stimulated with 0.1 and 0.01U/ml thrombin over time. (C) Average OCR quantified from (A). Upon stimulation with 0.1U/ml thrombin, there was a significant increase in OCR ($p<0.05$) compared to basal. (D) Average ECAR quantified from (B). Upon stimulation with 0.1U/ml thrombin, ECAR increased significantly compared to basal ($p<0.05$). Data shown as mean ± SEM, n=3, *<0.05.

3.4.4.2 Partitioning of glucose metabolism between OXPHOS and glycolysis with high dose thrombin

Since both OXPHOS and glycolysis are involved in thrombin activation of platelets, the partitioning of glucose through these pathways was examined with a high dose of thrombin. The contribution of fatty acid β-oxidation was first eliminated using etomoxir, which is an inhibitor of carnitine palmitoyltransferase-1 (Ito et al., 2012; Ravi et al., 2015). This resulted in conditions where OCR and ECAR were mostly glucose-dependent since there are no other substrates provided in the medium. Under basal conditions, etomoxir caused a small decrease in OCR, but had no effect on ECAR (Figure 3-20A), yet glucose was metabolised through both glycolysis and OXPHOS (Figure 3-20A and C). Thrombin (0.1U/ml) caused OCR to rise from 1.25 ± 0.02 to 1.96 ± 0.03 pmol/min/μg protein ($p<0.001$) (Figure 3-20A and B). The addition of the complex I/III inhibitors, antimycin A and rotenone (A/R), caused an almost complete abolition of basal OCR and ablated that induced by thrombin. The remaining non-mitochondrial OCR in thrombin-stimulated platelets was similar to control values, suggesting that thrombin did not alter non-mitochondrial OCR (Figure 3-20A). Parallel to the rise in OXPHOS, thrombin stimulated a rapid increase in in ECAR from 1.74 ± 0.10 to 7.1± 0.72 mpH/min/μg protein ($p<0.01$) (Figure 3-20C and D). Here, the addition of rotenone and antimycin increased ECAR in both resting and thrombin-stimulated platelets (Figure 3-20C), suggesting a compensatory increase in glycolysis when mitochondrial ATP synthesis is blocked. The subsequent addition of 2-deoxyglucose (2-DG; 50 mM) to inhibit glycolysis had no effect on OCR, but did abolish the thrombin-induced glycolysis, indicating a minimal non-glycolytic ECAR in platelets. Activation of platelets increased activity of both pathways (Figure 3-20E), but critically there was a shift to a glycolysis-dominated phenotype (almost 3 fold change in ECAR) where oxidative phosphorylation only changed minimally in the absence of β-oxidation.

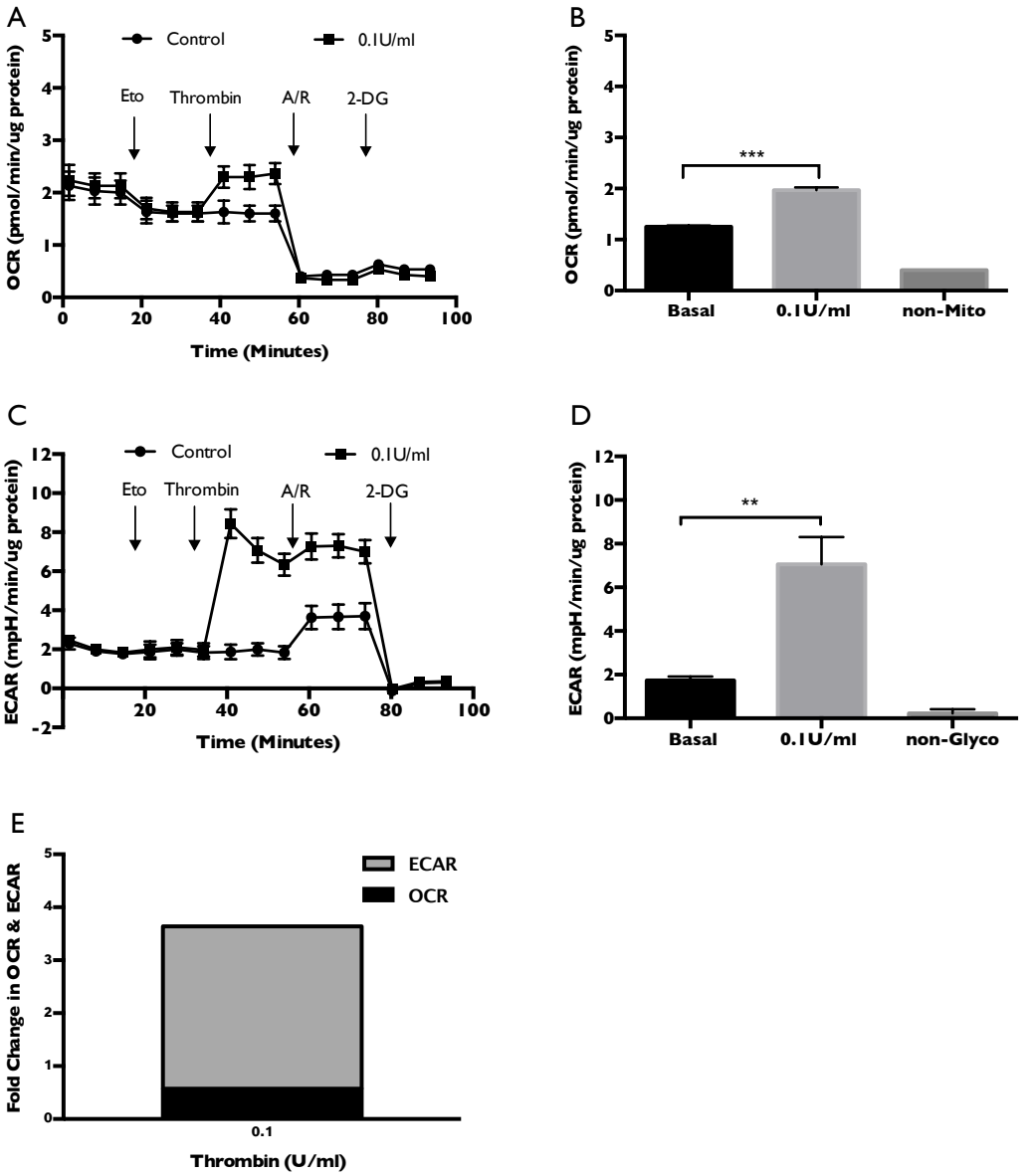

Figure 3-20: OCR & ECAR of platelets stimulated with high dose thrombin (A) OCR of platelets +/- 0.1U/ml thrombin. The glucose dependent oxygen consumption was distinguished by the addition of Etomoxir to block fatty acid oxidation. Non-mitochondrial OCR was distinguished by the OCR insensitive a combination of Antimycin/Rotenone. (B) Upon stimulation with 0.1U/ml thrombin, there was a significant increase in the OCR compared to basal after correcting for non-mitochondrial OCR ($p<0.001$). (C) ECAR of platelets +/- 0.1U/ml thrombin. 2-Deoxy glucose was added to correct for non-glycolytic extracellular acidification. (D) Upon stimulation with 0.1U/ml thrombin, there was a significant increase in the ECAR compared to basal after correcting for non-glycolytic acidification ($p<0.01$). (E) Fold change in OCR and ECAR after thrombin stimulation compared to basal. Values were corrected for non-mitochondrial OCR & non-glycolytic ECAR. Data expressed as mean ± SEM, n=3. **<0.01, ***<0.001.

3.4.4.3 Partitioning of glucose metabolism between OXPHOS and glycolysis with low dose thrombin

The partitioning of glucose between glycolysis and oxidative phosphorylation was next examined in response to a low dose of thrombin to discover whether OCR and ECAR responded in a dose-dependent and proportional manner. Under basal conditions, etomoxir caused a small decrease in OCR, but had no effect on ECAR (Figure 3-21A) and glucose was metabolised through both glycolysis and OXPHOS (Figure 3-21A and C). Thrombin (0.01U/ml) caused a small but significant increase in OCR from 1.25 ± 0.02 to 1.63 ± 0.06 pmol/min/μg protein ($p<0.001$) (Figure 3-21A and B). The addition of the complex I/III inhibitors, antimycin A and rotenone (A/R), caused an almost complete abolition of basal OCR and ablated that induced by thrombin. The remaining non-mitochondrial OCR in thrombin-stimulated platelets was similar to control values, again suggesting that thrombin did not alter non-mitochondrial OCR (Figure 3-21A). Parallel to the rise in OXPHOS, thrombin stimulated a rapid increase in in ECAR from 1.73 ± 0.10 to 5.1± 0.9 mpH/min/μg protein ($p<0.01$) (Figure 3-21C and D). Here, the addition of rotenone and antimycin increased ECAR in both resting and thrombin-stimulated platelets (Figure 3-21C), suggesting a compensatory increase in glycolysis when mitochondrial ATP synthesis is blocked. The subsequent addition of 2-deoxyglucose (2-DG; 50 mM) to inhibit glycolysis had no effect on OCR, but did abolish the thrombin-induced glycolysis, indicating a minimal non-glycolytic ECAR in platelets. Similar to the high dose thrombin, activation of platelets with ten-fold less of thrombin still increased activity of both pathways (Figure 3-21E), however, the shift to glycolysis (2 fold change in ECAR) was much more significant than to oxidative phosphorylation.

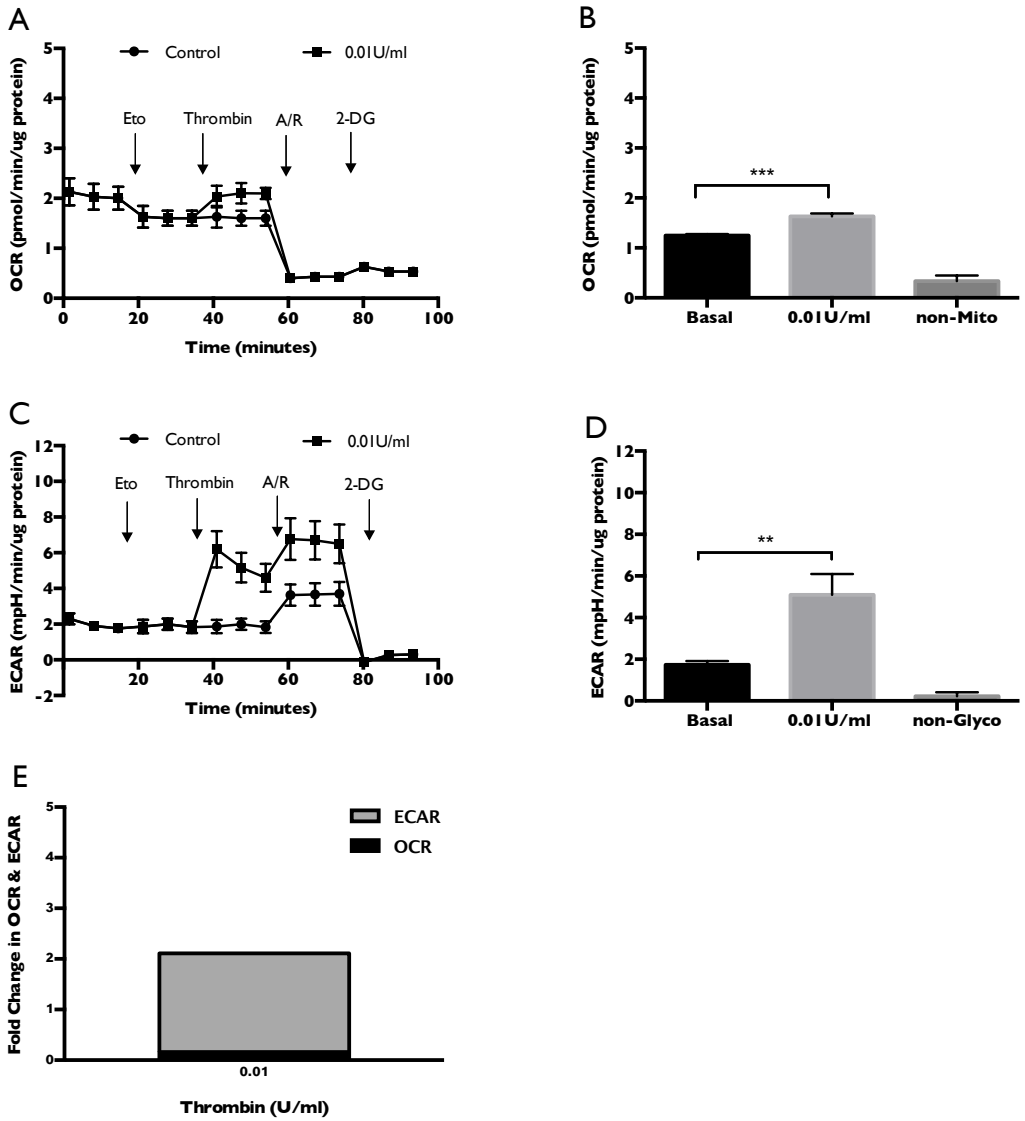

Figure 3-21: OCR & ECAR of platelets stimulated with low dose thrombin (A) OCR of platelets +/- 0.01U/ml thrombin. The glucose dependent oxygen consumption was measured by the addition of Etomoxir to inhibit fatty acid oxidation. Non-mitochondrial OCR was distinguished by the OCR insensitive a combination of Antimycin/Rotenone. (B) Upon stimulation with 0.01U/ml thrombin, there was a significant increase in the OCR compared to basal after correcting for non-mitochondrial OCR ($p<0.001$). (C) ECAR of platelets +/- 0.01U/ml thrombin. 2-Deoxy glucose was added to correct for non-glycolytic extracellular acidification. (D) Upon stimulation with 0.01U/ml thrombin, there was a significant increase in the ECAR compared to basal after correcting for non-glycolytic acidification ($p<0.01$). (E) Fold change in OCR and ECAR after thrombin stimulation compared to basal. Values were corrected for non-mitochondrial OCR & non-glycolytic ECAR. Data expressed as mean ± SEM, n=3. **<0.01, ***<0.001.

3.4.4.4 Energy phenotype of platelets at basal and activation with thrombin

Platelet energy phenotype was measured using the XFp cell phenotype test as described in 2.6.4. After establishing that platelets use both the glycolytic pathway and OXPHOS for energy generation following glucose addition and that platelets present glycolytic phenotype when activated in the absence of β-oxidation, an energy phenotype experiment was carried out to explore whether this was the case when endogenous fatty acids were present. Under basal condition, platelets utilise glycolysis and OXPHOS almost equally (Figure 3-22). Platelets became more energetic upon stimulation with thrombin, indicated by the increase in both glycolysis and OXPHOS, with the former being more significant than the latter. This suggested that platelets present a glycolytic phenotype upon activation regardless of the fuels being glucose or endogenous fatty acids.

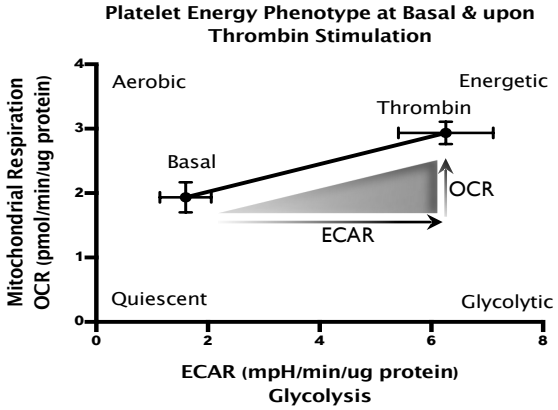

Figure 3-22: Platelet energy phenotype at basal and following activation with thrombin (0.1U/ml). The experiment was carried out in the absence of etomoxir in glucose containing XFp medium.

3.5 Discussion

The first aim of this chapter was to establish a system for examining platelet metabolism. This was achieved by comparing un-washed and washed platelets functionally in terms of glucose utilization, to investigate the potential effect of the purity of the platelet suspension on metabolism. Secondly, the basal metabolic profile of platelets isolated with the pH or PGE_1 method was compared using XFp, to identify suitable anti-aggregation reagent. Subsequently, platelet glucose uptake both at rest and activation and the demand of platelet primary and secondary aggregation on glucose was determined using enzyme-coupled fluorometric assay. This was further confirmed qualitatively using XFp assays with inhibitors of ADP and TxA_2 generation. Glycolytic capacity and its receptor mediation as well as the partitioning of glucose between glycolysis and OXPHOS were presented. In this series of experiments, it was also established that endogenous fatty acids contribute to basal platelet respiration.

3.5.1 Choosing a system for measuring platelet metabolism

Platelet aggregation assay is widely used for testing normal platelet function in response to various agonists both in clinical settings and *in vitro* experimentations (Jackson, 2007). *In vitro* experiments can be carried out on washed or unwashed platelets as defined in Chapter 2.2.2, however, un-washed platelets may carry over energy-rich plasma contents as well as plasma proteins in final platelet suspension (Niu et al., 1997). This is not ideal when measuring platelet substrate metabolism *in vitro* as the plasma content may interfere with platelet function specific energy metabolism. In this case, washed platelets are preferred as it provides relatively pure system.

In the first instance, the aggregation response of these two preparations were compared in Tyrode's buffer containing glucose with both thrombin and collagen to elucidate the effect of washing on platelet function. It was observed that although the amplitude of aggregation for high doses of thrombin (Figure 3-8) and collagen (Figure 3-9) were similar at the end of three and half minutes of aggregation, the initiation and progression of aggregation was significantly slower in washed platelets.

It is worth mentioning that this was not an effect of washing step. The wash buffer used in this study was a citrate based salt solution at pH 6.5, which has been shown to inhibit platelet aggregation by lowering the pH during isolation. Washed platelets prepared by this method have been shown to be sensitive to relatively weak agonists, such as ADP (Patscheke, 1981). The morphological as well as functional properties of platelets were maintained for up to 6 hours post isolation with this method (Patscheke, 1981).

The difference in the aggregation pattern that was observed in this study seems to be the effect of potentially large plasma proteins, such as von Willebrand factor, immunoglobulins, and factor V, remaining in the final suspension. These plasma proteins can further facilitate platelet aggregation in unwashed platelets, thus making platelets more sensitive to agonists. This implies that for achieving similar amplitude of aggregation for the same agonist, unwashed platelets require a smaller dose compared to the washed platelets. In other words, the use of unwashed cells could result in underestimation of the energy requirement induced by the given dose of agonist. Also, in the unwashed platelet suspension, there is the possibility of carrying over potential energy-rich components of plasma such as serum albumin bound fatty acids, glucose and triglycerides (Guppy et al., 1997; Niu et al., 1997). These will interfere with the investigation of fuel dependency and partitioning as well as the role of endogenous fatty acid metabolism. Taking these points into consideration, washed platelets were used throughout this study.

The basal ECAR and OCR were measured using the XFp assay. Platelets were isolated using either acidic pH or PGE_1 as an anti-aggregate during the preparation of washed platelets from PRP. The optimal cell number ($1*10^8$ platelets/ml) to achieve measurements of the OCR and ECAR within the detection limit of the XFp was first determined (Figure 3-10). Both methods gave similar basal ECAR and OCR values (Figure 3-11); however, there were large variations between samples from pH method. This was probably due in part to spinning of the cell culture miniplate for cell seeding procedure as described in 2.5.5, which may have induced spontaneous uncontrolled platelet aggregation. Platelets isolated and supplemented with prostaglandin before the spinning step exhibited improved cell adhesion with minimum platelet activation when observed under microscopy (Kramer et al.,

2014). To keep all the experimental conditions the same for platelet functional and metabolic experiments, the prostaglandin method was used throughout this study.

3.5.2 Glucose uptake by resting and activated platelets

3.5.2.1 Glucose uptake by resting platelets

Platelets have a large number of glycogen granules (Rocha et al., 2014), which make it difficult to quantify glucose consumption in terms of lactate formation since lactate could also be originating from glycogen. Bearing this in mind, the disappearance of exogenous glucose from the medium of platelet suspension was quantified directly in this study (Figure 3-12). As expected, there was a linear decrease in the concentration of glucose from the medium over two hours, indicating that resting platelets deplete exogenous glucose. There appeared to be a slight, non-significant, donor variation in the rate of glucose uptake (Figure 3-12C). At a higher platelet number ($5*10^8$ platelets/ml), the mean rate of glucose depletion from the medium was 0.21 ± 0.05 μmoles/hr/10^8, which was lower than the value of 0.29 ± 0.01 μmoles/hr/10^8 recorded for $3*10^8$ platelets/ml. This suggested that for a given volume and concentration of glucose, platelet number can become rate limiting for glucose uptake. These values were 10 times higher than those reported (0.021 μmoles/hr/10^8) previously by Karpatkin, (1967) using a similar enzymatic glucose assay. This may have been due to the harsh conditions during platelet isolation used by Karpatkin, which included a low temperature (5 °C) and a non-physiological pH (pH 7.1) in the final platelet suspension.

3.5.2.2 Glucose uptake by activated platelets

The physiological environment, in which platelets perform their function, is very dynamic and characterised by constant fluid motion. This implies that measuring platelet glucose uptake in a stagnant suspension might lead to the build-up of an unstirred layer around the cells and underestimation of the glucose uptake rate by platelets at rest. It was therefore not surprising that when the platelet suspension was stirred in the aggregometer at 1000rpm before adding the agonist thrombin, the mean rate of glucose uptake was 1.8 μmoles/hr/10^8, or six times higher than

that of platelets in a stagnant suspension (Figure 3-13 and 3-14). This speed of agitation was optimised so as not to cause platelet aggregation by the calibration process of aggregation assay as described in 2.3.2. . Although stirring the platelet suspension did not fully mimic fluid motion in the blood, these data highlight the importance of caution in interpreting results in different experimental conditions.

Thrombin plays a critical role in the coagulation cascade by activating platelets and converting the soluble fibrinogen into insoluble fibrin, consolidating the haemostatic plug (Chung et al., 2002). Thrombin has been shown to be the most potent platelet agonist *in vitro*, initiating a wide range of platelet responses such as shape change, release of ADP, serotonin and TxA_2 (Huang and Detwiler, 1986). However, for a given agonist, its strength is a function of its concentration, meaning that at a lower concentration, thrombin acts as a weak agonist. From a dose response experiment, 0.1 and 0.01U/ml thrombin were chosen as the 'high' and 'low' concentrations for the activation of platelets (Figure 3-13A and Figure 3-14A) in subsequent experiments. Both high and low doses of thrombin caused abrupt increase in the rate of glucose depletion, however, at considerably different rates and amplitude (Figure 3-13B and Figure 3-14B). This indicates that thrombin induces a dose-dependent glucose uptake by platelets.

With the high dose of thrombin, the aggregation of platelets was rapid (3 minutes) and the glucose depletion rate at a maximum at the initiation of the aggregation (15 fold higher than the resting rate). However, following the initial rapid increase in glucose uptake, which was linked to the early phase of aggregation, glucose depletion declined as the aggregation response plateaued. By contrast, the low dose of thrombin initiated shape change and primary aggregation, which only caused a 8-fold increase in the glucose depletion rate. This was increased further to 15-fold with the initiation of the release of secondary mediators from granules including ADP and TxA_2. This suggested that the release reaction requires more glucose than the initial aggregation response; a conclusion consistent with previous studies showing the ATP requirements of different platelet responses to be in the following order: shape change < primary aggregation < secondary aggregation (secretion of granule content) (Holmsen et al., 1982). This was also confirmed using the inhibitors of ADP and TxA_2: apyrase and indomethacin, respectively (Figure 3-15).

The glycolytic rate of platelets was significantly decreased in the indomethacin treated group compared to its thrombin control, and was not as significant in the apyrase treated platelets. ADP is released from dense granules upon platelet activation *in vitro*, which subsequently initiates the synthesis of TxA_2 (Jin et al., 2002). These data suggest that the synthetic machinery of TxA_2 is more energy dependent and has a greater glucose requirement.

3.5.3 Glycolytic capacity of resting and activated platelets

Having established that platelets take up glucose at rest and upon activation with thrombin in a dose dependent manner, it was decided to explore glycolytic capacity of platelets. This may be defined as the maximum glycolytic rate, and was measured both at rest and after activation with thrombin (Figure 3-16). Under basal conditions, before the addition of a physiological concentration of glucose (5.6mM), a minimal glycolytic rate was observed even after correcting for the non-glycolytic ECAR with 2-DG. This could be indicative of metabolism of intracellular glycogen (Akkerman et al., 1978; Niu et al., 1996). Addition of glucose increased the ECAR significantly, confirming that platelets take up exogenous glucose when provided despite the presence of intracellular glycogen. The injection of the mitochondrial ATP synthase inhibitor oligomycin prompted a further rise in ECAR, which was sustained for the duration of the experiment (20 minutes) before the abolition of ECAR by 2-DG. When platelets were stimulated with thrombin, the increase in ECAR was 3 times higher than basal. This confirms that thrombin-induced activation requires glucose uptake (Figure 3-13 & 3-14), and a glycolytic response. As observed earlier, the thrombin-induced ECAR was not sustained at its maximum level but reduced over the course of the following measurements. The addition of oligomycin increased the ECAR to value as high as that with thrombin, which was abolished by 2-DG. Combined, these data suggest that platelets have a relatively high glycolytic capacity, which can provide ATP purely dependent on glycolysis at rest and upon activation with thrombin. Under resting conditions, platelets have no need to reach full glycolytic capacity; however, thrombin activation requires a dramatic increase in glycolytic capacity to provide ATP under conditions when OXPHOS is inhibited. This further indicates the potential flexibility of platelets in

utilising glucose in glycolysis and oxidative phosphorylation. Chacko et al., (2013) reported similar response of platelets to oligomycin, measured as proton production rate with similar techniques as those used here, however, in that work, the glycolytic capacity was not measured.

3.5.3.1 Glycolytic capacity of platelets with PAR1 & PAR4

The action of thrombin on human platelets is mediated through PARs, 1 & 4, which belong to the G-protein coupled receptor superfamily. Activation of either is sufficient to trigger platelet activation and this can be achieved by the synthetic peptides of PAR1 and PAR4 to achieve thrombin-independent platelet activation (Chung et al., 2002; Candia, 2012). To understand whether one or both of these receptors mediated platelet glycolytic function, the glycolytic capacity of platelets was measured in response to activation with various doses of both PAR1 and PAR 4 (Figure 3-17 & 3-18). At the highest dose, both PAR1 and PAR4 induced similar amplitude of aggregation (Figure 3-17C & Figure 3-18C) to that observed with 0.1U/ml thrombin (Figure 3-13A), however, both failed to induce a similar ECAR to that observed when platelets were activated with 0.1U/ml thrombin. This suggests that when platelets are activated with high dose of thrombin, both receptors are required to induce the maximum glycolytic response. The ECAR for PAR1 was slightly higher than that of PAR4. Inhibition of mitochondrial ATP led to a further increase in ECAR as expected, of which PAR1 had a similar potency to that of thrombin, with PAR4 giving a lesser stimulation. This may be because PAR1 is the main receptor for thrombin on human platelets and PAR4 providing a redundancy in function by contributing to signalling at high thrombin concentrations for prolonged effect (Candia, 2012). These data suggest that PAR1 is sufficient to achieve maximum glycolytic capacity in platelets in the absence of OXPHOS.

3.5.4 Glycolytic and oxidative metabolism of glucose

Inhibition of mitochondrial ATP production with oligomycin decreased platelet oxygen consumption (Figure 3-16C) and increased ECAR (Figure 3-16A &B), indicating a role for platelet mitochondria in energy generation. This was confirmed by stimulating platelets with 0.1 and 0.01U/ml thrombin and measuring the OCR

and ECAR simultaneously (Figure 3-19). Thrombin increased both OCR and ECAR in a dose-dependent manner. The extent of increase in the ECAR was higher than that of OCR, suggesting that both glycolysis and OXPHOS are involved in platelet activation. This is in agreement with the data of Ravi et al., (2015) who used similar techniques, but a 5 fold-higher dose of thrombin, despite which the OCR increased to similar extent with that reported here in Figure 3-19. In addition, the basal OCR reported by Ravi et al., (2015) was double that reported in this study, possibly due to different media in the two studies.

3.5.4.1 Partitioning of glucose between OXPHOS and glycolysis with thrombin

The major alternative energy substrates to carbohydrates are fatty acids, which in the case of the experiments on platelet metabolism described above, will have been present within the cells, i.e., endogenous. The OCR and ECAR were therefore measured under conditions where the oxidation of endogenous long-chain fatty acids was inhibited (Figure 3-20 & 3-21). The inhibition of β-oxidation decreased the OCR, suggesting that platelets can use endogenous fatty acids under basal conditions. The inhibition of β-oxidation under basal condition did not alter the ECAR, and OCR was stabilized over a time course of 15 minutes. This suggests that glucose oxidation by platelets may compensate for the loss of β-oxidation. Ravi et al., (2015) published similar yet controversial results. They reported that inhibition of β-oxidation suppressed the OCR but increased the ECAR, suggesting that the increase in ECAR compensated for the loss of β-oxidation. However, this again may have been induced by the experimental conditions chosen by Ravi et al. Platelets were pre-treated with trimetazidine, inhibitor of long-chain 3-ketoacyl coenzyme A thiolase, for three hours before the measurements were taken. Trimetazidine was reported to increase the utilization of glucose (Chrusciel et al., 2014), thus potentially contributed to the the results observed by Ravi et al., (2015).

This study was the first to measure the partitioning of glucose between glycolysis and OXPHOS using different doses of thrombin. Stimulation of platelets with 0.1 and 0.01U/ml thrombin increased both the OCR and ECAR in a dose dependent manner (Figure 3-20 & 3-21) in the absence of β-oxidation. When the proportion

of glycolysis and OXPHOS were compared as a fold change, platelets presented a glycolytic phenotype upon activation regardless of thrombin dose. This was not driven by the inhibition of β -oxidation as indicated by the platelet energy phenotype map measured in the absence of etomoxir (Figure 3-22). In other words, these data suggest that platelets respond to external stimuli, such as thrombin, by choosing aerobic glycolysis over oxidative metabolism of glucose (or potentially glycogen). This is comparable to the 'Warburg effect' or aerobic glycolysis, described first in cancer cells (Warburg, 1956). Initially, this metabolic phenotype was ascribed to a mitochondrial defect; however, a contemporary view is that the shift to aerobic glycolysis is due to the requirements of rapidly proliferating cells for the biosynthetic precursor molecules produced in the process of glycolysis (Dimeloe et al., 2016; Smith and Sturmey, 2012). As platelets do not carry out extensive biosynthetic processes, it is somewhat unexpected that activated platelets commit to a less efficient energy-generating pathway as glycolysis only produces 2 ATP per molecule of glucose versus c. ≈32 ATP from OXPHOS. However, increased production of ATP from OXPHOS can limit glycolysis as high ATP levels inhibit PFK1, a rate-limiting enzyme in glycolysis (Zheng, 2012). In these circumstances, glycolysis can only continue by converting pyruvate to lactate, to regenerate NAD and maintain a high glycolytic rate. Moreover, although glycolysis produces less ATP than OXPHOS, its rate can be increased dramatically to satisfy the energy demands of rapid activation (Pearce et al., 2013). However, an added feature of the Warburg effect is the metabolism of glucose in PPP, an early branch point of glycolysis, which is essential for nucleotide biosynthesis and for production of NADPH, a critical coenzyme for fatty acid synthesis and regeneration of reduced glutathione. It is unlikely that nucleotide biosynthesis takes place in platelets, as they do not have nuclei. However, Thomas et al (2014) demonstrated that platelets do exhibit active PPP and that this plays an important role in redox management and prostaglandin synthesis, which is altered in aspirin-resistant platelets.

3.6 Conclusion

Platelet activation induces a cascade of energy-dependent events, including actin polymerisation, shape change, secretion of α and dense granules, and eventually, aggregation and clot formation (Simpson et al., 2008; Broos et al., 2012). This study has shown that glucose as the major substrate for fuelling these functional changes. This study is the first to demonstrate quantitatively that platelets consume glucose at rest and upon thrombin activation in a dose-dependent manner. The differentiation of primary and secondary aggregations showed that the secretion response required the highest glucose uptake. Moreover, platelets showed a relatively high capacity for glycolysis, which differed between resting and stimulated platelets, showing flexibility in the scope for glucose metabolism. Most importantly, it was shown that platelets present a glycolytic phenotype upon activation with thrombin despite the availability of other extracellular fuels and irrespective of the thrombin dose.

4. Glycogen in Platelets

4.1 Introduction

Reversible storage of glucose in the form of glycogen, a branched glucose polymer, is found in many organs, with liver and skeletal muscle having the largest storage pool. As in many other cell types, the existence of glycogen in platelets was visualised in electron micrographs, where it appeared as individual particles, randomly distributed in the cytoplasm (Symth et al., 2010; Figure 1-1). It is not clear whether platelet glycogen has a fundamental biological role (Scott, 1967), however, identification of enzymes related to glycogen metabolism, such as glycogen phosphorylase and phosphorylase kinase, support the notion that it might be an energy source in platelets (Rocha, et al., 2014).

Liver and skeletal muscle play key roles in maintaining whole-body glucose homeostasis, and consequently, the regulation of glycogen metabolism in these tissues is well characterised compared to other cells. Despite the fact that both liver and muscle store glycogen, there are differences in the ways and mechanisms that glycogen are mobilised and utilised. Glycogen derived glucose is used locally in skeletal muscles in cases of extreme physical activities, whereas it is exported from the liver for use by other tissues. The breakdown of glycogen in liver can be stimulated by adrenaline in response to extreme activities or glucagon in response to fasting, whereas in the muscles, it is stimulated only by adrenaline. In terms of mechanism, adrenaline induced cAMP-mediated phosphorylation of PKA inhibits glycolysis and stimulates gluconeogenesis in liver whereas it amplifies the breakdown of glycogen and glycolysis in muscle by activating phosphorylase kinase, which activates glycogen phosphorylase. In the muscle, phosphorylase kinase can also be activated by calcium due to the presence of calmodulin on its δ monomer, which has four regulatory sites that can bind calcium at concentrations as low as 0.1umol/L (Adeva-Andany et al., 2016; Figure 4-1).

It is generally agreed that glycogen degradation in platelets is mediated by an increase in glycogen phosphorylase activity (Scott, 1967; Karpatkin, 1967; Karpatkin et al., 1970; Chaiken et al., 1975; Agam et al., 1977); however, the mechanism for the activation of the glycogen phosphorylase remains unresolved.

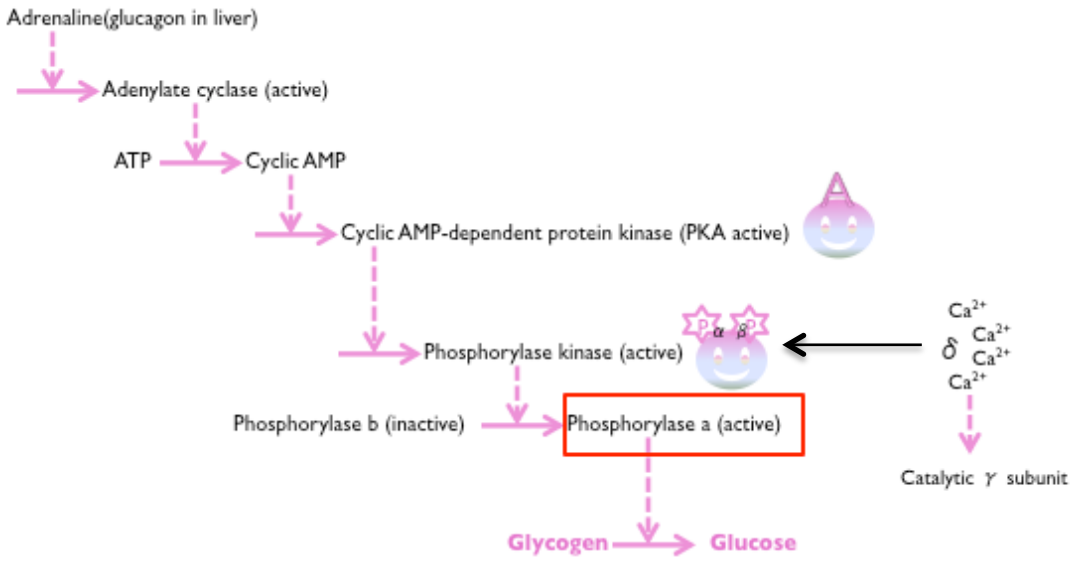

Figure 4-1: Simplified mechanism of glycogenolysis in muscle and liver

Platelets potentially do not require glycogen degradation at rest under physiological conditions (Karpatkin et al., 1970) where increased cAMP levels play central role in the inhibition of its activation. Thus, the inhibitory mechanism of platelet activation by cAMP-PKA pathway contradicts the notion of cAMP-PKA dependent activation of glycogen phosphorylase in platelets as in liver and muscle (Chaiken et al., 1975). However, the discovery of phosphorylase kinase in platelets (Scott, 1967) suggested the possibility of a cAMP-independent, calcium dependent activation pathway of glycogen phosphorylase in platelets, which was similar to skeletal muscle. This was supported by the decreased activity of phosphorylase in the presence of divalent cation chelaters, such as EDTA (Karpatkin et al., 1970); however, the difference between the role of calcium and magnesium cations was not addressed. Consequently, how and whether glycogen is mobilised and metabolised in the same way in platelets as skeletal muscles or other cell lines remains unclear. In terms of its metabolism, skeletal muscle switch to glycolysis dramatically under intense exercise where the ATP demand exceeds the capacity of oxidative metabolism (Egan and Zierath, 2013). As reviewed in Chapter 1, the existing literature suggests that platelets have the capacity to metabolise glycogen through glycolysis, however, the potential involvement of oxidative phosphorylation is not clear.

4.2 Aim

The aim of this chapter was to systematically explore the contribution of glycogen to platelet metabolic activity. To do this, 5 individual objectives were pursued to:

- Establish a simple method for glycogen quantification in platelets
- Establish the importance of exogenous glucose for various platelet functions
- Measure the maximal glycogen-dependent glycolytic capacity of platelets at rest and following activation
- Measure the partitioning of glycogen between glycolysis and oxidative phosphorylation
- Conduct a preliminary experiment to discover the mechanism for regulation of glycogenolysis in platelets

4.3 Material & Methods

Washed platelets were prepared as described in Chapter 2 using PGE_1 method unless stated otherwise. All the chemicals and buffer compositions are provided in Appendix 1&2. Unless stated otherwise, platelets were prepared for XFp assays as described in 2.5.3, cells were seeded as described in 2.5.5 and the cartridge was loaded as described in 2.5.6. All the XFp experiments were corrected for protein concentrations as described in 2.8, thus the OCR results are reported as pmol/min/μg protein, and ECAR reported as mpH/min/μg protein. In all experiments, unless stated otherwise, data were analysed from three independent experiments using platelets from three different individuals.

4.3.1 Platelet functions in response to the absence of glucose

In this series of experiments, the requirement of platelets for external glucose was examined by measuring various platelet functions in the presence and absence of glucose, using thrombin and collagen. For aggregation experiments, the data were presented as log (Thrombin dose) Vs. response (%Aggregation), from which the concentration of thrombin that gave half of the full aggregation response (EC_{50}) was compared for two time points, to better represent the aggregation pattern.

4.3.1.1 Aggregation of platelets with thrombin in Tyrode's buffer +/- glucose

Washed platelets were re-suspended in Tyrode's buffer containing glucose (5.6mM) or glucose-free Tyrode's buffer. The platelet count was adjusted to $2.5*10^8$ platelets/ml. Platelet aggregation was carried out for 3.5 minutes/dose on both suspensions with thrombin at doses 0.01, 0.0125, 0.025, 0.05 and 0.1U/ml. Aggregation experiments were carried out starting from the highest dose and alternating between the two groups for each dose.

4.3.1.2 ATP secretion by platelets with thrombin in Tyrode's buffer +/- glucose

Washed platelets were re-suspended in Tyrode's buffer containing glucose (5.6mM) or glucose-free Tyrode's buffer. The platelet count was adjusted to $2.5*10^8$ platelets/ml. ATP secretion was measured as described in 2.3.3 with thrombin

ranging from 0.01, 0.05 and 0.1U/ml. Aggregation experiments were carried out starting from the highest dose and alternating between the two groups for each dose.

4.3.1.3 Aggregation of platelets with collagen in Tyrode's buffer +/- glucose

The experimental procedure was as for 4.3.1.1. Platelet aggregation was measured for 3:30 minutes/dose on both suspensions with collagen added at 0.5, 1, 2.5, 5 and 10 μg/ml.

4.3.1.4 ATP secretion by platelets with collagen in Tyrode's buffer +/- glucose

The experimental procedure was as for 4.3.1.2. ATP secretion was measured as described in 2.3.3. Collagen was added at 1, 5 and 10 μg/ml. Aggregation was carried out starting from the highest dose and alternating between the two groups for each dose.

4.3.1.5 Adhesion of platelets on collagen in Tyrode's buffer +/- glucose

Washed platelets were re-suspended in Tyrode's buffer containing glucose (5.6mM) or glucose-free Tyrode's buffer and the count adjusted to $1*10^8$ platelets/ml. The platelet 96-well collagen adhesion assay was carried out as described in 2.3.1.

4.3.2 Measurement of platelet glycogen with acid hydrolysis

Glycogen can be hydrolysed using either amyloglucosidase or acid. Amyloglucosidase can hydrolyse the α-D-(1-4), the α-D-(1-6), and the α-D-(1-3) glucosidic bonds of oligosaccharides. However, the commercially available amyloglucosidase is stabilised with large amount of glucose, making it difficult to quantify the free glucose from glycogen in the samples using the enzyme-coupled fluorometric glucose assay. Therefore, the acid hydrolysis method of glycogen described by Rocha et al., (2014) was modified in this study. Briefly, Rocha et al., (2014) used a 30% KOH solution to lyse the platelets, precipitated glycogen using anhydrous ethanol followed by centrifugation and hydrolysed glycogen for 1h. In the

current study, a super sonication process was introduced (Scott and Still, 1969) to lyse platelets to release all the content into a glucose-free buffer, which was then subjected to acid hydrolysis for different times to discover the optimum time for maximum hydrolysis for the standard and sample.

4.3.2.1 Glycogen Standard

To test the modified method, 1mg/ml glycogen stock was prepared in PBS and a 5-point standard was diluted from the stock ranging from 0-200μg. 300μl of HCl 4M was added and the solution was boiled for 1 h before adding 300μl, 2M Na_2CO_3 to neutralise the mixture. The free glucose was quantified as described in 2.4. Before measuring the content of glycogen in platelets, a glycogen standard curve needed to be established using the acid hydrolysis method. A glycogen standard was created (Figure 4-2B) using the corresponding free glucose values for each glycogen standard point. These data show that for the glycogen standard ranging from 0-200 μg/ml, the liberated glucose could be measured using the glucose standard range chosen in this study (Figure 4-2A).

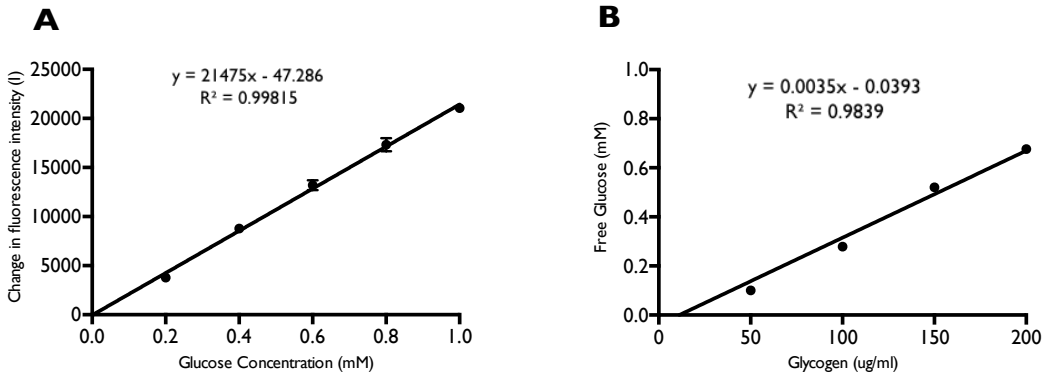

Figure 4-2: Creating glycogen standard A. Glucose standard ranging from 0-1.0mM. B. Glycogen standard calculated from the free glucose released from each glycogen standard point with A. n=1

4.3.2.2 Glycogen determination in platelets

Washed platelets were prepared from 15ml blood as described in 2.2.2. The final pellet was re-suspended in 500µl PBS and the platelet count was $6.4*10^8$/ml. Platelet samples were prepared as described in 2.4.1 and subjected to acid hydrolysis for 1h together with the glycogen standards as in 4.3.2.1. Glucose standards were prepared as described in 2.4, and used to calculate the glycogen content in standards and platelet sample.

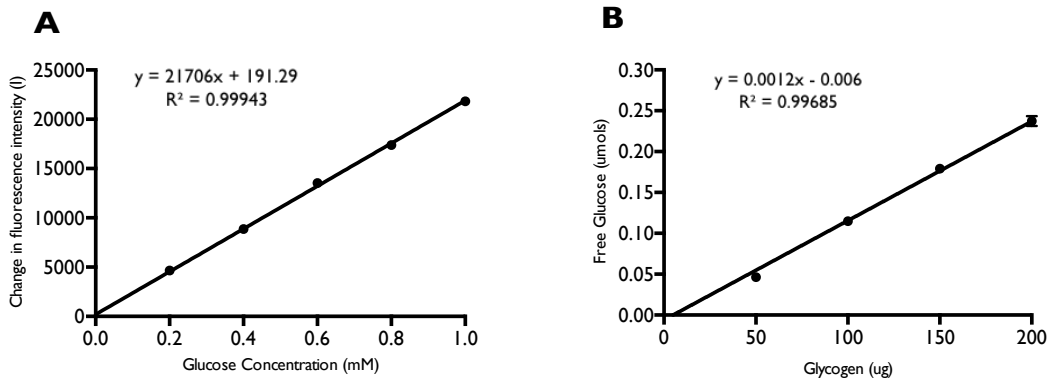

Figure 4-3: Determination of glycogen in platelet sample A. Glucose standard. B. Glycogen standard. The glycogen standard was created with the absolute amount of glucose in µmols and glycogen in µg, n=1

The amount of free glucose in 500µl of platelet suspension at $6.4*10^8$ platelets/ml was 0.1621µmols, which equals 140.08µg glycogen calculated from the glycogen standard (Figure 4-3B); a value comparable with the data reported by Rocha et al., (2014). These results confirm that the super sonication procedure was sufficient to release the glycogen from the platelet samples.

4.3.2.3 Glycogen standard hydrolysis time optimisation

200µg/ml of glycogen was hydrolysed for 60, 90 and 120 minutes and the free glucose quantified using the method described in 2.4.

4.3.2.4 Platelet sample preparation

The final washed platelet pellet was re-suspended in glucose-free Tyrode's buffer (Appendix 2). The platelet count was adjusted to $2.5*10^8$ platelet/ml or $3*10^8$ platelet/ml. Platelet aggregation was compared for 250μl, $2.5*10^8$ platelet/ml and 500μl, $3*10^8$ platelet/ml using 0.1U/ml thrombin.

4.3.2.5 Platelet sample glycogen hydrolysis time optimisation

The final washed platelet pellet was re-suspended in glucose-free Tyrode's buffer (Appendix 2) and the platelet count adjusted to $3*10^8$ platelet/ml. The suspension was split into three 500μl aliquots. The samples were prepared as described in 2.4.1 and subjected to acid hydrolysis for 60, 90 and 120 minutes. Glucose standards were prepared as described in 2.4, and used to calculate the glycogen in standards as well as in the platelet samples.

4.3.2.6 Basal glycogen level in platelets from different donors

Washed platelets were isolated from six different donors and re-suspended in glucose-free Tyrode's buffer. The platelet count was adjusted to $3*10^8$ platelet/ml. The samples were sonicated and subjected to acid hydrolysis along with the glycogen standards for 60 minutes as described in 2.4.1. The free glucose from the samples and glycogen standards were quantified as described in 2.4 and the amount of glycogen in the samples calculated.

4.3.2.7 Glycogen level in platelets stimulated with thrombin

Washed platelets were prepared and re-suspended in glucose-free Tyrode's buffer. Platelet aggregation was carried out as described in 4.3.2.4 with 500μl, $3*10^8$ platelet/ml using 0.1U/ml thrombin. Platelet glycogen level was measured before and after stimulation with thrombin as described in 2.4.1. The data were analysed from four independent experiments using platelets from three different individuals.

4.3.3 Glycogen dependent glycolytic capacity of platelets

Washed platelets were re-suspended in glucose-free XFp assay medium (Appendix 2). Platelets were seeded into an XFp plate from wells B to G. Wells A and H acted as absolute controls without cells. The A well was treated with the same compounds as B-D and H treated with the same compounds as E-G. The cartridge compound-loading map is shown in Figure 4-4. Cells were stimulated with 0.1U/ml thrombin.

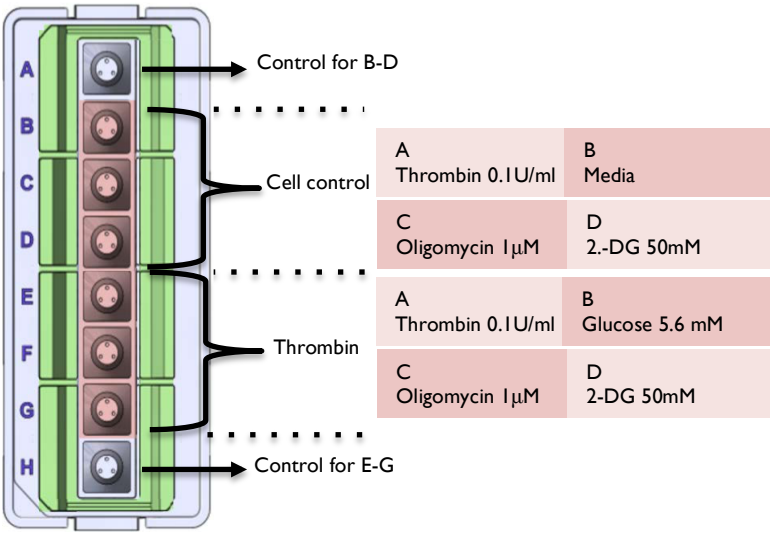

Figure 4-4: Cartridge compound loading map for measuring glycogen-dependent glycolytic function. Platelets are stimulated with 0.1U/ml thrombin. Shown are the final well concentrations of the compounds added.

4.3.4 Glycolytic and oxidative metabolism of glycogen

4.3.4.1 Glycogen-dependent OCR & ECAR of platelets stimulated with thrombin

Washed platelets were re-suspended in glucose-free XFp assay medium (Appendix 2). Platelets were seeded into an XFp plate from wells B to G and treated with 0.01 and 0.1U/m thrombin (Figure 4-5). Both OCR and ECAR were measured simultaneously.

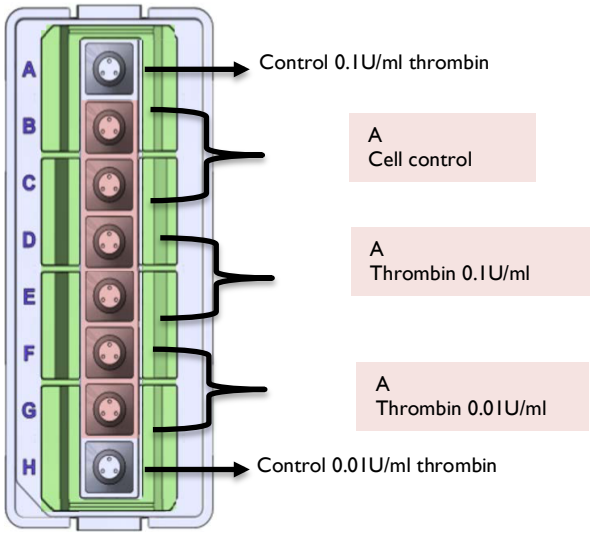

Figure 4-5: Cartridge compound loading map for measuring glycogen-dependent OCR & ECAR. Platelets are stimulated with either 0.01 or 0.1U/ml thrombin. Shown are the final well concentrations of the compounds added.

4.3.4.2 Partitioning of glycogen in glycolysis and OXPHOS with thrombin

Washed platelets were re-suspended in glucose-free XFp assay medium (Appendix 2). Platelets were seeded into XFp plate from wells B to G and treated with sequential injections of etomoxir, media/thrombin, a combination of antimycin and rotenone (A/R), and finally with 2-DG as shown in Figure 4-6.

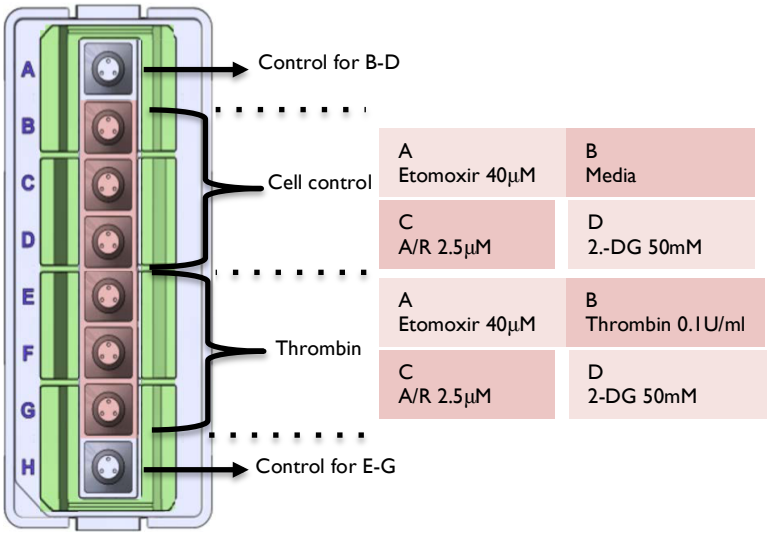

Figure 4-6: Cartridge compound loading map for measuring the partitioning of glycogen between OXPHOS and glycolysis. The final well concentrations of the compounds added are indicated in the shaded boxes.

4.3.5 Mechanism of platelet glycogenolysis

Washed platelets were re-suspended in glucose-free XFp assay medium (Appendix 2). The cell suspension was split into two equal portions and one was treated with BAPTA-AM (20μM). Both suspensions were placed in an incubator for 20 minutes at 37°C. Platelets were seeded into XFp plates from wells B to G. Wells B-D were kept as cell control and wells E-G were seeded with BAPTA-AM treated platelets (Figure 4-7). Platelets were stimulated with 0.1U/ml thrombin.

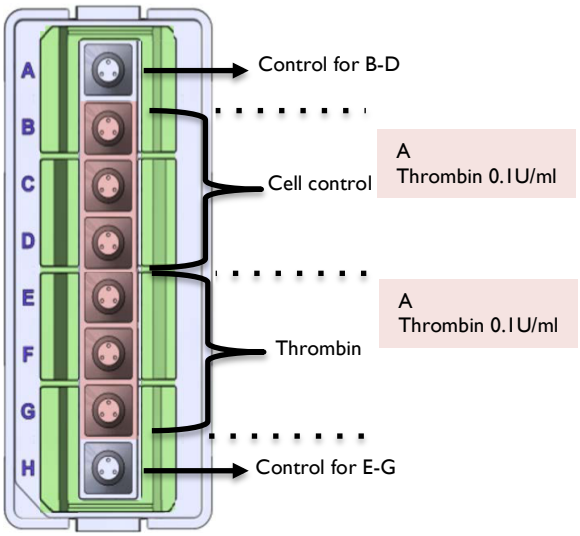

Figure 4-7: Cartridge compound loading map for measuring the mechanism of platelet glycogenolysis. Shown are the final well concentrations of the compounds added.

4.4 Results

4.4.1 Platelet functions in response to the absence of glucose

4.4.1.1 Aggregation of platelets with thrombin in Tyrode's buffer +/- glucose

The role of endogenous glycogen in platelet aggregation was compared with various doses of thrombin in Tyrode's buffer +/- glucose. The aggregation was carried out for three and half minutes, however, the data were analysed at 1.5 and 3 minutes of aggregation to better understand the aggregation pattern (Figure 4-8A, B). The EC_{50} values for platelets in both +/- glucose suspensions at 1.5 minutes were 0.03 and 3 minutes were 0.07 (+glucose) and 0.06 (-glucose), indicating that the absence of exogenous glucose did not affect the EC_{50} at both 1.5 and 3 minutes ($p>0.05$).

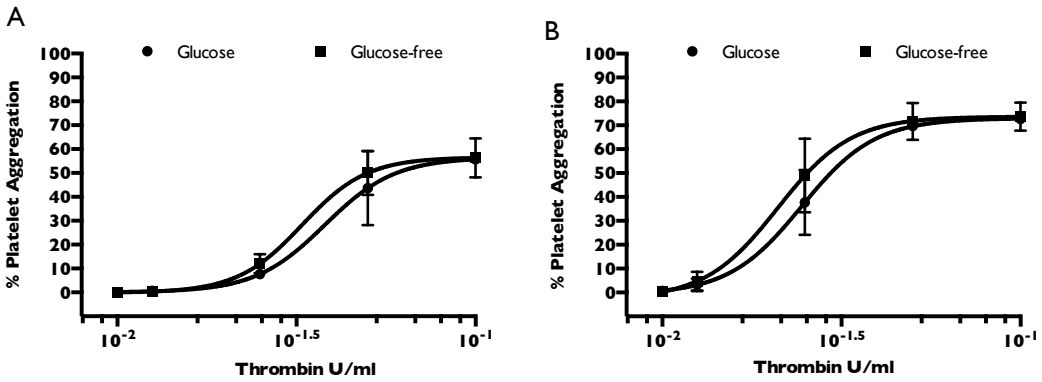

Figure 4-8: Aggregation of platelets with thrombin in Tyrode's buffer +/- glucose. Dose response curves of platelets stimulated with 0.01, 0.0125, 0.025, 0.05 and 0.1U/ml thrombin in Tyrode's buffer +/- glucose. Data presented as log (thrombin dose) Vs. response (%Aggregation), n=3. (A) Dose response curve for platelets stimulated with thrombin in +/- glucose Tyrode's buffer at 1.5 minutes. (B) Dose response curve for platelets stimulated with thrombin +/- glucose in Tyrode's buffer at 3 minutes.

4.4.1.2 ATP secretion of platelets with thrombin in Tyrode's buffer +/- glucose

ATP is stored in dense granules in platelets (Papen et al., 2013). To understand whether the omission of exogenous glucose affected platelet secretion response, ATP secretion was measured in Tyrode's buffer +/- glucose with various doses of thrombin (Figure 4-9). Surprisingly, ATP secretion did not differ between groups at all doses ($p>0.05$).

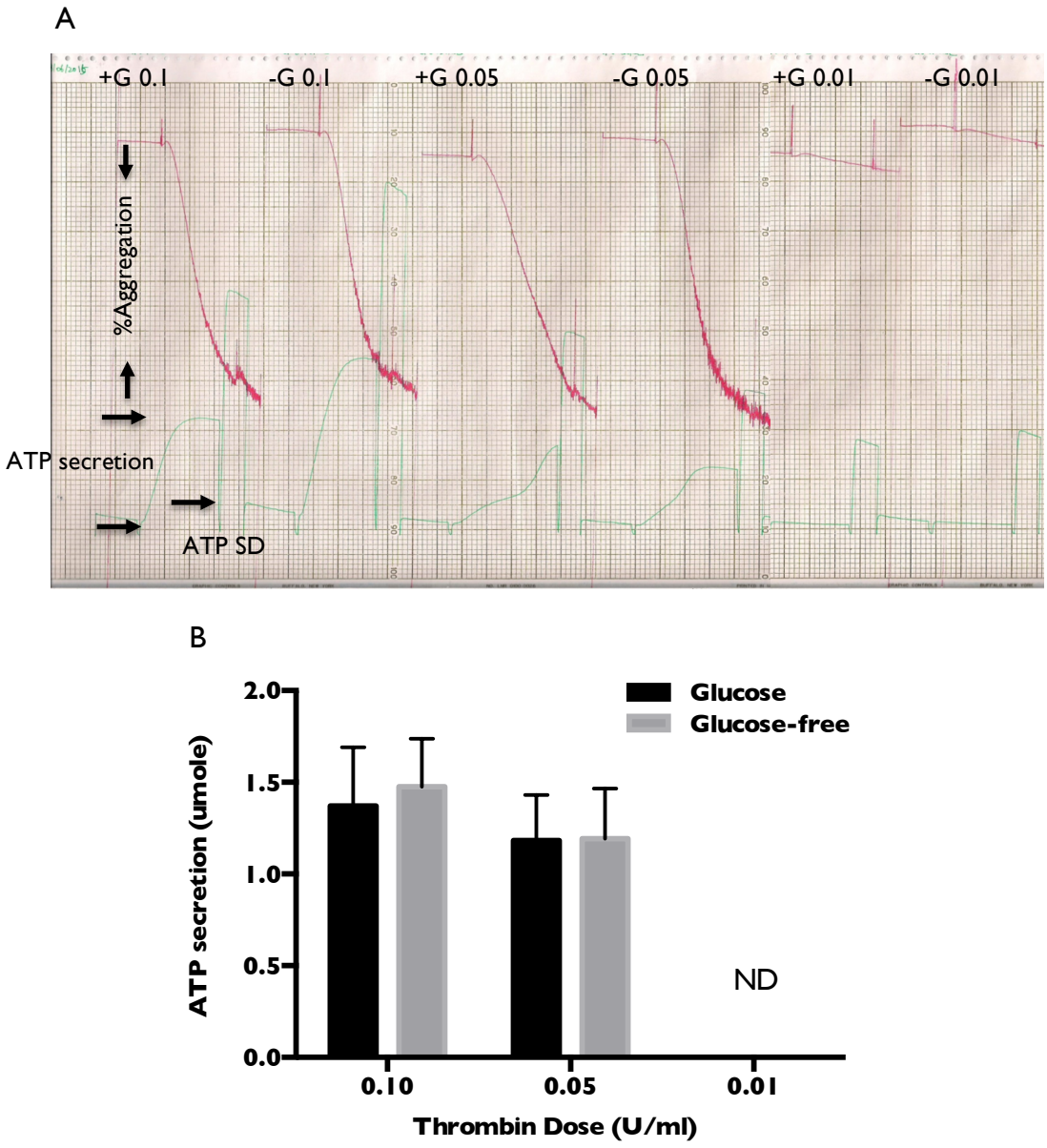

Figure 4-9: Platelet ATP secretion with thrombin in Tyrode's buffer +/- glucose (A) Platelet ATP secretion stimulated with thrombin, from left to right: +/- G (glucose) 0.1U/ml, +/-G 0.05 U/ml, +/-G 0.01U/ml thrombin. (B) ATP secretion by platelets stimulated with 0.1, 0.05, 0.01 U/ml thrombin over 90 seconds. The data are shown as mean ± SD, n=3. ND= not detected

4.4.1.3 Adhesion of platelets on collagen in Tyrode's buffer +/- glucose

Platelet interaction with collagen is one of the earliest steps in the initiation of haemostasis (Grabowska et al., 2003). The requirement for exogenous glucose in this process was measured by re-suspending platelets in Tyrode's buffer +/- glucose and measuring platelet adhesion on a collagen coated plate. The absence of exogenous glucose did not alter platelet adhesion to collagen ($p>0.05$).

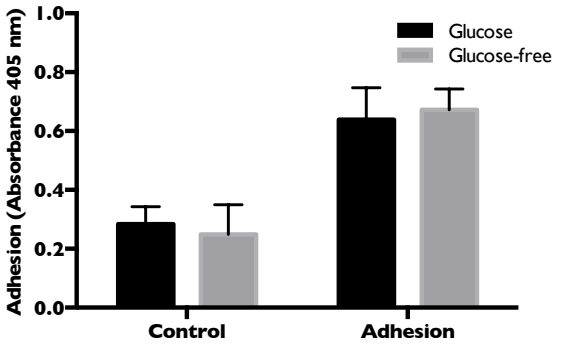

Figure 4-10: Platelet-collagen adhesion for platelets suspended in Tyrode's buffer +/- glucose. The data are shown as mean ± SD, n=3.

4.4.1.4 Aggregation of platelets with collagen in Tyrode's buffer +/- glucose

To discover whether the aggregation response seen with thrombin was specific for a given agonist, a similar experiment was carried out with a range of doses of collagen (Figure 4-11). The data were again analysed for 1.5 and 3minutes of the aggregation experiment. The EC_{50} were not different for platelets in the presence and absence of glucose ($p>0.05$).

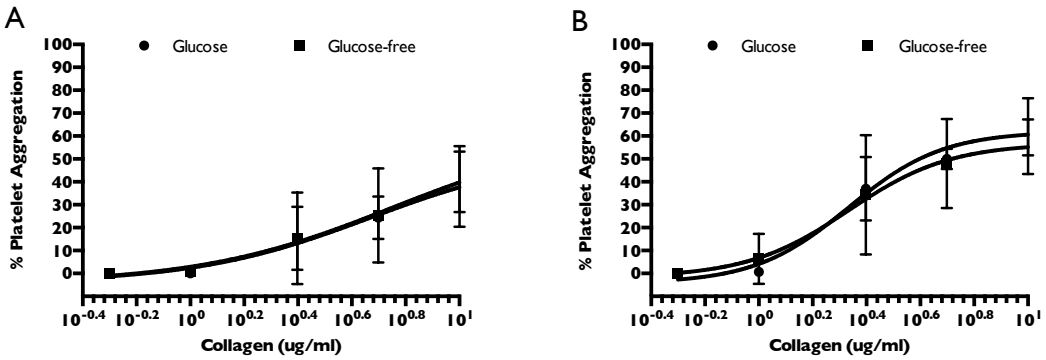

Figure 4-11: Aggregation of platelets with collagen in Tyrode's buffer +/- glucose. Dose response curves of platelets stimulated with 0.5, 1, 2.5, 5 and 10 μg/ml collagen in Tyrode's buffer +/- glucose. Data presented as log (collagen dose) Vs. response (%Aggregation), n=3. (A) Dose response curve for platelets stimulated with collagen in Tyrode's buffer +/- glucose at 1.5 minutes. EC_{50} for +/- glucose were 14.7 and 13.6 (B) Dose response curve for platelets stimulated with collagen in Tyrode's buffer +/- glucose at 3 minutes. EC_{50} was 0.3 for both +/- glucose conditions.

4.4.1.5 ATP secretion of platelets with collagen in Tyrode's buffer+/- glucose

The ATP secretion of platelets in Tyrode's buffer +/- glucose was also compared with various doses of collagen (Figure 4-12). ATP secretion did not differ between groups for all doses ($p>0.05$).

A

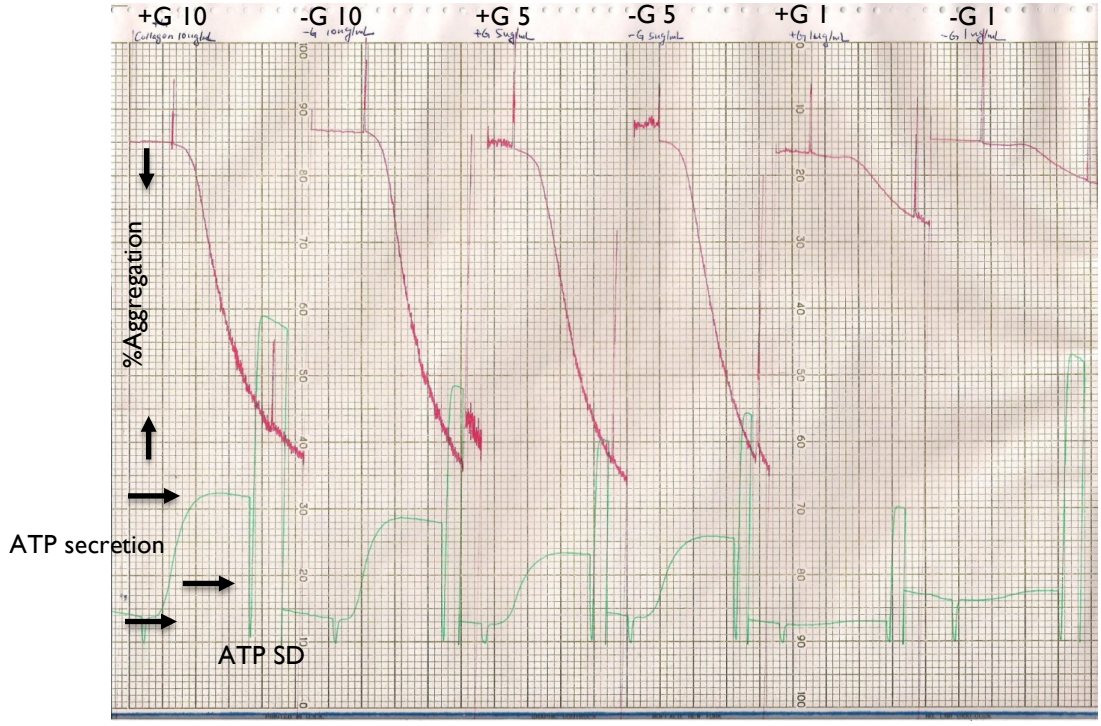

B

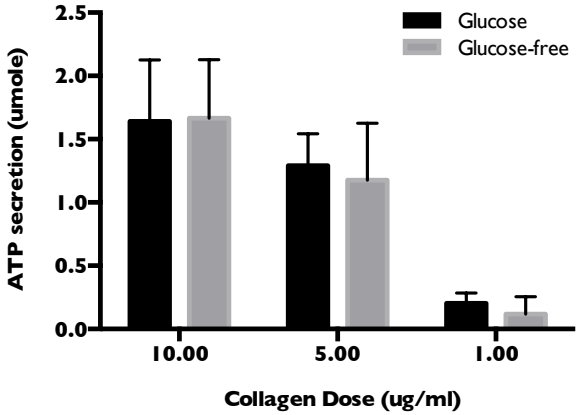

Figure 4-12: Platelet ATP secretion with collagen in Tyrode's buffer +/- glucose (A) Platelet ATP secretion stimulated with collagen, from left to right: + G (glucose) 10 μg/ml, - G 10 μg/ml, +G 5 μg/ml, - G 5 μg/ml, + G 1 μg/ml, - G 1 μg/ml. (B) ATP secretion by platelets stimulated with 10, 5, 1 μg/ml collagen over 90 seconds. The data are shown as mean ± SD, n=3

4.4.2 Quantification of platelet glycogen with acid hydrolysis

The optimised acid hydrolysis method for glycogen determination was tested for both glycogen standard (4.3.2.1) and samples (4.3.2.2). However, the optimal hydrolysis time for both standards and a given number of platelets required further optimisation. After optimising these parameters, the amount of basal glycogen levels from different donors as well as the amount of glycogen required for aggregation response was quantified.

4.4.2.1 Optimisation of hydrolysis time for glycogen standard

To discover the optimal hydrolysis time for converting all the glycogen in the standards into free-glucose, the highest concentration in the standard 200 μg/ml of glycogen was subjected to 60, 90 and 120 minutes of hydrolysis and the amount of free glucose released was 0.23±0.04, 0.24±0.05 and 0.22±0.02μmols respectively, which did not differ significantly ($p>0.05$). The data therefore shows that 1h of hydrolysis was sufficient to liberate all of the glucose from glycogen.

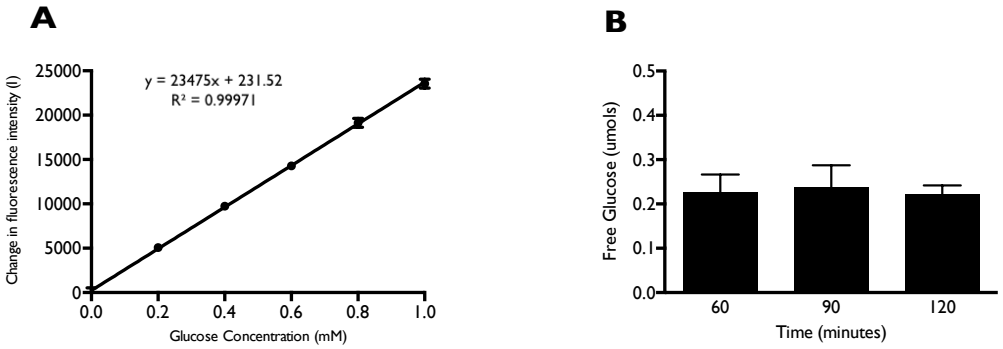

Figure 4-13: Glycogen standard hydrolysis time optimization (A) Glucose standard. (B) The absolute amount of glucose released by 200μg/ml glycogen at 60, 90 and 120 minutes of hydrolysis. Data shown as means ± SD, n=3.

4.4.2.2 Platelet sample preparation

The aggregation experiments in this study were carried out with 250µl, $2.5*10^8$ platelets/ml for three and half minutes. To measure the glycogen content in platelets before after aggregation, the experiment was modified to increase the volume and platelet number of the suspension for the same dose of thrombin. To achieve a similar % of aggregation ($p>0.99$) with 0.1U/ml thrombin, 500µl, $3*10^8$ platelets/ml (Figure 4-14A) took 5 minutes compared to 250µl, $2.5*10^8$ platelets/ml (Figure 4-14B).

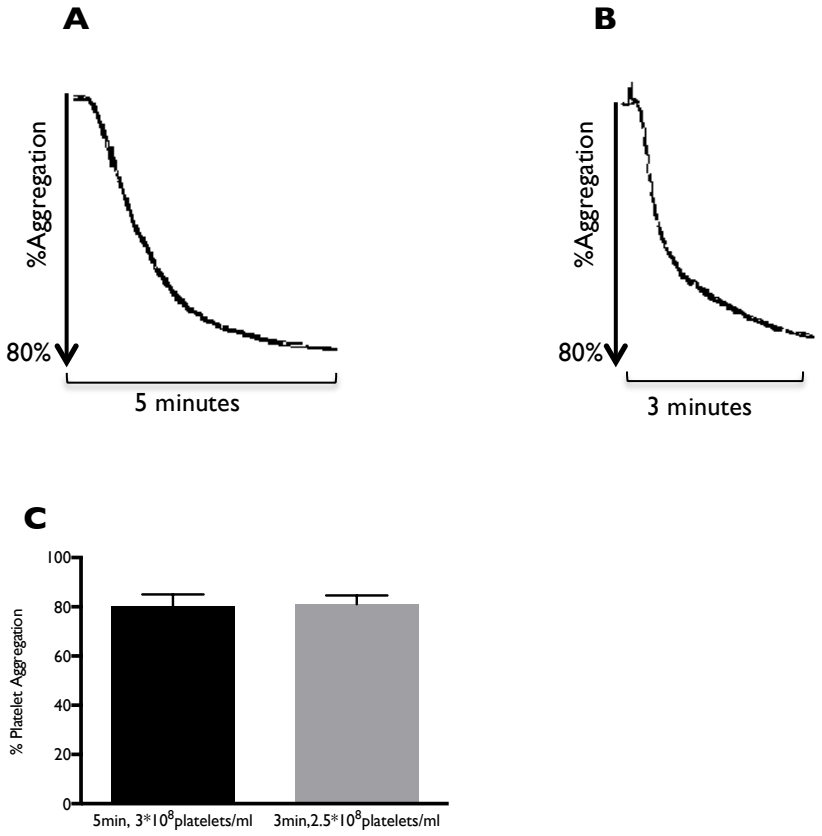

Figure 4-14: Aggregation traces for two different cell concentrations and for volumes (A) Representative aggregation trace for 500µl, $3*10^8$ platelets/ml stimulated with 0.1U/ml thrombin. (B) Representative aggregation trace of 250µl, $2.5*10^8$ platelets/ml stimulated with 0.1U/ml thrombin. (C) %Aggregation of A&B over 5 and 3 minutes, n=3, Data shown as mean ± SD.

4.4.2.3 Optimisation of hydrolysis time for platelet glycogen samples

To ensure that the glycogen standard and samples required the same amount of time to achieve maximum hydrolysis, 500µl of $3*10^8$/ml platelet was subjected to acid hydrolysis for 60, 90 and 120 minutes. The amount of free glucose (Figure 4-15C) and glycogen (Figure 4-15D) were quantified. The amount of glycogen ($p>0.05$) did not differ across all time points and so 60 minutes hydrolysis time was chosen for this study.

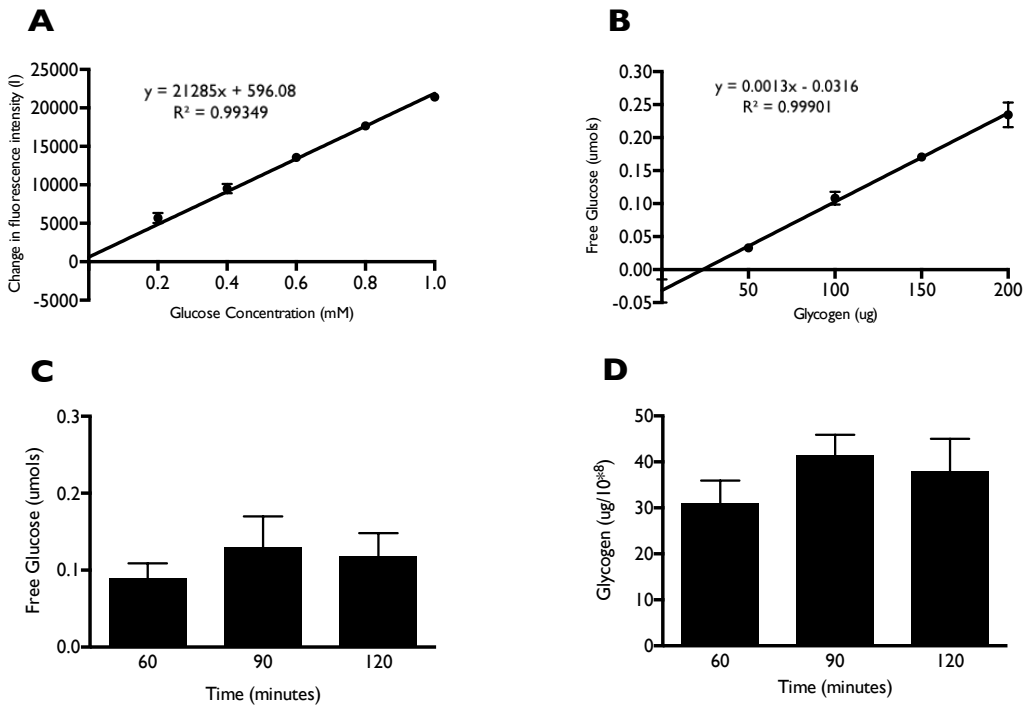

Figure 4-15: Platelet sample hydrolysis time optimization for glycogen analysis (A) Glucose standard. (B) Glycogen Standard. (C) Absolute amount of free glucose from 500µl, $3*10^8$/ml platelets at 60, 90 and 120 minutes of hydrolysis. (D) Absolute amount of glycogen in 500µl, $3*10^8$/ml platelets at 60, 90 and 120 minutes of hydrolysis; Data shown as mean ± SD, n=3.

4.4.2.4 Basal glycogen level in platelets from different donors

After establishing the method for the quantification of platelet glycogen, the basal glycogen levels in six different donors were measured (Figure 4-16). There were donor variations in the level of basal glycogen. The minimum was 28.9 μg glycogen/10^8 platelets and maximum 44.98 μg glycogen/10^8 platelets.

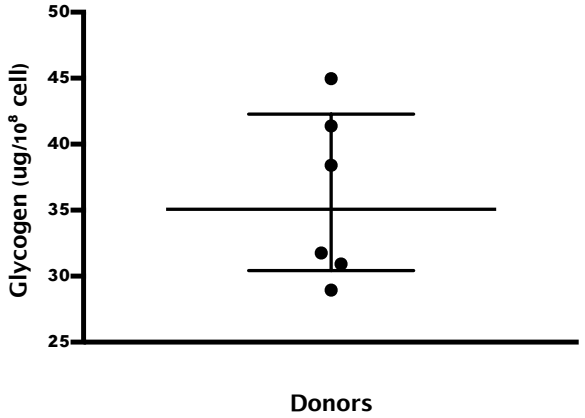

Figure 4-16: Basal glycogen level of platelets from six different donors. Data shown as median with interquartile range.

4.4.2.5 Glycogen level in platelets stimulated with thrombin

The amount of glycogen in platelets before and after stimulation with 0.1U/ml thrombin in glucose-free Tyrode's medium was quantified (Figure 4-17). The initial glycogen level, 26.5 ± 4.2 μg glycogen/10^8 platelets, dropped significantly to 12.3 ± 3.4 μg glycogen/10^8 platelets ($p<0.01$) after aggregation.

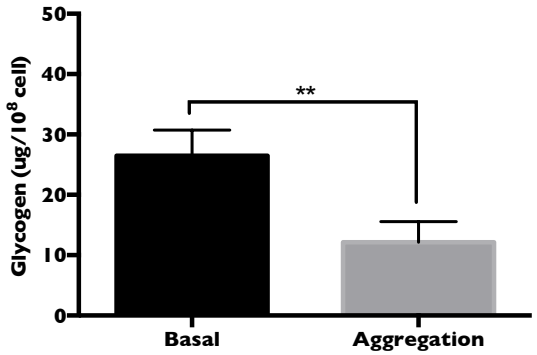

Figure 4-17: Platelet glycogen level before and after thrombin stimulation. Data shown as mean ± SD, n=4. **<0.01.

4.4.3 Glycogen-dependent glycolytic capacity of platelets

The glycolytic capacity of platelets at rest and following activation was assessed using the XFp glycolytic stress test (2.6.1). After establishing a basal ECAR in glucose-free XFp medium (Appendix 2), 0.1U/ml thrombin was injected (Figure 4-18A). The ECAR increased from 0.7 ± 0.1 to a mean of 3.2 ± 1.2, and maximum 4.6± 0.4mpH/min/μg protein ($p < 0.05$), due to the glycogen-dependent glycolytic function of platelets when extracellular glucose was absent. The injection of the mitochondrial complex V inhibitor oligomycin did not further elevate the ECAR unlike the case when exogenous glucose was provided (3-16A). The addition of 2-DG ablated the ECAR, indicating that the ECAR was due to glycolysis and there was minimum non-glycolytic ECAR only. Surprisingly, when exogenous glucose was provided after the stimulation of platelets with thrombin, platelets sustained a higher glycolytic rate, and were able to respond to oligomycin. The injection of thrombin increased the ECAR from 0.6 ± 0.2 to a maximum 5.0 ± 0.4mpH/min/μg protein ($p < 0.001$). The subsequent injection of 5.6mM glucose sustained the glycolytic rate, despite the plateau response as previously observed. Platelets could therefore respond to the inhibition of mitochondrial ATP synthase, by increasing the glycolytic rate to 5.4 ± 0.2mpH/min/μg protein ($p<0.05$). The addition of 2-DG again suggested that this ECAR was from glycolysis and that platelets present minimal non-glycolytic ECAR (Figure 4-18B).

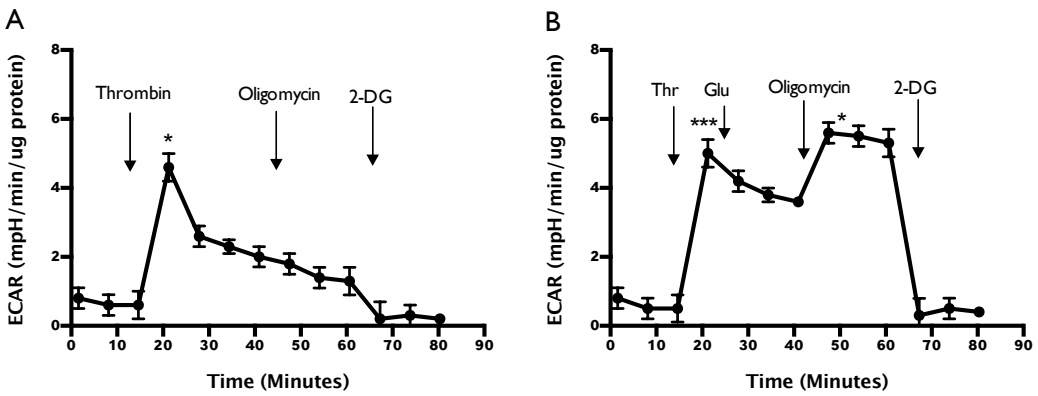

Figure 4-18: Glycogen-dependent glycolytic capacity of platelets at rest and following activation (A) ECAR of platelets with sequential injection with thrombin (0.1U/ml), oligomycin (1μM) and 2-deoxy glucose (2-DG, 50mM) in glucose free medium. The injection of thrombin increased ECAR significantly ($p<0.05$). 2-DG was added to correct for non-glycolytic extracellular acidification. (B) ECAR of platelets after the sequential addition of thrombin (0.1U/ml), glucose (5mM), oligomycin and 2-DG. Thrombin stimulation increased ECAR drastically ($p<0.001$) above basal ECAR. Oligomycin further increased ECAR ($p<0.05$). Data shown as mean ± SEM, n=3. *<0.05, ***<0.001.

4.4.4 Glycolytic and oxidative metabolism of glycogen

4.4.4.1 Glycogen-dependent OCR and ECAR of platelets stimulated with thrombin

To understand whether OXPHOS is involved in glycogen dependent platelet activation, the OCR and ECAR of platelets were measured in the resting state and after activation with thrombin in glucose-free medium. When stimulated with 0.1U/ml thrombin, platelet OCR increased from 2.6±0.03pmol/min/μg protein to 3.8±0.02pmol/min/μg protein ($p<0.05$) (Figure 4-19A, C). 0.01U/ml thrombin failed to induce an increase in OCR. ECAR was measured simultaneously and showed a pattern similar to the OCR (Figure 4-19C, D). 0.1U/ml thrombin increased ECAR drastically from 1.9 ± 0.2 mpH/min/μg protein to an average 6.1 ± 1.6 mpH/min/μg protein ($p<0.05$) compared to 0.01U/ml, which failed to increased ECAR.

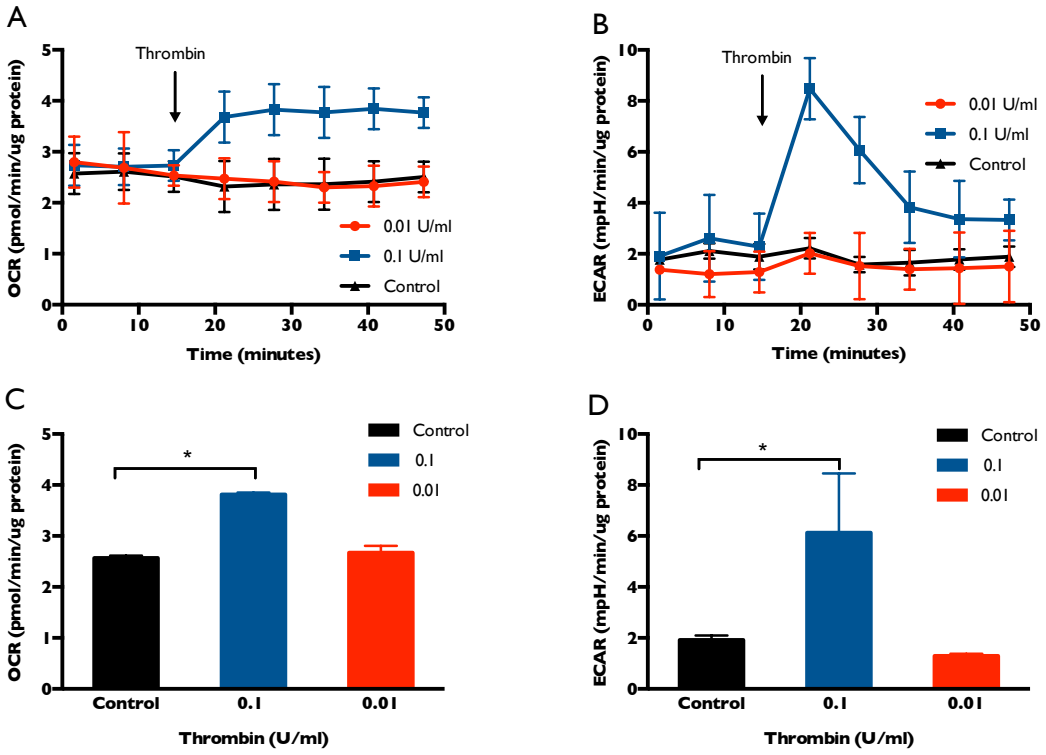

Figure 4-19: OCR and ECAR of platelet stimulated with high and low dose of thrombin in glucose-free medium (A) OCR of platelets stimulated with 0.1and 0.01U/ml thrombin over time. (B) ECAR of platelets stimulated with 0.1 and 0.01U/ml thrombin over time. (C) Mean OCR quantified from (A). Upon stimulation with 0.1U/ml thrombin, there was a significant increase in OCR ($p<0.05$) compared to basal. (D) Average ECAR quantified from (B). Upon stimulation with 0.1U/ml thrombin, ECAR increased significantly compared to basal ($p<0.05$). Data shown as mean ± SEM, n=3, *<0.05.

4.4.4.2 Partitioning of glycogen in glycolysis and OXPHOS in response to thrombin

Since both OXPHOS and glycolysis are involved in glycogen-dependent thrombin activation of platelets, the partitioning of glycogen into glycolysis and oxidation culminating in oxidative phosphorylation was examined in response to a high dose of thrombin. The contribution of fatty acid β-oxidation was first inhibited using etomoxir (Ito et al., 2012; Ravi et al., 2015), to produce conditions where OCR and ECAR were largely glycogen-dependent since there were no other substrates provided in the medium. In contrast to experiments performed in the presence of external glucose (Figure 3-20A), inhibition of β-oxidation caused a sustained and significant fall in OCR (Figure 4-20A). Under resting conditions, glycogen was metabolised through both glycolysis and OXPHOS (Figure 4-20A and C). Thrombin (0.1U/ml) caused the OCR to rise from 0.8 ± 0.07 to 2.1 ± 0.06pmol/min/μg protein ($p<0.01$) (Figure 4-20A and B). The addition of the complex I/III inhibitors, antimycin A and rotenone (A/R), caused an almost complete abolition of basal OCR and ablated that induced by thrombin. The remaining non-mitochondrial OCR in thrombin-stimulated platelets was similar to the control suggesting that thrombin did not alter non-mitochondrial OCR (Figure 4-20A). In parallel to the rise in OXPHOS, thrombin stimulated a rapid increase in the ECAR from 0.4 ± 0.06 to an average 2.9 ± 0.5 mpH/min/μg protein ($p<0.01$) (Figure 4-20C and D). In this case, similar to oligomycin in Figure 4-18A, the addition of rotenone and antimycin failed to increase ECAR in both resting and thrombin-stimulated platelets (Figure 4-20C), suggesting that endogenous glycogen was insufficient to support the compensatory increase in glycolysis when mitochondrial ATP synthesis was blocked. The subsequent addition of 2-deoxyglucose (2-DG; 50 mM) to inhibit glycolysis had no effect on OCR, but did abolish the thrombin-induced glycolysis, indicating a minimal non-glycolytic ECAR in platelets. Activation of platelets increased the activity of both pathways (Figure 4-20E), but critically, there was a shift to a glycolysis-dominated phenotype (almost 5 fold change in ECAR) whereas oxidative phosphorylation changed only minimally in the absence of β-oxidation. Under conditions where β-oxidation was inhibited in glucose-free Tyrode's buffer, platelets aggregated normally (EC_{50} did not change, $p>0.05$) in response to thrombin (Figure 4-20F).

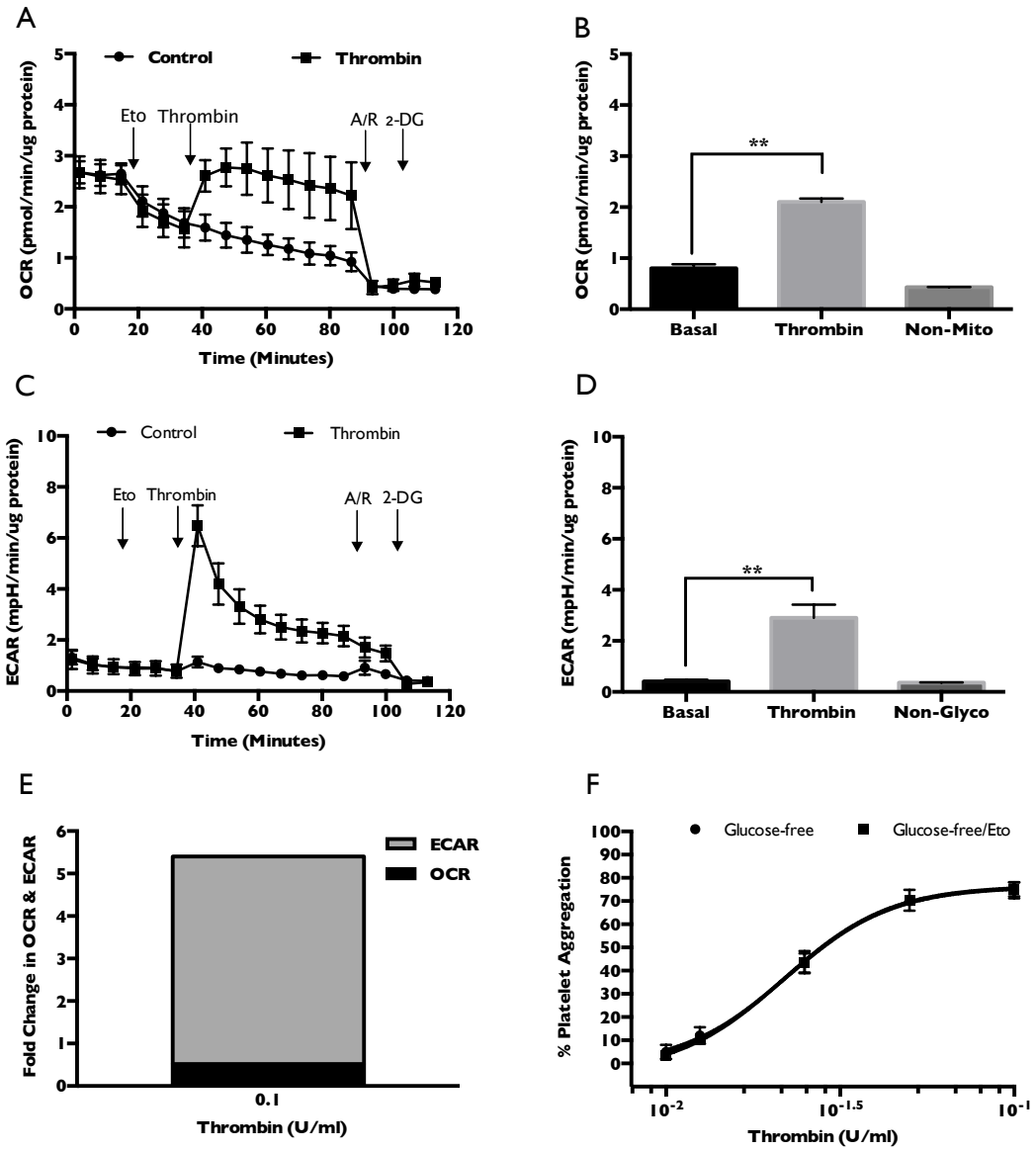

Figure 4-20: OCR & ECAR of platelets stimulated with thrombin in glucose free medium (A) OCR of platelets +/- 0.1U/ml thrombin. The glycogen-dependent oxygen consumption was differentiated from that of endogenous fatty acids by the addition of Etomoxir. Non-mitochondrial OCR was accounted by the OCR, which was insensitive to the combination of Antimycin/Rotenone. (B) Upon stimulation with 0.1U/ml thrombin, there was a significant increase in the OCR compared to basal after correcting for non-mitochondrial OCR ($p<0.01$). (C) ECAR of platelets +/- 0.1U/ml thrombin. 2-Deoxy glucose was added to correct for non-glycolytic extracellular acidification. (D) Upon stimulation with 0.1U/ml thrombin, there was a significant increase in the ECAR compared to basal after correcting for non-glycolytic acidification ($p<0.01$). (E) Fold change in OCR and ECAR after thrombin stimulation compared to basal. The values were corrected for non-mitochondrial OCR & non-glycolytic ECAR. Data expressed as mean ± SEM, n=3 F. Dose response curve of platelets stimulated with 0.01, 0.0125, 0.025, 0.05 and 0.1U/ml thrombin in glucose-free Tyrode's buffer +/- etomoxir. Data presented as log (thrombin dose) Vs. response (%Aggregation), n=3, **<0.01.

4.4.5 Mechanism of platelet glycogenolysis

To understand whether Ca^{2+} plays a role in platelet glycogen metabolism, platelets were treated with BATPA-AM (20μM), a chelator of intracellular Ca^{2+}, and glycogen metabolism was examined. Under these conditions the basal OCR and ECAR were unaffected, but the shift towards a glycolytic phenotype induced by thrombin as well the increase in oxygen consumption was abolished (Figure 4-21).

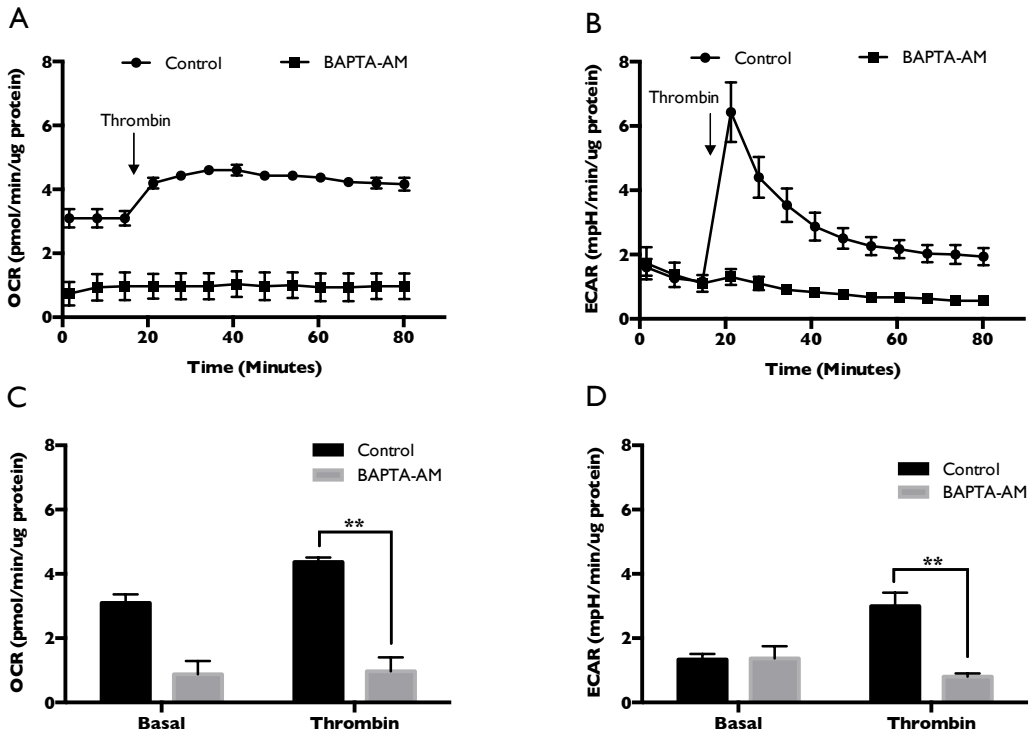

Figure 4-21: Platelet OCR and ECAR measured with +/- BAPTA-AM (A) OCR of platelets +/- BAPTA-AM stimulated with 0.1U/ml thrombin. (B) ECAR of platelets +/- BAPTA-AM stimulated with 0.1U/ml thrombin. (C) OCR quantified from (A). Upon thrombin stimulation, OCR increased significantly in the control group compared to BAPTA-AM treated group ($p<0.01$). (D) ECAR quantified from (B). Upon thrombin stimulation, ECAR increased significantly in the control group compared to BAPTA-AM treated group ($p<0.01$), Data shown as mean ± SEM, n=3, **<0.01.

4.5 Discussion

The first aim of this chapter was to investigate the relative importance of exogenous glucose on platelet functions. Consequently, platelet aggregation, ATP secretion and adhesion were tested with thrombin and collagen in the presence or absence of glucose. A simplified method was then developed to quantify glycogen content in platelets basally as well as after activation with thrombin. After confirming that platelets utilised glycogen in the absence of glucose, the glycogen-dependent glycolytic capacity and the partitioning of glycogen between glycolysis and OXPHOS were measured. Also, a preliminary experiment was carried out to investigate the potential regulation of glycogenolysis in platelets.

4.5.1 Platelet function in response to the absence of glucose

This study is the first to compare the functional responses of platelets in the presence or absence of glucose. Platelet secretion and aggregation with both thrombin and collagen were similar in the presence and absence of glucose, and platelet-collagen interaction was also unaffected by the omission of exogenous glucose (Figure 4-8 to Figure 4-12). Quantification of platelet glycogen content before and after thrombin stimulation indicated that endogenous glycogen could provide platelets with sufficient energy when glucose supply was limited (Figure 4-13 to Figure 4-17). These findings support the notion that the platelet glycogen store is biologically active, serving as an energy reserve. Interestingly, platelets are not the only blood cells to have a glycogen reserve; common myeloid progenitor cells, such as neutrophils (Borregaard and Herlin, 1982), monocyte derived dendritic cells (Amiel and Thwe, 2016) and inflammatory macrophages (Gudewicz, 1975) also have an active glycogen metabolism though its role has yet to explored in these cell types.

4.5.2 Glycogen-dependent glycolytic capacity

In a medium lacking glucose or other exogenous substrates, the potential fuel sources for washed platelets are endogenous fatty acids and glycogen (Broekman et al., 1980; Ravi et al., 2015). In studies that have investigated platelet metabolism in glucose-free medium, the production of lactate has strongly suggested the utilization of endogenous glycogen through glycolysis, and mitochondrial respiration without exogenous glucose has indicated a possible role for both glycogen and endogenous fatty acids in sustaining platelet metabolism (Vehoeven et al., 1984). The ability of platelets to utilise glycogen by glycolysis was therefore investigated in the present study. In the absence of glucose, the maximal ECAR of platelets in response to thrombin (Figure 4-18) was lower than that in the presence of glucose (Figure 3-16) and the glycolytic response decreased abruptly over time. However, the glycolytic response seemed to be sufficient to support platelet aggregation. To explore the maximal glycogen-dependent glycolytic capacity, oligomycin was added to inhibit oxidative phosphorylation. In the absence of exogenous substrates, platelets were unable to increase ECAR to compensate for the loss of ATP generated from OXPHOS. This could be because after thrombin stimulation, platelets were drained of glycogen (Figure 4-18A) in agreement with earlier studies that have measured lactate production in the absence of glucose which lasted as long as 60-90 minutes (Karpatkin, 1967; Verhoeven et al., 1984). In the present study, glycolysis in the presence of external glucose continued despite the inhibition of ATP generation by OXPHOS before being abolished by 2-DG (Figure 3-16). This suggests that platelets can rely on glycolysis for energy generation; a feature also observed in neutrophils, where defective respiration has been reported not to affect their energy metabolism (Borregaard and Herlin, 1982). As circulatory cells, this property is likely to equip platelets to function under conditions where the oxygen supply may be limited, such as in a thrombus.

Interestingly, if glucose was provided after stimulation with thrombin in a glucose-free buffer, the maximal ECAR peaked at a level similar to that seen when glucose was present throughout stimulation (Figure 3-16) and the elevated glycolytic response could be sustained for longer (Figure 4-18B). Apart from this, platelets were able to compensate for the loss of ATP generation with OXPHOS by

increasing ECAR in response to oligomycin. These data indicate that platelets can support various functions without reaching the maximal glycolytic capacity, providing them with plasticity in the presence and absence of glucose.

4.5.3 Glycolytic and oxidative metabolism of glycogen

Low dose (0.01U/ml) thrombin in the absence of glucose did not prompt an increase in OCR and ECAR, potentially suggesting a failure to achieve the mobilization of glycogen. The response of OCR and ECAR to stimulation with the high dose (0.1U/ml) thrombin, did suggest the mobilisation of glycogen through both glycolysis and OXPHOS (Figure 4-19). However, OXPHOS could be potentially from endogenous fatty acids. Consequently, the relative contribution of endogenous fatty acids and glycogen to OXPHOS was then explored by inhibiting the β-oxidation of long chain fatty acids with etomoxir (Figure 4-20). Inhibiting β-oxidation did not affect platelet aggregation, indicating that aggregation can be achieved solely by relying on glycogen. However, the inhibition of β-oxidation did prompt a fall in OXPHOS over time, suggesting that in order to sustain oxidative phosphorylation in the absence of glucose, endogenous fatty acids were required. The fall in OCR was less significant when platelets were activated with thrombin (0.1U/ml), which induced a sustained increase in OCR, which was slightly higher than in the presence of glucose (Figure 3-20). These data suggest that glycogen may also be metabolised via OXPHOS under stimulatory conditions. Although the change in ECAR was nearly five times higher than that of OCR, in the absence of exogenous glucose and endogenous fatty acids, it appears that platelets can maximize ATP generation from OXPHOS. This suggests a fine cooperation between glycolysis and OXPHOS under the circumstances of nutrient deficiency.

4.5.4 Regulation of glycogenolysis in platelets

In both liver and muscle, the enzyme controlling the breakdown of glycogen is phosphorylase a, which also exists in a less active b form. Transformation from phosphorylase b to a is regulated by glycogen phosphorylase kinase, which is itself activated by a cAMP-PKA dependent pathway. However, in skeletal muscle, this

transformation can also be mediated by calcium, independent of cAMP pathway resulting in the breakdown of glycogen. The present study showed that glycogen breakdown in platelets requires calcium and is cAMP/PKA pathway independent (Figure 4-21). This is consistent with the observation that the cAMP/PKA signalling cascade plays a central role in the inhibition of platelet activation (Beck et al. 2014) by increasing cAMP levels. During platelet activation and aggregation, glycogenolysis continues to occur despite a fall in cAMP levels. Additionally, blocking calcium with BAPTA-AM (20μM) completely abolished glycolysis in glucose-free buffer, indicating that there is no redundancy of pathways controlling glycogenolysis in platelets.

The precise role of platelet glycogen in circulating platelets has yet to be investigated. However, platelet glycogen has been shown to play an important role in various diseases. Deficiency in hexokinase, the first rate-limiting enzyme in glycolysis, can cause anaemia in patients. However, the hexokinase deficient platelets of these patients have been shown to have normal glycogen metabolism and can support normal platelet function (Akkerman, 1984), as glycogen breakdown by-passes the first reaction in glycolysis, suggesting a backup role for platelet glycogen reserve in diseases such as hexokinase deficiency. The absence of glycogen reserve as in glycogen storage disease type 1, patients have an impaired coagulation system and suffer prolonged bleeding upon injury (Czapek et al., 1973), consistent with a vital role for glycogen in sustaining platelet function in people without this disorder.

4.6 Conclusion

In summary, this study has provided evidence that the platelet glycogen store was metabolically active for supporting various platelet functions under conditions where exogenous nutrients were limited. It also showed that the metabolic fate of glycogen was similar to that of glucose, involving both glycolysis and OXPHOS. Most importantly, it showed that platelet glycogenolysis was mediated by calcium dependent pathway, providing the first new knowledge in this area since the publication by Verhoeven et al., (1984).

5. Metabolic flexibility of platelets

5.1 Introduction

A fundamental role of mammalian mitochondria is energy transduction in the form of ATP, via the oxidation of nutrients in oxidative phosphorylation. Platelets have fully functional mitochondria (Symth et al., 2010; Figure 1-1), which, in addition to generating ATP are involved in redox signalling (Pietraforte et al., 2014), platelet activation (Bozza and Weyrich, 2008), initiation of the inflammatory response (Boudreau et al., 2014) and apoptosis (Leytin, 2012; Zharikov and Shiva, 2013). Of these functions, the focus in this thesis is on the role of platelet mitochondria in energy metabolism.

Metabolism of glucose, fatty acids and amino acids converge in the mitochondria, where fuel oxidation can be modified in response to changes in the availability of nutrients and the energy demand of the cell under various conditions (Galgani et al., 2008). Although glucose and fatty acids are considered to be the major oxidative substrates for platelets (Karpatkin, 1967; Garcia-Souza and Oliveira, 2014; Ravi et al., 2015) evidence on the role of the third potential substrate in the energy metabolism of platelets amino acids, is lacking. The carbon skeletons from amino acid deamination can be transformed into metabolic intermediates that can be oxidised in mitochondria or, in some tissues, converted to glucose via gluconeogenesis. Of all the amino acids, the role of glutamine as a substrate for platelet mitochondria has received most attention, yet the role as an oxidative fuel is controversial (Murphy et al., 1992; Ravi et al., 2015).

Above all, the relative dependency and flexibility of platelets in oxidising glucose, endogenous fatty acids and amino acids under various conditions remain unclear. This is partially due to the inflexibility of existing methods on separating different fuel oxidation by platelets in same platelet suspension; however, XFp Seahorse bioanalyser provides an easy approach for the differentiation of various fuel oxidations, by injecting inhibitors of corresponding metabolic pathways. The serial injections of the inhibitors of mitochondrial complexes enable the interrogation of the components of mitochondrial respiration as described in Chapter 1.4.4 in detail. In this chapter, these measures are also used to investigate the impact of potential metabolic disturbance on the function of platelet mitochondria.

5.2 Aims

The aim of this chapter is to determine the metabolic flexibility of platelets in terms of their ability to utilise a variety of substrates. In order to address this, the following series of experiments have been carried out:

- Measurement of amino acid utilisation by human platelets at rest and following activation
- Determine the relative ability of platelets to utilise glutamine, glucose and endogenous fatty acids
- Measurement of the relative dependency of platelets on glycolysis and OXPHOS generated ATP to respond to activation
- Measurement of the function of human platelet mitochondria at rest and activation
- Measurement of the impact of a high fat diet on murine platelet mitochondrial function

5.3 Materials & Methods

All the chemicals and buffer compositions are provided in Appendix 1&2. Unless stated otherwise, platelets were prepared as described in 2.5.3 for the XFp assays, cells were seeded as described in 2.5.5 and the cartridge was loaded as described in 2.5.6. All the XFp experiments were corrected for protein concentrations as described in 2.8, thus the OCR results are reported as pmol/min/μg protein, and ECAR reported as mpH/min/μg protein. In all experiments, unless stated otherwise, data were analysed from three independent experiments using platelets from three different individuals.

5.3.1 Amino acid utilisation by platelets at rest and activation

For each experiment, the concentrations of amino acids were calculated by relating the area under the curve obtained from HPLC chromatograms to that given by certified standards.

5.3.1.1 Amino acid utilisation by platelets with thrombin and collagen activation

Washed platelets were prepared and re-suspended at $2.5*10^8$ platelets/ml in Tyrode's buffer (pH 7.4) supplemented with 16 amino acids (Table 5-1). Platelets were then incubated at 37°C for 1 hour before a sample was collected for HPLC analysis of amino acid content. Platelet aggregation was carried out for 4 minutes/dose of thrombin (0.01 and 0.1 U/ml) as described in 2.3.2. Collagen doses were 1 and 10μg/ml. The aggregation experiment was carried out beginning with the highest dose. After the aggregation, platelet suspensions were collected and centrifuged (1200×*g*) to isolate the aggregate from the supernatant. The supernatant was then stored at -20°C before HPLC analysis (Chapter 2.7).

Table 5-1: Amino acid concentrations in this study and plasma reference range in healthy Caucasian population

Amino Acids	Stock Concentration (mM)	Assay Medium Concentration (μM)	Caucasians Reference Range[1] Age: 17-65 years (n=280)
Aspartic Acid	20	200	2-11
Asparagine	20	400	18-106
Serine	20	160	71-165
Histidine	20	100	58-104
Glutamine	10	900	352-689
Glycine	20	200	142-297
Threonine	20	200	69-182
Arginine	20	300	48-146
Alanine	20	200	191-531
Trypotophan	20	200	missing
Methionine	20	200	13-43
Valine	20	200	109-300
Phenylalanine	20	200	36-88
Isoleucine	20	160	26-95
Leucine	20	160	56-189
Lysine	20	100	112-271

Tan and Gajra, (2006)

5.3.1.2 Platelet flexibility to oxidise glutamine

Washed platelets were re-suspended in XFp assay medium (Appendix 2) containing 4mM glutamine (pH 7.4). Platelet flexibility to oxidise glutamine was investigated by measuring the 'dependency' and 'capacity' as described in 2.6.5. The compound-loading map is shown in Figure 5-1 and the concentrations of the inhibitors are shown in 2.6.5.

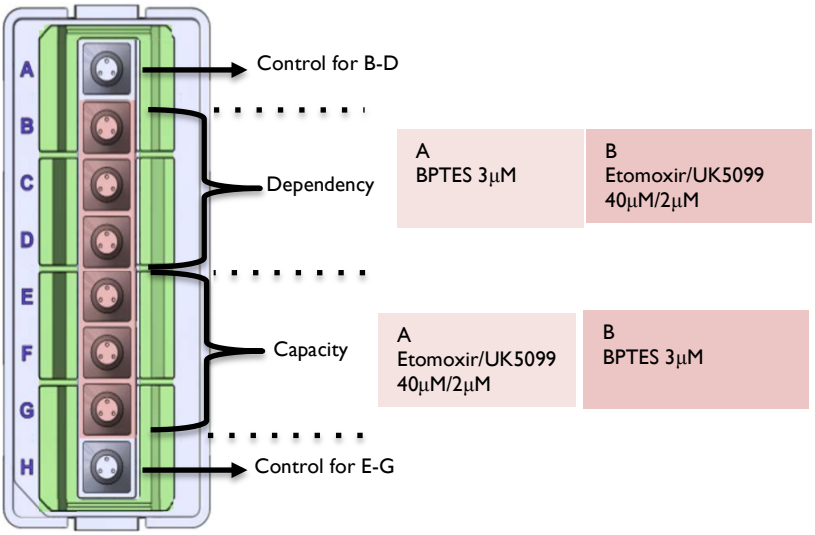

Figure 5-1: Cartridge compound loading map for measuring platelet dependency and capacity to oxidize glutamine. For each well, the cartridge port A, and B were loaded with BPTES and Etomoxir plus UK5099 for measuring dependency. For measuring capacity, the sequence was reversed.

5.3.2 Platelet flexibility to oxidise glucose and endogenous fatty acids

5.3.2.1 Platelet aggregation with glucose and endogenous fatty acid oxidation inhibitors

Washed platelets at a concentration of $2.5*10^8$ platelets/ml were treated with UK5099 (2μM), etomoxir (40μM) or UK5099 and etomoxir combination for 20 minutes. Platelet aggregation was carried out for three minutes with 0.1U/ml thrombin for each sample as described in 2.3.2.

5.3.2.2 Platelet flexibility to oxidise glucose and endogenous fatty acids at rest and activation

Washed platelets were re-suspended in XFp assay medium (Appendix 2) containing 4mM glutamine (pH 7.4). A series of experiments using conditions as described in Chapter 2.6.5 were performed to examine platelet flexibility by measuring dependency and capacity of platelet to a) oxidise glucose at rest (Figure 5-2) and in response to thrombin (Figure 5-3); b) oxidise fatty acids at rest (Figure 5-4) and in response to thrombin (Figure 5-5).

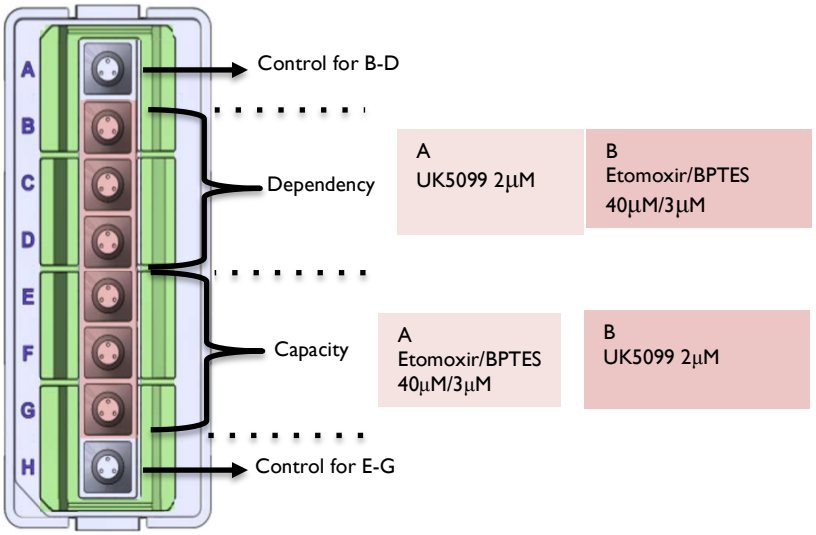

Figure 5-2: Cartridge compound loading map for measuring platelet dependency and capacity to oxidize glucose. For each well, the cartridge port A, and B were loaded with UK5099 and Etomoxir plus BPTES for measuring dependency. For measuring capacity, the sequence was reversed.

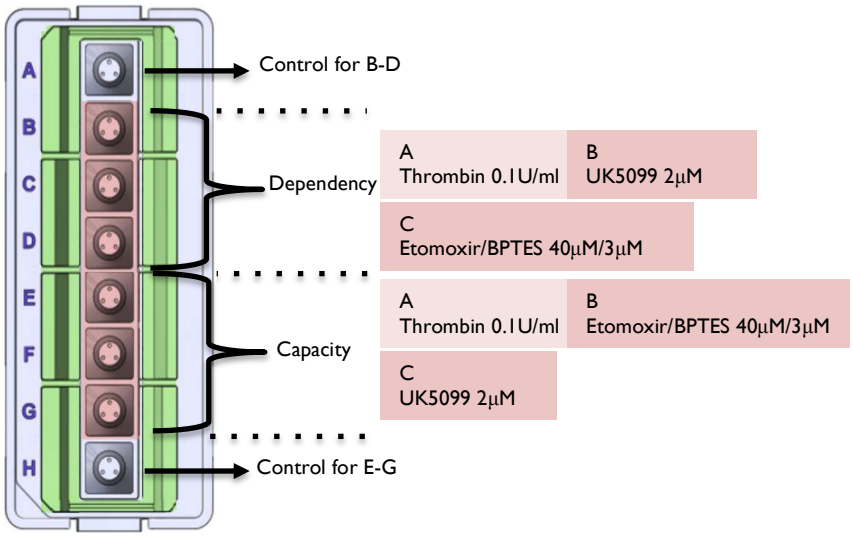

Figure 5-3: Cartridge compound loading map for measuring platelet dependency and capacity to oxidize glucose with thrombin. For each well, the cartridge ports A, B and C were loaded with thrombin (0.1U/ml), UK5099 and Etomoxir plus BPTES for measuring dependency. For measuring capacity, the sequence was reversed.

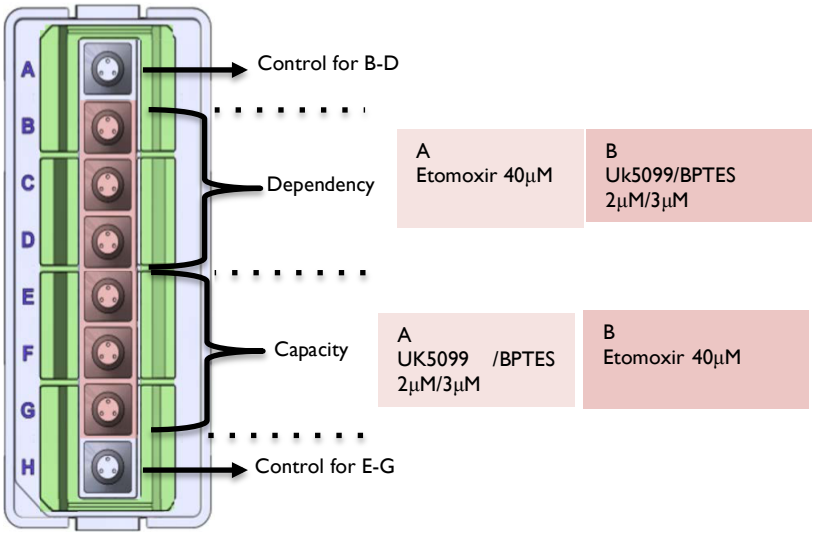

Figure 5-4: Cartridge compound loading map for measuring platelet dependency and capacity to oxidise endogenous fatty acids. For each well, the cartridge ports A and B were loaded with Etomoxir and UK5099 plus BPTES for measuring dependency. For measuring capacity, the sequence was reversed.

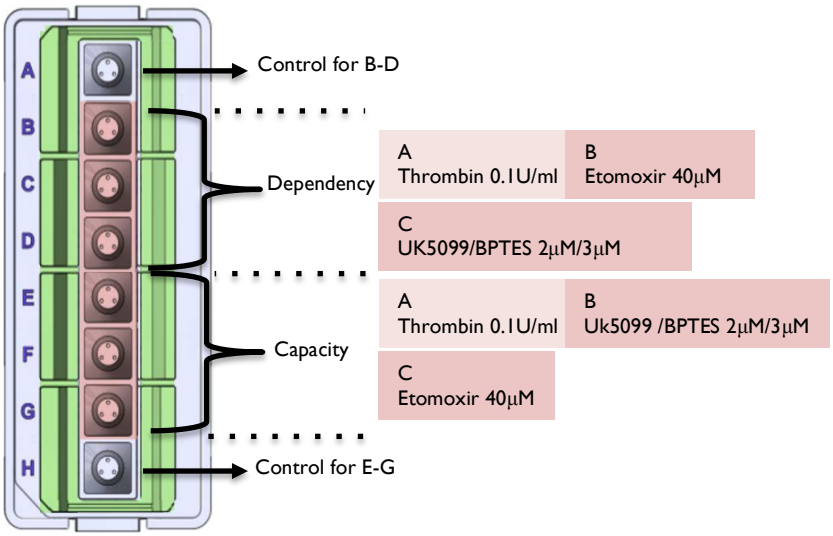

Figure 5-5: Cartridge compound loading map for measuring platelet dependency and capacity to oxidise endogenous fatty acids with thrombin. For each well, the cartridge ports A, B and C were loaded with thrombin (0.1U/ml), Etomoxir and UK5099 plus BPTES for measuring dependency. For measuring capacity, the sequence was reversed.

5.3.3 Platelet functional dependency on ATP from glycolysis and oxidative phosphorylation

Washed platelets were prepared and re-suspended at $2.5*10^8$ platelets/ml in Tyrode's buffer and incubated for one hour at 37°C. They were then divided into four groups and treated with oligomycin (1μM), 2-DG (50mM) or oligomycin plus 2-DG for 20 minutes. Platelet aggregation was monitored for three minutes using 0.1U/ml thrombin (Chapter 2.3.2).

5.3.4 Function of mitochondria in human platelets at rest and activation

To examine mitochondrial function of human platelets at rest and after activation it was first necessary to optimise the concentrations of key inhibitors, such as FCCP, antimycin A and rotenone. A series of experiments were therefore performed to optimise the concentration of FCCP as described in Chapter 2.6.3, where OCR was measured in the presence of 1μM oligomycin. Subsequently, concentrations of antimycin A and rotenone were used in combination at 2.5μM instead of the 0.5μM (Figure 3-16C) in the mitochondrial stress test.

5.3.4.1 Human platelet mitochondrial components of respiration

A modified mitochondrial stress test to discover the effect of thrombin was carried out as described in 2.6.2 (Table 2-5). B, C, D wells were kept as controls and E, F, G wells were stimulated with thrombin (0.1U/ml) (Figure 5-6). The concentrations of the inhibitors were as optimised in 5.3.4.

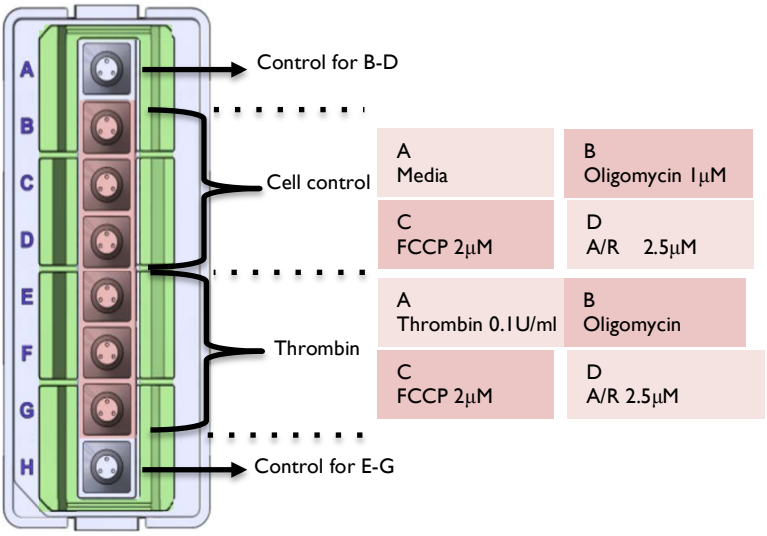

Figure 5-6: Cartridge compound loading map for measuring platelet mitochondrial function. For each well, the cartridge ports A, B, C and D were loaded with media/thrombin (0.1U/ml), oligomycin, FCCP and Antimycin A plus rotenone (A/R).

5.3.4.2 The effect of secondary mediators on human platelet mitochondrial components of respiration

Washed platelets were prepared and split into three equal portions. One was kept as control, one was treated with 2U/ml apyrase, and the last was treated with 10μM indomethacin. All the samples were incubated for 20 minutes in a non-CO_2 incubator at 37 °C before seeding into XFp plates (Figure 5-7). All the wells were stimulated with 0.1U/ml thrombin except for A.

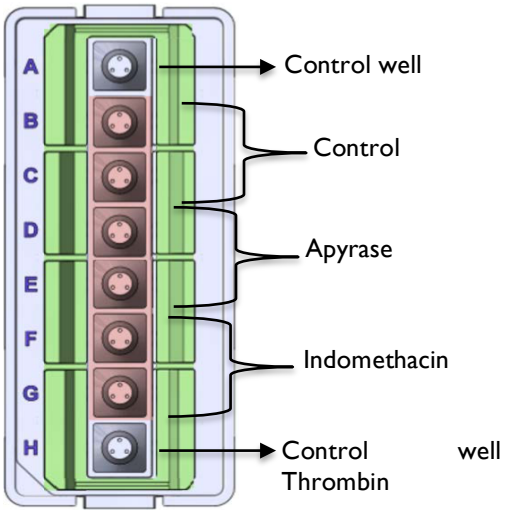

Figure 5-7: Cell seeding plan for measuring the effect of secondary mediators on platelet mitochondrial function. A & H wells were kept as controls with no cells; H well was injected with thrombin and the other wells used to correct for the protein. B & C wells were kept as controls. D & E wells were seeded with platelets treated with apyrase. F & G wells were seeded with platelets treated with indomethacin. All the wells were stimulated with 0.1U/ml thrombin.

5.3.4.3 Glycogen-dependent human platelet mitochondrial components of respiration

Washed platelets were re-suspended in glucose-free XFp medium (Appendix 2). Platelets were seeded into an XFp plate in wells B to G. The experimental procedure and cartridge-loading map was as in Figure 5-6.

5.3.5 Function of mitochondria in murine platelets at rest and activation

5.3.5.1 Murine platelet mitochondrial components of respiration

Blood was obtained by cardiac puncture from wild type C57BL/6 mice (Charles River) under terminal CO_2 narcosis. The mice had been fed a standard chow diet, and the blood was collected into PPACK. PRP was obtained by centrifugation of the blood at 300×*g* for 10 minutes at room temperature. The PRP was then centrifuged at 100×*g* in the presence of prostacyclin (0.1mg/ml) for 6 minutes at room temperature. The pellet was re-suspended in modified Tyrode's buffer, spun again at 100×*g* for 5 minutes and finally re-suspended at a concentration of 1×10^8 platelets/ml in XFp medium (Appendix 2). Platelets were seeded into B to G wells of an XFp plate as described in 2.5.5. The experimental procedure and cartridge-loading map was as in Figure 5-6.

5.3.5.2 High fat diet-induced murine platelet mitochondrial dysfunction

Wild type C57BL/6 (Charles River) animals were fed a standard laboratory mouse chow diet (Harlan Laboratories, Indianapolis, USA) for 4 weeks. The mice were then split into two groups with the control group maintained on normal chow and the experimental group fed on a 'Western' diet from special diet services (SDS) with 45, 20 and 35 % of total energy intake deriving from fat, protein and carbohydrates, respectively (diet code: 824053) for a further 12 weeks. Washed platelets were prepared as described in 5.3.5.1 and examined using the XFp mitochondrial stress test. Platelets were seeded into B to G wells of an XFp plate as described in 2.5.5. B, C and D were seeded with wild type platelets and E, F and G with the high-fat diet group. The experimental procedure and cartridge-loading map was as in B-C wells in Figure 5-6, except for not being stimulated with thrombin.

5.4 Results

5.4.1 Amino acid profile of platelet suspension at rest and activation

For measuring the amino acid profile of platelet suspension, the amino acid standards were first established (Figure 5-8). The percentage error fell within 0.5% for identification based on retention time (Figure 5-8A) of the amino acids using HPLC. This indicates that the possibility of misidentification is effectively zero and the amino acid concentration of a standard should be interpreted as 12.5±0.06μM considering the inherent technical variability.

A

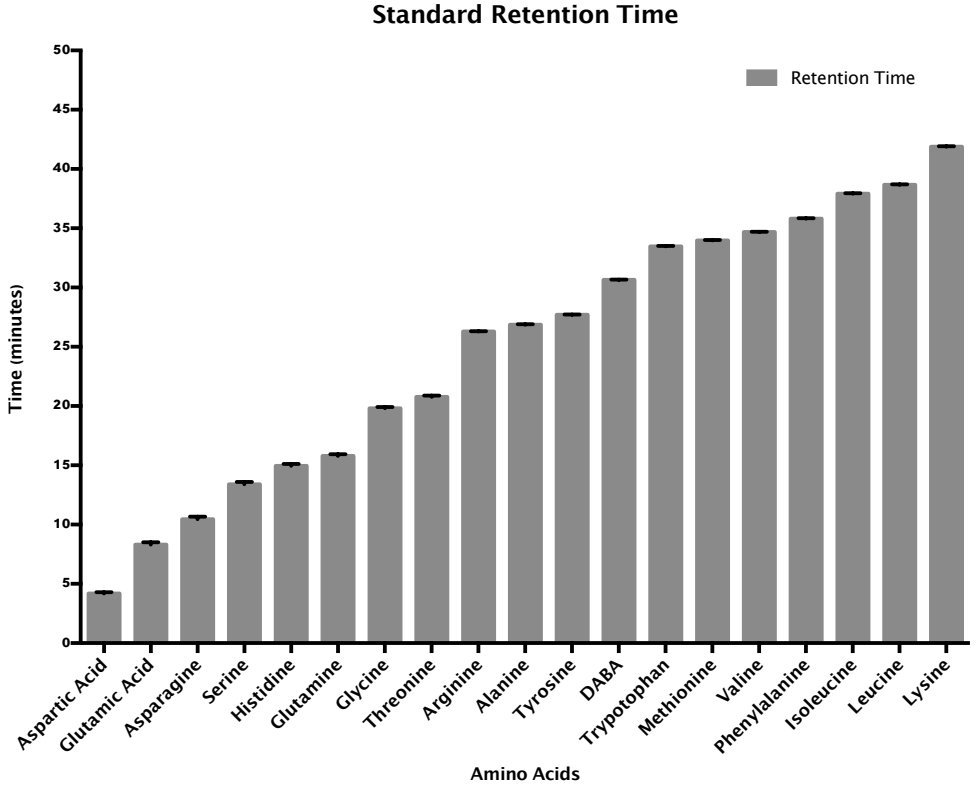

B

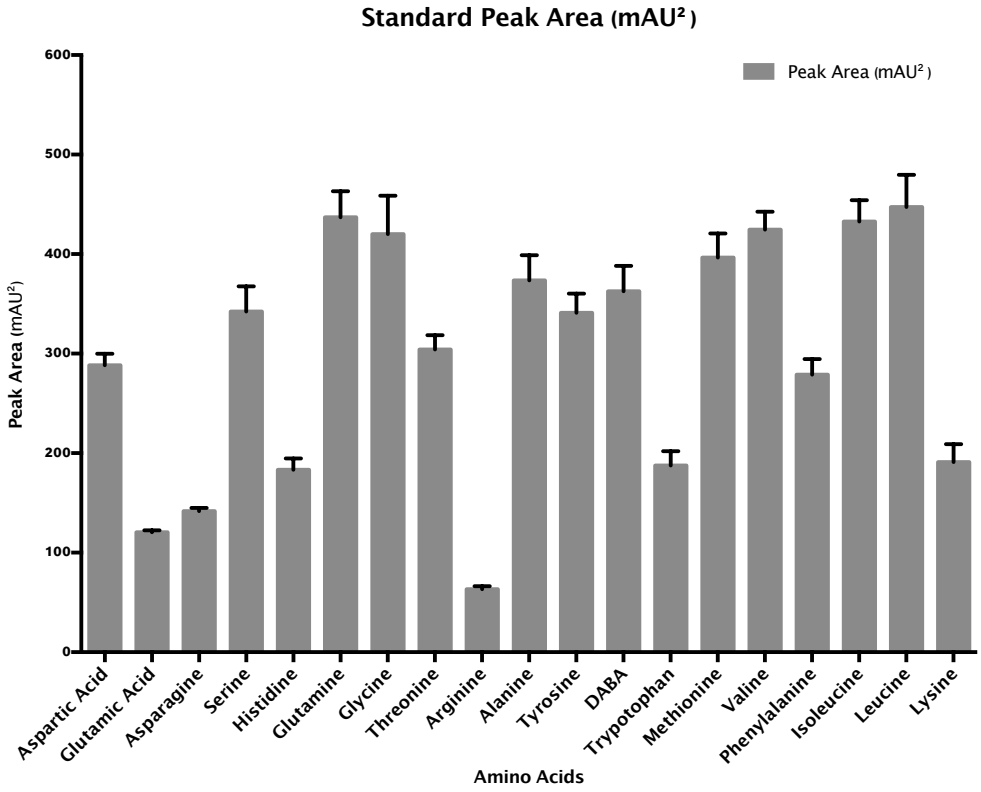

Figure 5-8: Amino acid standard (A) Average retention time corresponding to 12.5μM of the 18 amino acid standards. Mean± SD, n=3. (B) Average peak area corresponding to 12.5μM of the 18 amino acid standards. Data are presented as mean± SD, n=3.

5.4.1.1 Amino acid profile of platelet suspension at rest and after thrombin activation

Changes in amino acid profile in platelet suspension were measured (Figure 5-9). The concentrations of 16 amino acids were measured in the platelet-free samples taken from the medium (base), after 1-hour incubation with platelets at rest, and stimulation with low (0.01 U/ml) and high (0.1U/ml) doses of thrombin. Asparagine and glutamine were depleted, indicated by a fall in the concentration, after one hour of incubation in basal conditions as well as in response to stimulation with thrombin compared to the concentrations in the medium. However, arginine accumulated, indicated by a rise in concentration. The concentration of asparagine fell significantly after stimulation with both doses of thrombin compared to the concentrations in basal medium (367.6±45μM, $p<0.05$; 365.0±26.8μM, $p<0.01$ vs. 396.6±25.6μM). Glutamine decreased after an hour of incubation (834.5±80.8μM vs 866.4±71.2μM, $p<0.01$) with greater falls evident in response to thrombin (781.4±83.3μM, 774±94.4μM $p<0.0001$) compared to the concentration of glutamine in the medium. Interestingly, the concentration of arginine was higher in all the samples compared to the medium. After an hour of incubation, the concentration of arginine increased from 298.5±17.8μM to 352.6 ± 49.1μM ($p<0.0001$), which was further increased after stimulation with 0.1U/ml thrombin to 508.8 ± 76.2μM ($p<0.0001$). 0.01U/ml thrombin increased arginine concentration, but to a lesser extent compared to 0.1U/ml thrombin, yet significantly higher than that from the basal medium (431.9±48.9μM, $p<0.0001$).

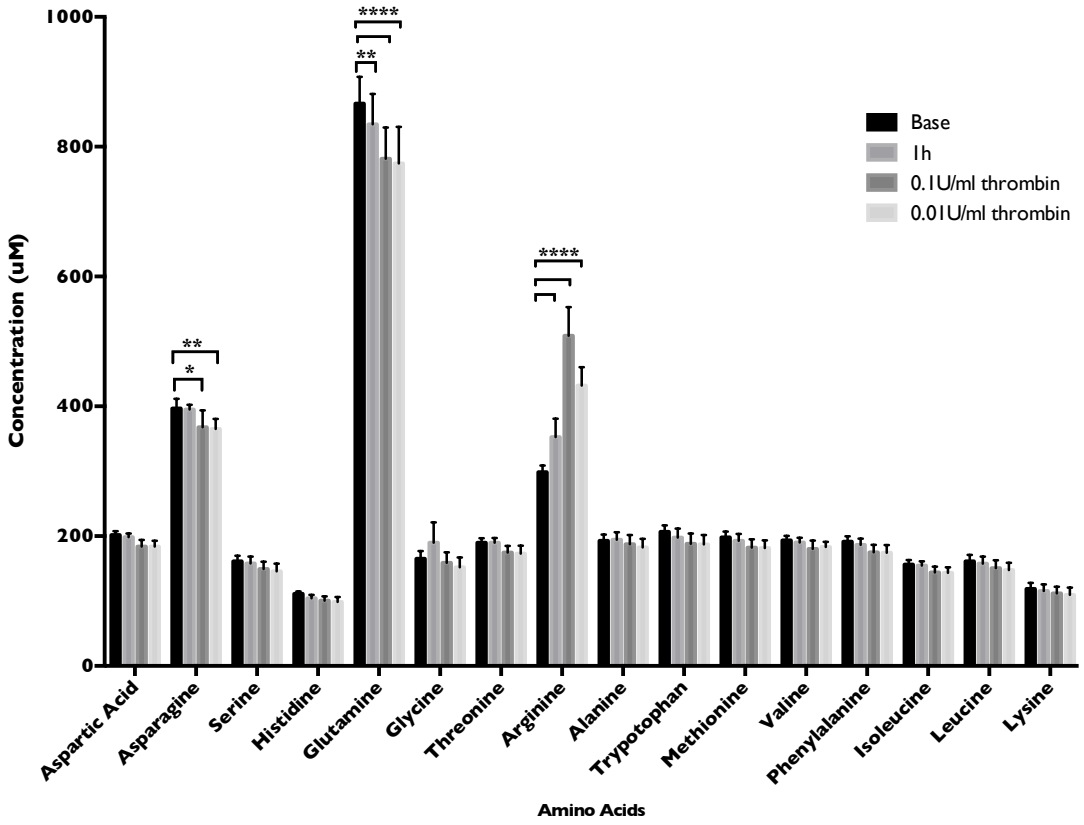

Figure 5-9: 16 amino acid profile in platelet suspension stimulated with thrombin (0.01 and 0.1U/ml). Concentrations of asparagine in the supernatants from platelets stimulated with 0.01 and 0.1U/ml thrombin were significantly higher than that of basal medium ($p<0.01$, $p<0.05$). Glutamine decreased significantly after an hour of incubation ($p<0.01$), and further decreased with the stimulation of thrombin ($p<0.0001$). The concentration of arginine increased significantly after an hour of incubation as well as stimulation with thrombin ($p<0.0001$). Data are presented as mean± SD, n=3. *<0.05, **<0.01, ****<0.0001.

5.4.1.2 Amino acid profile of platelet suspension at rest and after collagen activation

The changes in amino acid profile of the platelet suspension in response to collagen stimulation compared to basal medium were similar to that of thrombin (Figure 5-10). Asparagine and glutamine were depleted, indicated by a fall in the concentration, after one hour of incubation as well as in response to stimulation with collagen compared to the concentrations in the medium; however, arginine accumulated, indicated by a rise in concentration. The concentration of asparagine in the supernatant of platelets incubated with 10μg/ml collagen decreased significantly compared to base medium ($p<0.01$). Glutamine decreased after an hour of incubation ($p<0.01$), with further changes apparent in response to collagen stimulation (771.5±62.9.3μM, 805±85.5μM $p<0.0001$) compared to the concentration in the medium. The concentration of arginine increased significantly after stimulation with both 1μg/ml and 10μg/ml collagen to 436.1± 50.9 and 499.7 ± 61.2μM ($p<0.0001$) from 298.5±17.8μM.

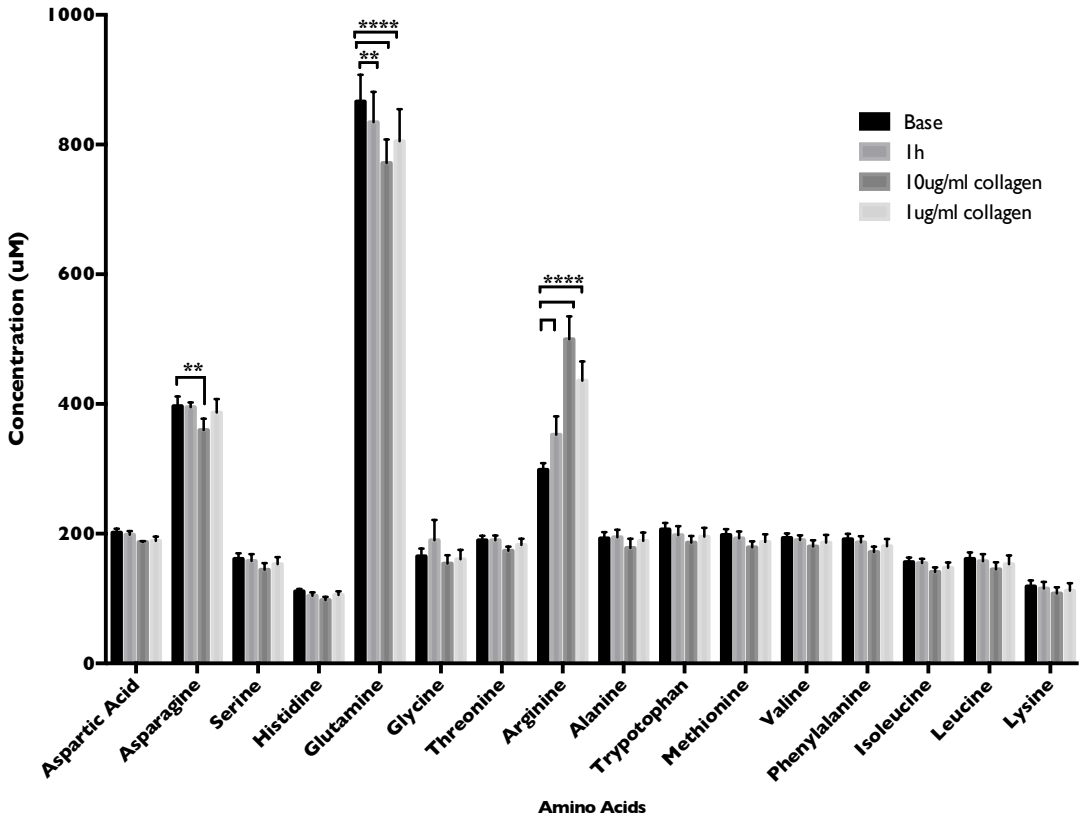

Figure 5-10: 16 amino acid profile of platelet suspension stimulated with collagen (1 and 10μg/ml). Concentration of asparagine in the supernatant from platelets stimulated with 10μg/ml collagen was significantly higher than that of basal medium ($p<0.01$). Glutamine decreased significantly after an hour of incubation ($p<0.01$), and further decreased with the stimulation of collagen ($p<0.0001$). The concentration of arginine increased significantly after an hour of incubation as well as stimulation with collagen ($p<0.0001$). Data are presented as mean± SD, n=3. **<0.01, ****<0.0001.

5.4.1.3 Platelet flexibility to oxidise glutamine

As observed in Figure 5-9 and 5-10, there was a significant depletion in the concentration of the glutamine from the medium after stimulation with both thrombin and collagen. The mitochondrial flexibility, that is the difference between capacity and dependency as defined in Chapter 2.6.5, to oxidise glutamine was measured using the XFp mitochondrial fuel flexibility test kit (Figure 5-11). To measure platelet dependency on glutamine oxidation, an allosteric inhibitor of glutaminase, BPTES was injected after basal OCR was established (Robinson et al., 2007; Vacanti et al., 2014). BPTES did not change basal oxygen consumption (Figure 5-11A) ($p>0.99$), indicating that the contribution of glutamine to mitochondrial oxygen consumption was minimal. However, the subsequent inhibition of platelet glucose oxidation with a mitochondrial pyruvate carrier inhibitor, UK5099, and of fatty acid oxidation with the carnitine palmitoyl-transferase 1A inhibitor, etomoxir, decreased OCR. The mitochondrial capacity to oxidise glutamine was measured by inhibiting the metabolism of glucose and fatty acids leaving glutamine as the only fuel source for platelet mitochondria. In this situation, the oxidation of glucose and endogenous fatty acids by platelets fell, as measured by a drop in OCR (Figure 5-11B), but did not fall further on the addition of BPTES to inhibit glutaminase ($p>0.99$), indicating minimal contribution of glutamine to mitochondrial OCR.

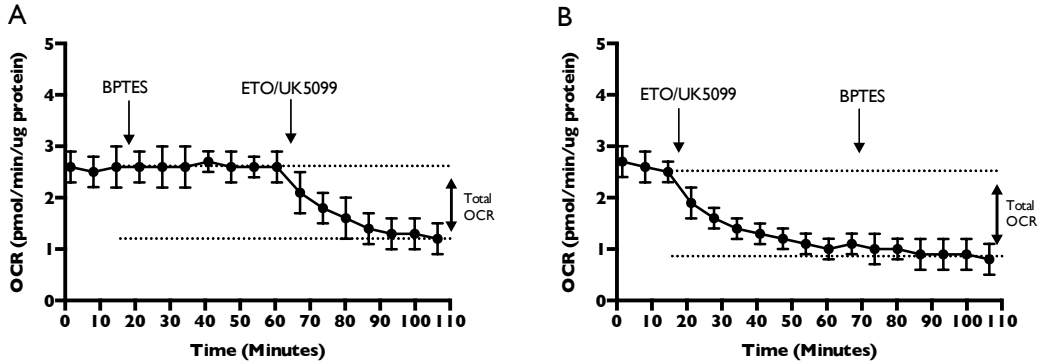

Figure 5-11: Platelet dependency and capacity to oxidise glutamine (A) Platelet mitochondrial dependency on oxidising glutamine. After establishing a basal OCR, BPTES was injected and 7 measurements were taken before injection the combination of etomoxir plus UK5099. (B) Platelet mitochondrial capacity to oxidising glutamine. After establishing a basal OCR, the combination of etomoxir plus UK5099 was injected and 7 measurements were taken before injection of BPTES. Data are presented as mean± SEM, n=3

5.4.2 Platelet flexibility to oxidise glucose and endogenous fatty acids

Having observed that glutamine made a minimal contribution to platelet mitochondrial fuel oxidation, the contribution of glucose and endogenous fatty acids was next investigated.

5.4.2.1 Platelet aggregation with glucose and endogenous fatty acid oxidation inhibitors

Inhibiting glucose oxidation with UK5099 and fatty acid oxidation with etomoxir alone or in combination, did not affect platelet aggregation compared to control (P>0.05).

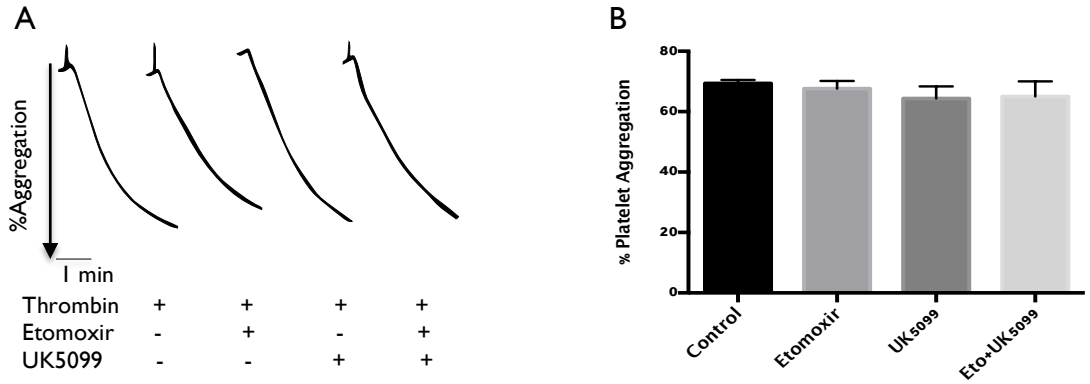

Figure 5-12: Platelet aggregation with glucose and fatty acid oxidation inhibitors (A) Representative platelet aggregation trace of thrombin, thrombin+etomoxir, thrombin+UK5099 and thrombin+UK5099+etomoxir for three minutes of aggregation. (B) % aggregation quantified from (A) for three minutes of aggregation. Data are presented as mean± SD, n=3. %Aggregation in all groups did not differ significantly compared to control group (p>0.05).

5.4.2.2 Platelet flexibility to oxidise glucose at rest

After observing that inhibiting glucose and fatty acid oxidation independently or in combination did not affect platelet aggregation, the potential fuel flexibility supporting this capability in the absence of either fuel was investigated. Addition of UK5099 caused OCR to fall (Figure 5-13A), indicating platelet dependency on glucose oxidation (36.0± 3.5%; Figure 5-13B). The subsequent injection of etomoxir and BPTES further reduced OCR, giving a value for total OCR responsible for the oxidation of glucose/carbohydrate, fatty acids and the minimal amount of glutamine. Alternatively, when etomoxir and BPTES were injected first, OCR fell, leaving glucose as the only major fuel for ultimate oxidation. The subsequent injection of UK5099 further reduced OCR, to a level indicative of the full capacity of platelet mitochondria to complete the oxidation of glucose (58.3±2.1%; Figure 5-13B). The difference between the full capacity and dependency on glucose was equivalent to the platelets flexibility to oxidise glucose (22.2±0.6%), in the absence of other fuels (Figure 5-13B). The corresponding ECAR was reported in Figure 5-13C&D. The inhibition of glucose and fatty acids oxidation pathways independently, did not affect ECAR; however, inhibiting all the major fuel oxidation increased ECAR significantly ($p<0.05$).

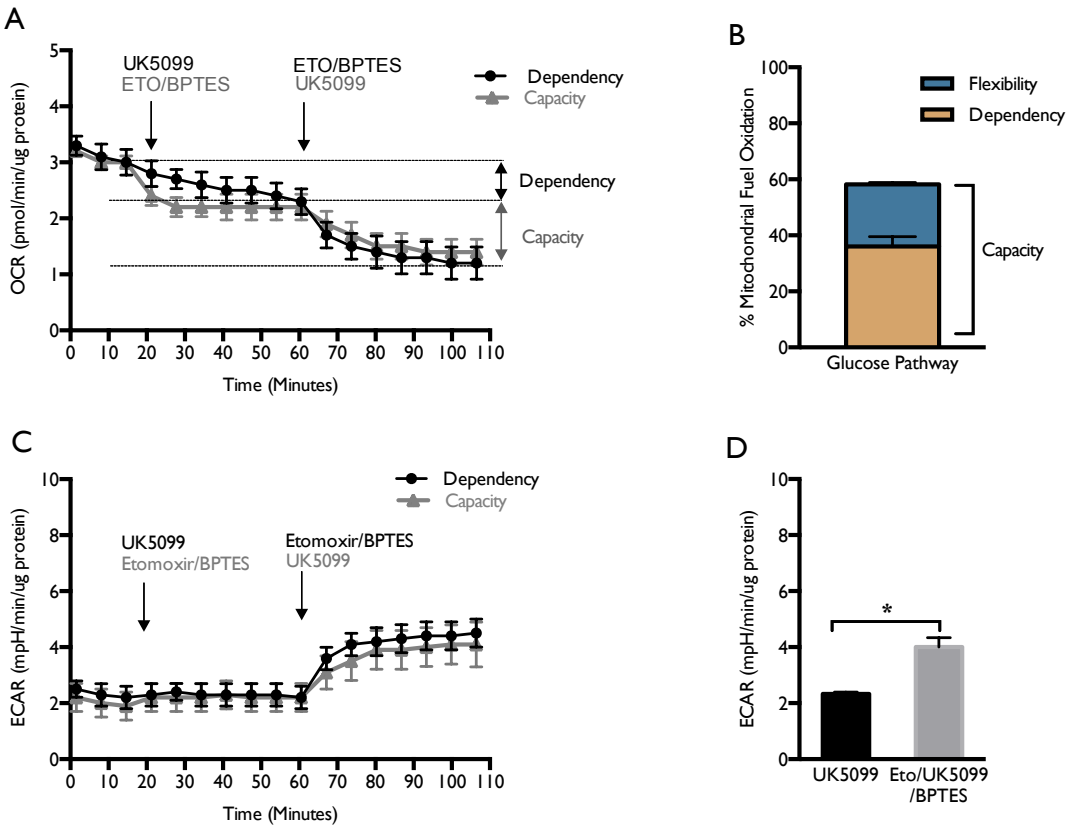

Figure 5-13: Platelet flexibility to oxidise glucose at rest (A) Platelet dependency and capacity to oxidise glucose. For measuring dependency, a basal OCR was established before the sequential injection of UK5099 and the combination of etomoxir and BPTES. The sequence was reversed for measuring capacity. (B) % Platelet dependency, capacity and flexibility calculated from (A) as defined in Chapter 2.6.5. (C) ECAR of (A). (D) ECAR quantified from (C). Inhibition of the oxidation of all the fuels increased ECAR significantly compared to the inhibition of individual fuels ($p<0.05$). Data are presented as mean± SEM, n=3, *<0.05.

5.4.2.3 Effect of thrombin on platelet flexibility to oxidise glucose

The flexibility of platelets to oxidise glucose was also investigated with thrombin-stimulated platelets (Figure 5-14). Addition of 0.1U/ml thrombin increased both OCR and ECAR as shown previously. The addition of UK5099 resulted in a fall in OCR, which was equivalent to platelet dependency on glucose oxidation (48.6±3.8%) when stimulated with thrombin (Figure 5-14B). Platelet capacity for glucose oxidation, as measured with the sequential injection of the combination of etomoxir and BPTES, followed by UK5099, was 54.3±1.5% (Figure 5-14B). The difference between the full capacity and dependency on glucose oxidation was equivalent to the platelets' flexibility to oxidise glucose (5.6±1.5%) when activated with thrombin (Figure 5-14B). The corresponding ECAR was reported in Figure 5-14C&D. The inhibition of glucose and fatty acids oxidation pathways independently, did not affect ECAR; however, inhibiting all the major fuel oxidation increased ECAR significantly ($p<0.05$).

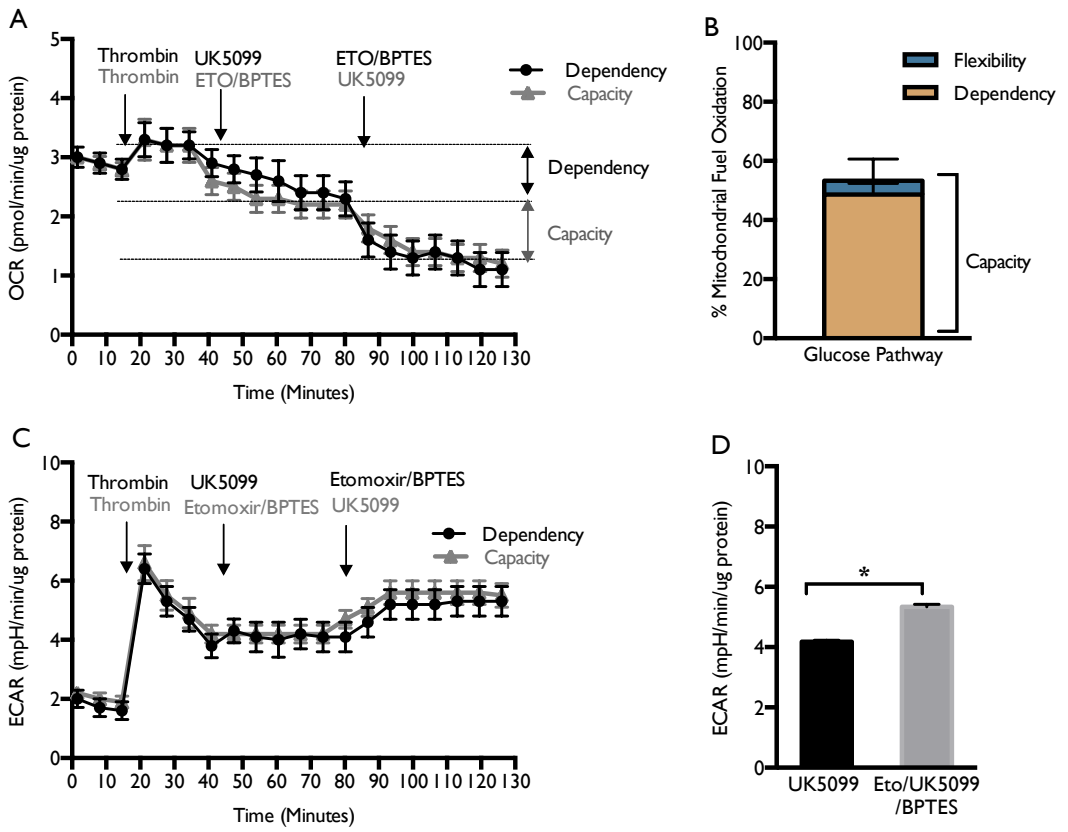

Figure 5-14: Platelet flexibility to oxidise glucose following thrombin activation (A) Platelet dependency and capacity to oxidise glucose. For measuring dependency, a basal OCR was established before the sequential injection of thrombin, UK5099 and the combination of etomoxir and BPTES. The sequence was reversed for measuring capacity. (B) % Platelet dependency, capacity and flexibility calculated from (A). (C) ECAR of (A). (D) ECAR quantified from (C). Inhibition of all the fuel oxidation increased ECAR significantly compared to the inhibition of individual fuels ($p<0.05$). Data are presented as mean± SEM, n=3, *<0.05.

5.4.2.4 Platelet flexibility to oxidise endogenous fatty acids at rest

Platelet dependency on fatty acid oxidation was investigated (Figure 5-15). OCR fell in response to etomoxir (Figure 5-15A), which indicated the oxidative dependency of platelets on fatty acid oxidation (30.63±7.9%; Figure 5-15B). The subsequent addition of UK5099 and BPTES further reduced OCR by an amount equivalent to the total OCR responsible for the oxidization of glucose, fatty acids and minimal amount of glutamine. The addition of UK5099 and BPTES (i.e., without etomoxir) first reduced OCR from basal, leaving the fatty acids as the only major fuel for platelet oxidation. As the other major fuels for platelet oxidation were inhibited, the oxidation of fatty acids reached full capacity, potentially compensating for the loss of the other two fuels. The subsequent injection of etomoxir further reduced OCR, which was equivalent of the full capacity of platelets to oxidise fatty acids (56.02±7.39%; Figure 5-15B). The difference between the full capacity and dependency on fatty acid oxidation is equivalent to platelets' flexibility to oxidise fatty acids (25.4±6.9%), in the absence of other fuels (Figure 5-15B). The corresponding ECAR was reported in Figure 5-15C&D. The inhibition of fatty acids and glucose oxidation pathways independently, did not affect ECAR; however, inhibiting all major fuel oxidation increased ECAR significantly ($p<0.05$).

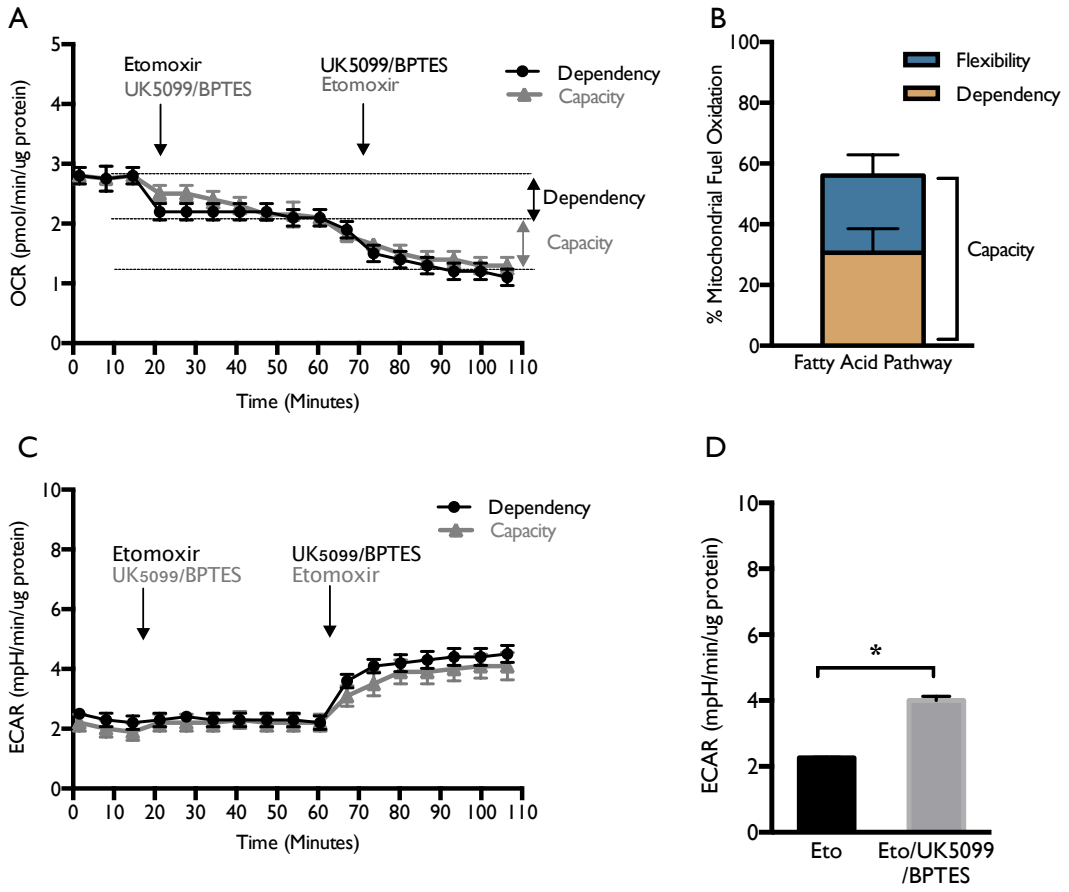

Figure 5-15: Platelet flexibility to oxidise endogenous fatty acids at rest (A) Platelet dependency and capacity to oxidise fatty acids. For measuring dependency, a basal OCR was established before the sequential addition of etomoxir and the combination of UK5099 and BPTES. The sequence was reversed for measuring capacity. (B) % Mitochondrial dependency, mitochondrial capacity and flexibility calculated from (A). (C) ECAR of (A). (D) ECAR quantified from (C). Inhibition of all fuel oxidation increased ECAR significantly compared to the inhibition of individual components ($p<0.05$). Data are presented as mean± SEM, n=3, *<0.05.

5.4.2.5 Effect of thrombin on platelet flexibility to oxidise endogenous fatty acids

The flexibility to oxidise fatty acids was also investigated in thrombin-stimulated platelets (Figure 5-16). After establishing basal OCR (Figure 5-16A) and ECAR (Figure 5-16C), the injection of 0.1U/ml thrombin increased both OCR and ECAR. The injection of etomoxir caused OCR to fall, which was equivalent to platelet dependency on fatty acid oxidation (37.71±4.0%) when stimulated with thrombin (Figure 5-16B). Platelet capacity, as measured with the sequential injection of the combination of UK5099 and BPTES, followed by etomoxir, was 54.3±1.5% (Figure 5-16B). The difference between the full capacity and dependency on fatty acid oxidation was equivalent to the platelet flexibility to oxidise fatty acids (23.2±0.5%), in the absence of other fuels (Figure 5-16B). The corresponding ECAR was reported in Figure 5-16C&D. The inhibition of fatty acid and glucose oxidation pathways independently, did not affect ECAR; however, inhibiting all major fuel oxidation increased ECAR significantly ($p<0.05$).

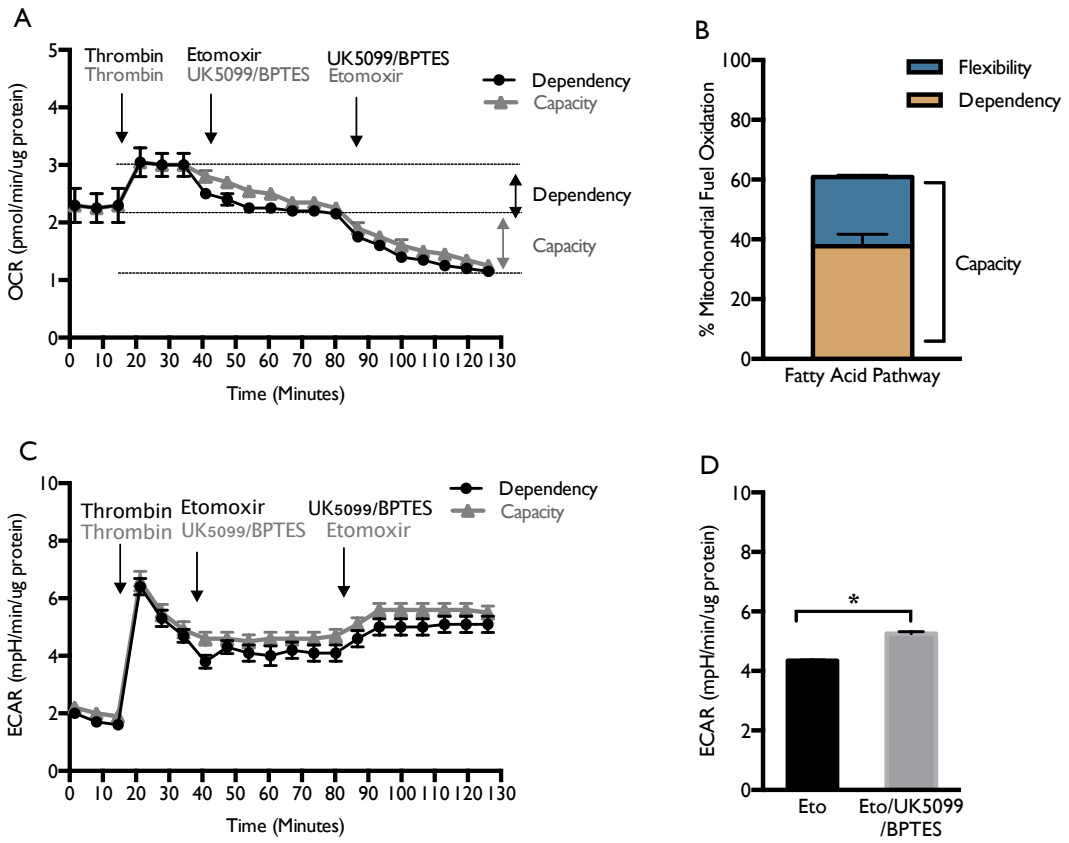

Figure 5-16: Platelet flexibility to oxidise endogenous fatty acids following thrombin activation (A) Platelet dependency and capacity to oxidise fatty acids. For measuring dependency, a basal OCR was established before the sequential injection of thrombin, etomoxir and the combination of UK5099 and BPTES. The sequence was reversed for measuring capacity. (B) % Mitochondrial dependency, mitochondrial capacity and flexibility calculated from (A). (C) ECAR of (A). (D) ECAR quantified from (C). Inhibition of all the fuel oxidation increased ECAR significantly compared to the inhibition of individual components ($p<0.05$). Data are presented as mean± SEM, n=3, *<0.05.

5.4.3 Platelet functional dependency on ATP from glycolysis and oxidative phosphorylation

Metabolic pathway flexibility was investigated using pharmacological inhibition of key metabolic processes (Figure 5-17). Inhibition of mitochondrial ATP synthesis with oligomyocin, or glucose/glycogen metabolism with 2-DG, did not influence platelet aggregation over three minutes (Figure 5-17A and B). However, the aggregation response caused by thrombin was abolished when oligomycin and 2-DG were added together ($p<0.05$).

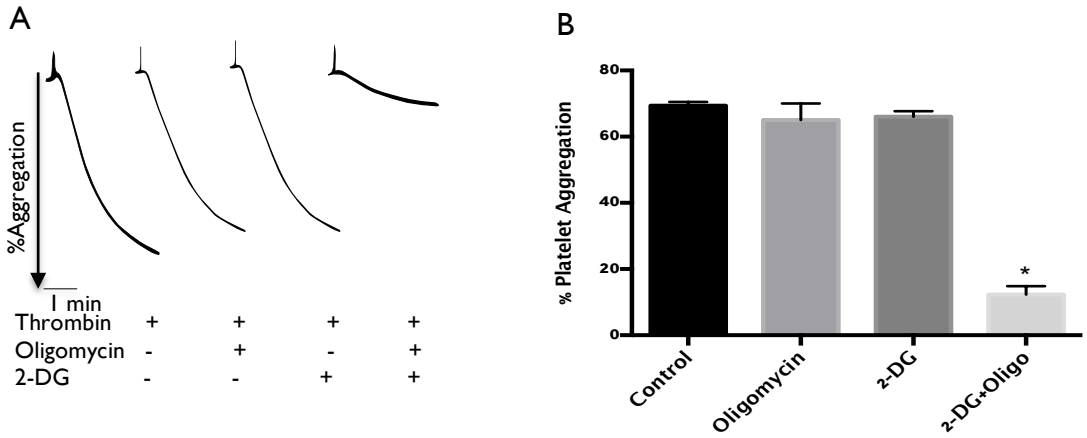

Figure 5-17: Platelet functional dependency on ATP from glycolysis and OXPHOS (A) Representative aggregation traces of platelets in response to thrombin stimulation with oligomycin, 2-DG or in combination; the concentration of the inhibitors used was as in metabolic assays. (B) % Platelet aggregation quantified from (A) for three minutes of aggregation. Platelet aggregation was significantly inhibited by the combination of 2-DG and oligomycin, $p<0.05$. Data are presented as mean± SD, n=3, *<0.05.

5.4.4 Function of mitochondria in human platelets at rest and activation

5.4.4.1 FCCP titration

In order to measure the mitochondrial components of respiration, the concentration of FCCP was optimised. OCR was measured in the presence of 1μM oligomycin (Figure 3-12C). The maximal respiration was achieved with the high range FCCP3 injection, which was 2μM (Figure 5-18). This concentration was used in subsequent experiments.

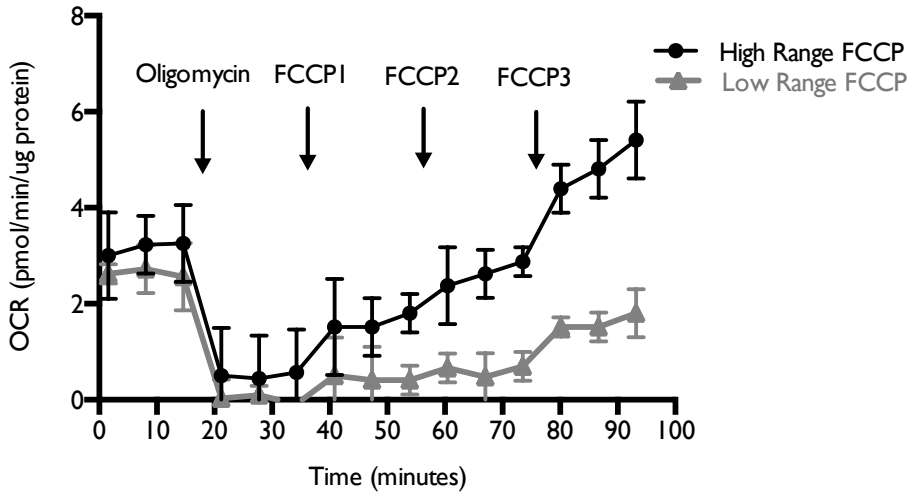

Figure 5-18: FCCP concentration optimization. Oligomycin 1μM. Low range FCCP: 0.125, 0.25, 0.5μM; High range FCCP: 0.5,1.0, 2.0μM. Data are presented as mean± SEM, n=3.

5.4.4.2 Optimisation of Antimycin & Rotenone concentrations

The recommended concentration of antimycin and rotenone (0.5μM) in mitochondrial stress test of Seahorse bioscience was used in Figure 3-16C, which resulted high non-mitochondrial respiration. Platelet mitochondrial components of respiration were measured with the sequential injection of oligomycin (1μM), FCCP (2μM) and a combination of antimycin A and rotenone (2.5μM each; Figure 5-19, A). 2.5μM A/R resulted in minimum non-mitochondrial respiration compared to that at 0.5μM (Figure 3-16). The ethanol vehicle had no effect (Figure 5-19, B). ATP-linked OCR, non-mitochondrial OCR, proton leak and spare respiratory capacity were calculated as the % of basal (Figure 5-19, C). ATP-linked OCR, non-mitochondrial OCR, proton leak and spare respiratory capacity were 76.6 ± 5.0%, 11.6 ± 7.0%, 11.7 ± 6.0% and 34.5± 7.0%, respectively.

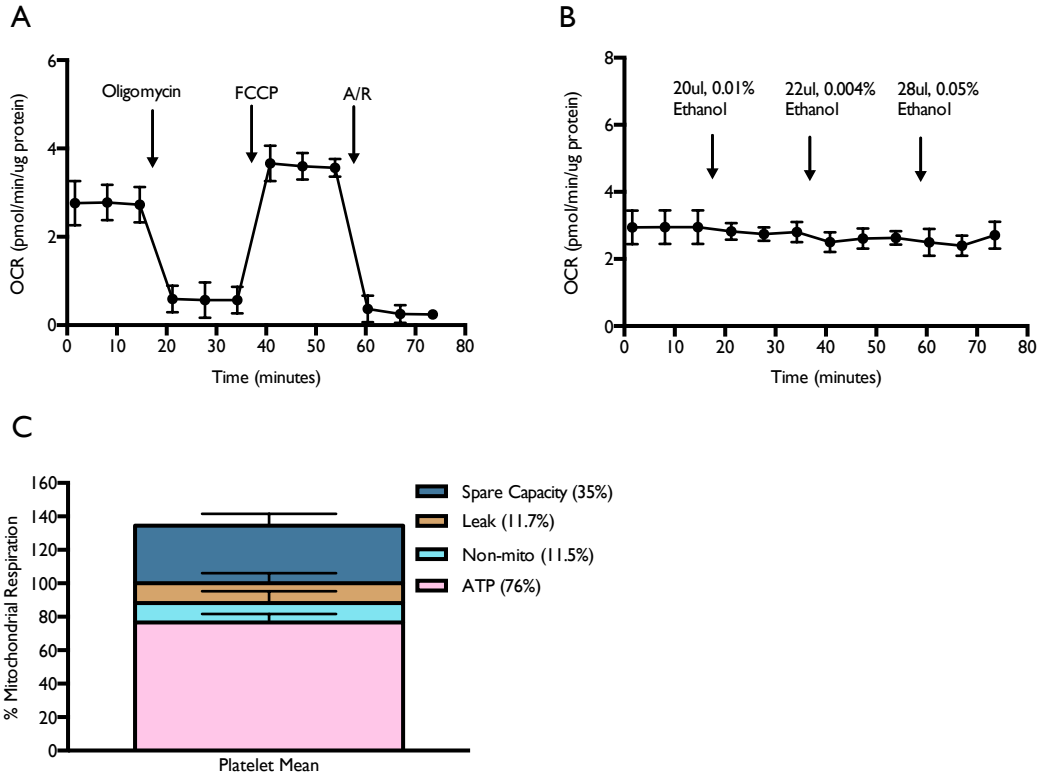

Figure 5-19: Platelet mitochondrial components of respiration with 2.5μM of antimycin & Rotenone (A/R). (A) Platelet OCR was measured with sequential injection of oligomycin, FCCP and A/R. (B) Ethanol control for (A). (C) ATP-linked OCR, non-mitochondrial OCR, proton leak and spare capacity was calculated as % of basal OCR. Data are presented as mean± SEM, n=3.

5.4.4.3 Components of human platelet mitochondrial respiration

Thrombin (0.1U/ml) increased OCR from 2.1±0.2 to 3.1±0.4 pmol/min/μg protein ($p<0.05$) (Figure 5-20A&C). Under these conditions, the oligomycin-sensitive OCR was higher (2.8±0.4 pmol/min/μg protein) compared to non-stimulated platelets (1.69 ±0.135 pmol/min/μg protein) (Figure 5-20A&C), indicating an increased ATP demand in thrombin-stimulated platelets. Interestingly, the maximal respiration rate of activated platelets, as determined by the addition of the proton ionophore FCCP, was similar (3.5±0.5 pmol/min/μg protein) to the OCR induced by thrombin (Figure 5-20A&C). ECAR was measured simultaneously (Figure 5-20B&D). ECAR rose in response to thrombin from 1.36±0.2 to mean 4.06±0.6mpH/min/μg protein ($p<0.05$). The addition of oligomycin resulted in a compensatory increase in the ECAR in both control and thrombin stimulated platelets. Compared to basal, ECAR increased significantly in the control group from 1.07±0.08 to 3.7±0.6 mpH/min/μg protein ($p<0.05$) and to 5.7±0.5 mpH/min/μg protein ($p<0.01$) in the thrombin stimulated group.

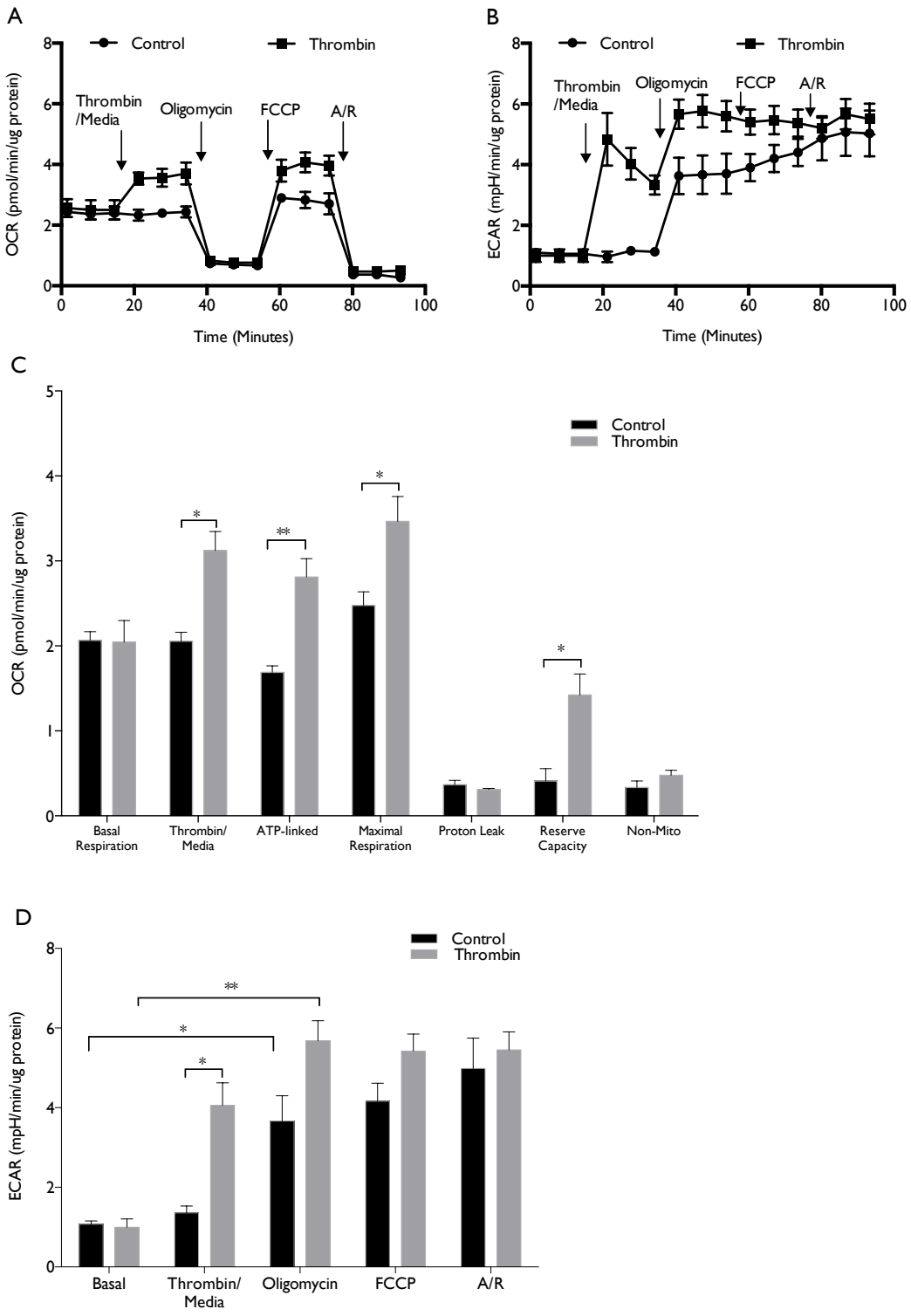
A
Control
Thrombin
Thrombin /Media
Oligomycin
FCCP
A/R
OCR (pmol/min/ug protein)
Time (Minutes)
B
Control
Thrombin
Thrombin /Media
Oligomycin
FCCP
A/R
ECAR (mpH/min/ug protein)
Time (Minutes)
C
Control
Thrombin
OCR (pmol/min/ug protein)
Basal Respiration
Thrombin/ Media
ATP-linked
Maximal Respiration
Proton Leak
Reserve Capacity
Non-Mito
D
Control
Thrombin
ECAR (mpH/min/ug protein)
Basal
Thrombin/ Media
Oligomycin
FCCP
A/R

Figure 5-20: Components of mitochondrial respiration of human platelets and corresponding ECAR (A) OCR of platelets with sequential injection of media or 0.1 U/ml thrombin, oligomycin, FCCP and antimycin & rotenone (A/R). (B) ECAR of (A). (C) Parameters of platelet mitochondrial function +/- thrombin. "Basal" indicates the difference between Basal and A/R sensitive OCR; "thrombin" indicates the difference between thrombin stimulated OCR and Basal; "ATP-linked" indicates the difference between media/thrombin stimulated OCR and oligomycin sensitive OCR; "maximal respiration" indicates the difference between FCCP induced OCR and A/R sensitive OCR; "proton leak" indicates the difference between oligomycin and A/R sensitive OCR; "reserve capacity" indicates the difference between FCCP and media/thrombin stimulated OCR; "non-mitochondrial OCR" indicates the A/R sensitive OCR. OCR rose significantly ($p<0.05$) after thrombin stimulation compared to basal and there were statistically significant increases in ATP-linked ($p<0.01$), maximal ($p<0.05$) and reserve capacity ($p<0.05$) of thrombin-stimulated platelets. (D) Average ECAR quantified from (B). Thrombin and oligomycin induced a significant increase in ECAR compared to basal ($p<0.05$; $p<0.01$) in thrombin stimulated platelets. Oligomycin induced a compensatory increase in ECAR in the control group that was significantly higher than basal ($p<0.05$). Data presented as mean± SEM, n=3. *<0.05, **<0.01.

5.4.4.4 The effect of secondary mediators on human platelet mitochondrial components of respiration

Inhibition of platelet derived ADP formation with apyrase had no significant effect on OCR (Figure 5-21). In contrast, inhibition of TxA_2 generation by indomethacin significantly reduced thrombin induced OCR (4.0±0.3 to 3.0±0.3 pmol/min/μg protein; $p<0.05$), ATP-linked OCR (3.0±0.3 to 2.2±0.2 pmol/min/μg protein; $p<0.05$), maximal respiration (5.1±0.3 to 3.8±0.2 pmol/min/μg protein; $p<0.01$) and reserve capacity (2.6±0.1 to 1.0±0.1 pmol/min/μg protein; $p<0.001$).

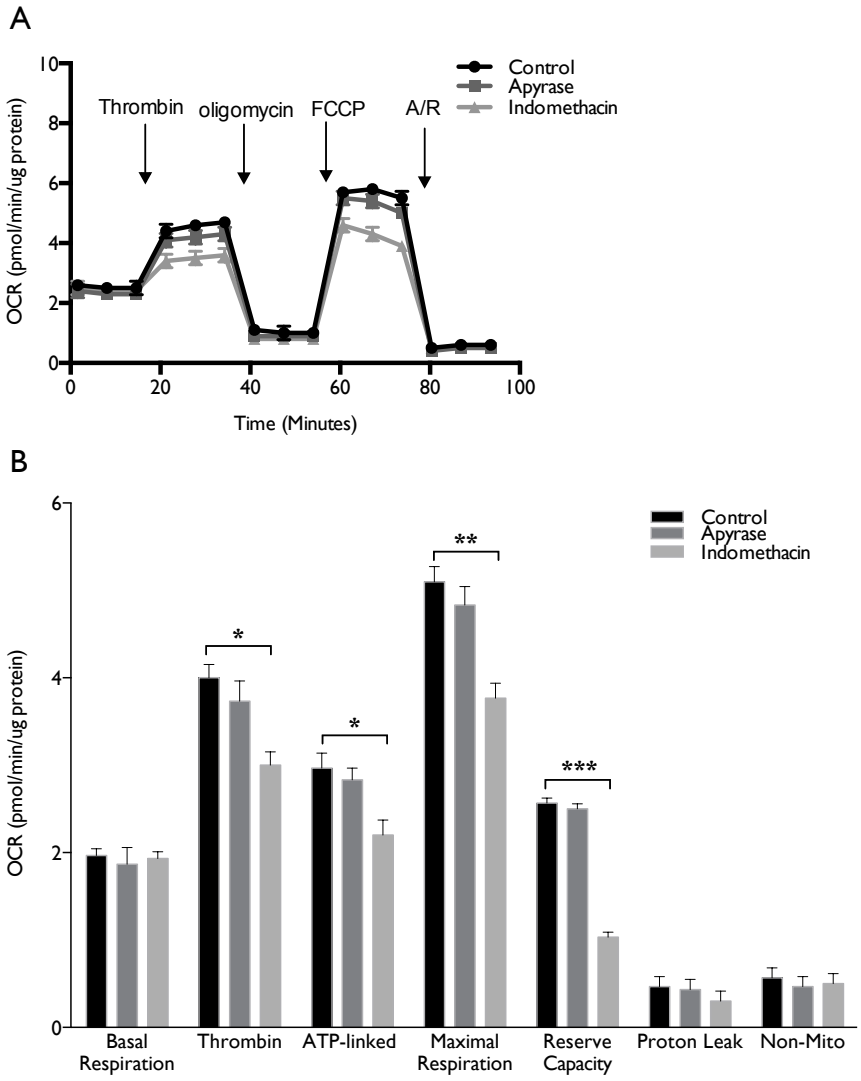

Figure 5-21: The effect of secondary mediators on human platelet mitochondrial components of respiration (A) OCR of platelets pre-incubated with apyrase and indomethacin with sequential injection of either media or 0.1 U/ml thrombin, oligomycin, FCCP and antimycin/rotenone (A/R). (B) Indomethacin significantly decreased thrombin induced OCR ($p<0.05$), ATP-linked OCR ($p<0.05$), maximal respiration ($p<0.01$), and reserve capacity ($p<0.001$). Data presented as mean± SEM, n=3. *<0.05, **<0.01, ***<0.001.

5.4.4.5 Glycogen-dependent human platelet mitochondrial components of respiration

The components of mitochondrial respiration were measured in the absence of glucose in the media. Both OCR and ECAR were measured simultaneously with the mitochondrial inhibitors of mitochondrial respiration (Figure 5-22). Thrombin (0.1U/ml) increased OCR from 3.0±0.2 to 4.9±0.5 pmol/min/μg protein ($p<0.05$) (Figure 5-22A&C). Under these conditions, the oligomycin-sensitive OCR was higher in thrombin-stimulated (4.1±0.3 pmol/min/μg protein) compared to non-stimulated platelets (1.9 ±0.2 pmol/min/μg protein; Figure 5-22A&C), indicating an increased ATP demand in thrombin-stimulated platelets ($p<0.001$). Interestingly, the maximal respiration rate of activated platelets, as determined by the addition of the proton ionophore FCCP, was slightly higher (6.4±0.6 pmol/min/μg protein) than the OCR induced by thrombin (Figure 5-22A&C). Thrombin induced a significant increase in ECAR (Figure 5-22B&D) from 1.06±0.2 to 3.8±0.7mpH/min/μg protein ($p<0.05$). The inhibition of mitochondrial ATP synthesis with oligomycin resulted in a compensatory increase in the ECAR in the control group but not in the thrombin stimulated platelets as shown previously. Compared to basal, ECAR increased significantly in the control group from 1.06±0.2 to 2.3±0.2 mpH/min/μg protein ($p<0.01$).

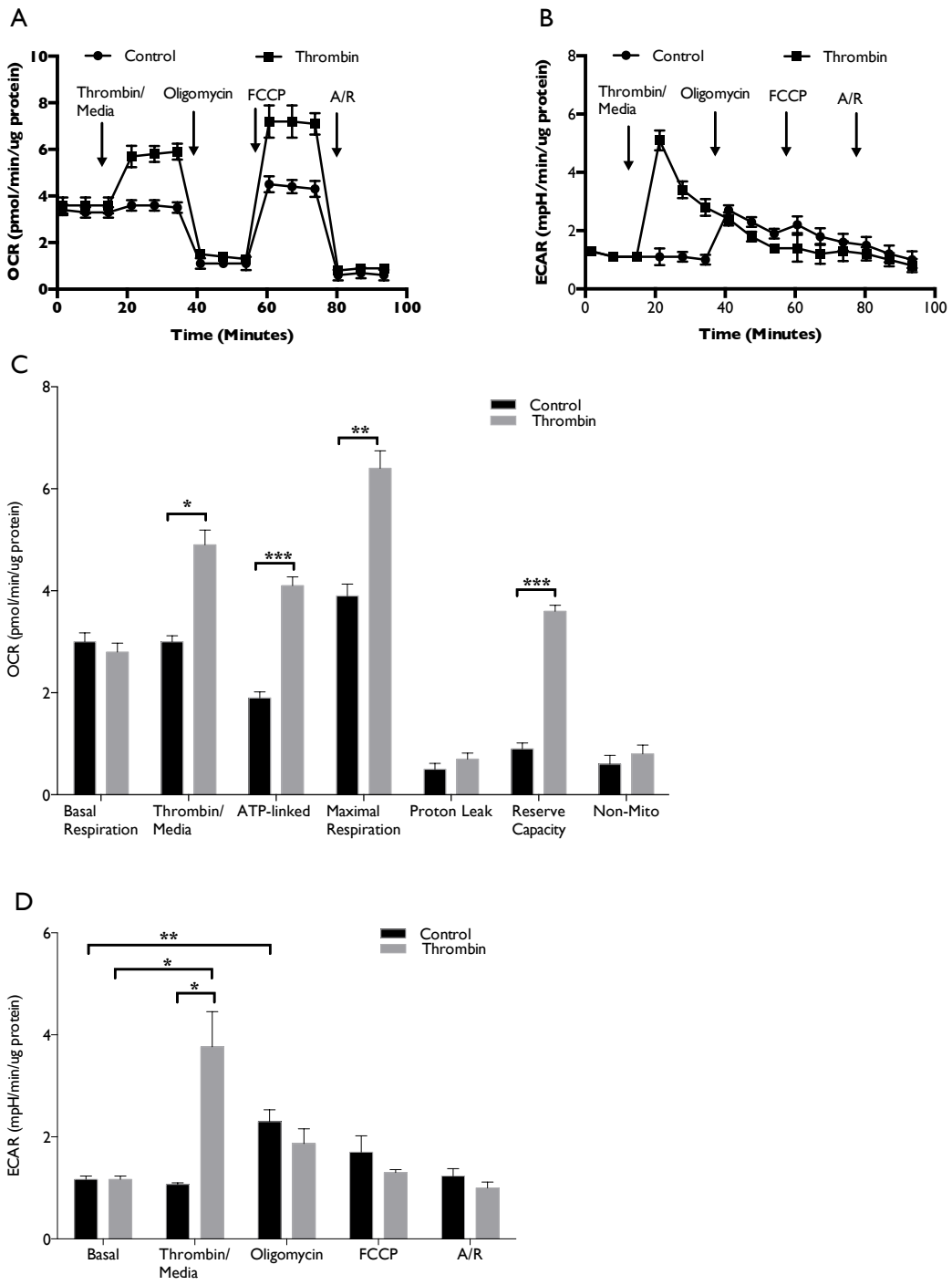

Figure 5-22: Glycogen-dependent human platelet mitochondrial components of respiration and corresponding ECAR in glucose-free medium (A) OCR of platelets with sequential injection of media or 0.1 U/ml thrombin, oligomycin, FCCP and antimycin/rotenone (A/R). (B) ECAR of (A). (C) Parameters of platelet mitochondrial function +/- thrombin. OCR rose significantly ($p<0.05$) after thrombin stimulation compared to basal and there were statistically significant increases in ATP-linked ($p<0.001$), maximal ($p<0.01$) and reserve capacity ($p<0.001$) of thrombin-stimulated platelets. (D) Average ECAR quantified from (B). Thrombin induced a significant increase in ECAR compared to basal ($p<0.05$) in thrombin-stimulated platelets. Oligomycin induced a compensatory increase in ECAR in the

control group that was significantly higher than basal ($p<0.01$). Data presented as mean± SEM, n=3. *<0.05, **<0.01, ***<0.001.

5.4.5 Function of mitochondria in murine platelets at rest and activation

5.4.5.1 Murine platelet mitochondrial components of respiration

Thrombin caused a significant increase in OCR from 2.23 ±0.5 to 4.23±0.8 pmol/min/μg protein ($p<0.05$) (Figure 5-23) in murine platelets. The addition of oligomycin reduced the basal and thrombin induced OCR, indicative of that fraction linked to ATP production. FCCP stimulated both groups to reach their maximal respiration rate (4.0±0.3 and 5.1 ±0.5 pmol/min/μg protein). However, the thrombin-stimulated group showed a significantly higher maximal respiration rate, giving higher reserve capacity (2.5±0.3 pmol/min/μg protein) ($p<0.05$).

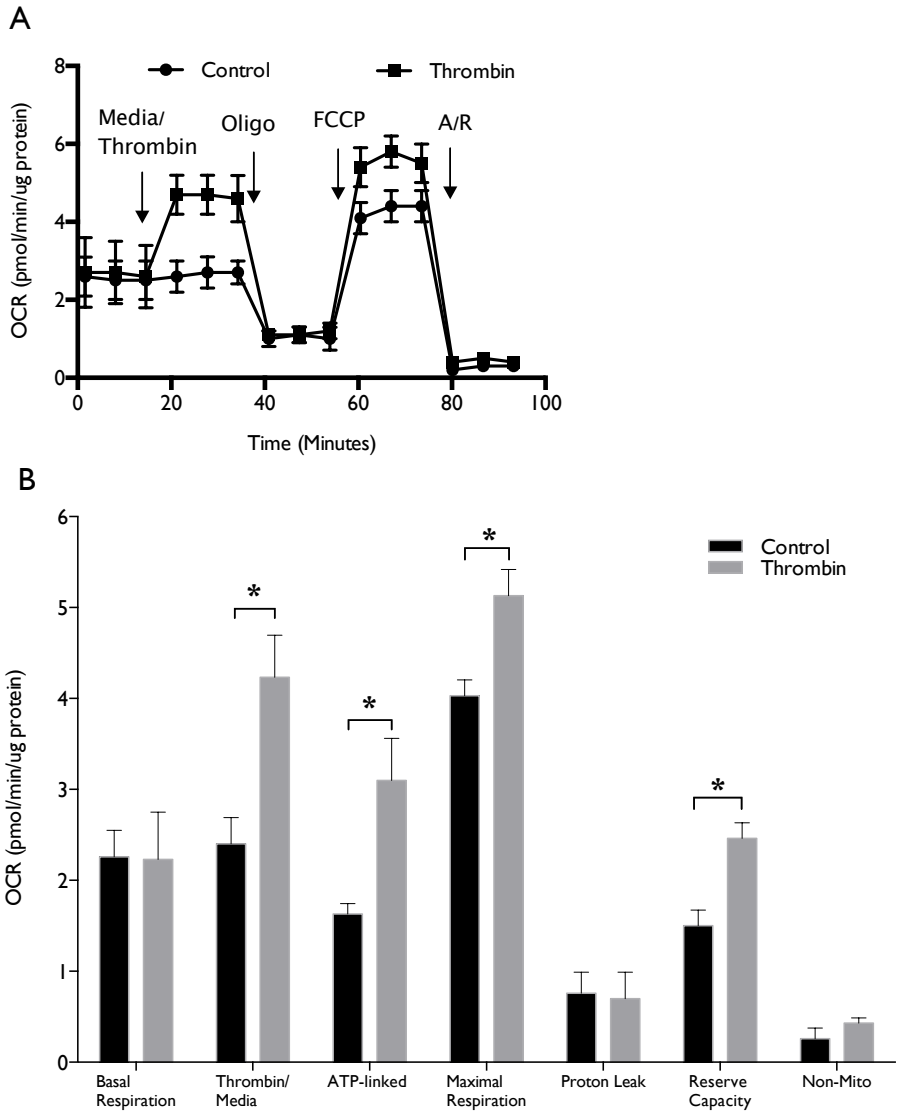

Figure 5-23: Mitochondrial respiratory function of murine platelets (A) OCR of murine platelets with sequential injection of media or 0.1 U/ml thrombin, oligomycin, FCCP and antimycin/rotenone (A/R). (B) Parameters of platelet mitochondrial function +/- thrombin. OCR rose significantly ($p<0.05$) after thrombin stimulation compared to basal and there were statistically significant increases in ATP-linked ($p<0.05$), maximal ($p<0.05$) and reserve capacity ($p<0.05$) of thrombin-stimulated platelets. Data presented as means ±SEM, n=3, *<0.05.

5.4.5.2 High fat diet induced murine platelet mitochondrial dysfunction

Hyperlipidaemic murine platelets had significantly elevated basal respiration (3.6±0.6 pmol/min/μg protein) compared to the wild type (2.0±0.2 pmol/min/μg protein) ($p<0.05$). This resulted in an increased ATP-coupled respiration in the hyperlipidaemic group (2.3±0.1 pmol/min/μg protein) compared to those fed normal chow (1.4±0.3 pmol/min/μg protein). Platelets from hyperlipidaemic mice had an increased mitochondrial proton leak (1.19±0.17 pmol/min/μg protein vs. 0.53±0.2 pmol/min/μg protein $p<0.01$). However, most strikingly, it was found that FCCP increased the OCR from platelets from hyperlipidaemic mice to a level equivalent to that measured at rest (Figure 5-24).

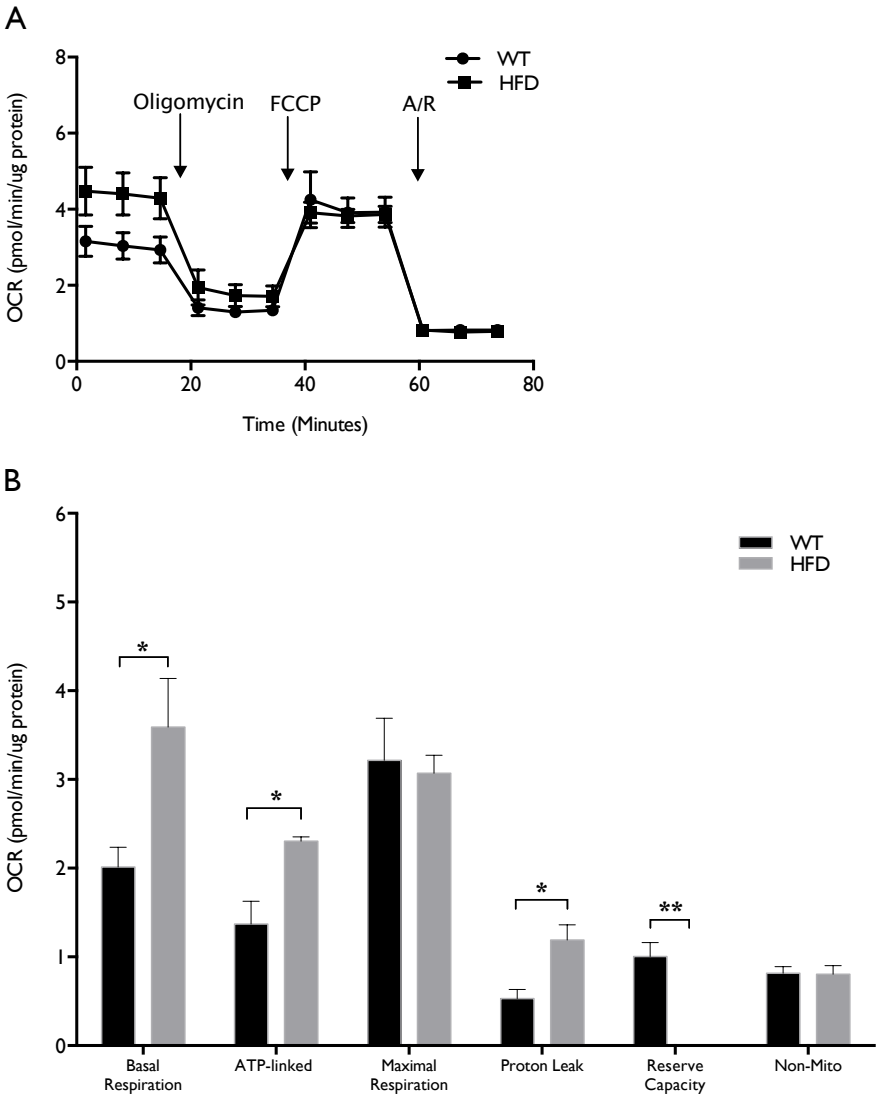

Figure 5-24: Mitochondrial respiratory function of platelets from wild type and 12 weeks high fat diet fed mice (A) OCR of platelets from wild type and HFD fed mice. (B) Platelet mitochondrial indices quantified from (A). HFD-fed mice had significantly elevated basal OCR ($p<0.05$), ATP-linked ($p<0.05$) and proton leak ($p<0.05$); however, the reserve respiratory capacity of HFD group was lost ($p<0.01$). Data presented as means ±SEM, n=3. *<0.05, **<0.01.

5.5 Discussion

The aim of this chapter was first to investigate the amino acid profile of platelet suspension at rest and activation with both thrombin and collagen. Consequently, the metabolic fate of glutamine as an oxidative fuel for platelets was investigated using BPTES, a glutaminase inhibitor, in XFp assay. Subsequently, the functional dependency of platelets on glucose and fatty acid oxidation was determined using inhibitors of these pathways (UK5099 and etomoxir) respectively both in the aggregation assay and the XFp assay. Platelet aggregation was also measured in the presence of glycolysis and mitochondrial ATP synthase inhibitors, 2-DG and oligomycin, to elucidate the platelet functional dependency on ATP from these two pathways. Last but not the least, the function of platelet mitochondria in both human and murine platelets was measured.

5.5.1 Amino acid utilisation by platelets at rest and activation

Amino acids may be classified as essential, non-essential and conditionally essential (Gannon and Nuttal, 2010). The human body is unable to synthesise *de novo* phenylalanine, valine, threonine, tryptophan, methionine, leucine, isoleucine, lysine and histidine, which are thus categorized as essential amino acids and must be derived from dietary sources. The human body can synthesize the remaining 11 amino acids, tyrosine, aspartate, asparagine, alanine, serine, glycine, cysteine, glutamate, glutamine, proline and arginine. However, some non-essential amino acids can become essential in times of illness and stress; i.e. the body cannot make them in sufficient quantities, these are described as 'conditional amino acids'. Examples include arginine, cysteine, glutamine, tyrosine, glycine, proline and serine. All amino acids are used to synthesize proteins, biomolecules, and can be oxidised to urea and carbon dioxide to provide energy. Here the utilisation by resting and activated platelets of 16 amino acids, including all the essential amino acids plus alanine, aspartic acid, asparagine, serine, arginine, glycine and glutamine were studied.

13 out of 16 amino acids in the platelet suspension did not change significantly; however, asparagine and glutamine were depleted (decreased in the concentration compared to the starting medium concentration) while arginine was accumulated

(increase in the concentration compared to the starting medium concentration) after one hour of incubation with platelets and stimulation with both thrombin and collagen (Figure 5-9 & 5-10). However, the inhibition of glutaminase, the major enzyme that converts glutamine to glutamate with BPTES (Robinson et al., 2007; Vacanti et al., 2014), did not affect platelet oxygen consumption, suggesting redundancy for glutamine as an oxidative fuel (Figure 5-11).

Earlier studies also support the notion that glutamine has minimum role in platelets as an oxidative fuel. In an earlier study, Murphy et al (1992) examined the metabolic fate of glutamine given as a single amino acid and reported that nearly 75% of that consumed was converted to glutamate, a figure that did not change in response to thrombin stimulation. However in that study, glutamine accounted for most of the ammonia that was produced by platelets supporting the idea of a minimal role for glutamine as an oxidative fuel (Murphy et al., 1992). This view was challenged by a recent study conducted by Ravi et al., (2015) claiming that the omission of glutamine compromised platelet mitochondrial function both at rest and following stimulation with thrombin. Furthermore azaserine (25 and 50μM) reduced oxygen consumption by 40%. However, that study used a mixture of fresh and 6-8 day old platelets, which potentially have reduced oxidative metabolism compared to fresh platelets (Cohen and Wittles, 1970). Notably azaserine inhibits all the glutamine-dependent enzymes in the hexosamine pathway (Hensley et al., 2013), but does not specifically inhibit glutaminase (Robinson et al., 2007; Vacanti et al., 2014). In the present study and in contrast to Ravi et al., (2015), the omission of glutamine did not affect mitochondrial function of platelets (Figure 5-20, 5-22), both at rest and after stimulation with thrombin, even in the absence of glucose.

It has been reported that isolated immune cells, such as lymphocytes, macrophages and neutrophils utilize glutamine at a high rate, yet, despite the high expression of glutaminase in these cells, the rate of oxidation is low (Curi et al., 1999; Newsholme, 2001; Newsholme et al., 2003; Altman et al., 2016). It has therefore been proposed that one of the main roles of glutamine in these immune cells is to produce NADPH in pyruvate/malate cycle, via the action of $NADP^+$ dependent malic enzyme, which converts the malate to pyruvate. NADPH can be generated via PPP in platelets; however, glucose might not be spared towards the PPP under

stressed or activated conditions (Thomas et al., 2014). Thus, providing substrate for the generation of NADPH using the pyruvate/malate cycle as in immune cells might be one of the functions of glutamine in platelets.

Both asparagine and glutamine were depleted whereas arginine accumulated (Figure 5-9 & 5-10), observation not previously been reported in platelets. A possible explanation is that glutamine and asparagine are used by platelets to form arginine. Glutamine is an important precursor for arginine synthesis in other systems (Ligthart-Melis et al., 2008), and the first catabolic product of asparagine, aspartate, is required for the argininosuccinate synthase to form arginine from citrulline. In some tissues and cell lines arginine serves as a precursor for nitric oxide production via the action of nitric oxide synthase (NOS), which includes endothelial (eNOS), neuronal (nNOS), and inducible (iNOS) isoenymes. There are numerous data in the literature suggesting the expression of two isoforms of NOS in platelets, eNOS and iNOS (Cozzi et al., 2015), however, the expression, regulation and function of these isoforms in platelets is highly controversial (Bohmer et al., 2014; Gambaryan and Tsikas, 2015). These controversies arise from the reliability of the assay for measuring NOS expression as well as the absence of positive and negative controls such as in endothelial cells or cells from NOS knock-out mice (Gambaryan and Tsikas, 2015). Thus it is difficult to know whether platelets synthesize nitric oxide from arginine itself, which seems unlikely as platelets secrete arginine both at rest and dose-dependently when activated. The metabolic fate of platelet secreted arginine needs to be further investigated, however, it is tempting to speculate that platelet derived arginine is taken up by other immune cells, such as macrophages. It was shown that under prolonged NO synthesis, macrophages take up arginine via the cationic amino acid transporter 2 (CAT2) during inflammation, which is either catabolised through iNOS to NO in M1 macrophages or hydrolysed by arginase in M2 macrophages (Rath et al., 2014). This points to a potential metabolic co-operation between platelets and other immune cells under physiological or pathological conditions.

5.5.2 Platelet dependency and capacity to oxidise glucose and endogenous fatty acids

Glucose was provided at physiologically relevant concentrations in order to examine the level of individual contribution, competition and cooperation between glucose and endogenous fatty acids in platelet metabolism. The individual inhibition of glucose or endogenous fatty acid oxidation or in combination did not affect platelet aggregation with thrombin (Figure 5-12). This suggests that glucose and endogenous fatty acids are interchangeable as metabolic substrates. The way in which this is achieved was investigated (Figure 5-13 to 5-16).

When expressed as a proportion of platelet fuel oxidation, of which the major fuels being glucose and endogenous fatty acids, the dependency and capacity to oxidise the two fuels were almost equal at rest. The dependency on glucose increased after stimulation with thrombin. However, the capacity of glucose oxidation decreased slightly, whereas endogenous fatty acids did not change when platelets were stimulated with thrombin. This resulted in similar flexibility, (the difference between capacity and dependency), for glucose and fatty acids at rest. However, the flexibility for glucose oxidation was significantly reduced when platelets were stimulated with thrombin, due to the glucose flux change towards glycolysis that was shown previously (Chapter 3 & 4). The flexibility for endogenous fatty acid oxidation did not change before or after thrombin stimulation, probably due to the limited pool of fatty acids that can be spared for ATP generation without compromising platelet membrane integrity. The glycolytic rate was measured when both glucose and endogenous fatty acid oxidation were inhibited in the same series of experiments. The individual inhibition of either glucose or fatty acid oxidation did not affect glycolysis, whereas in combination, inhibition increased the glycolytic rate significantly. These data therefore suggest that in both the quiescent and activated state, platelets may switch between glucose and endogenous fatty acid oxidation and that these substrates can compensate for each other's availability. This could explain the functional outcome of platelet aggregation in the presence of glucose/fatty acid oxidation inhibition. Thus, when both fuels are restricted, platelets up-regulate glycolysis to meet the energy demand for functional responses, indicating not only fuel, but metabolic pathway flexibility in order to respond to a

thrombotic signal. It should be cautioned that the dependency on each fuel might be underestimated in this work as the inhibition of either pathway may up-regulate the other. As dependency is calculated in terms of total fuel oxidation, this would be larger than usual due to the compensation. The remaining oxygen consumption can be accounted for the non-mitochondrial oxygen consumption, proton leak, lactate derived TCA intermediates such as succinate, and the small amount of medium chain fatty acids (Niu et al., 1997).

Few blood cells possess such flexibility as platelets in terms of fuel oxidation. The inhibition of fatty acid oxidation prevents T cell differentiation into T_{reg} (Byersdorfer, 2013) and the polarization of M2 macrophages is fatty acid dependent, such that inhibition of fatty acid oxidation drives M2 macrophages to the M1 state (Galvan-pena and O'Neil, 2014). Dendritic cell maturation is highly fatty acid dependent, and mature dendritic cells have both OXPHOS and aerobic glycolysis where the inhibition of glycolysis prevents dendritic cell maturation (Malinarich et al., 2015). These differences between platelets and other blood cells may have arisen due to platelets being terminally differentiated, which spares them from many anabolic processes involved in cell differentiation and proliferation. Moreover, the innate flexibility of platelets to respond in a range of metabolic challenges illustrates the fundamental nature of platelets in sustaining haemostasis and vascular integrity.

Although a few other studies have reported on the oxidative capability of platelets using similar techniques (Chacko et al., 2013; Kramer et al., 2014; Ravi et al., 2015), the present work is the first to show metabolic flexibility in platelets. While, Ravi et al., (2015) demonstrated the role of exogenous and endogenous fatty acids as substrates for platelets by adding BSA-palmitate or incubating platelets with etmoxir, the BSA control reduced the mitochondrial components of respiration. Etomoxir reduced basal oxygen consumption as shown here, however, platelet oxygen consumption did not respond to thrombin activation possibly a result of prolonged incubation and the use of aged platelets (Cohen and Wittles, 1970). However, in agreement with the data obtained here, Ravi et al., (2015) did report a role for endogenous fatty acids as an energy source for platelets

5.5.3 Platelet functional dependency on ATP from glycolysis and oxidative phosphorylation

The fuel flexibility of platelets prompted the investigation of platelet functional dependency on ATP from glycolysis and oxidative phosphorylation. The inhibition of glycolysis or of mitochondrial ATP synthase separately did not inhibit the ability of platelets to respond to thrombin. However, when these pathways were inhibited simultaneously, platelet aggregation with thrombin was prevented (Figure 5-17). The data do show evidence of platelet shape change, which was potentially due to the small amount of intracellular metabolically available ATP (Akkerman and Holmsen, 1981) or of ATP derived from creatine phosphate via creatine kinase (Arnold et al., 2012) in platelets. The conditions *in vivo* might not be as extreme as *in vitro,* but these data suggest that there is ample scope to generate ATP in platelets as well as the metabolic pathway plasticity.

From a functional perspective, this flexibility may be important to enable platelets to perform physiologically *in vivo* inside a thrombus, where the availability of oxygen may be limited (partial or complete hypoxia). The functional outcome of limited oxygen is cellular metabolic adaptation, which is mediated by mitochondrial oxygen sensing, in part regulated by mitochondria induced expression of hypoxia inducible factor (HIF) in a variety of cell types. A key role of HIF is activation of anaerobic glycolysis and the inhibition of mitochondrial oxidative phosphorylation, without leading to paralysis of mitochondria sufficient to cause cell death (Solaini et al., 2010). The mechanisms of how this process is modulated in platelets under potentially hypoxic condition inside a thrombus, need further investigation; however, the availability of endogenous glycogen as well as exogenous glucose and the flexibility to produce ATP from glycolysis or OXPHOS in platelets indicates a potential survival mechanism in adverse microenvironments.

5.5.4 Function of mitochondria in human platelets at rest and activation

Platelets have sufficient glycolysis to support the need for ATP even when mitochondrial ATP machinery is compromised (Figure 5-17). This allows experiments to be carried out to measure aspects of mitochondrial coupling and respiratory control such as basal, ATP-coupled, non-mitochondrial, maximal respiration, proton leak, and spare respiratory capacity (Figure 5-18 to 5-20). These components were measured after carefully titrating the concentrations of inhibitors of oxidative phosphorylation (Brand and Nicholls 2011). The coupling efficiency was 76% (ATP-coupled O_2/basal-non mitochondrial O_2). Proton leak represented 12% of total OCR, non-mitochondrial respiration was 11.5% and the spare capacity was 35%. These results are broadly comparable with those of Kramer et al., (2014) and Chacko et al., (2013), however, the coupling efficiency and spare respiratory capacity are higher in this study. The differences can be accounted by factors such as different cell preparation methods and the absence of experiments combining antimycin and rotenone in those studies.

Compared to other blood cells, such as monocytes and lymphocytes (Chacko et al., 2013; Kramer et al., 2014), platelet mitochondrial respiration is highly coupled to ATP generation and the contribution of non-mitochondrial oxygen consuming enzymes, such as membrane-bound NADPH oxidase, to mitochondrial oxygen consumption is relatively modest. Similarly, the non-ATP coupled proportion of mitochondrial OCR, proton-leak, is relatively small, potentially limiting the generation of mitochondrial ROS. The spare respiratory capacity is an important characteristic of platelet mitochondria, which enables platelets to survive in conditions where a sudden increase in energy demand is imposed, such as platelet activation. These data also suggest that measurement of the individual components of mitochondrial respiration can provide a full assessment of platelet mitochondrial function; changes to which might reflect defects in platelet mitochondria.

The present experiments were therefore repeated to determine the components of respiration in thrombin-activated platelets (Figure 5-20), with the inhibitors of secondary mediators of platelet activation (Figure 5-21) as well as under conditions where glucose was omitted from the medium (Figure 5-22). Thrombin induced an

increase in mitochondrial respiration roughly equal to the value of maximal respiration, suggesting that platelets utilise the spare respiratory capacity to supply the increased ATP demand required by thrombin stimulation. The experiments also confirmed the potential of platelets to use glycolysis to generate ATP as required. Indomethacin, which inhibits the generation of TxA_2, reduced spare respiratory capacity significantly, suggesting that the production of TxA_2 is highly coupled to the increase in energy demand. Interestingly, the omission of glucose did not affect mitochondrial function, again highlighting the metabolic plasticity of platelets. There was a spare glycolytic capacity (Figure 5-22B) in un-stimulated platelets in the absence of glucose, presumably from glycogen, indicated by the increase in glycolytic rate after oligomycin injection, which was not observed in thrombin stimulated platelets (Figure 4-16). These data suggests that thrombin stimulated platelets without access to external sources of glucose lose the spare glycolytic capacity as they potentially exhaust their supply of glycogen under conditions where nutrients are limited.

5.5.5 Mitochondrial function of murine platelets at rest and activation

In order to investigate the impact of hyperlipidaemia on platelet mitochondrial function, it was first established that murine platelet mitochondria have similar characteristics as those in the human (Figure 5-23). After establishing that this was the case the impact of a high fat diet on platelet mitochondrial function was examined. Platelets from mice fed a high fat diet (HFD) demonstrated significant platelet mitochondrial dysfunction in response to dietary hyperlipidaemia (Figure 5-24). Platelets isolated from HFD mice had significantly elevated basal respiration, increased ATP-coupled respiration and increased proton leak compared to animals fed standard chow. Most strikingly, platelets from the HFD group completely lost spare respiratory capacity compared to wild type. Together, these data directly demonstrate that mitochondrial dysfunction in blood platelets in response to HFD.

The mechanisms of this HFD induced phenotype needs further investigation, however, the increase in the basal respiration in the HFD group could potentially be due to the adaptation of platelets to lipid overload or its response to HFD induced

stress. The HFD platelets were working to maximal capacity at rest, indicated by the elevated basal respiration, which was almost equal to the maximal respiration. This resulted in increased ATP-linked oxygen consumption; however, the increased proton leak suggested less energy-coupled mitochondria in HFD platelets. It is still not established whether cellular ATP-demand is altered under high fat conditions but a similar increase in mitochondrial efficiency was also observed in HFD rat skeletal muscle mitochondria, which contribute to the onset of insulin resistance (Crescenzo et al., 2015). The increase in proton leak in HFD platelets could be due to an increase in mitochondrial anion carrier protein activities, damaged inner mitochondrial membrane or ETC complexes, as well as electron slippage, where electrons reduce oxygen prematurely, resulting in the generation of ROS (Mailloux et al., 2013). The mechanism for the contribution of basal proton leak to respiration is not fully understood, however, inducible proton leak is regulated by ANT and UCPs. Both ANT and UCPs can be activated by fatty acids, which are potentially increased in HFD platelets. It was recently shown that platelets express fully functional UCP2, which contributed to the decreased membrane potential in sickle cell disease platelets (Shiva et al., 2014). However, the contribution of these proteins to increased proton leak in HFD model needs further investigation.

Mitochondria are the main site of lipid metabolism, and lipid overload has been associated with mitochondrial dysfunction in a range of other cell types such as skeletal muscle (Koves et al., 2008) endothelial cells (Tang et al., 2014), macrophages (Yao and Tabas, 2001), and ovarian oocytes (Saben et al., 2016). It has long been agreed that mitochondrial impairment in hyperlipideamia is associated with decreased fat oxidation; however, this has now been overtaken by the theory that increased mitochondrial fat oxidation coexists with elevated mitochondrial stress and reactive oxygen species production as cells try to dismiss the metabolic stress caused by lipid overload (Muoio and Neufer, 2012). Although the overall mechanisms of platelet mitochondrial dysfunction in hyperlipidaemia have yet to be discovered, one of the possible reasons could be that persistent lipid overload led to metabolic inflexibility and defective energy haemostasis in platelets.

5.6 Conclusion

The main aim of this chapter was to investigate the metabolic flexibility of platelets in terms of glucose, endogenous fatty acids and amino acids utilisation under rest and activated conditions. This study has described the amino acid profile of platelet suspension before and after thrombin and collagen activation. Among 16 amino acids that were investigated, asparagine and glutamine were depleted from the medium, whereas arginine was accumulated (increase in the concentration). The metabolic fate of these amino acids however needs further investigation. After showing that glutamine had little contribution to mitochondrial oxygen consumption, the flexibility of platelets to oxidise glucose and endogenous fatty acids were investigated. This series of experiments revealed that platelets can switch freely between glucose and fatty acid oxidation both at rest and under activated conditions. Under conditions where these are limited for mitochondrial oxidation, platelets can up-regulate glycolysis to meet the energy demand of activation.

Subsequently, functions of mitochondria were investigated in both human and murine platelets, and they showed similar profile, strengthening the case for using murine platelets as models for human disease states. Stimulated platelets had higher ATP-coupled respiration and spare respiratory capacity, which did not change in the absence of glucose in human platelets. However, indomethacin, the TxA2 inhibitor, decreased both ATP-coupled respiration and spare respiratory capacity, indicative of the high energy demand of secretion process during platelet activation. Last but not least, the affect of HFD on functions of murine platelet mitochondria was investigated. It was shown that hyperlipidaemia induced elevated basal respiration, ATP-coupled respiration, however, there were also increased proton leak as well as diminished spare respiratory capacity. Together, these data suggested severe mitochondrial dysfunction in HFD murine platelets.

6. General Discussion

The fundamental role of platelets is in primary haemostasis. They prevent excessive bleeding and promote the repair of vascular wall by forming a haemostatic plug at the site of vascular injury. Beyond their role in haemostasis, there is growing evidence in the literature showing that platelets are also involved in inflammation (Hundelshausen and Weber, 2007). Platelet response to vascular perturbation or inflammation requires the transition between the relatively quiescent to active state. This is achieved by a series of biochemical signalling events, which bring about morphological changes, such as shape change and spreading, in addition to the expression of large numbers of proteins and the release of various mediators of coagulation or inflammation (Simpson et al., 2008; Broos et al., 2012). The activation of a platelet from a quiescent state requires dramatic changes in the ATP demand (Holmsen et al., 1982;Verhoeven *et al*., 1984&1985). Platelets can generate ATP through both glycolysis and oxidative phosphorylation (Karpatkin, 1967; Cohen and Wittels, 1970; Ravi et al. 2015). However, the relative importance, integration and quantitative contribution to overall energy supply of these pathways under different conditions are unclear (Chaudhry et al., 1973; Mant, 1980) and the potential role of platelet mitochondria in these processes has received little attention.

Under normal physiological conditions, most cells exhibit metabolic flexibility, in which mitochondria are able to switch between different metabolic substrates. This is important in view of recent observations linking mitochondrial dysfunction in platelets to the aetiology of diabetes (Avila et al. 2011; Ran et al. 2009), which suggests that metabolic alterations may provide a link between blood cell dysfunction and disease. However, given the paucity of information on the metabolic profiles relating to platelet function, it is difficult to understand how they become compromised in metabolic diseases known to be associated with platelet dysfunction. Thus, the aim of this study was to investigate the metabolic profiles of platelets in a defined system as well as showing the effect of metabolic disturbance, such as hyperlipidaemia, on the functions of platelet mitochondria. To achieve this, experiments have been carried out to further our understanding of the roles of the major metabolic substrates; carbohydrate, fat and protein in sustaining platelet physiology as well as platelet metabolic flexibility in terms of these fuels and pathways.

6.1 Summary of major findings

6.1.1 System for investigating platelet metabolism

To my knowledge, this is the first study to explore how various preparation methods affect platelet metabolism. Platelet metabolism can be influenced by technical factors, for example, the anticoagulant, temperature, platelet suspension medium and anti-aggregation reagents used for platelet purification processes (Table 1-2). An attempt was therefore made to optimise these factors, by reference to the literature as well as experimentally testing. First, the effect of anti-aggregating reagents, citric acid and prostaglandin, on basal platelet metabolism was tested (Figure 3-11). The basal metabolic profile did not differ between two preparations; however, the so-called prostaglandin method was more effective in preventing spontaneous aggregation during the spinning of the XFp miniplate. Consequently, the prostaglandin method was used throughout this study. Secondly, washed and un-washed platelets were compared functionally in glucose containing medium (Figure 3-8 & 3-9). Unwashed platelets were more sensitive to a given dose of agonist, suggesting that plasma components, which remained in platelet suspension, can interfere with platelet function and potentially with platelet metabolism. The extent to which platelet metabolism changes in various disease conditions, such as in the risk factors of MS mentioned in Chapter 1, independent of the increased systemic inflammation, is unknown. To understand these metabolic changes independent of other risk factors therefore requires a relatively pure platelet population with the minimum of plasma carry over. Thus using washed platelets throughout this study provided a relatively pure system compared to un-washed platelets to investigate various aspects of platelet metabolism and potential impact of high-fat diet on platelet mitochondria.

6.1.2 Glucose metabolism in platelets

6.1.2.1 Glucose uptake by platelets

This study has quantified glucose uptake by platelets at rest and during primary and secondary aggregation. The results were confirmed qualitatively by experiments on

the Seahorse bio-analyser. The data showed that both primary and secondary aggregation processes are highly energy dependent. Secondary aggregation is characterised with the secretion of ADP and TxA_2. Presumably this increase in energy demand is in part necessary to support the synthesis of TxA_2. This proposition agrees with early studies that measured platelet energy requirements using ATP equivalents as reviewed in Chapter 1.5.6 (Akkerman et al., 1982; Holmsen et al., 1982; Vorhoeven et al., 1984 & 1985), however, the present work has provided more reliable, quantitative data (Figure 3-13 to 3-15). Increased TxA_2 generation by platelets is a feature of diabetes related vascular complications (Sobol and Watala, 2000; Natarajan et al., 2008). Further investigation is required for understanding the metabolic control over the TxA_2 synthetic machinery in platelet, which will have a potential for exploitation in a clinical context for disease management by developing drug targets.

6.1.2.2 Platelet glycolytic capacity

This study was also the first to measure the glycolytic capacity and maximal glycolytic rate of platelets at both rest and in response to receptor activation (Figure 3-16 to 3-18). These experiments revealed that glycolysis increases in response to the inhibition of OXPHOS, suggesting the compensatory mechanism known as the Pasteur effect. Indeed, platelets were able to survive reliant solely on glycolysis. The maximal glycolytic rate for resting platelets was lower than that of thrombin-stimulated platelets, suggesting that platelets did not require full glycolytic capacity at rest. By contrast, in response to thrombin, platelets reached full glycolytic capacity, mediated mainly through the PAR1 receptor. These results are important, as previous studies have only measured the aerobic respiration of the cell as an indicator of the metabolic capacity (Ravi et al., 2015). However, it is important to note that sufficient glycolytic capacity to support cell function when mitochondrial respiration is manipulated is a prerequisite for this line of investigation (Brand and Nicholls, 2011). In addition, the discovery of the involvement of PAR1 in the mediation of glycolytic capacity of platelets can potentially be exploited as a drug target; however, the molecular mechanism of how this metabolic process is regulated would need further investigation. Given the potent activatory effect of thrombin on platelets, thrombin-mediated activation via

PAR1 and PAR4 has been explored as a novel target for anti-thrombotic drugs. As previously mentioned (Chapter 3), PAR1 has a higher affinity for thrombin than PAR4, thus, two PAR1 antagonists, atopaxar and vorapaxar, have recently entered phase 3 clinical trials. However, their clinical significance was disappointing, due to intracranial bleeding observed in some patients when used in combination with other anti-platelet agents, such as aspirin (Lee et al., 2012; Sidhu et al., 2014). In other words, investigating the potential metabolic pathways regulating the expression and function of PARs *in vivo* might benefit the development of novel drug targets with fewer complications as well as enhancing our understanding of PARs' mode of action.

6.1.2.3 Glycolytic and oxidative metabolism of glucose

This study agrees with those of others: Karpatkin, 1967 Doery et al. 1970, Akkerman et al. 1978, and Ravi et al., 2015, that the pathways of glycolysis and glucose oxidation are present in platelets. However, this thesis is the first to show that activated platelets adopt a glycolytic phenotype regardless of fuel availability and that endogenous fatty acids can serve as a fuel source (Figure 3-19 to 3-22). The adoption of a Warburg-type phenotype upon activation has been reported in a number of cell types related to the innate immune system regardless of their function. For example, most hemocytoblasts adopt aerobic glycolysis upon activation, and glycolysis is closely linked to proinflammatory responses of cells such as natural killer cells (Finlay, 2015), effector T cell, B cells, M1 macrophages (Murray et al., 2015), and monocytes (Pearce and Pearce, 2013). Thus, a glycolytic switch upon stimulation observed in platelets appears to be a feature shared by many cells of the blood lineages and may represent the new field of 'immunometabolism' 'in developmentally related cells, as reviewed by O'Neill and Pearce (2016). However, the signalling pathways to govern these processes in platelets are not as well characterised as in the other blood cells (O'Neill and Pearce, 2016). For example, several signalling pathways contribute to the Warburg Effect, such as PI3K/Akt and Ras signalling pathways, which promote glycolysis through activation of hexokinase and phosphofructokinase. Thus, the molecular mechanisms involved in platelet metabolic reprogramming need further investigation to facilitate our current understanding of why and how platelets adopt this metabolic phenotype.

6.1.3 Glycogen in platelets

A simplified method for the quantification of platelet glycogen *in vitro* was developed (Figure 4-10 to 4-14) and used to show that different individuals had different basal glycogen levels, which agreed with the findings of Rocha et al., (2014). The cause and function of this difference have yet to be investigated. However, these data might suggest that platelet glycogen store is active, where glycogenolysis and glycogenesis take place constantly, a notion supported by the confirmed presence of enzymes involved in these processes as reviewed in 1.5.2 (Scott, 1967; Karpatkin, 1967; Karpatkin et al., 1970). Although the enzymes were not measured in the present study, it was the first to measure glycogen levels before and after thrombin stimulation as well as their metabolic fate via glycolysis and oxidation (Figure 4-18 to 4-20). The data suggest a role for platelet glycogen in the absence of glucose. Most importantly, the mechanism of glycogenolysis was shown to be dependent on calcium (Figure 4-22). Glycogen shares similar metabolic fate with glucose in stimulated platelets, however, the interaction between exogenous glucose and glycogen as well as the role of glycogen *in vivo* need further research.

6.1.4 Metabolic flexibility of platelets

6.1.4.1 Amino acid profile of platelet suspension at rest and activation

This study measured the amino acid profile (16 amino acids) of platelet suspension before and after thrombin and collagen stimulation and showed that the concentrations of glutamine and asparagine in the incubation medium fell in a dose dependent manner, while the concentration of arginine increased (Figure 5-9 to 5-11). The potential metabolic fate of these amino acids was discussed in 5.5.1, from which it was concluded that glutamine does not seem to be used as an oxidative fuel, in agreement with previously published data (Murphy et al., 1992).

6.1.4.2 Platelet metabolic fuel and pathway flexibility

The data in this work show that platelets can switch between glycolysis and OXPHOS, in order to satisfy the metabolic demands of aggregation (Figure 5-12 to

5-17). Although aerobic glycolysis is a key feature in the normal activation of platelets, inhibiting glycolysis with 2-DG or inhibiting glucose originated pyruvate oxidation with UK5099 did not affect platelet aggregation *in vitro*. Under such conditions, platelets presumably satisfy their metabolic need for aggregation by mitochondrial respiration and metabolism of other substrates, such as endogenous fatty acids. Similarly, inhibiting mitochondrial ß-oxidation of fatty acids and mitochondrial ATP synthase did not inhibit platelet aggregation, presumably since glycolysis could compensate for the loss of mitochondrial ATP. This switch, or in another word, fine cooperation between glycolysis and OXPHOS might have functional implications beyond energy metabolism in platelets as mitochondrial respiration was sustained in the presence of increased glycolysis. Accumulating evidence suggest that in addition to their role in generating ATP, platelet mitochondria are important in regulating platelet activation, apoptosis (Zharikov and Shiva, 2013; Garcia-Souza and Oliveira, 2014) and triggering inflammatory response (Boudreau et al., 2014). One of the potential roles of platelet mitochondria, as in the most mammalian cells, is required for the regeneration of NADH to NAD+ to support TCA cycle for producing biosynthetic precursors or to maintain mitochondrial integrity to avoid apoptosis. Apart from this, mitochondrial ROS generation has been reported in resting platelets, and increased upon platelet activation. Elimination of this ROS had negative affect on phosphatidylserine (PS) exposure, a membrane protein that plays a central regulatory role in platelet activation (Pignatelli et al., 1998; Carrim et al. 2015).

6.1.4.3 Function of mitochondria in platelets

This study mainly focused on the function of platelet mitochondria in terms of energy generation. It was the first to measure platelet mitochondrial components of respiration in healthy murine platelets, which had a similar profile to healthy human platelets. This validates the animal model as an effective system to investigate the effect of potential metabolic disturbance on platelet mitochondria. Thrombin-stimulated platelets had higher ATP-coupled respiration and spare respiratory capacity compared to non-stimulated platelets, which was reduced by the inhibition of TxA_2 generation (Figure 5-20 to 5-23). This indicates that platelets utilise their spare respiratory capacity to satisfy the increased need for both ATP synthesis and

TxA_2 generation in response to thrombin-stimulation. Combined with the data shown in Chapter 3, Figure 3-14 & 3-15, it further confirms that the secondary aggregation, which is associated with the synthesis of TxA2 and ADP release, is most energy dependent. These data also show platelets increase glycolysis and OXPHOS simultaneously, however predominantly glycolysis, to meet the energy demand imposed on platelets by activation. Despite presenting a glycolytic phenotype, there was an increase in the proportion of glucose derived pyruvate oxidation upon activation with thrombin, suggesting not only cooperation but also competition for substrates between glycolysis and OXPHOS (Figure 5-14). This was also observed in bone marrow derived dendritic cell (BMDC). It was suggested that pyruvate produced by the Warburg metabolism fed into mitochondria, which facilitated a transient increase in spare respiratory capacity, making activated BMDC more metabolically capable than resting cells (Hill et al., 2012; Pearce and Everts, 2015). The spare respiratory capacity in activated platelets was much higher than that of resting platelets, probably supported by the increased glucose derived pyruvate feeding into platelet mitochondria as shown in BMDC.

6.1.4.4 Impact of high fat diet on function of mitochondria in platelet

To understand the effect of disturbed metabolic balance on platelet metabolism, it was decided to examine the impact of a HFD. Analysis of platelet mitochondrial respiration from mice fed a HFD demonstrated significant mitochondrial dysfunction (Figure 5-24). Platelets isolated from HFD mice had elevated basal respiration, increased ATP-coupled respiration and increased proton leak compared to animals fed standard chow. Most strikingly, platelets from the HFD group completely lost their spare respiratory capacity compared to wild type. This study is the first to demonstrate that platelet mitochondrial function is altered in response to hyperlipidaemia independent of other complications and opens up a new area for investigating the potential impact of altered platelet metabolism on disease outcome.

6.2 Limitations

Areas where this work might have been strengthened include:

- The concentrations of 2-DG, etomoxir, UK5099 and BPTES were used as recommended by Seahorse Bioscience Assay kits (Agilent) and were not titrated in the current study. However the response induced by each inhibitor was confirmed as the maximum by repeated measurements and referencing to the published data on platelets using similar techniques (Ravi et al., 2015). As an alternative, the specificity and efficacy of these inhibitors could have been tested using other techniques, such as Western Blotting.
- Due to the lack of effective glycogen phosphorylase inhibitors and to simplify the experimental procedures, glycogen metabolism was mainly investigated in the absence of glucose. Consequently, although this study has shown that glycogen can provide an energy source for platelets, the interaction between exogenous glucose and glycogen could not be investigated.
- Assessment of human and murine platelet mitochondrial respiration was achieved after carefully titrating the mitochondrial inhibitors. However, analysis of mitochondrial polarisation and the use of TEM to test mitochondrial physiology/structural integrity would have been desirable in studying the mitochondrial dysfunction observed in HFD platelets.

6.3 Further work

Due to time constraints, two original aims were not included in this study. The first was to measure simultaneously the oxidation of exogenous and endogenous fatty acids. It will provide first the intrinsic rate and reserve/spare capacity of platelets to oxidise fatty acids in the absence or limitation of other exogenous substrates. This could have been achieved by measuring the components of mitochondrial respiration and treating platelets with BSA-etomoxir and Fatty acid: BSA: etomoxir (Seahorse Bioscience, UK). Apart from this, free fatty acids are weak lipophilic acids and can mildly uncouple mitochondria, resulting in increased proton leak, which can lead to an increase in oxygen consumption not due to fatty acid oxidation. Measuring the mitochondrial components of respiration in the presence of free fatty acids will provide readouts on both aspects, fatty acid oxidation and fatty acid induced proton leak. This will have potential implications in assessing the effect of increased free fatty acids concentration, such as in hyperlipidaemia, on platelet function. It was previously reported that unsaturated fatty acids, such as oleic, linoleic and linolelaidic acids inhibited platelet aggregation when stimulated with collagen and arachidonic acid (MacIntyre et al., 1984; Sato et al., 1987; Mutanen, 1997; Phang et al., 2009). It was suggested that free fatty acids interfered with signal transductions and TxA_2 generation by platelets. However, this might be due to the effect of free fatty acids on platelet mitochondrial metabolism, which this assay might provide further insights.

A second original aim was to investigate the signalling pathways underpinning the glycolytic shift in activated platelets by using inhibitors of PI3K/Akt and AMP-activated protein kinase (AMPK) pathways. The balance between PI3K/Akt and AMPK pathways was shown to determine the metabolic fate of T cells and dendritic cells, which have similar metabolic transition as platelets when activated. In activated T cell and dendritic cells, PI3K/Akt/mTOR (mechanistic target of rapamycin) pathway plays an important role in the metabolic shift towards a glycolytic phenotype via several mechanisms (O'Sullivan and Pearce, 2014; O'Neill and Pearce, 2016), notably, by inducing transcription factors Myc and HIF-1a. AMPK is activated by the increased ratio of AMP to ATP, and antagonises the mTOR-mediated anabolic pathway, promoting mitochondrial biogenesis. The role of mTOR

(Aslan and McCarty, 2012; Razmara et al., 2013) and AMPK (Randriamboavonjy et al., 2010) in regulating platelet spreading, aggregation, integrin signalling and thrombus stability have began to emerge, yet their role in platelet metabolism needs investigation.

6.4 Concluding Remarks

There is increasing evidence showing that transition between resting to activated state of the activatory cells require specific metabolic patterns (O'Sullivan and Pearce, 2015; O'Neil and Pearce, 2016) to support functional changes, including platelets (Chacko et al., 2013; Pearce and Pearce, 2013; Ravi et al., 2015). In this context, improving our understanding of platelet metabolism and its regulation could lead to the development of novel therapeutic targets for treating arterial thrombosis and potentially other inflammatory diseases.

This study has performed a detailed analysis of fuel choice made by human platelets at rest and under activating conditions. The roles of glucose and endogenous fatty acids, and in addition, the importance of endogenous glycogen in facilitating a platelet response were demonstrated. Of note, platelets adopt a glycolytic phenotype when stimulated with thrombin regardless of the nutrient availability and thrombin dose. Most importantly, this study was the first to uncover a remarkable metabolic plasticity, switching freely between substrates and metabolic pathways, of blood platelets under physiological conditions. Moreover, using an animal model, we have demonstrated that the metabolic disturbance induced by hyperlipidaemia result in platelet mitochondrial dysfunction (Figure 6-1).

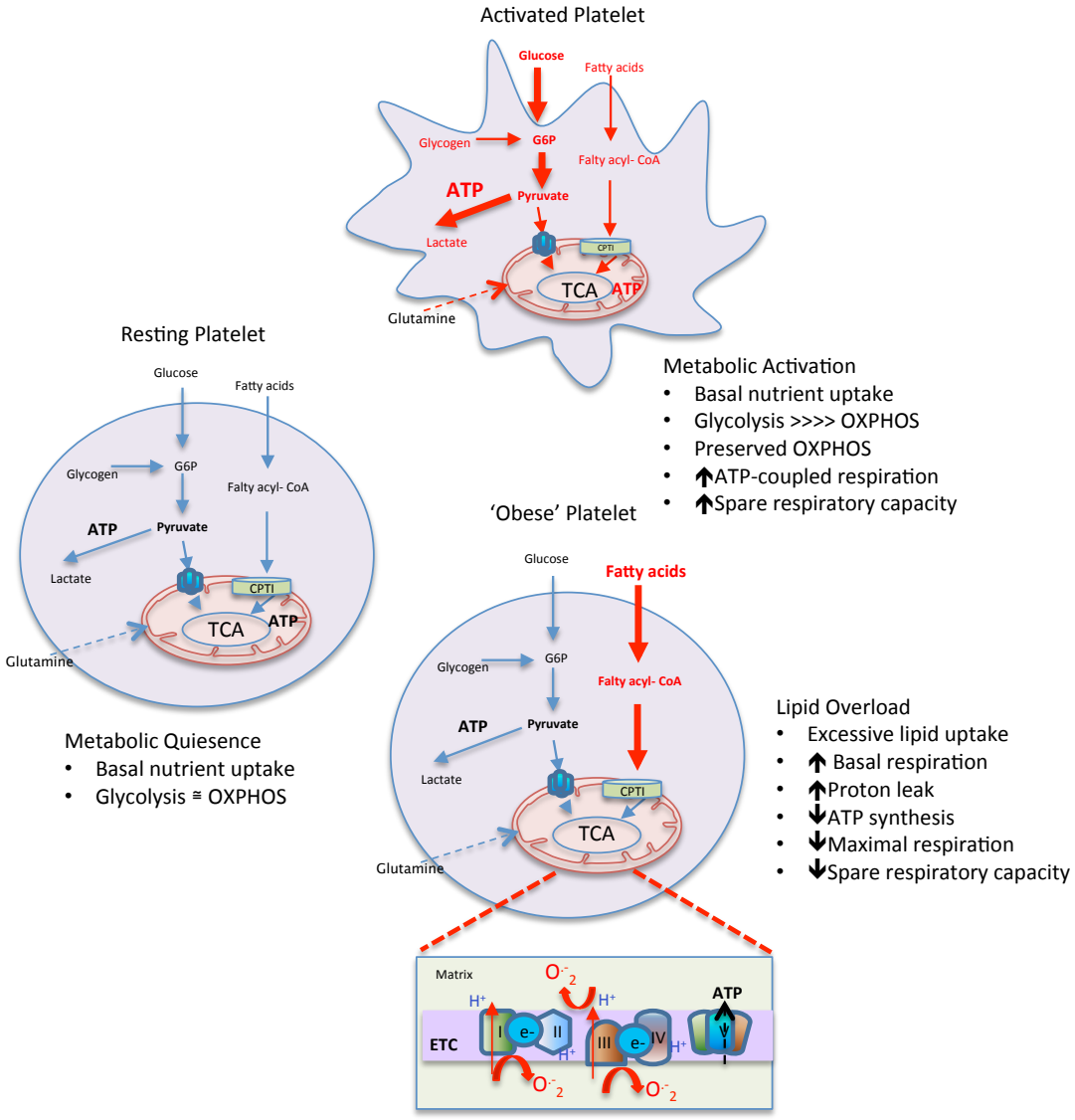

Figure 6-1: Summary figure combining the key data from chapter 3-5. Basally, platelets can use exogenous glucose and endogenous fatty acids, and potentially minimal amount of glutamine to generate ATP. Glucose is metabolised through both glycolysis and OXPHOS. Upon activation, platelets increase glucose uptake and lactate formation, shifting to a glycolytic phenotype, yet preserving mitochondrial function, indicated by increased ATP-coupled respiration and spare respiratory capacity. During this process, endogenous fatty acid oxidation increases but not significantly and platelets take up more glutamine. HFD platelets exhibit mitochondrial dysfunction indicated by increased basal respiration, proton leak and decreased maximal respiration and spare respiratory capacity.

Reference:

Adeva-Andany, M.M. et al., 2016. Glycogen metabolism in humans. *BBA Clinical*, 5, pp.85–100.

Agam, G., Gutman, A. & Djaldetti, M., 1977. Abnormal platelet glycogen metabolism in multiple myeloma patients. *Clinica Chimica Acta*, 79, pp.437–445.

Akkerman, J.W.N. et al., 1983. A novel technique for rapid determination of energy consumption in platelets. *Biochemical Journal*, 210, pp.145–155.

Akkerman, J.W.N. & Holmsen, H., 1981. Interrelationships among platelet responses: studies on the burst in proton liberation, lactate production, and oxygen uptake during platelet aggregation and Ca2+ secretion. *Blood*, (57), pp.956–966.

Akkerman, J.W.N., Gorter, G. & Sixma, J.J., 1978. Regulation of glycolytic flux in human platelets: relation between energy production by glyco(geno)lysis and energy consumption. *Biochimica et biophysica Acta*, 541(2), pp.241–50.

Altman, B.J., Stine, Z.E. & Dang, C. V, 2016. From Krebs to clinic: glutamine metabolism to cancer therapy. *Nature Reviews Cancer*, 16(10), pp.619–634.

Amiel, E. & Thwe, P.M., 2016. Intracellular glycogen reserves fuel early glycolytic metabolism associated with dendritic cell maturation and immune function. *The Journal of Immunology*, 196(1 Supplement), p.202.31 LP-202.31.

Anfossi, G., Russo, I. & Trovati, M., 2009. Platelet dysfunction in central obesity. *Nutrition, metabolism, and cardiovascular diseases*, 19(6), pp.440–9.

Arnold, H. et al., 2012. High levels of brain-type creatine kinase activity in human platelets and leukocytes: A genetic anomaly with autosomal dominant inheritance. *Blood Cells, Molecules, and Diseases*, 48(1), pp.62–67.

Agilent, 2017. *Chemical Analysis, Life Sciences, And Diagnostics*. Agilent. Web. 8 Mar. 2017. http://www.agilent.com/en-us/products/cell-analysis-(seahorse)/how-seahorse-xf-analyzers-work

Aslan, J.E. & McCarty, O.J.T., 2012. Regulation of the mTOR-Rac1 axis in platelet function. *Small GTPases*, 3(1), pp.67–70.

Atkinson, D.E., 1977. Functional Stoichiometric Coupling and Metabolic Prices. In *Cellular Energy Metabolism and its Regulation*. pp. 31–83.

Avila, C. et al., 2012. Platelet Mitochondrial Dysfunction is Evident in Type 2 Diabetes in Association with Modifications of Mitochondrial Anti-Oxidant Stress Proteins. *Experimental and Clinical Endocrinology & Diabetes*, 120, pp.248–251

Aster, R.H. & Jandl, J.H., 1964. Platelet sequestration in man. I. Methods. *Journal of Clinical Investigation*, 43, 843.

Agilent, *XFp Basic Procedure,* 08/03/2017. http://www.agilent.com/en-us/products/cell-analysis-(seahorse)/seahorse-analyzers/seahorse-xfp-analyzer/basic-procedures-to-run-an-xfp-assay

Agilent, *Seahorse XFp Cell Mito Stress Test Kit User Guide*, 08/03/2017. http://www.agilent.com/en-us/products/cell-analysis-(seahorse)/seahorse-xfp-consumables/kits-reagents-media/seahorse-xfp-cell-mito-stress-test-kit

Agilent, *Seahorse XFp cell Glycolysis Stress Test Kit User Guide*, 08/03/2017. http://www.agilent.com/en-us/products/cell-analysis-(seahorse)/seahorse-xfp-consumables/kits-reagents-media/seahorse-xfp-glycolysis-stress-test-kit

Agilent, *Seahorse XFp Cell Phenotype Test Kit User Guide*, 08/03/2017. http://www.agilent.com/en-us/products/cell-analysis-(seahorse)/seahorse-xfp-consumables/kits-reagents-media/seahorse-xfp-cell-energy-phenotype-test-kit

Agilent, *Seahorse XFp Mito Fuel Flex Test Kit User Guide*, 08/03/2017. http://www.agilent.com/en-us/products/cell-analysis-(seahorse)/seahorse-xfp-consumables/kits-reagents-media/seahorse-xfp-mito-fuel-flex-test-kit

Bartolomeo, M.P. & Maisano, F., 2006. Validation of a reversed-phase HPLC method for quantitative amino acid analysis. *Journal of bimolecular techniques*, 17(2), pp.131–137.

Beck, F. et al., 2014. Time-resolved characterization of cAMP/PKA-dependent signalling reveals that platelet inhibition is a concerted process involving multiple signalling pathways. *e-Blood*, 123(5), pp.1–11.

Bellavite, P. et al., 1994. A colorimetric method for the measurement of platelet adhesion in microtiter plates. *Analytical biochemistry*, 216(2), pp.444–450.

Benz, R. & McLaughlin, S., 1983. The molecular mechanism of action of the proton ionophore FCCP (carbonylcyanide p-trifluoromethoxyphenylhydrazone). *Biophysical journal*, 41(3), pp.381–98.

Berg, J.M., Tymoczko, J.L., Stryer, L., 2002. Chapter 17, The Citric Acid Cycle. In: Freeman, W.H., 5th edition. *Biochemistry*. New York; Available from: https://www.ncbi.nlm.nih.gov/books/NBK21163/

Berg, J.M., Tymoczko, J.L., Stryer, L., 2002. Section 30.1 Metabolism Consist of Highly Interconnected Pathways. In: Freeman, W.H., 5th edition. *Biochemistry*. New York; Available from: https://www.ncbi.nlm.nih.gov/books/NBK22553/

Berg, J.M., Tymoczko, J.L., Stryer, L., 2002. Section 16.1, Glycolysis Is an Energy-Conversion Pathway in Many Organisms. In: Freeman, W.H., 5th edition. *Biochemistry*. New York; Available from: https://www.ncbi.nlm.nih.gov/books/NBK22593/

Borregaard, N. & Herlin, T., 1982. Energy metabolism of human neutrophils during phagocytosis. *The Journal of clinical investigation*, 70(3), pp.550–7.

Boudreau, L.H. et al., 2014. Platelets release mitochondria serving as substrate for bactericidal group IIA-secreted phospholipase A2 to promote inflammation. *Blood*, 124(14), pp.2173–2183.

Bozza, F.A. & Weyrich, A.S., 2008. Mitochondria push platelets past their prime. *Hemostasis*, 111(5), pp.2496–2497.

Born, G. V. R. & Cross, M. J., 1963. The aggregation of blood platelets. *Journal of Physiology*. 168, 2 178–195.

Brand, M.D. & Nicholls, D.G., 2011. Assessing mitochondrial dysfunction in cells. *The Biochemical journal*, 435(2), pp.297–312.

Broekman, M.J., Ward, J.W. & Marcus, A.J., 1980. Phospholipid Metabolism in Stimulated Human Platelets: CHANGES IN PHOSPHATIDYLINOSITOL, PHOSPHATIDIC ACID, AND LYSOPHOSPHOLIPIDS. *Journal of Clinical Investigation*, 66(August), pp.275–283.

Bode, A.P.1 & Norris, H.T., 1992. The use of inhibitors of platelet activation or protease activity in platelet concentrates stored for transfusion. *Blood Cells*; 18(3): 361-80;

Böhmer, A., Gambaryan, S. & Tsikas, D., 2014b. Human blood platelets lack nitric oxide synthase activity. *Platelets.* doi:10.3109/09537 104.2014.974024

Broos, K. et al., 2012. Blood platelet biochemistry. *Thrombosis research*, 129(3), pp.245–9.

Broos, K. et al., 2011. Platelets at work in primary hemostasis. *Blood reviews*, 25(4), pp.155–67.

Bye, A.P., Unsworth, A.J. & Gibbins, J.M., 2016. Platelet signaling: A complex interplay between inhibitory and activatory networks. *Journal of Thrombosis and Haemostasis*, 14(5), pp.918–930.

Born, G.V.R., 1962. Aggregation of blood platelets by adenosine diphosphate and its reversal. *Nature* 194: 927-929.

Born, G.V.R. & Cross, M. J., 1963. The aggregation of blood platelets. *Journal of Physiology* 168, 2 178–195

Bergmeyer, H.U., 1974. *Methods of Enzymatic Analysis*. Academic Press, New York; p. 481

Carrim, N. et al., 2015. Thrombin-induced reactive oxygen species generation in platelets: A novel role for protease-activated receptor 4 and GPIbα. *Redox Biology*, 6, pp.640–647.

Cazenave, J.P. et al., 2004. Preparation of Washed Platelet Suspensions From Human and Rodent Blood. *Methods in molecular biology*, 272(5), pp.13–28.

Chacko, B.K. et al., 2013. Methods for defining distinct bioenergetic profiles in platelets, lymphocytes, monocytes, and neutrophils, and the oxidative burst from human blood. *Laboratory investigation*, 93(6), pp.690–700.

Chaiken, R., Pagano, D. & Detwiler, T.C., 1975. Regulation of platelet phosphorylase. *Biochimica et biophysica acta*, 403, pp.315–325.

Chaudhry, A.A. et al., 1973. Relationship of Glucose Oxidation to Aggregation of Human Platelets of Glucose of Human. *Blood*, 41, pp.249–258.

Chrusciel, P., Rysz, J. & Banach, M., 2014. Defining the role of trimetazidine in the treatment of cardiovascular disorders: Some insights on its role in heart failure and peripheral artery disease. *Drugs*, 74(9), pp.971–980.

Chung, A.W.Y. et al., 2002. Mechanisms of action of proteinase-activated receptor agonists on human platelets. *British journal of pharmacology*, 135(5), pp.1123–32.

Clemetson, K.J., 2012. Platelets and primary haemostasis. *Thrombosis research*, 129(3), pp.220–4.

Cohen, P., Derksen, a & Van den Bosch, H., 1970. Pathways of fatty acid metabolism in human platelets. *The Journal of clinical investigation*, 49(1), pp.128–39.

Cohen, P. & Wittels, B., 1970. Energy substrate metabolism in fresh and stored human platelets. *The Journal of clinical investigation*, 49(1), pp.119–27.

Coughlin, S.R., 2000. Thrombin signalling and protease-activated receptors. *Nature*, 407(6801), pp.258–264.

Cozzi, M.R. et al., 2015. Visualization of nitric oxide production by individual platelets during adhesion in flowing blood. *Blood*, 125(4), pp.697–706.

Cooper, G.M. 2000. Metabolic Energy. In: *The Cell: A Molecular Approach*. 2nd edition. Sunderland (MA): Sinauer Associates; Available from: https://www.ncbi.nlm.nih.gov/books/NBK9903/

Cooper, G.M., 2000. The Mechanism of Oxidative Phosphorylation. In: *The Cell: A Molecular Approach*. 2nd edition. Sunderland (MA): Sinauer Associates; Available from: https://www.ncbi.nlm.nih.gov/books/NBK9885/

Crescenzo, R. et al., 2015. Mitochondrial efficiency and insulin resistance. *Frontiers in Physiology*, 6(JAN), pp.1–5.

Curi, R. et al., 1999. Metabolic fate of glutamine in lymphocytes, macrophages and neutrophils. *Brazilian Journal of Medical and Biological Research*, 32(1), pp.15–21.

Czapek, E.E., Deykin, D. & Salzman, W.E., 1973. Platelet Dysfunction in Glycogen Storage Disease Type 1. *Blood*, 41(2), pp.235–247.

Craik, D.J., Stewart, M. & Cheeseman, I.C., 1995. GLUT-3 (Brain-Type) Glucose Trasporter Polypeptide in Human Blood Platelets. *Thrombosis Research*, 79, pp.461–469.

Dashty, M., 2013. A quick look at biochemistry: Carbohydrate metabolism. *Clinical Biochemistry*, 46(15), pp.1339–1352.

Davi, G. & Patrono, C., 2008. Platelet activation and atherothrombosis. *The New England journal of medicine*, 358, p.1638; author reply 1638-1639.

Daví, G. & Santilli, F., 2007. Atherothrombotic disease and the metabolic syndrome. *International Congress Series*, 1303, pp.74–82.

De Candia, E., 2012. Mechanisms of platelet activation by thrombin: A short history. *Thrombosis Research*, 129(3), pp.250–256.

Deykin, D. & Desser, R.K., 1968. The incorporation of acetate and palmitate into lipids by human platelets. *The Journal of clinical investigation*, 47(7), pp.1590–602.

Dimeloe, S. et al., 2016. T cell metabolism governing activation, proliferation and differentiation:a modular view. *Immunology*. Available at: http://doi.wiley.com/10.1111/imm.12655.

Divakaruni, A.S. & Brand, M.D., 2011. The regulation and physiology of mitochondrial proton leak. *Physiology*, 26(3), pp.192–205.

Doery, J.C.G., Hirsh, J. & Cooper, I., 1970. Energy metabolism in human platelets: interrelationship between glycolysis and oxidative metabolism. *Blood*, 36(2), pp.159–68.

Durina, J. & Remkova, A., 2007. Prothrombotic state in metabolic syndrome. *Bratislavské lekárske listy*, 108(6), pp.279–80.

Dudkina, N. V et al., 2010. Structure and function of mitochondrial supercomplexes. *Biochimica et biophysica acta,* 1797(6-7), pp.664–70.

Du, Y.B., Liu, X.S. & Guo, S.W., 2017. Platelets impair natural killer cell reactivity and function in endometriosis through multiple mechanisms. *Hum Reprod* 1-17. doi: 10.1093/humrep/dex014

D'Alessandro, M.P. & Bergman, R.A., 2017. *Anatomy Atlases: A Digital Library Of Human Anatomy*. Web. 8 Mar. 2017. http://www.anatomyatlases.org

Egan, B. & Zierath, J.R., 2013. Exercise metabolism and the molecular regulation of skeletal muscle adaptation. *Cell Metabolism*, 17(2), pp.162–184.

El Haouari, M. & Rosado, J.A., 2008. Platelet signalling abnormalities in patients with type 2 diabetes mellitus: a review. *Blood cells, molecules & diseases*, 41(1), pp.119–23.

Ferreira, I.A. et al., 2005. Glucose uptake via glucose transporter 3 by human platelets is regulated by protein kinase B. *The Journal of biological chemistry*, 280(38), pp.32625–32633.

Fink, B.D. et al., 2012. Endothelial cell and platelet bioenergetics: effect of glucose and nutrient composition. *PloS one*, 7(6), p.e39430.

Flatow, F. A. & Freireich, E. J., 1966. The increased effectiveness of platelet concentrates prepared in acidified plasma. *Blood*, 27, 449-59.

White, G.J. & Krivit, W., 1967. An ultrastructural basis for the shape changes induced in platelets by chilling. *Blood*, 30(5).

Gale, A.J., 2011. Current Understanding of Hemostasis. *Toxicol Pathology*, 39(1999), pp.43–65.

Galgani, J.E., Moro, C. & Ravussin, E., 2008. Metabolic flexibility and insulin resistance. *American journal of physiology. Endocrinology and metabolism*, 295(5), pp.E1009-17.

Galván-Peña, S. & O'Neill, L.A.J., 2014. Metabolic reprograming in macrophage polarization. *Frontiers in Immunology*, 5(SEP), pp.1–6.

Gambaryan, S. & Tsikas, D., 2015. A review and discussion of platelet nitric oxide and nitric oxide synthase: do blood platelets produce nitric oxide from L-arginine or nitrite? *Amino Acids*.

Gannon, M.C. & Nuttall, F.Q., 2010. Amino acid ingestion and glucose metabolism--a review. *IUBMB life*, 62(9), pp.660–8.

Garcia-Souza, L.F. & Oliveira, M.F., 2014. Mitochondria: Biological roles in platelet physiology and pathology. *The international journal of biochemistry & cell biology*, 50, pp.156–160.

Ghoshal, K. & Bhattacharyya, M., 2014. Overview of platelet physiology: its hemostatic and nonhemostatic role in disease pathogenesis. *The Scientific World Journal*, 10.1155, p.781857.

Gudewicz, P., 1975. Mechanisms and Regulation of Macrophage Glycogen Metabolism. *eCommons*, p.1579.

Guppy, M. et al., 1997. Fuel choices by human platelets in human plasma. *European journal of biochemistry*, 244(1), pp.161–7.

Guerif, F. et al., 2013. A Simple Approach for COnsumption and RElease (CORE) Analysis of Metabolic Activity in Single Mammalian Embryos. *PLoS ONE* 8(8): e67834. doi:10.1371/journal.pone.0067834

Hawker, R.J., Turner, V.S. & Mitchell, S.G., 1996. Use of prostaglandin E 1 during preparation of platelet concentrates. *Transfusion Medicine*, 6(3), pp.249–254.

Heijnen, H.F. et al., 1997. Thrombin stimulates glucose transport in human platelets via the translocation of the glucose transporter GLUT-3 from alpha-granules to the cell surface. *The Journal of cell biology*, 138(2), pp.323–30.

Hensley, C.T., Wasti, A.T. & Deberardinis, R.J., 2013. Glutamine and cancer: cell biology, physiology, and clinical opportunities. *The Journal of Clinical Investigation*, 123(9), pp.3678–3684.

Hundelshausen, V.P. & Weber, C., 2007. Platelets as immune cells: bridging inflammation and cardiovascular disease. *Circulation research*, 100(1), pp.27–40.

Hill, B.G. et al., 2012. Integration of cellular bioenergetics with mitochondrial quality control and autophagy. *The Journal of biological chemistry*, 393(12), pp.1485–1512.

Hinkle, P.C., 2005. P/O ratios of mitochondrial oxidative phosphorylation. *Biochimica et Biophysica Acta*, 1706(1–2), pp.1–11.

Holmsen, H., Kaplan, K.L. & Dangelmaier, C.A., 1982. Differential energy requirements for platelet responses:A simultaneous study of aggregation, three secretory processes, arachidonate liberation, phosphatidylinositol breakdown and phosphatidate production. *Biochemical Journal*, 208, pp.9–18.

Huang, M.E. & Detwiler, T.C., 1981. Characteristics of the Synergistic Actions of Platelet Agonists. *Blood*, 57(4), pp.685–692.

Hussain, O.Z. & Newcomb, T.F., 1964. Thrombin Stimulation of Platelet Oxygen Consumption Rate. *Journal of applied physiology*, 19, pp.297–300.

Ito, K. et al., 2012. A PML-PPAR-delta pathway for fatty acid oxidation regulates hematopoietic stem cell maintenance. *Nature Medicine*, 18(9), pp.1350–1358.

Jackson, S.P., 2007. The growing complexity of platelet aggregation. *Blood*, 109(12), pp.5087–5095.

Jastroch, M. et al., 2010. Mitochondrial proton and electron leaks. *Essays Biochem*, 47, pp.53–67.

Jennings, L.K., 2009. Role of Platelets in Atherothrombosis. *American Journal of Cardiology*, 103(3 SUPPL.), pp.4–10.

Jin, J. et al., 2002. Adenosine diphosphate (ADP)–induced thromboxaneA2 generation in human platelets requires coordinated signalling through integrin

aIIb3 and ADP receptors. *Hemostasis, Thrombosis and Vascular Biology*, 99(1), pp.193–198.

Joist, J.H. et al., 1976. Phospholipid transfer between plasma and platelets in vitro. *Blood*, 48(2), pp.199–211.

Kadenbach, B., 2003. Intrinsic and extrinsic uncoupling of oxidative phosphorylation. *Biochimica et Biophysica Acta - Bioenergetics*, 1604(2), pp.77–94.

Kadenbach, B. et al., 2010. New extension of the Mitchell Theory for oxidative phosphorylation in mitochondria of living organisms. *Biochimica et Biophysica Acta*, 1800(3), pp.205–212.

Kakouros, N. et al., 2011. Platelet function in patients with diabetes mellitus: From a theoretical to a practical perspective. *International Journal of Endocrinology*, 742719.

Kaplan, Z.S. & Jackson, S.P., 2011. The role of platelets in atherothrombosis. *Hematology*, pp.51–61.

Karpatkin, S., 1967. Studies on human platelet glycolysis. Effect of glucose, cyanide, insulin, citrate, and agglutination and contraction on platelet glycolysis. *The Journal of clinical investigation*, 46(3), pp.409–417.

Karpatkin, S., Charmatz, A. & Langer, R.M., 1970. Glycogenesis and glyconeogenesis in human platelets: incorporation of glucose, pyruvate and citrate into platelet glycogen; glycogen synthetase and fructose-1,6-diphosphatase activity. *Journal of Clinical Investigation*, 49(August 1969), pp.140–149.

Keaney, J.F. & Loscalzo, J., 1999. Diabetes, Oxidative Stress, and Platelet Activation. *Circulation*, 99(2), pp.189–191.

Kelly, B. & O'Neill, L.A., 2015. Metabolic reprogramming in macrophages and dendritic cells in innate immunity. *Cell research*, 25(7), pp.771–84.

Kieffer, N. et al., 1987. Biosynthesis of major platelet proteins in human blood platelets. *European journal of biochemistry*, 164(1), pp.189–95.

Kocsis, J.J. et al., 1973. Duration of inhibition of platelet prostaglandin formation and aggregation by ingested aspirin or indomethacin. *Prostaglandins*, 3(2), pp.141–144.

Koves, T.R. et al., 2008. Mitochondrial Overload and Incomplete Fatty Acid Oxidation Contribute to Skeletal Muscle Insulin Resistance. *Cell Metabolism*, 7(1), pp.45–56.

Kramer, P. a et al., 2014. Bioenergetics and the oxidative burst: protocols for the isolation and evaluation of human leukocytes and platelets. *Journal of visualized experiments : JoVE*, 10.3791/51(85).

Lee, H. et al., 2012. Safety and efficacy of targeting platelet proteinase-activated receptors in combination with existing anti-platelet drugs as antithrombotic in mice. *British Journal of Pharmacology*, 166(7), pp.2188–2197.

Lewis, N. & Majerus, P.W., 1969. Lipd metabolism in human platelets. II. De novov phospholipid synthesis and the effect of thrombin in the pattern of synthesis. *The Journal of Clinical Investigation*, 48, pp.2114–2123.

Leytin, V., 2012. Apoptosis in the anucleate platelet. *Blood reviews*, 26(2), pp.51–63.

Ligthart-Melis, G.C. et al., 2008. Glutamine is an important precursor for de novo synthesis of arginine in humans. *American Journal of Clinical Nutrition*, 87(5), pp.1282–1289.

Lümmen, P., 1998. Complex I inhibitors as insecticides and acaricides. *Biochimica et Biophysica Acta (BBA) - Bioenergetics*, 1364(2), pp.287–296.

Lodish, H., Berk, A., Zipursky, S.L et al., 2000. Section 16.2, Electron Transport and Oxidative Phosphorylation. In: Freeman, W.H., 4th edition. *Molecular Cell Biology*. New York: Available from: https://www.ncbi.nlm.nih.gov/books/NBK21528/

Lodish, H., Berk, A., Zipursky, S.L., et al. 2000. Section 16.2, Electron Transport and Oxidative Phosphorylation. In: Freeman, W.H., 4th edition. *Molecular Cell Biology* New York: Available from: https://www.ncbi.nlm.nih.gov/books/NBK21528/)

Langer, H.F., Geisler, T. & Gawaz, M., 2013. Chapter 32 Atherosclerosis and Coronary Artery Disease. In: Michelson, A.D., 3rd edition. *Platelets*, England: British medical association, Pages 653-668

Ma, X. et al., 2011. Mitochondrial Electron Transport Chain Complex III Is Required for Antimycin A to Inhibit Autophagy. *Chemistry & Biology*, 18(11), pp.1474–1481.

Machlus, K.R. & Italiano, J.E., 2013. The incredible journey: From megakaryocyte development to platelet formation. *The Journal of cell biology*, 201(6), pp.785–96.

MacIntyre, D.E. et al., 1984. Inhibition of platelet function by cis unsaturated fatty acids. *Blood*, 63(4), pp.848–857.

Magwenzi, S. et al., 2015. Oxidized LDL activates blood platelets through CD36 / NOX2 – mediated inhibition of the cGMP / protein kinase G signalling cascade. *Platelets and Thrombopoiesis*, 125(17), pp.2693–2704.

Mailloux, R.J., McBride, S.L. & Harper, M.E., 2013. Unearthing the secrets of mitochondrial ROS and glutathione in bioenergetics. *Trends in Biochemical Sciences*, 38(12), pp.592–602.

Majerus, P.W., Smith, M.B. & Clamon, G.H., 1969. Lipid Metabolism in human platelets Evidence for a complete fatty acid synthesizing system. *The Journal of Clinical Investigation*, 48(4), pp.156–164.

Malinarich, F. et al., 2015. High Mitochondrial Respiration and Glycolytic Capacity Represent a Metabolic Phenotype of Human Tolerogenic Dendritic Cells. *The Journal of Immunology*, 194(11), pp.5174–5186.

Mant, M.J., 1980. Platelet adherence to collagen: Metabolic energy requirements. *Thrombosis Research*, 17(5), pp.729–736.

Mason, R.G., Read, M.S. & Shermer, R.W., 1974. Comparison of Certain Functions of Human Platelets Separated from Blood by Various Means. *The American journal of pathology*, 77(2), pp.255–67.

Mathur, D. et al., 2014. Perturbed Glucose Metabolism: Insights into Multiple Sclerosis Pathogenesis. *Frontiers in Neurology*, 5(December), pp.1–7.

Maughan, R., 2013. Carbohydrate metabolism. *Surgery*, 31(6), pp.273–277.

May, J.A., Heptinstall, S., 2004. Effects of anticoagulants used during blood cell collection on human platelet function, in: Gibbons, J.M. & Mahaut-Smith, M.P. (Eds.), *Methods and Molecular Biology, vol. 272: Platelets and Megakaryocytes, vol. 1: Functional Assays*, Humana Press, Inc., Totowa.

Menitove, J., Frenzke, M. & Aster, R., 1986. Use of PGE1 for preparation of platelet concentrates. *Transfusion*, 26(4), pp.346–350.

Menitove, J., Kagen, L. & Aster, R., 1988. Recovery and survival in vivo of platelet concentrates prepared with prostaglandin E1. *Transfusion*, 28(1), pp.56–58.

Michno, A. et al., 2007. Alterations of adenine nucleotide metabolism and function of blood platelets in patients with diabetes. *Diabetes*, 56(2), pp.462–7.

Mookerjee, S.A., Nicholls, D.G. & Brand, M.D., 2016. Determining Maximum Glycolytic Capacity Using Extracellular Flux Measurements. *PloS one*, 11(3), p.e0152016.

Muenzer, J., Weinbach, E.C. & Wolfe, S.M., 1975. Oxygen consumption of human blood platelets: Effect of thrombin. *Biochhnica et Biophysica Acta,*, 376, pp.243–248.

Muoio, D.M. & Neufer, P.D., 2012. Lipid-induced mitochondrial stress and insulin action in muscle. *Cell Metabolism*, 15(5), pp.595–605.

Murphy, M.P., 2001. How understanding the control of energy metabolism can help investigation of mitochondrial dysfunction, regulation and pharmacology. *Biochimica et Biophysica Acta - Bioenergetics*, 1504(1), pp.1–11.

Murphy, S. et al., 1992. Amino acid metabolism during platelet storage for transfusion. *British Journal of Haematology*, 81(4), pp.585–590.

Mustard, J.F., Kinlough-Rathbone, R.L. & Packham, M. a, 1989. Isolation of human platelets from plasma by centrifugation and washing. *Methods in enzymology*, 169(1975), pp.3–11.

Mustard, J.F., Perry, D. W., Ardlie, N. G., Packham, M. A., 1972. Preparation of suspensions of washed platelets from humans. *British Journal of Haematology* 22: 193-204.

Mutanen, M., 1997. Cis-unsaturated fatty acids and platelet function. *Prostaglandins, leukotrienes, and essential fatty acids*, 57(4–5), pp.403–410.

Natarajan, A., Zaman, A.G. & Marshall, S.M., 2008. Platelet hyperactivity in type 2 diabetes: role of antiplatelet agents. *Diabetes & vascular disease research*, 5(2), pp.138–44.

Neufeld, E.J. et al., 1983. High affinity esterification of eicosanoid precursor fatty acids by platelets. *The Journal of clinical investigation*, 72(1), pp.214–20.

Newsholme, P. et al., 2003. Glutamine and glutamate as vital metabolites. *Brazilian Journal of Medical and Biological Research*, 36(2), pp.153–163.

Newsholme, P., 2001. Why Is L-Glutamine Metabolism Important to Cells of the Immune System in Health, Postinjury, Surgery or Infection. *Journal of Nutrition*, 131, pp.2552–2555.

Newsholme, P. et al., 2003. Glutamine and glutamate — their central role in cell metabolism and function. *Cell biochemistry and function*, (April 2002), pp.1–9.

Niu, X., Whisson, M.E. & Guppy, M., 1997. Types and sources of fuels for platelets in a medium containing minimal added fuels and a low carryover plasma. *British journal of haematology*, 97(4), pp.908–16.

Niu, X. et al., 1996. Carbohydrate metabolism in human platelets in a low glucose medium under aerobic conditions. *Biochimica et Biophysica Acta*, 1291, pp.97–106.

Nording, H.M., Seizer, P. & Langer, H.F., 2015. Platelets in Inflammation and Atherogenesis. *Frontiers in Immunology*, 6, p.98.

Nicholls, D.G. & Hampton, J.R., 1972. Density gradient separation of human platelets from plasma and the role of plasma in adenosine diphosphate induced platelet electrophoretic mobility changes. *Thrombosis et Diathesis Haemorrhagica* 27:425- 433

O'Neill, L.A.J. & Pearce, E.J., 2016. Immunometabolism governs dendritic cell and macrophage function. *The Journal of experimental medicine*, 213(1), pp.15–23.

O'Sullivan, D. & Pearce, E.L., 2015. Targeting T cell metabolism for therapy. *Trends in Immunology*, 36(2), pp.71–80.

Palomo, I. et al., 2010. Pathophysiology of the proatherothrombotic state in the metabolic syndrome. *Frontiers in bioscience (scholar edition)*, 2(7), pp.194–208.

Patel, I., Aledort, L. & Puszkin, E.G., 1976. Amino Acid Metabolism of Platelets in Leukemia. *Cancer Research*, 36, pp.1263–1266.

Patzelt, J., Verschoor, A. & Langer, H.F., 2015. Platelets and the complement cascade in atherosclerosis. *Frontiers in Physiology*, 6(MAR), pp.1–9.

Pearce, E.J. & Everts, B., 2015. Dendritic cell metabolism. *Nature Review Immunology*, 15(1), pp.18–29

Pearce, E.L. et al., 2013. Fueling immunity: insights into metabolism and lymphocyte function. *Science*, 342(6155), p.1242454.

Pearce, E. & Pearce, E., 2013. Metabolic pathways in immune cell activation and quiescence. *Immunity*, 38(4).

Phang, M., Garg, M.L. & Sinclair, A.J., 2009. Inhibition of platelet aggregation by omega-3 polyunsaturated fatty acids is gender specific-Redefining platelet response to fish oils. *Prostaglandins Leukotrienes and Essential Fatty Acids*, 81(1), pp.35–40.

Pietraforte, D. et al., 2014. Redox Control of Platelet Functions in Physiology and Pathophysiology. *Antioxidants & Redox Signaling*, 21(1), pp.177–193.

Polanowska-Grabowska, R., Gibbins, J.M. & Gear, A.R.L., 2003. Platelet adhesion to collagen and collagen-related peptide under flow: Roles of the a2b1 integrin, GPVI, and Src tyrosine kinases. *Arteriosclerosis, Thrombosis, and Vascular Biology*, 23(10), pp.1934–1940.

Protti, A. et al., 2012. Metformin overdose causes platelet mitochondrial dysfunction in humans. *Critical care*, 16(5), p.R180.

Papen, V.M. et al., 2013. Determination of ATP and ADP secretion from human and mouse platelets by an HPLC assay. *Transfusion Medicine and Hemotherapy*, 40(2), pp.109–116.

Patscheke H., 1981. Shape and functional properties of human platelets washed with acid citrate. *Haemostasis*, 10(1):14-27.

Pignatelli, P. et al., 1998. Hydrogen peroxide is involved in collagen-induced platelet activation. *Blood*; 91:484–90.

Randriamboavonjy, V. et al., 2010. AMPK α2 subunit is involved in platelet signalling, clot retraction, and thrombus stability. *Blood*, 116(12), pp.2134–2140.

Rath, M. et al., 2014. Metabolism via arginase or nitric oxide synthase: Two competing arginine pathways in macrophages. *Frontiers in Immunology*, 5(OCT), pp.1–10.

Ravi, S. et al., 2015. Metabolic Plasticity in Resting and Thrombin Activated Platelets. *Plos One*, 10(4), p.e0123597.

Razmara, M., Heldin, C.-H. & Lennartsson, J., 2013. Platelet-derived growth factor-induced Akt phosphorylation requires mTOR/Rictor and phospholipase C-γ1, whereas S6 phosphorylation depends on mTOR/Raptor and phospholipase D D. *Cell communication and signaling*, 11(1), p.3.

Ren, J. et al., 2010. Mitochondrial biogenesis in the metabolic syndrome and cardiovascular disease. *Journal of molecular medicine*, 88(10), pp.993–1001.

Rivera, J. et al., 2009. Platelet receptors and signalling in the dynamics of thrombus formation. *Haematologica*, 94(5), pp.700–711.

Robinson, M.M. et al., 2007. Novel mechanism of inhibition of rat kidney-type glutaminase by bis-2-(5-phenylacetamido-1,2,4-thiadiazol-2-yl)ethyl sulfide (BPTES). *The Biochemical journal*, 406(3), pp.407–14.

Russo, I., 2012. The Prothrombotic Tendency in Metabolic Syndrome: Focus on the Potential Mechanisms Involved in Impaired Haemostasis and Fibrinolytic Balance. *Scientifica*, (525374), pp.1–17.

Saben, J.L. et al., 2016. Maternal Metabolic Syndrome Programs Mitochondrial Dysfunction via Germline Changes across Three Generations. *Cell Reports*, 16, pp.1–8.

Sahai, S., 1983. Glutaminase in human platelets. *Cilinica Chimica Acta*, 127, pp.197–203.

Santilli, F. et al., 2012. Platelet activation in obesity and metabolic syndrome. *Obesity reviews*, 13(1), pp.27–42.

Santilli, F. et al., 2015. Platelets and diabetes mellitus. *Prostaglandins and Other Lipid Mediators*, 120, pp.28–39.

Santos Rocha, D. et al., 2014. A Simple Method to Quantify Glycogen from Human Platelets. *Journal of Cytology & Histology*, 5(2), pp.5–7.

Sato, T. et al., 1987. Inhibition of platelet aggregation by unsaturated fatty acids through interference with a thromboxane-mediated process. *Biochimica et biophysica acta*, 931(2), pp.157–164.

Scott, R.B., 1967. Activation of glycogen phosphorylase in blood platelets. *Blood*, 30(3), pp.553–558.

Shiva, S. et al., 2014. Mitochondrial Uncoupling Protein 2 Is Present in Human Platelets and Regulates Platelet Activation. *Blood*, 124(21), p.4147 LP-4147..

Sidhu, T.S., French, S.L. & Hamilton, J.R., 2014. Differential signaling by protease-activated receptors: Implications for therapeutic targeting. *International Journal of Molecular Sciences*, 15(4), pp.6169–6183.

Simonnet, H., Vigneron, A. & Pouysségur, J., 2014. Conventional techniques to monitor mitochondrial oxygen consumption. *Methods in Enzymology*, 542, pp.151–161.

Simpson, I.A. et al., 2008. The facilitative glucose transporter GLUT3 : 20 years of distinction. *American journal of physiology Endocrinology and metabolism*, 295, pp.242–253.

Sjövall, F. et al., 2013. Mitochondrial respiration in human viable platelets-Methodology and influence of gender, age and storage. *Mitochondrion*, 13(1), pp.7–14.

Smith, D.G. & Sturmey, R.G., 2013. Parallels between embryo and cancer cell metabolism. *Biochemical Society transactions*, 41(2), pp.664–9.

Smyth, S.S. et al., 2010. CHAPTER 114 PLATELET MORPHOLOGY , BIOCHEMISTRY , AND FUNCTION. In *Hemostasis and Thrombosis*. pp. 1735–1814.

Sobol, A.B. & Watala, C., 2000. The role of platelets in diabetes-related vascular complications. *Diabetes Research and Clinical Practice*, 50(1), pp.1–16.

Solaini, G. et al., 2010. Hypoxia and mitochondrial oxidative metabolism. *Biochimica et biophysica acta*, 1797(6–7), pp.1171–7..

Sorbara, L.R. et al., 1997. Thrombin induced translocation of GLUT 3 glucose transporters in human platelets. *Biochemical Journal*, 516, pp.511–516.

Spector, A., Hoak, J. C., Warner, E. D. & Fry, G., 1970. Utilization of long-chain free fatty acids by human platelets, *Journal of Clinical Investigation*. 49, 1489-1496.

Stock, D., Leslie, A.G. & Walker, J.E., 1999. Molecular architecture of the rotary motor in ATP synthase. *Science*, 286(5445), pp.1700–5.

Suslova, T.E. et al., 2015. Platelet haemostasis in patients with metabolic syndrome and type 2 diabetes mellitus: cGMP- and NO-dependent mechanisms in the insulin-mediated platelet aggregation. *Frontiers in Physiology*, 6(JAN), pp.1–8.

Schwertz, H., Köster, S., Kahr, W.H.A., et al., 2010. Anucleate platelets generate progeny. *Blood*.115(18):3801-3809

Tan, I.K. & Gajra, B., 2006. Plasma and urine amino acid profiles in a healthy adult population of Singapore. *Annals of the Academy of Medicine, Singapore*, 35, pp.468–475.

Tangen, O., Berman, H.J., Marfey, P., 1971. Gel filtration: a new technique for separation of blood platelets from plasma. *Thrombosis et Diathesis Haemorrhagica* 25:268- 278

Tang, X. et al., 2014. Mitochondria, endothelial cell function, and vascular diseases. *Frontiers in physiology*, 5(May), p.175.

Terada, H., 1990. Uncouplers of oxidative phosphorylation. *Environmental Health Perspectives*, 87, pp.213–218.

Thomas, A. et al., 2014. Network reconstruction of platelet metabolism identifies metabolic signature for aspirin resistance. *Scientific reports*, 4, p.3925

Tziomalos, K. et al., 2010. Endothelial dysfunction in metabolic syndrome: prevalence, pathogenesis and management. *Nutrition, metabolism, and cardiovascular diseases*, 20(2), pp.140–146.

Vacanti, N.M. et al., 2014. Role of mitochondrial pyruvate carrier in substrate regulation. *Molecular Cell*, 56(3), pp.425–435.

Van Rooy, M.J. & Pretorius, E., 2015. Metabolic syndrome, platelet activation and the development of transient ischemic attack or thromboembolic stroke. *Thrombosis Research*, 135(3), pp.434–442.

Vasta, V. et al., 1995. Glutamine transport and enzymatic activities involved in glutaminolysis in human platelets. *BBA - General Subjects*, 1243(1), pp.43–48.

Verhoeven, A.J.M., Mommersteeg, M.E. & Akkerman, J.W., 1984. Quantification of energy consumption in platelets during thrombin-induced aggregation and secretion. Tight coupling between platelet responses and the increment in energy consumption. *The Biochemical journal*, 221(3), pp.777–87.

Verhoeven, A.J.M. et al., 1985. The energetics of early platelet responses: Energy consumption during shape change and aggregationwith special reference to protein phosphorylation and the polyphosphoinositide cycle. *Biochemical Journal*, 228, pp.451–462.

Wachowicz, B. et al., 2016. The physiology of blood platelets and changes of their biological activities in multiple sclerosis. *Acta Neurobiol Exp*, 76, pp.269–281.

Watala, C., 2005. Blood platelet reactivity and its pharmacological modulation in (people with) diabetes mellitus. *Current pharmaceutical design*, 11(18), pp.2331–65.

Weber, A.A., Reiman, S. & Schror, K., 1999. Specific inhibition of ADP induced platelet aggregation by clopidogrel in vitro. *British journal of pharmacology*, 126(1), pp.415–420.

White, J.G., 1979. Current concepts of platelet structure. *American Journal of Clinical Pathology*, 71(4), pp.363–378.

Walsh, P.N., 1972. Albumin density gradient separation and washing of platelets and the study of platelet coagulant activities. *British Journal of Haematology,* 22:205-217

Warburg, O., 1956. On the Origin of Cancer Cells. *Science* 24 FEB : 309-314

World Health Organisation, 2016. Fact sheet: Cardiovascular Diseases (CVDs), WHO Media Centre, 08/03/2017; http://www.who.int/mediacentre/factsheets/fs317/en/

Yao, P.M. & Tabas, I., 2001. Free Cholesterol Loading of Macrophages Is Associated with Widespread Mitochondrial Dysfunction and Activation of the Mitochondrial Apoptosis Pathway. *Journal of Biological Chemistry*, 276(45), pp.42468–42476.

Zharikov, S. & Shiva, S., 2013. Platelet mitochondrial function: from regulation of thrombosis to biomarker of disease. *Biochemical Society transactions*, 41(1), pp.118–23.

Zheng, J., 2012. Energy metabolism of cancer: Glycolysis versus oxidative phosphorylation. *Oncology Letters*, 4(6), pp.1151–1157.

Zucker, W.H., Shermer, R.W. & Mason, R.G., 1974. Ultrastructural comparison of human platelets separated from blood by various means. *The American journal of pathology*, 77(2), pp.255–67.

Appendix 1

Chemicals	Supplier	Cat.No & Size
Antimycin A	Sigma-Aldrich	A8674-25MG
Apyrase	Sigma-Aldrich	A6237-100UN
Adenosine 5triphosphate disodium salt hydrate (ATP)	Sigma-Aldrich	A6419
Amino Acid Standard 1	Sigma-Aldrich	AAS18
BAPTA/AM	Calbiochem	196419-25MG
BPTES	Sigma-Aldrich	SML0601-5MG
Beta mercaptoethanol	Santa Cruz	CAS60242
Collagen Reagens HORM® Suspension (KRH)	Takeda	1*4ml Reagent, 4*10ml diluting solution
Carbonyl cyanide 4-(trifluoromethoxy)phenylhydrazone (FCCP)	Sigma-Aldrich	C2920-10MG
Citric Acid	Sigma-Aldrich	251275-500G
Cell-Tak Cell Adhesive	Corning	354240
Dithiothreitol	Sigma-Aldrich	D0632-1G
(+)-Etomoxir Sodium Salt Hydrate	Sigma-Aldrich	E1905-5MG
EPPS	Sigma-Aldrich	E9502-10G
Ethylenediaminetetraacetic acid (EDTA)	Sigma-Aldrich	E9884-500G
D-(+)- Glucose	Sigma-Aldrich	G6152-100G
Glycogen	Sigma-Aldrich	G0885-1G
Glucose Standard, 5.0mmol/L	Analox	GMRD-010, 30ML
Glacial Acetic Acid	SLS	CHE1018
HEPES Sodium Salt	Sigma-Aldrich	H7006-100G
Hexokinase/G-6-P	Roche Life Science	127-825
Indomethacin	Sigma-Aldrich	I7378-5G
Luciferin-luciferase	Fisher	A22066
Magnesium Sulphate	Fisher Scientific	M/1050-500G

Magnesium Chloride ($MgCl_2$)	Sigma-Aldrich	M8266-1KG
Methanol (HPLC grade)	Fisher Scientific	M/4056/17
Nicotinamide adenine dinucleotide phosphate (NADP)	Roche Life Science	128 040
Oligomycin	Sigma-Aldrich	O4876-5MG
Phenol Red	Sigma-Aldrich	P3532-5G
Potassium Chloride (KCl)	Sigma-Aldrich	P5405-250G
Potassium Phosphate Monobasic (KH_2PO_4)	Sigma-Aldrich	P5655-100G
Prostaglandin (PGE_1)	Sigma-Aldrich	P5640-1MG
Prostacycin (PGI_2)	Sigma-Aldrich	P6188-1MG
p-Nitrophenyl phosphate disodium hexahydrate	Sigma-Aldrich	N4645-5G
Phthaladialdehyde Reagent (OPA)	Sigma-Aldrich	P0532
PPACK	Ceyman Chemicals	15160
Rotenon	Sigma-Aldrich	R8875-1G
Sodium Bicarbonate ($NaHCO_3$)	Sigma-Aldrich	S4772-500G
Sodium Chloride (NaCl)	Sigma-Aldrich	S5886-500G
Sodium Hydroxide	Fisher Scientific	S4920/60
Sodium Phosphate Monobasic (NaH_2PO_4)	Sigma-Aldrich	S8282-500G
Sodium Citrate Dihydrate ($C_6H_5Na_3O_7 \cdot 2\ H_2O$)	Fisher Scientific	BP327-500
Sodium Acetate	Sigma-Aldrich	W302406
Tri-sodium Citrate	Life Science	106447
Triton *100	Sigma-Aldrich	X100-100ML
Thrombin	Sigma-Aldrich	10602400001
Tetrahydrofuran (THF)	Sigma-Aldrich	34865
UK5099	Sigma-Aldrich	PZ0160-5MG

Appendix 2

Preparation of Modified Tyrode's Buffer

Compound	Molarity (m M)	F.W.	g/L
NaCl	15	58.44	8.77
HEPES *sodium salt*	5	260.29	1.30
NaH_2PO_4 anh.	0.55	120	0.086
$NaHCO_3$ anh.	7	84.01	0.59
KCl	2.7	74.55	0.20
$MgCl_2$	0.5	203.31	0.10
D-glucose anh.	5.6	180.16	1.01

Equipment: Balance; pH meter; Magnetic stirrer

Method: Weigh out the appropriate amount of chemicals and dissolve in approximately 800ml of dH_2O, adjust the pH to 7.4 and make up to 1 L. Store at 4 °C. Filter through a 0.22 μm filter before use and warm to 37°C.

Preparation of Glucose- free Modified Tyrode's Buffer

Compound	Molarity (mM)	F.W.	g/L
NaCl	15	58.44	8.77
HEPES *sodium salt*	5	260.29	1.30
NaH_2PO_4 anh.	0.55	120	0.086
$NaHCO_3$ anh.	7	84.01	0.59
KCl	2.7	74.55	0.20
$MgCl_2$	0.5	203.31	0.10

Equipment: Balance; pH meter; Magnetic stirrer

Method: Weigh out the appropriate amount of chemicals and dissolve in approximately 800ml of dH_2O, adjust the pH to 7.4 and make up to 1 L. Store at 4 °C. Filter through 0.22 μm filter before using it and warm to 37°C.

Preparation of xF Base Medium

Compound	Molarity (m M)	F.W.	g/L
NaCl	15	58.44	8.77
NaH_2PO_4 anh.	0.55	120	0.086
KCl	2.7	74.55	0.20
$MgCl_2$	0.5	203.31	0.10
Phenol Red	0.0084	354.38	0.003

Equipment: Balance; pH meter; Magnetic stirrer

Method: Weigh out the appropriate amount of chemicals and dissolve in approximately 800ml of dH_2O, adjust the pH to 7.4 and make up to 1 L. Store at 4 °C. Filter through 0.22 μm filter before using it and warm to 37°C. Measure the pH every time before use and re-adjust the pH to 7.4. Add glucose, 5.6 mM when required for the specific assay before checking pH.

Preparation of Wash Buffer

Compound	Molarity (M)	F.W.	g/100 ml
Citric Acid	0.036	192.12	0.757
EDTA	0.01	372.24	0.380
Glucose	0.005	180.16	0.090
KCl	0.005	74.55	0.037
NaCl	0.09	58.44	0.526

Equipment: Balance; pH meter; Magnetic stirrer

Method: Weigh out the appropriate amount of chemicals and dissolve in approximately 80ml of dH_2O, adjust the pH to 6.5 and make to 100 ml. Store at 4 °C. Filter through 0.22 μm filter before use and warm to 37°C.

Preparation of PBS

Compound	Molarity (mM)	F.W.	g/L
KCl	2.7	74.55	0.2
KH_2PO_4	1.5	136.09	0.2
$MgCl_2$	0.2	203.31	0.047
NaCl	136.9	58.44	8.0
NaH_2PO_4 anh.	9.6	120	1.15

Equipment: Balance; pH meter; Magnetic stirrer

Method: Weigh out the appropriate amount of chemicals and dissolve in approximately 800ml of dH_2O, adjust the pH to 7.4 and make up to 1 L. Store at room temperature. Filter through 0.22 μm filter before use and warm to 37°C.

Preparation of Acid-Citrate Dextrose Buffer (ACD)

Compound	Molarity (mM)	F.W.	g/L
D-glucose anh.	113.8	180.16	20.5
Tri-Na Citrate	29.9	294.10	8.79
NaCl	72.6	58.44	4.24
Citric Acid	2.9	210.14	0.59

Equipment: Balance; pH meter; Magnetic stirrer

Method: Weigh out the appropriate amount of chemicals and dissolve in approximately 800ml of dH_2O, adjust the pH to 6.4 and make up to 1 L. Store at 4 °C. Filter through 0.22 μm filter before use and warm to 37°C.

Preparation of Citrate Buffer

Compound	Molarity (mM)	F.W.	g/L	g/250 ml
Citric Acid	29	210.14	6.148	1.537
Sodium Citrate Dehydrate	68	294.1	19.99	4.998

Prepare fresh on the day 15ml/plate of citrate buffer to be assayed and add:

Compound	Molarity (mM)	F.W.	g/L	g/15 ml
p-nitrophenyl phosphate	5	317.2	1.856	0.028
Triton*100	0.1%		1 ml	15 ul

Equipment: Balance; pH meter; Magnetic stirrer

Method: Weigh out the appropriate amount of chemicals and dissolve in approximately 200ml of dH_2O, adjust the pH to 5.4 and make up to 250 ml of Citrate Buffer fresh every time.

Preparation of Glucose Cocktail

Compound	Weight (mg)	dH_2O (ml)
Dithiothreitol	7.715	10
Magnesium sulphate	91.2	10
NADP	39.37	5
ATP	30.26	5

Equipment: Balance; pH meter; Magnetic stirrer

Method: Prepare EPPS buffer first by adding 2.52g of EPPS and dissolve in 150 ml of distilled water. pH to 8 using 1M NaOH (4g in 100ml of distilled water) then make up to 200 ml. Store at 4 °C and discard after 3 months.

Add together in a 50 ml glass beaker 15 ml of EPPS buffer, 1ml of Hexokinase glucose 6-phosphate dehydrogenase, and from table above 2ml Dithiothreitol, 2ml Magnesium sulphate, 3ml of NADP, and 1ml of ATP. Mix together and aliquot into 1.5 ml Eppendorf tubes. Store at -20 °C, discard after 8 weeks.

HPLC Analysis

Mobile Phases: 83mM Sodium Acetate (pH5.9); 56.45g Sodium Acetate in water, pH to 5.9 with glacial Acetic Acid, and made up to 5L

Buffer A:

Component	Final Percentage (v/v)	Volume (ml)
83mM Sodium Acetate (pH5.9)	80%	2000
Methanol	20%	500
Degas		
Tetrahydrofuran	0.5%	12.5

Buffer B:

Component	Final Percentage (v/v)	Volume (ml)
83mM Sodium Acetate (pH5.9)	20%	500
Methanol	80%	2000
Degas		